

Genetic and autoimmune modulators of brain function in neuropsychiatric illness and health

Dissertation

for the award of the degree

‘Doctor of Philosophy’ (Ph.D.)

Division of Mathematics and Natural Sciences

of the Georg-August-Universität Göttingen

within the doctoral program Center for Systems Neuroscience

of the Georg-August University School of Science (GAUSS)

submitted by

Bárbara Oliveira

born in Vila Nova de Famalicão, Portugal

Göttingen 2018

Doctoral thesis committee:

Prof. Dr. Dr. Hannelore Ehrenreich (1st referee)

Clinical Neuroscience

Max Planck Institute of Experimental Medicine

Prof. Dr. Wolfram-Hubertus Zimmermann (2nd referee)

Institute of Pharmacology

University Medical Center Göttingen

Prof. Dr. Nils Brose

Department of Molecular Neurobiology

Max Planck Institute of Experimental Medicine

Dr. Sonja Wojcik

Department of Molecular Neurobiology

Max Planck Institute of Experimental Medicine

Members of the examination board:

Prof. Dr. Jürgen Wienands

Institute for Cellular and Molecular Immunology

University Medical Center Göttingen

Prof. Dr. Klaus-Armin Nave

Department of Neurogenetics

Max Planck Institute of Experimental Medicine

Prof. Dr. Ralf Heinrich

Department of Neurobiology

Institute for Zoology and Anthropology

Date of oral examination: 17.04.2018

Declaration

I hereby declare that the thesis “Genetic and autoimmune modulators of brain function in neuropsychiatric illness and health” has been written independently and with no other sources and aids than quoted.

Bárbara Oliveira

Göttingen, 02.03.2018

ACKNOWLEDGEMENT

“The value of things is not the time they last, but the intensity with which they occur. That is why there are unforgettable moments and unique people!” *Fernando Pessoa*

Going through my thoughts of what the last four years have been, I cannot feel anything but gratitude. All the good and bad moments, the tears and laughter and the “I will never finish my PhD” breakdowns come together to put a smile on my face. I have been blessed with incredible people that shared this journey with me and to whom I will never be able to thank enough for so many unforgettable moments!

I start with the “Captain” ;) my supervisor, Prof. Hannelore Ehrenreich. You gave me the opportunity of joining an incredible team and to be a part of several interesting projects. I am sincerely grateful for all the challenges and learning experiences you provided me with. I realize now, that even in the moments when we disagreed, you helped me to become a more confident and outspoken person. I will always be grateful for the trust you had in me and the scientific guidance during my PhD.

I would like to thank my thesis committee members, Prof. Wolfram-Hubertus Zimmermann, Prof. Nils Brose and Dr. Sonja Wojcik for their valuable guidance and scientific input during my PhD. Your inquisitive minds challenged me to be and to do better! Thank you also to my examination board members, Prof. Jürgen Wienands, Prof. Klaus-Armin Nave and Prof. Ralf Heinrich for taking the time to consider my work.

Moreover, I would like to express my gratitude to all the people with whom I collaborated during my PhD; The Bochum team: Prof. Michael Hollmann, Daniel and Christina for all the fun data discussions over the phone; To Krasimira, Iris and Daria for your priceless help in introducing me to stem cell culture; To my dear Patapia, which was always ready to help and cheer me up, I would not have made it without you! And finally, to Prof. Silvio Rizzoli and Eugenio for your guidance and great scientific discussions during my calcium imaging experiments. A special thank you to Eugenio, for making me believe that everything would work out. You always had time for me, even when you did not have any time left.

My lovely colleagues at Clinical Neuroscience (past and present), you made this journey a hell of a ride! Every single one of you provided me with sweet memories that I will forever cherish. I have been more than lucky to be a part of such a nice team. I truly enjoyed our lunch and coffee breaks and all the scientific discussions over the last years. A special thank you to Nadine, the best technical assistant ever, for putting all of your heart in our cultures. It was amazing to work with you.

A special thank you to Martin, Julia and Michelle for sharing the "PhD representative adventure" with me: I enjoyed all the crazy moments we lived together, the pancakes marathon...the stress of organizing the retreat and the summer party... even the abstract book drama seems funny now ;)

The amazing people that I am lucky to have as friends, that always supported and encouraged me:

To the amazing women, without whom I would not have come to Göttingen: Isabel, Ines, Liliana and Catarina. Your support gave me the courage necessary to make a change and for that I will be forever grateful.

My Extrabrain colleagues: being a part of this program with such an amazing group of people was one of the best experiences of my life... all the meetings around Europe and the time we spent together were truly special!

To Olaf and Gwen for always pulling me higher... Literally! Our climbing sessions helped me to keep my sanity during these four years. Your positive energy was a miracle worker.

To Umer, for always being so attentive and kind to me, and off course thank you for all the delicious food!

Anja, my sweet Anja! I will miss your positive energy! And your muffins ;) You are the sunshine of the office.

Fernandella! Thank you for being such a kind person! I am so lucky to have as a friend!

Bekir, the Wolf, my antibody dealer. Thank you for always being ready to listen.

Beate, we had to become friends after bumping into each other in pretty much every GGNB course we attended ☺ You are one of the gifts that Göttingen provided me with.

Vikas, I don't know anyone else with such a positive attitude in life! Spending time with you is always good for my immune system ☺

Ludo, thank you for your random acts of friendship: the countless bounties and pringles, the mushroom risotto for dinner and for keeping me company in the late nights of working in the lab. You always put up with all the pranks kindly and most importantly without killing me. Thank you for teaching me how to dance, I am aware of how big the challenge was ;) not as big as having German class together though!

Giulia, Marina, Mara, Edda and Livia...my girls! Life in Göttingen would not be the same without you...As we once sang in the back of a taxi in a cold November night: I will always love youuuuuuuuu! We shared so many adventures... from Copenhagen to Barcelona, Rome, Basel, Leiden, Berlin, Edinburgh, Amsterdam, Oslo and so many more! Mara visiting you was always amazing! And that picture with Santa! OMG! Your thesis writing survival kit

brought me so much joy! Edda, my dear...Göttingen is so small that we even had the same stalker ☺ And Livia...that weekend in the Vatican with Francesco, zucchini flowers and cacao pepe forever!!!

As for the other two ladies... my "work wives":

Giulia, my constant source of entertainment and support. Thank you for turning the bad moments into a good laugh and for being such a good partner in crime! Great minds think alike, evil minds work together ☺. You were always ready to cross Europe and live new adventures. Thank you for Columbus and after Columbus...for singing Edelweiss on the train in Salzburg, for the best walking tour ever in Edinburgh! And for all the silly things we did together like planting tulips in July. Most of all, thank you for your believe in me.

Marina, my life guru! You always push me to be better and do better... even things that I did not think I was able to do like participating in the Great Barrier Run. In the past years I had a lot of muscle pain to blame you for! You are my rock, and in the difficult moments you are always there to support me and make me believe in myself. May we always celebrate surviving the tough moments with a glass of red wine on a roof top ☺ thank you for the shitake burgers, the pouched eggs and all the cookie sessions! Your positive energy is contagious and I am incredible lucky to be your friend!

Joana and Ginie, my examples of women's strength and power! You inspire me always! I am super lucky to have you in my life.

César and Monique, the best flat mates ever! You are family! And despite of the distance you are always present in the most important moments!

Finally, my family: the source of all my strength and inspiration in life! Filipe (my beloved George) and Adolfo, you thought me the wonders of being different. It is for you and because of you that every day I try to be a better researcher. Papi, Miquinhas & Diogo. None of this or whatever I have accomplished in life would be possible without your love and support. Your constant care and attention, despite the distance, are my driving force! Papi, you proved me that love is timeless, and every day I feel your support and encouragement to be better. You taught me that it is up to me to set my own limits. Miquinhas, my cheerleader! It is overwhelming to feel your love and belief in me. You are always the first one to say that I can do it! Diogo, you are always there when I need you, and growing up together made me a stronger and more independent person. All I am today, I owe to the three of you!

So, lovely people! For all we lived so far and the many amazing moments ahead of us I am deeply thankful!

To Papi, my hero.

"I am nothing.

I'll never be anything.

Apart from that, I have in me all the dreams in the world."

Fernando Pessoa

TABLE OF CONTENTS

1. Introduction.....	15
<i>Scope of the present work</i>	35
2. Establishing a cell culture system for translational studies.....	39
3. PROJECT I – All naturally occurring autoantibodies against the NMDA receptor subunit GluN1 have pathogenic potential irrespective of epitope and immunoglobulin class	47
Overview of Project I	47
Original publication.....	49
4. PROJECT II – Uncoupling the widespread occurrence of anti-NMDAR1 autoantibodies from neuropsychiatric disease in a novel autoimmune model	63
Overview of Project II	63
Original publication.....	67
5. PROJECT III – Excitation-inhibition dysbalance as predictor of autistic phenotypes	85
Overview of Project III	85
Original publication.....	87
6. Summary and Conclusions.....	91
7. Bibliography.....	97
8. Appendix.....	113
Accepted co-author publications	113
Manuscript under revision	147
List of abbreviations	161
<i>Curriculum vitae</i>	163
List of publications.....	165

1. INTRODUCTION

Brain development and function

The outstanding complexity of the human brain is the product of an evolutionary journey that started millions of years ago. The human connectome is a myriad of specialized neuronal cell types and its synaptic connections, which add up to assemble the neural circuits and networks (van den Heuvel *et al.* 2016). Much more than the sum of its individual components, the structural and functional connectivity of the brain is shaped by the unique interaction between an individual and its environment.

In its most simple definition, the human adult brain is composed by an average of 86.1 billion neurons and an approximately equal number of glial cells with a heterogeneous distribution (Azevedo *et al.* 2009, Herculano-Houzel 2009). To achieve such numbers, tightly regulated molecular and cellular processes take place, starting from early stages in embryonic development until adulthood. In the ectoderm, undifferentiated cells are recruited to give rise to neural stem cells. Once in the neural plate, they acquire their identity and begin the first steps of differentiation to neuronal and glial lineages. A coordinated spatial and temporal regulation of gene expression takes place along with extensive cell proliferation. The default mode of neural induction proposes that, in the embryonic ectoderm cells adopt a neural fate as a result of inhibition of the bone morphogenic protein (BMP) (Kandel *et al.* 2000, Munoz-Sanjuan *et al.* 2002). The balance between self-renewal and differentiation allows neural stem cells to either remain in a multipotent status or develop to neural progenitor cells and, ultimately, to a mature progeny. Notch signalling is highly involved in controlling the balance between expansion of neural stem cells/neural progenitor cells and neural differentiation, by blocking neuronal differentiation and maintaining neural stem cells in an undifferentiated state (Kandel *et al.* 2000).

After neuroectoderm induction, neurulation takes place to form the neural tube. Cellular diversity in the central nervous system (CNS) depends on spatial patterning cues, responsible for production of different types of neural progenitor cells. Early neural induction and spatial patterning involves the transcription factors orthodenticle homeobox 1 (OTX1), LIM homeobox 1 (LIM1) and forkhead box protein A2 (FoxA2), and specify anterior neural tissue. Further refinement of anterior/posterior patterning is regulated by gradients of Wnts, and Wnt antagonism. Patterning of the telencephalon occurs along the dorsal-ventral axis by dorsally produced fibroblast growth factor 8 (FGF8), BMPs, and Wnts and by a ventral gradient of sonic hedgehog (Kandel *et al.* 2000, Germain *et al.* 2010).

The output of neural stem cells overtime is a dynamic process in which these cells either commit to a neuronal or glial cell fate. In the developing neocortex, cortical laminar organization is dictated by radial migration of neuronal progeny. In the ventricular and subventricular zones, expansion of the progenitor pool starts with several rounds of

INTRODUCTION

symmetric division of the neural stem cells. Later on, a small percentage of these cells undergo asymmetric cell divisions to generate the early born neurons. With the progression of neurogenesis, these earlier born neurons differentiate to radial glia cells, progenitor cells with the dual role of serving as a migratory scaffold for neurons and as neuronal progenitors themselves. Later-born neurons migrate past the earlier-born neurons, migrating radially to the cortical plate and resulting in six distinct cortical layers formed in an inside-out fashion. The end of the neurogenic period dictates a switch from neurogenesis to gliogenesis. Following the formation of the cortical layers, the radial glia cells in the ventricular zone lose competence to produce neurons and acquire competence to produce glia, terminally differentiating to astrocytes. Oligodendroglia originate in the anterior entopeduncular area of the telencephalon and later migrate tangentially to populate the cortex. The cerebral cortex is comprised primarily of glutamatergic projection neurons, originating from dorsal telencephalic progenitors, and of GABAergic interneurons of ventral origin that migrate tangentially from the ganglionic eminences into the cortical plate. Upon arriving to the cortical plate, both neuronal populations are instructed to stop migrating and proceed with differentiation, forming and extending dendrites and establishing synaptic connections (Schuurmans *et al.* 2002, Molyneaux *et al.* 2007, Germain *et al.* 2010, Kohwi *et al.* 2013, Silbereis *et al.* 2016).

In the cortex, glutamatergic and GABAergic neurons are responsible for information processing, with excitatory and inhibitory synaptic inputs being tightly coupled. In fact, interneurons inhibit glutamatergic cells and are excited by them. Excitatory glutamatergic signalling is mediated by a series of glutamate receptors, grouped in two main categories: the ionotropic or metabotropic receptors. The α -amino-3-hydroxy-5-methyl-4-isoxazolepropionic acid (AMPA), kainate (KA) and N-methyl-D-aspartate (NMDA) receptors represent the three main subtypes of ionotropic receptors. Inhibitory GABAergic signalling, triggered by γ -aminobutyric acid (GABA) is associated with type A GABA ionotropic receptors (GABA_AR) and the type B GABA metabotropic receptors (GABA_BR). Cortical transmission is largely mediated by ionotropic neurotransmitter receptors. Glutamate elicits excitation via the activation of AMPAR and NMDAR, while GABA evokes inhibition via GABA_AR (Kandel *et al.* 2000, Isaacson *et al.* 2011). Inhibition is somehow proportional to the excitation produced, resulting in a relatively constant excitation/inhibition (E/I) ratio that controls neural excitability. At the network level, balanced inhibition allows a progressive recruitment of firing neurons and prevents epileptiform discharges and excitotoxicity. Disruption of the E/I balance might impair brain function, and possibly contribute to neurological disorders such as autism and schizophrenia (Tao *et al.* 2014).

NMDA receptors

NMDA receptors (NMDAR) are ionotropic glutamate-gated ion channels, assembled as heteromers in a tetrameric conformation, which are essential mediators of brain plasticity (Sheng *et al.* 1994, Paoletti *et al.* 2013). Their molecular composition is variable and usually associates two copies of the obligatory GluN1 subunit with two GluN2 subunits or a mixture of GluN2 and GluN3 subunits, resulting in different biophysical and pharmacological properties (Mayer 2011). Sequence homology within the seven subunits divides them into three subfamilies: GluN1 subunit, GluN2 subunits (GluN2A, GluN2B, GluN2C and GluN2D) and GluN3 subunits (GluN3A and GluN3B) (Paoletti 2011, Paoletti *et al.* 2013). Alternative splicing increases GluN1 variability and together with receptor subunit composition influences receptor properties such as ion conductance, affinity to agonistic agents and sensitivity to allosteric modulation, receptor desensitization characteristics and association with intracellular signalling molecules. Post-translational modifications influencing receptor function include glycosylation, palmitoylation, S-nitrosylation and phosphorylation (Paoletti *et al.* 2013, Lussier *et al.* 2015, Hogan-Cann *et al.* 2016, Iacobucci *et al.* 2017).

Each NMDAR subunit comprises four elements spanning the extracellular, transmembrane and intracellular regions (Figure 1). NMDAR extracellular epitopes sense diffusible ligands such as glutamate, glycine, H^+ , Zn^{2+} and respond by gating a Ca^{2+} -rich cationic current. Flow of Na^+ , K^+ and Ca^{2+} depends on the controlled gating of the transmembrane pore (Paoletti *et al.* 2013).

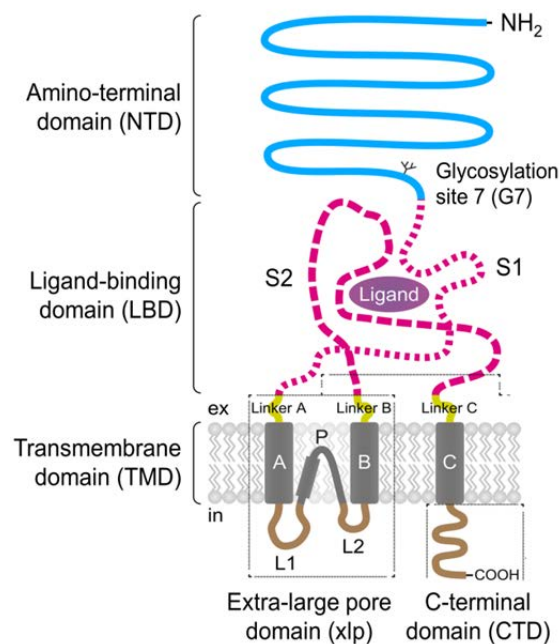


Figure 1. Structure of the GluN1 subunit of NMDAR. The extracellular amino-terminal domain (NTD) participates in allosteric regulation and subunit assembly; the ligand-binding domain (LBD; consisting of the S1 and S2 segments) is the binding site for glycine in GluN1 and glutamate in GluN2 or D-serine in GluN3 subunits. Three transmembrane helices (A, B and C) and a pore loop that contains the ion channel constitute the

INTRODUCTION

transmembrane domain (TMD). Finally, the intracellular carboxy-terminal domain (CTD) is involved in receptor trafficking, anchoring, and binding to downstream signalling molecules (Furukawa *et al.* 2005, Gielen *et al.* 2009, Mayer 2011, Paoletti 2011, Paoletti *et al.* 2013).

NMDAR activity is required for synaptogenesis, experience-dependent synaptic remodelling and long-term potentiation and depression (Lau *et al.* 2007, Paoletti *et al.* 2013). NMDAR subunit composition and number are not static. Different receptor subtypes coexist in the CNS depending on the developmental stage, cellular type, sub-cellular location and neuronal activity (Lau *et al.* 2007). Typically, they are found in the post-synapse in a di-heteromeric GluN1/GluN2A or tri-heteromeric GluN1/GluN2A/GluN2B conformation (Lau *et al.* 2007, Iacobucci *et al.* 2017). Peri-synaptic and extra-synaptic sites are enriched in GluN2B-containing receptors while at the synapse the GluN1/GluN2A conformation is more frequent. Enrichment in GluN1/GluN2A occurs upon a postnatal developmental switch in synaptic NMDAR phenotype from GluN2B to GluN2A (Lau *et al.* 2007, Gladding *et al.* 2011, Paoletti *et al.* 2013). Receptor number at the synapses is regulated by neuronal activity. While blocking neuronal activity promotes alternative ribonucleic acid (RNA) splicing and export of NMDAR from the endoplasmic reticulum to the synapse, receptor internalization and degradation through the ubiquitin–proteasome system is driven by chronic activity (Lau *et al.* 2007, Horak *et al.* 2014).

The presence of NMDAR and glutamate signalling goes beyond the CNS. NMDAR are expressed across a wide range of non-neuronal cells and tissues, including glial and endothelial cells, kidney, bone, pancreas, among others. Physiological tasks attributed to these non-neuronal receptors include bone deposition, wound healing, inhibition of insulin secretion, blood brain barrier (BBB) integrity and activity-dependent myelination (Skerry *et al.* 2001, Hogan-Cann *et al.* 2016).

NMDAR dysfunction is linked to synaptic defects and ultimately neurological and psychiatric conditions. Altered subunit expression, trafficking, localization or activity might underlie several phenotypes. These include neurodegenerative conditions such as Parkinson's and Alzheimer's disease in which glutamate toxicity contributes to neuronal loss (Mehta *et al.* 2013). Associated neuropsychiatric conditions include schizophrenia, anti-NMDAR encephalitis and autism spectrum disorders in which altered glutamate signalling due to either reduced or enhanced NMDAR function is implicated (Paoletti *et al.* 2013).

The blood brain barrier

The BBB is a dynamic interface between the CNS and the blood. Together with the blood-cerebrospinal fluid (CSF) barrier, the blood-retinal barrier, the blood-nerve barrier and the blood-labyrinth barrier, the BBB exerts a bi-directional control of the molecular and cellular trafficking into the brain (Blanchette *et al.* 2015).

The development of the BBB starts with the vascularization of the neuroepithelium via sprouting angiogenesis and consequent invasion of the neural epithelium by endothelial progenitor cells and pericytes in a later stage (Hellstrom *et al.* 1999, Stenman *et al.* 2008, Engelhardt *et al.* 2014). The brain endothelial cells interact with neural, vascular and immune cells to regulate its permeability via intra and intercellular events (Neuwelt *et al.* 2008, Ransohoff 2009, Neuwelt *et al.* 2011). The extracellular matrix, located at the abluminal endothelial surface acts as central scaffold, linking different cells and molecules of the BBB and providing a physical barrier for leukocyte migration (Correale *et al.* 2009, Blanchette *et al.* 2015).

The maintenance of the BBB properties involves the interaction of brain endothelial cells with different cell types and environmental cues. On the luminal side, a paracellular barrier is created via tight junctions to seal the space between adjacent brain endothelial cells and prevent unspecific influx of ions and small charged molecules from the blood stream (Huber *et al.* 2001, Blanchette *et al.* 2015). The assembly of tight junctions requires the transmembrane proteins occludin, claudin and junctional adhesion molecules. On the abluminal side, astrocyte-derived signals regulate the BBB phenotype by preventing immune cell infiltration and sealing the paracellular space (sonic hedgehog) (Alvarez *et al.* 2011); decreasing vascular permeability (angiopoietin) (Lee *et al.* 2003); and regulating tight junction integrity (angiotensin and Apolipoprotein E; ApoE) (Wosik *et al.* 2007, Bell *et al.* 2012). ApoE immunoreactivity in the brain is evident in astrocytic end-feet (Boyles *et al.* 1985) (Figure 2A). There, it regulates tight junction integrity through the activation of protein kinase C and phosphorylation of occludin (Nishitsuji *et al.* 2011). In fact, *ApoE*^{-/-} mice display extravasation of serum immunoglobulin G (IgG) in the cerebellum and discrete cortical and subcortical areas such as the hippocampus (Fullerton *et al.* 2001).

Homeostasis in the brain is kept by specific transport systems and enzymes in the BBB. While drug and nutrient-metabolizing enzymes process neuroactive blood-borne compounds, specific transport systems in the plasma membrane of brain endothelial cells allow the passage of nutrients and water-soluble compounds (Correale *et al.* 2009). This balance can be altered by inflammatory cytokines, hormones and drugs (Blanchette *et al.* 2015). During neuroinflammation, inflammatory cytokines in the CNS or blood, as interleukin-1 β (IL-1 β), tumour necrosis factor α (TNF- α), CC-chemokine ligand 2 (CCL-2), and interleukin-17A (IL-

INTRODUCTION

17A), modulate the BBB permeability by degrading tight junction proteins, modifying their phosphorylation status or affecting their turnover rate (Argaw *et al.* 2006, Stamatovic *et al.* 2009, Marchiando *et al.* 2010). Breakdown of the BBB allows a free flow of blood-derived components and neurotoxic proteins that can accumulate in the CNS and lead to neuronal toxicity and progressive neurodegeneration (Winkler 2012; Montagne 2015). Additionally, influx of immunoglobulins (Ig) through the brain can occur via modulation of barrier properties due to brain endothelial cells activation or by transfer of antibodies in the absence of brain endothelial cell activation. Efflux to the circulation of up taken antibodies is mediated by neonatal Fc receptors, present in brain endothelial cells which actively transport immunoglobulins out of the brain (Figure 2B) (Zhang *et al.* 2001). Additionally, the BBB is not a homogenous structure. There is a differential distribution of the receptors for the modulating molecules of BBB permeability that, ultimately, can mediate different effects of the same circulating Ig on brain function by determining its primary entry site (Brimberg *et al.* 2015).

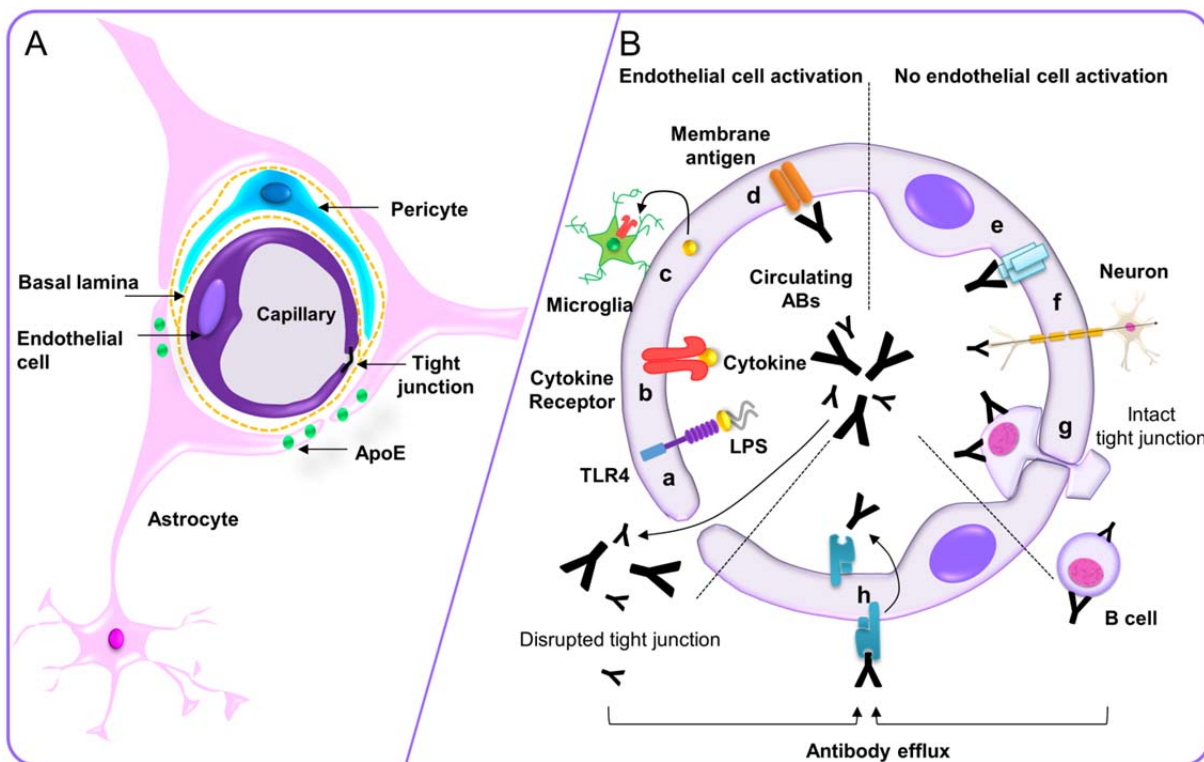


Figure 2. BBB and Ig access to the brain parenchyma. (A) Basic cellular composition of the BBB. **(B)** Mechanisms of Ig influx to the brain: via endothelial cell activation due to interaction of pro-inflammatory molecules with Toll-like receptor 4 (TLR4) **(a)** or cytokine receptors **(b)**; transcellular-dependent mechanisms can transport cytokines and chemokines through the BBB and activate CNS immune cells **(c)** or by direct binding of circulating antibodies **(d)**. Transfer of antibodies in the absence of endothelial cell activation can occur by receptor-mediated endocytosis **(e)**, retrograde axonal transport by neurons protruding towards the lumen of BBB capillaries **(f)** or by transendothelial migration of B cells **(g)**. Neonatal Fc receptors present in endothelial cells mediate efflux of Ig back to the circulation **(h)** (Fabian *et al.* 1987, Roth *et al.* 2004, Ge *et al.* 2008, Diamond *et al.* 2009). ApoE: apolipoprotein E; LPS; lipopolysaccharide; ABs: autoantibodies; Fc: Fragment crystallisable.

Synergies between nervous and immune systems

Both the CNS and the immune system are self-organizing: they start with genetically encoded primary instructions, to which information retrieved from environmental cues is added to develop individualized systems. Once seen as two unrelated systems, the bi-directional interaction between brain and immune molecules has been challenging this view.

Two major classes of immune effector molecules – cytokines and antibodies – have been linked to brain development and function (Boulanger 2009, Deverman *et al.* 2009, Brimberg *et al.* 2015). The BMPs, belonging to the transforming growth factor β (TGF- β) cytokine superfamily, regulate induction of the neuroepithelium and signalling via the gp130 cytokine family maintains the radial glia cells pool by promoting its self-renewal during embryogenesis (Hatta *et al.* 2002, Munoz-Sanjuan *et al.* 2002). Also chemokines, small cytokines with chemoattractant properties, are implicated in migration, proliferation and differentiation of neurons and glia. The stromal cell-derived factor 1 (SDF-1) chemokine and its receptor C-X-C chemokine receptor type 4 (CXCR4) regulate cell proliferation and migration in the brain (Lu *et al.* 2002, Stumm *et al.* 2003).

Microglia, the resident macrophage-like cells in the brain are responsible for immune surveillance, responding to infection and injury by secreting a large repertoire of cytokines and chemokines. They scan the brain parenchyma making transient contacts with synapses (Wake *et al.* 2009). During embryogenesis, microglia promotes astrocyte proliferation by secreting IL-1 and regulates developmental apoptosis and synaptogenesis by secreting TNF- α (Giulian *et al.* 1988, Deverman *et al.* 2009). Immature astrocytes induce the expression of the complement cascade protein C1q on retinogeniculate neurons. The complement system, besides their opsonizing functions plays a role in synaptic elimination. Indeed, C1q and C3 complement components localize at the synapses and tag unwanted synapses for elimination by microglia during synaptic pruning (Stevens *et al.* 2007, Schafer *et al.* 2012). The class I major histocompatibility complex (MHC) engages antigen presentation to T cells during adaptive immune responses. In the brain it modulates plasticity in the hippocampus and participates in synapse refinement processes (Huh *et al.* 2000, Bhat *et al.* 2009, Lee *et al.* 2014). Antibodies targeting brain proteins also impact brain function and homeostasis, and the effects of brain exposure will be discussed later in the “*Neurological diseases driven by autoimmunity*” section of the introduction.

The crosstalk between the nervous and immune systems is not unidirectional and CNS molecules also interact with immune cells in the periphery. Of particular interest is the role of neurotransmitter signalling in immune cells. In the CNS, GABA is the major neurotransmitter involved in inhibitory processes. Additionally, immune cells like macrophages, T cells and antigen presenting cells (APC) express functional GABA_AR. GABA synthesis by

INTRODUCTION

macrophages, dendritic cells and T cells has immunoinhibitory effects as downregulation of CD4⁺ T cell-mediated autoimmune processes (Tian *et al.* 2004, Bhat *et al.* 2010, Dionisio *et al.* 2011). In dendritic cells, GABAergic signalling potentiates chemotactic responses by promoting hypermotility (Fuks *et al.* 2012, Barragan *et al.* 2015).

Glutamate is another player in neurotransmitter-driven immunomodulation extending its role beyond excitatory processes in the brain. After maturation in the thymus, resting T cells express several metabotropic glutamate receptors (mGluR): mGlu2/3R, mGlu5R, mGlu8R and ionotropic receptors like NMDAR, AMPAR and KA receptors. Dendritic cells undergoing maturation and in contact with T cells release glutamate to prevent T cell activation (Levite 2008). T cells initially uptake glutamate via the constitutively expressed mGluR5. Upon antigen presentation by dendritic cells and T cell activation, mGluR1 are expressed for glutamate uptake and attenuate the mGluR5-triggered effects, mediating enhanced T cell proliferation and secretion of pro-inflammatory cytokines (Levite 2008). Hence, during cross talk between dendritic and T cells, glutamate signalling appears to control the proliferation of T cells depending on which receptor is involved on its uptake (Pacheco *et al.* 2006, Pacheco *et al.* 2007). Additionally, T cell responses seem to be modulated by glutamate signalling via NMDAR upregulation upon CD4⁺ T cell activation. T helper 1 *versus* T helper 2 cell functions such as proliferation, cytokine production and cell survival seem to be differentially affected by NMDAR signalling. *In vitro*, pharmacological stimulation of NMDAR results in reduced T helper 1-like cytokine production and unaltered T helper 2-like or IL-10 responses, most probably due to susceptibility of T helper 1 cells to NMDAR-dependent physiological cell death (Orihara *et al.* 2018). However, a direct link between glutamate and NMDAR signalling in immune cells has not been established yet.

Innate and adaptive immunity

Down the road of (auto)immunity there are two ways to go: the innate or the adaptive one (Figure 3). When a prompt response to danger is required, innate immunity takes place and immune events are driven by transmembrane receptors like Toll-like receptors, cytokine and chemokine receptors or fragment crystallisable (Fc) receptors (Figure 3A) (Alberts *et al.* 2002, Church *et al.* 2008, Bhat *et al.* 2009). On the other side, adaptive immunity involves antigen-specific T cells and an orchestrated antibody response by B cells to antigen-driven stimulation (Figure 3B). In the core of adaptive immune responses is the production of high affinity antibodies able to recognize virtually any antigen due to somatic hypermutation events of Ig genes (Bhat *et al.* 2009). Both innate and adaptive immunity can be involved in autoimmune events. While innate-related autoimmunity events are mainly associated with the inflammasome in adaptive-related autoimmunity, involvement of immune cells as

macrophages, T and B cells as well as production of antibodies recognizing self-antigens and activation of the complement system are possible (Church *et al.* 2008).

Antibody production is the result of the combined activity of innate and adaptive immunity. In fact, immunostimulants, secreted during innate responses can promote inflammation and trigger adaptive immune responses in which macrophages and dendritic cells can engage in antigen presentation to naïve T cells (Alberts *et al.* 2002). T cell receptors (TCR) recognize both peptide segments of antigenic proteins and fragments of the antigen-bound MHC on the surface of APCs (Figure 3B). If on one side naïve T cells interact with dendritic cells during its activation, B cells require stimulation via activated T helper cells (Alberts *et al.* 2002). In the germinal centres of the lymph nodes activated B cells can differentiate to plasma cells or memory B cells. Differentiation of B cells into antibody-synthesizing plasma cells allows mass production and secretion of specific antibodies. Post-proliferative plasma cells usually secrete IgM, IgG or IgA antibodies with moderate affinity. Further cycles of B cell proliferation, somatic hypermutation and affinity purification leads to differentiation to plasma cells able to secrete antibodies with increased affinity. Additionally, memory B cells can be re-stimulated during a second encounter with the antigen and engage secondary antibody responses (Janeway *et al.* 2001).

Antigen recognition leads to lymphocyte activation and clonal expansion, producing clones of lymphocytes carrying the same antigen-specific receptor (Rose 2015). Mechanisms of tolerance to self-antigens must take place to prevent severe autoimmune reactions. Immunological tolerance is acquired by clonal deletion and inactivation of developing lymphocytes. Thus, the mature lymphocyte repertoire is shaped by negative and positive selection. Self-tolerance is granted by elimination or neutralization of lymphocytes with strongly self-reactive receptors during negative selection. Positive selection identifies and preserves lymphocytes fit to respond to foreign antigens (Janeway *et al.* 2001).

Immunoglobulin diversification

Immunoglobulins are Y-shaped molecules presenting two distinct regions: the variable (V) region that controls the specificity to bind to the antigen and the constant (C) region that determines how the antigen is eliminated, upon binding by recruiting cells and immune molecules to destroy the antigen source via phagocytosis or the complement system (Figure 3C). Membrane bound Ig on B cell surface, serve as cell receptor (BCR) for the antigen and have no effector functions. Its V regions, exposed on the cell surface, recognize and bind to antigens in order to activate B cells, promote clonal expansion and the production of specific antibodies (Janeway *et al.* 2001).

INTRODUCTION

In early stages of B cell development, the primary antibody repertoire is created by assembly of exons encoding the antigen-binding variable regions of Ig heavy and light chains (Hwang *et al.* 2015). Diversification of Ig genes in mature B cells can occur via two deoxyribonucleic acid (DNA) modifying mechanisms: somatic hypermutation and class switch recombination (Kracker *et al.* 2011). Somatic hypermutation takes place in the germinal centres and enables the selection of antibodies with increased antigen affinity by introducing point mutations in the exons of Ig heavy and light chains (Rajewsky 1996). This stochastic process generates an extensive repertoire of immunoglobulins able to recognize virtually any antigen. To produce high affinity antibodies antigen-activated B cells undergo affinity maturation processes, including multiple rounds of somatic hypermutation and selection of clones with high antigen affinity followed by clonal expansion (Hwang *et al.* 2015). Class switch recombination modulates antibody's effector function. Immature B cells express mainly IgM and, upon antigen stimulation and interaction with T cells in the periphery they proliferate, differentiate and acquire the ability to produce antibodies of other isotypes. During class switch recombination events, the coding exons of the C region, within the *IgH* gene, are replaced by DNA recombination between switch (S) region DNA segments, while the binding specificity (V region) of the BCR is maintained (Selsing 2006, Kracker *et al.* 2011).

In mammals there are five isotypes of antibodies: IgA, IgD, IgE, IgG, and IgM (Lefranc *et al.* 2001). In the bone marrow, the first isotype produced by a developing B cell is IgM, to be inserted in the plasma membrane as the BCR of immature naïve B cells. Upon migration to peripheral lymphoid organs, these cells start to express IgD at their surface evolving to mature naïve B cells responsive to foreign antigens. IgM is the major isotype secreted into the bloodstream upon first exposure to the antigen. In its secreted form, IgM is a pentameric molecule with a total of ten antigen-binding sites and the ability to activate the complement system, while IgD seem to function mostly as cell-surface receptors. IgG is a monomer heavily produced during secondary immune responses and the main isotype present in the blood. Besides activating the complement system, its Fc region can signal to phagocytic cells via Fc receptors present in macrophages and neutrophils and, ultimately, trigger phagocytosis. IgA is the main antibody isotype in body fluids. Present in the blood as a monomer, it acquires a dimeric conformation, when present in secretions, thought to be protective against the proteolytic action of enzymes. IgE molecules are monomers that serve as cell-surface receptors for antigen in mast cells and basophils. After being secreted, IgE bind to Fc receptors in mast cells and, upon binding to an antigen, it signals the mast cell to release histamine (Janeway *et al.* 2001, Lefranc *et al.* 2001, Alberts *et al.* 2002).

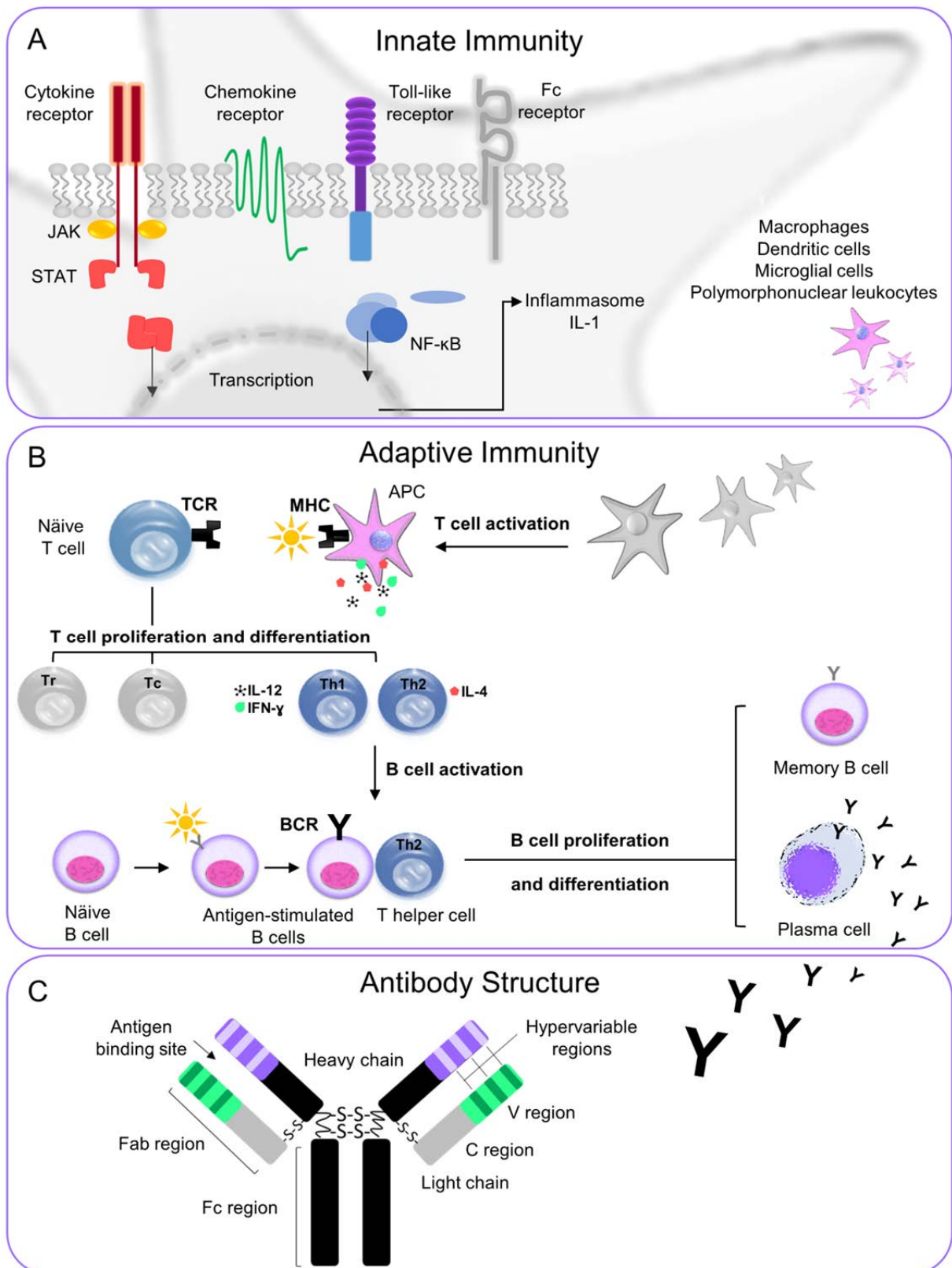


Figure 3. Innate and adaptive immunity. (A) Innate responses are mediated by recognition of foreign molecules by transmembrane receptors located in antigen presenting cells (APCs). Stimulation of these receptors activates intracellular signalling pathways as Janus kinase/Signal Transducer and Activator of Transcription (JAK/STAT) or nuclear factor kappa B (NF-κB) that culminate in triggering the inflammasome and its major player interleukin 1 (IL-1). **(B)** Adaptive responses rely partially in pre-existing elements of innate immunity for T cell activation. Näive T cells are able to bind to antigen-MHC complexes via its T cell receptor (TCR) and engage proliferation and

INTRODUCTION

differentiation to effector cells as regulatory (Tr), cytotoxic (Tc) and helper (Th) T cells. APCs secrete cytokines that influence the functional differentiation of T cells. CD4⁺ T cells differentiate to Th1 in the presence of IL-12 and IFN- γ , while secretion of IL-4 promotes Th2 differentiation. This has a direct impact on the outcome of the immune response as Th1 preferentially activate macrophages and Th2 activate B cells. Upon activation by Th2 cells in the germinal centres, antigen-stimulated B cells undergo proliferation and differentiation events that culminate in high affinity antibody production by plasma cells and acquisition of immunological memory. **(C)** Antibody structure. Four polypeptide chains: two identical light (L) chains and two identical heavy (H) chains connected by a combination of noncovalent and covalent disulphide bonds (Alberts *et al.* 2002). IFN- γ : interferon gamma; MHC: major histocompatibility complex; Fc: fragment crystallisable region; Fab: antibody-binding fragment.

Autoimmunity – a case of molecular misunderstanding?

An autoimmune condition occurs when a specific adaptive immune response develops against a self-antigen, leading to chronic inflammatory tissue damage. As in a protective immune response, self-antigen triggered T cytotoxic cell responses and activation of macrophages by T helper 1 can cause tissue damage, whereas inappropriate T helper 2-mediated activation of self-reactive B cells can initiate detrimental autoantibody responses. Although the T and B cell repertoire are purged of most self-antigen high-affinity receptors by clonal deletion, they still include low-affinity self-reactive receptors. Transient autoimmune responses are common and pathological status arises only when they are sustained and a cause of tissue damage. Susceptibility to autoimmune disease has been most consistently associated with human leukocyte antigen (*HLA*) gene complex. The T cell response to an antigen depends on the *HLA* haplotype. Being so, susceptibility to autoimmunity can be determined by different levels of efficacy of *MHC* variants, coded by the *HLA* complex, in presenting autoantigenic peptides to autoreactive T cells. Additionally, during the selection of the TCR repertoire, self-antigens associated with certain *MHC* variants might induce positive selection of cells bearing TCRs specific for these self-antigens. A scenario only possible if these self-antigens are expressed at low levels or bind too poorly to self-MHC molecules and do not trigger negative selection events (Janeway *et al.* 2001).

Autoimmune responses can be initiated by molecular mimicry events during immune responses to foreign antigens, possibly due to sequence homology between human and the pathogen peptides. According to the molecular mimicry hypothesis, autoreactive T cells and autoantibodies are initially directed to microbial antigens and further react with similar self-antigens (Fujinami *et al.* 1985, Ang *et al.* 2004, Atassi *et al.* 2008). Immunological cross-reactivity can occur due: (i) to homology between amino acid sequences, (ii) recognition of non-homologous peptide sequences by a single BCR or TCR due to their high level of degeneracy, (iii) variability in antigen recognition by T cells during antigen presentation by influence of *HLA* haplotypes and (iv) recognition of structural similarity in complex molecular

structures by immunological receptors, that might include double-stranded DNA molecules or glycolipids for example (Fujinami *et al.* 1985, Mason 1998, Ang *et al.* 2004). Being so, one can define molecular mimicry as a dual recognition of self and non-self-peptides by a single BCR or TCR, in which cross-reactive antibodies and T cells can engage autoimmune events (Ang *et al.* 2004). A role for molecular mimicry has been proposed in some immune-mediated diseases including acute rheumatic fever (Group A *streptococci*), Chagas' disease (*Trypanosoma cruzi*) and Guillain–Barre' syndrome (*Campylobacter jejuni*) as examples (Ang *et al.* 2004, Sheikh *et al.* 2004, Teixeira *et al.* 2011, Cunningham 2012).

Neurological diseases driven by autoimmunity

In several autoimmune conditions, the presence of autoantibodies can be a direct cause of the disease as it happens in systemic lupus erythematosus, myasthenia gravis and Rasmussen encephalitis or it can contribute to the severity of the disease as in rheumatoid arthritis. When it comes to autoimmune responses to brain antigens, autoantibodies can induce brain damage and likely initiate or worsen multiple neurologic conditions (Brimberg *et al.* 2013, Mader *et al.* 2017). Their contribution to brain pathology is dependent on BBB function that usually prevents their access to the brain (Hammer *et al.* 2014, Platt *et al.* 2017). Brain-reactive autoantibodies can target neuronal or non-neuronal antigens. In neuropsychiatric systemic lupus erythematosus, autoantibodies targeting double stranded DNA molecules, can cross react with the GluN2A and GluN2B subunits of the NMDAR and induce excitotoxic neuronal death due to prolonged channel opening time and exacerbated calcium influx (DeGiorgio *et al.* 2001, Faust *et al.* 2010). In neuromyelitis optica autoantibodies target the astrocytic aquaporin 4 water channel present in astrocytic endfeet, resulting in astrocyte loss and demyelination (Lennon *et al.* 2004).

In utero exposure to certain brain-reactive autoantibodies can lead to neurodevelopmental changes in the fetal brain. Contactin-associated protein 2 (CASPR2) autoantibodies, isolated from seropositive mothers of autistic children, when injected to female mice lead to neuronal abnormalities and an autistic-like phenotype in their male offspring upon *in utero* exposure. These include abnormal cortical development, decreased dendritic complexity of excitatory neurons and reduced numbers of inhibitory neurons in the hippocampus, as well as impairments in sociability, flexible learning and repetitive behaviour (Brimberg *et al.* 2013, Brimberg *et al.* 2016).

Two outcomes are possible upon entry of brain-reactive autoantibodies in the brain. Remission of the neuropsychiatric symptoms can be achieved by removal of the autoantibodies, as it is the case in limbic encephalitis, associated predominantly with antibodies targeting the leucine-rich glioma inactivated protein 1 (LGI1) (Mader *et al.* 2017).

INTRODUCTION

Alternatively, exposure to brain-reactive autoantibodies might have persistent effects by triggering irreversible mechanisms that cannot be reverted by autoantibodies elimination. In neuropsychiatric systemic lupus erythematosus patients, acute exposure to GluN2A/GluN2B autoantibodies leads to neuronal apoptosis and chronic damage of surviving neurons mediated by microglia-dependent synaptic loss persistent upon autoantibodies removal (DeGiorgio *et al.* 2001, Faust *et al.* 2010, Bialas *et al.* 2017).

Rasmussen's encephalitis was one of the first autoimmune conditions to be associated with neuronal surface autoantibodies targeting the glutamate system (Rogers *et al.* 1994). Since the identification of the pathogenic role of GluR3 autoantibodies in this condition, several other CNS disorders have been related to autoimmune processes targeting ion channel and synaptic proteins in the brain (Table 1). Of those, anti-NMDAR encephalitis was one of the first synaptic autoimmune encephalitides to be characterized at the molecular level (Dalmau *et al.* 2007).

Table 1. Antibodies targeting neuronal or synaptic proteins and associated disorders.

Target	Antibody effects	Associated disorder	Phenotype
GluN1	Endocytosis of NMDAR in neurons with disruption of epitope function	Anti-NMDAR encephalitis	Psychosis, seizures, dyskinesia
AMPA	Endocytosis of AMPAR in neurons	Limbic encephalitis	Memory loss, confusion
mGluR1	Blockade of induction of long-term depression in Purkinje cells Reduction of AMPAR clusters at the synapse	Cerebellar ataxia, limbic encephalitis	Reduction of basal activity of Purkinje cells
mGluR5	Unknown	Limbic encephalitis, Ophelia syndrome	Memory loss, confusion
GABA_AR	Reduction of GABA _A R at the synapse and extrasynaptic sites	Encephalitis	Seizures
GABA_BR	Unknown	Limbic encephalitis	Memory loss, seizures
GlyRα1	Endocytosis of GlyR α 1 in HEK cells	PERM	Muscle rigidity, spasms
D2R	Unknown	Basal ganglia encephalitis, Tourette syndrome	Parkinsonism
Neurexin3α	Decreased expression of Neurexin3 α on synapses and decreased synapse formation	Encephalitis	Seizures, confusion
CASPR2	Alteration of gephyrin clusters in inhibitory synapses	Morvan syndrome, limbic encephalitis	Memory loss, sleep disorder, neuromyotonia
LG11	Inhibition of interaction with ADAM22; Decrease of postsynaptic AMPAR with disruption of epitope function	Limbic encephalitis	Memory loss, seizures
Amphiphysin	Disruption of vesicle endocytosis in neurons	Stiff-person encephalomyelitis	Rigidity, spasms, confusion, memory loss
IgLON5	Decrease of cell surface IgLON5 in neurons	Sleep disorder	Sleep apnea, brainstem dysfunction
DPPX	Hyperexcitability of enteric neurons	PERM, cerebellar ataxia, encephalitis	Hyperekplexia, diarrhoea and other GI symptoms

Notes: GluN1: glutamate ionotropic receptor NMDA type subunit 1; AMPAR: α -amino-3-hydroxy-5-methyl-4-isoxazolepropionic acid receptor; mGluR1/5: metabotropic glutamate receptor 1/5; GABA_AR: γ -aminobutyric acid type A receptor; GABA_BR: γ -aminobutyric acid type B receptor; GlyR α 1: glycine receptor α 1 subunit; D2R: dopamine D2 dopamine receptor; CASPR2: contactin-associated protein 2; LG11: leucine-rich glioma inactivated protein 1; IgLON5: immunoglobulin G superfamily member 5; DPPX: dipeptidyl aminopeptidase-like protein 6; NMDAR: N-methyl-D-aspartate receptor; HEK: human embryonic kidney; ADAM22: disintegrin and metalloproteinase domain-containing protein 22; PERM: progressive encephalitis with rigidity and myoclonus; GI: gastrointestinal (Diamond *et al.* 2013, Crisp *et al.* 2016, Dalmau 2016).

Anti-NMDAR encephalitis

Anti-NMDAR encephalitis patients develop psychosis, cognitive problems and seizures, and its clinical picture can progress to altered status of consciousness, dyskinesias and autonomic dysfunction (Dalmau *et al.* 2007). At the cellular level, binding of GluN1 autoantibodies (NMDAR-AB) leads to a reduction of NMDAR cluster density, mediated by direct disruption of the epitope upon binding, receptor internalization and degradation (Hughes *et al.* 2010, Gleichman *et al.* 2012). This decrease in NMDAR has been reported *in vitro* using mouse or rat hippocampal neurons exposed to CSF or IgG extracts of anti-NMDAR encephalitis patients or individuals with other conditions (Hughes *et al.* 2010, Hammer *et al.* 2014, Moscato *et al.* 2014). Additionally, surface and total GluN2A and GluN2B protein levels which assemble with GluN1 to form functional NMDARs, decrease upon exposure to patients autoantibodies (Hughes *et al.* 2010).

In the context of anti-NMDAR encephalitis, only IgG antibodies have been reported to bind to the extracellular NTD of the GluN1 subunit. The NTD domain includes seven *N*-linked consensus glycosylation sites (G1-G7); and glycosylation and deamidation of the G7 site contribute to epitope formation and recognition by NMDAR-AB (Gleichman *et al.* 2012). Exposure to patient-derived CSF prolongs the duration of NMDAR opening in HEK293 cells expressing GluN1-GluN2B, and induces reduction of long-term potentiation in acute hippocampal slices (Gleichman *et al.* 2012, Zhang *et al.* 2012, Jezequel *et al.* 2017). Moreover, injection of IgG or CSF into rodent brains leads to increased glutamate levels and excitability of the motor cortex (Manto *et al.* 2010, 2011). *In vitro*, NMDAR-AB have no binding preference to inhibitory or excitatory neurons (Moscato *et al.* 2014). Thus, in theory, the acute effects of antibody exposure, such as seizures might be due to a hyper-glutamatergic state and consequent increase in network excitability coupled with homeostatic changes in inhibitory neurotransmission (Crisp *et al.* 2016). Although NMDAR-AB do not induce compensatory changes in glutamate receptor gene expression upon receptor internalization *in vitro*, they cause a decrease in inhibitory synapse density onto excitatory hippocampal neurons. In fact, a reduction on GABA_AR cluster density has been observed in hippocampal neurons exposed to NMDAR-AB⁺ CSF with no change in GABA_AR-mediated miniature inhibitory postsynaptic currents (Moscato *et al.* 2014).

Studies using patient serum or CSF report a strong binding of NMDAR-AB to the hippocampal region, with no evidence of neuronal loss as consequence (Dalmau *et al.* 2008, Hughes *et al.* 2010). In the hippocampus, the binding pattern of patient's NMDAR-AB is dependent on NMDAR density, with higher intensities observed in proximal dendrites of the dentate gyrus (Hughes *et al.* 2010). In line with the pivotal role of NMDAR signalling in mediating synaptic plasticity in the hippocampus, long term effects in anti-NMDAR

encephalitis patients include deficits in executive function and memory (Finke *et al.* 2012, Planaguma *et al.* 2015).

Presence of NMDAR-AB has been associated with contact with influenza A and B, CNS herpes simplex virus infection, a diagnosis of ovarian teratoma, and a genome-wide significant marker (rs524991) in the proximity of nuclear factor I A (*NFIA*) gene, a transcription factor that mediates neuroprotection upon NMDAR activation (Dalmau *et al.* 2007, Zheng *et al.* 2010, Pruss *et al.* 2012, Armangue *et al.* 2014, Hammer *et al.* 2014, Pruss *et al.* 2015). Regardless of the triggering events leading to autoantibody production, NMDAR-AB seem to be generated in secondary lymphoid organs and potentially gain access to the CNS upon BBB disruption or via the choroid plexus. This hypothesis is supported by NMDAR-AB seropositivity in healthy individuals (Busse *et al.* 2014, Dahm *et al.* 2014). In the lymph nodes, antigen-presenting cells expose naïve B cells to NMDAR that differentiate into memory B cells and antibody-producing plasma cells. Plasma cell-secreted NMDAR-AB and circulating memory B cells can potentially access the brain. NMDAR-AB can exert their effects by direct contact with their target antigens and memory B cells can undergo re-stimulation, antigen-driven affinity maturation, clonal expansion, differentiation into antibody-producing plasma cells and ultimately engage intrathecal production of NMDAR-AB (Moscato *et al.* 2014, Dalmau 2016).

Post mortem or biopsy histopathological studies of anti-NMDAR encephalitis patients revealed that complement-mediated cell death mechanisms are not related with the pathogenesis of the disease. NMDAR-AB (IgG1) are able to fix complement *in vitro*, however, no evidence of complement deposition and only residual neuronal and glial cell death has been reported (Martinez-Hernandez *et al.* 2011, Bien *et al.* 2012). Overall, there is a low density of inflammatory cells in the parenchyma with the majority of them locating in perivascular and Virchow-Robin spaces. In fact, B and T cell lymphocytic perivascular cuffing along with the presence of antibody secreting plasma cells or plasmablasts (CD138⁺) and microglial activation are the main histopathological findings reported thus far (Camdessanche *et al.* 2011, Martinez-Hernandez *et al.* 2011, Bien *et al.* 2012). The presence of CD138⁺ cells in the parenchyma supports additional intrathecal synthesis of NMDAR-AB and the fact that memory B cells can migrate to the brain, cross the BBB and differentiate to antibody secreting plasma cells. Both mouse and human studies have reported immunoglobulin deposition in the brain upon exposure to NMDAR-AB (Martinez-Hernandez *et al.* 2011, Bien *et al.* 2012, Planaguma *et al.* 2015, Wright *et al.* 2015).

Scope of the present work

In the introduction of this thesis, the synergetic interaction between the nervous and immune systems and the potential pathological outcomes mediated by autoimmune processes targeting the brain was addressed, with a particular focus on autoantibodies targeting NMDAR in the context of anti-NMDAR encephalitis.

The first two projects were designed to understand the role of these autoantibodies beyond this pathological condition and gain insight to its effects upon access to the brain. Specifically, Project I aimed at (i) determining the functional properties of NMDAR-ABs of different isotypes; for this purpose a new assay employing human induced pluripotent stem cell-derived neurons was developed. (ii) Identifying which NMDAR epitopes are recognized by these autoantibodies. Project II focused on (i) determining if these NMDAR-AB are present and functional in other mammal species; (ii) assessing the protective role of the BBB and the effects of endogenously produced NMDAR-AB on the brain, in the presence of an open BBB.

Additionally, I have briefly mentioned that disruption of the balance between excitation and inhibition in the brain can contribute to brain diseases as autism and schizophrenia. The contributors for such disruption are not completely understood and might have a common ground between diseases. In Project III, we focused on dissecting the relationship between the severity of autistic traits in schizophrenic patients and imbalances in excitation and inhibition. Specifically, using transcranial magnetic stimulation (TMS), we aimed at determining if individuals with low severity of autistic traits and individuals with high severity of autistic traits would differ in terms of glutamatergic or GABAergic neurotransmission.

2. ESTABLISHING A CELL CULTURE SYSTEM FOR TRANSLATIONAL STUDIES

2. ESTABLISHING A CELL CULTURE SYSTEM FOR TRANSLATIONAL STUDIES

To address the aims of the projects aforementioned, with a particular focus on the translational potential of project I and II, a new methodology was implemented. The generation of induced pluripotent stem cell (IPS)-derived neurons from human fibroblasts has been previously described (Shi *et al.* 2012). To implement this method, different molecular biology techniques were applied in a workflow that comprised reprogramming of fibroblasts to pluripotent stem cells, several steps of quality control of pluripotency, induction of neuronal differentiation and assessment of neuronal maturity and activity (Figure 4). Here, it will be briefly described how this was achieved, and examples of applications of this tool will be addressed in Projects I and II.

Resorting to the Göttingen Research Association for Schizophrenia (GRAS) sample collection, fibroblasts were obtained from five different individuals, complying with Helsinki Declaration, and approved by the Ethics Committees of Georg-August-University, Göttingen. All subjects provided written informed consent.

To achieve pluripotency, fibroblasts were reprogrammed using either Sendai virus (SeV) or the STEMCCA excisable polycistronic lentiviral vector to overexpress the four reprogramming factors: the octamer-binding transcription factor 4 (OCT4), the Kruppel-like factor 4 (KLF4), the sex determining region Y-box 2 (SOX2), and the MYC proto-oncogene (c-MYC) (Figure 4A). These two reprogramming strategies differ essentially in their interaction with the host genome. The STEMCCA system requires the integration of the polycistronic vector into the host genome, under the promoter of the elongation factor 1 alpha (*EF1 α*) gene (Sommer *et al.* 2009, Sommer *et al.* 2010). In contrast, the SeV-based vector is a non-integrative system, in which the vectors containing the reprogramming factors replicate in the form of negative-sense single stranded RNA in the cytoplasm of infected cells (Fusaki *et al.* 2009). Different clones, produced using the two reprogramming strategies, were selected and further expanded for pluripotency assessment (Streckfuss-Bomeke *et al.* 2013). Our strategy included (i) detection of placental alkaline phosphatase expression; (ii) immunofluorescent detection of a panel of markers specific to human embryonic stem cell physiology and fundamental to maintain an undifferentiated state: OCT4, Nanog, SOX2, podocalyxin (Tra1-60), zinc finger CCHC domain-containing protein 1 (LIN28), and stage-specific embryonic antigen-4 (SSEA4); (iii) detection of pluripotency markers at the RNA level and its upregulation from patient fibroblasts to patient IPS using quantitative real time polymerase chain reaction (qPCR). Expression of nuclear (OCT4) and surface (Tra1-60) pluripotency markers was monitored regularly using flow cytometry to assess the pluripotency level overtime.

ESTABLISHING A CELL CULTURE SYSTEM FOR TRANSLATIONAL STUDIES

Neuronal conversion and differentiation was based on a dual SMAD inhibition protocol (Figure 4B) (Shi *et al.* 2012). Here, IPS cells are exposed to a neural induction medium complemented with SB431542 and dorsomorphin molecules. The synergistic action of these neural fate-inducing molecules selectively blocks the TGF- β and the BMP pathways, promoting differentiation towards the neuroectodermal lineage (Chambers *et al.* 2009, Zhou *et al.* 2010). Signalling through the nodal/activin branch of the TGF- β pathway induces mesodermal gene expression in ectodermal cells and activation of the BMP pathway leads to the acquisition of epidermal fates. Conversely, inhibition of both Activin/Nodal and BMP signalling, promotes neuroectoderm specification (Munoz-Sanjuan *et al.* 2002). Successful neural induction results in the formation of a homogeneous neuroepithelial sheet after ten days, with downregulation of pluripotency markers and upregulation of neural stem cell markers such as paired box 6 (PAX6), OTX1/2, Nestin, forkhead box G1 (FOXP1), empty spiracles homeobox 1 (EMX1) and SOX2. Dissociation of the neuroepithelial sheath leads to rearrangement of neural stem cells (SOX2⁺) in a rosette-like structure, further expanded by application of the mitogen fibroblast growth factor 2 (FGF2). Neuronal progenitors (doublecortin; DCX⁺) emerge from these structures during the neurogenesis period. A coordinated differentiation of these progenitors is promoted with the application of the small molecule N-[N-(3,5-Difluorophenacetyl)-L-alanyl]-S-phenylglycine t-butyl ester (DAPT), giving rise to neurons (positive for microtubule-associated protein 2; MAP2⁺). DAPT inhibits γ -secretase, necessary for canonical Notch signalling (Nelson *et al.* 2007). The Notch signalling pathway is critical for several aspects of neural development: it promotes the survival of neural stem and progenitor cells and newly generated neurons, helps progenitor cells to maintain their undifferentiated state throughout the neurogenic period and promotes the glial fate in multipotent progenitor cells (Mason *et al.* 2006, Yaron *et al.* 2006, Nelson *et al.* 2007). Thus, transient inhibition of Notch signalling using DAPT, leads to delayed G1/S-phase transition committing cells to neurogenesis and a synchronized differentiation of neural progenitors (Nelson *et al.* 2007, Borghese *et al.* 2010). Neuronal identity and maturation was confirmed by combining RNA expression and protein markers for DCX, β -Tubulin III, MAP2, NeuN, GluN1, CAMKII and Synapsin1 (Figure 4C). Functional analysis by calcium imaging coupled with field stimulation revealed both spontaneous and evoked activity (Figure 5).

This *in vitro* tool enabled us to add a translational aspect to several projects. Specifically, it allowed to assess the expression of erythropoietin receptor in human stem cells (Ott *et al.* 2015 – see Appendix) and the effects of autoantibodies targeting the NMDAR, using a receptor endocytosis assay based on human-derived IPS-neurons as described in detail in Protects I and II (Castillo-Gomez&Oliveira *et al.* 2017, Pan&Oliveira *et al.* 2018, Ehrenreich 2016 – see Appendix).

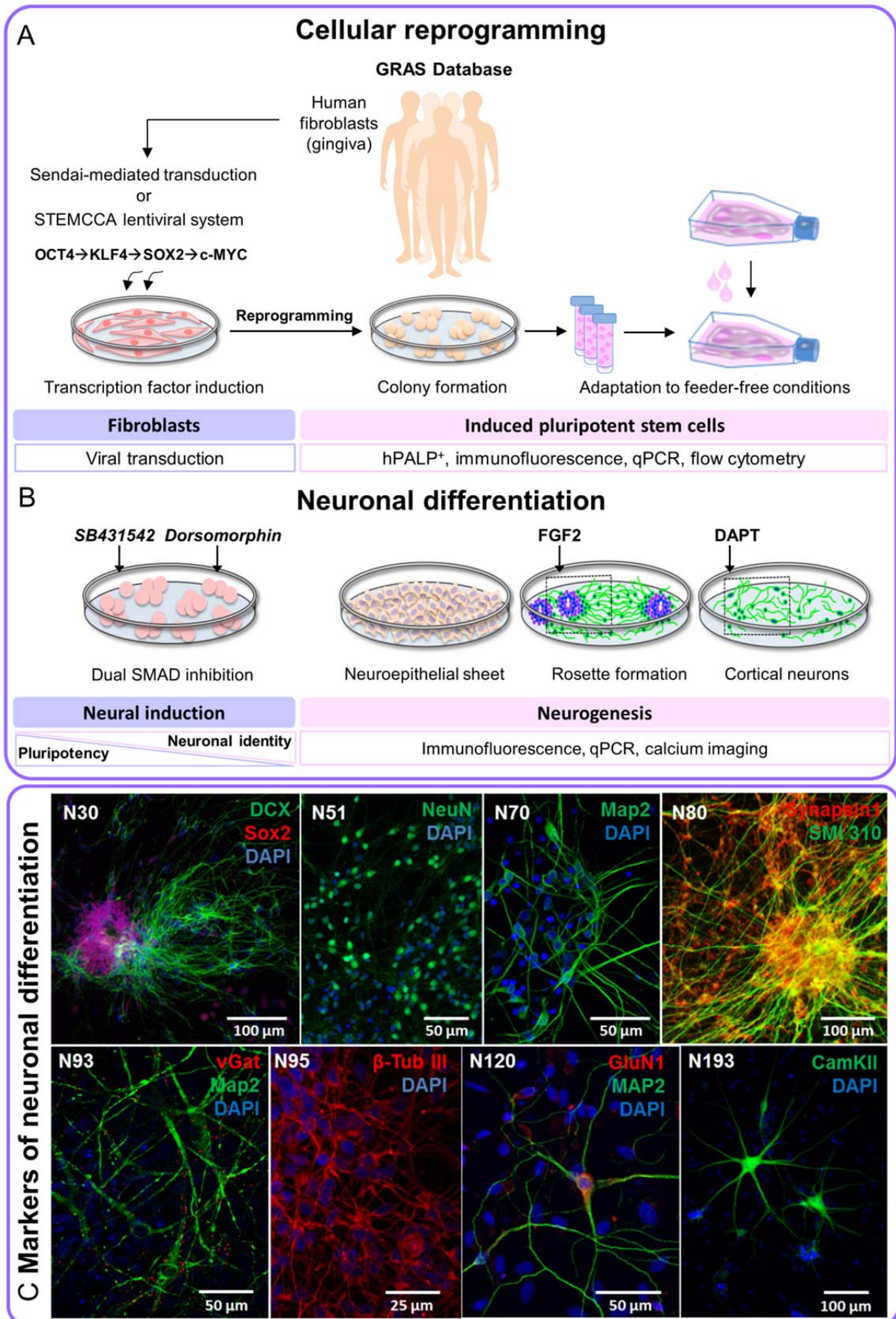


Figure 4. Reprogramming of human fibroblasts and differentiation into neurons. (A) Cellular reprogramming of fibroblasts collected from patient's gingiva involved cell transduction via Sendai or lentiviral systems to

ESTABLISHING A CELL CULTURE SYSTEM FOR TRANSLATIONAL STUDIES

overexpress the four transcription factors: OCT4, KLF4, SOX2 and c-MYC. Successful reprogramming leads to formation of colonies of IPS cells expressing high levels of hPALP, OCT4, Nanog, SOX2, Tra-1-60, LIN28 and SSEA4 markers. Pluripotent colonies can be selected and adapted to feeder-free conditions. **(B)** Induction of a neuronal phenotype can be achieved by dual SMAD inhibition, upon which cells form a neural stem cell monolayer. Dissociation of the neuroepithelial sheath leads to rearrangement of neural stem cells into a rosette-like structure, further expanded by application of the mitogen FGF2. Neuronal progenitors emerge from these structures during the neurogenesis period and are further differentiated with the application of the small molecule DAPT to give rise to mature neurons. **(C)** Immunofluorescent stainings of neuronal markers over several days after induction of the neuronal phenotype. N represents the number of days after the beginning of dual SMAD inhibition (Castillo-Gomez&Oliveira *et al.* 2017). hPALP: human placental alkaline phosphatase; qPCR: real time quantitative polymerase chain reaction; FGF2: fibroblast growth factor 2; DAPT: N-[N-(3,5-Difluorophenacetyl)-L-alanyl]-S-phenylglycine t-butyl ester;

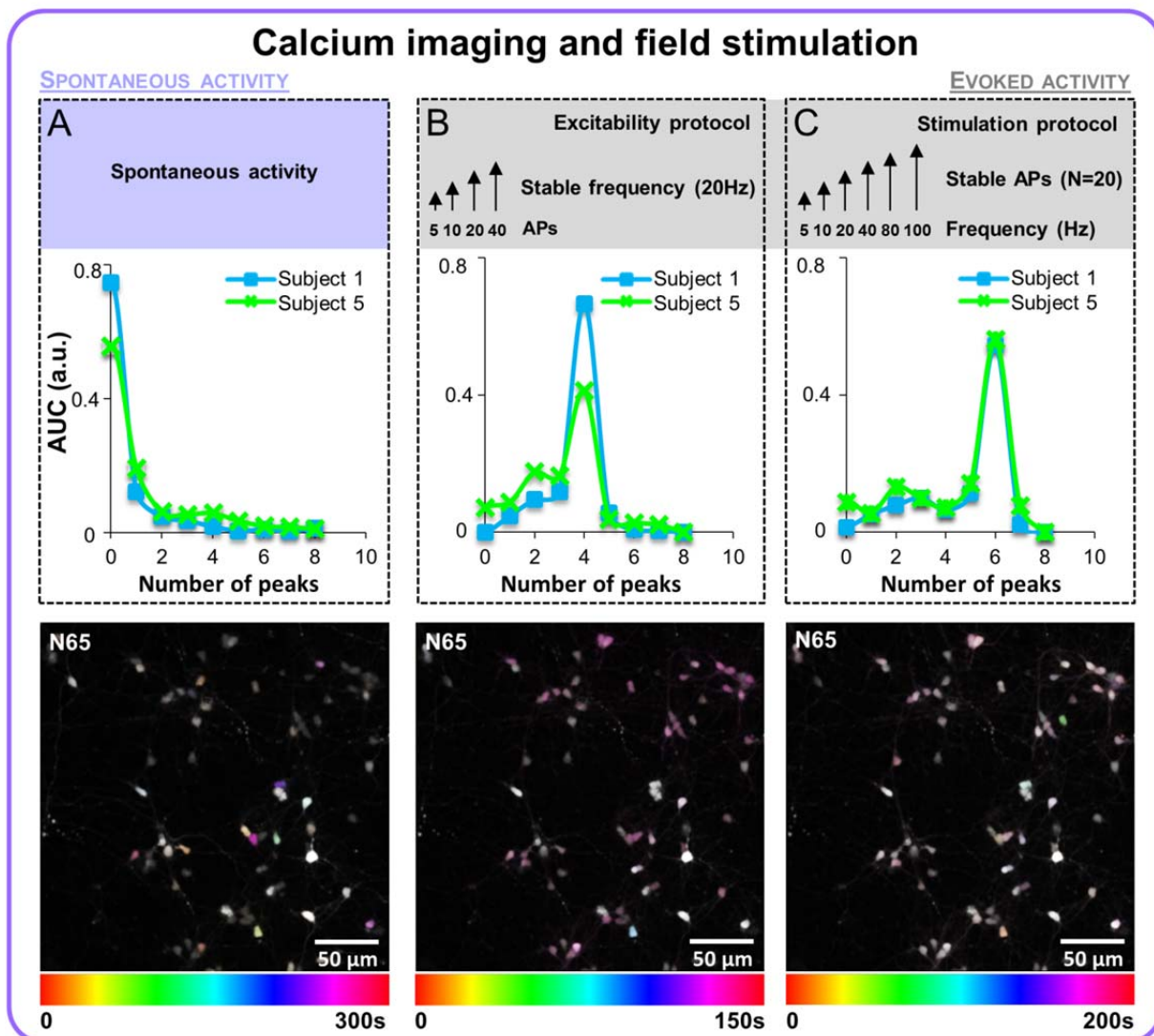


Figure 5. Calcium imaging and field stimulation of N65 IPS-derived neurons labelled with Fluo-4 AM calcium dye. (A) Spontaneous activity was detected with transient changes in fluorescence intensity, over a period of 300 seconds. The number of times the emission of fluorescence surpassed the baseline fluorescence and decayed to close to baseline was determined as a peak of activity. In the bottom figure, the temporal colour code represents the asynchronous nature of the spontaneous activity and some cells with no spontaneous activity

ESTABLISHING A CELL CULTURE SYSTEM FOR TRANSLATIONAL STUDIES

(white) for the recorded period. **(B)** Evoked activity – excitability protocol: cells were stimulated at a constant frequency of 20 Hz with an increasing series of action potentials (APs) triggered from 5 to 40, in a total of four stimuli. The majority of the cells were responsive to the four stimuli (line graph) with stronger responses to the highest number of APs (temporal colour code figure; pink). **(C)** Evoked activity – stimulation protocol: cells were stimulated with a constant number of APs (20) at an increasing frequency ranging from 5 to 100 Hz, in a total of six stimuli. The majority of the cells were responsive to the six stimuli (line graph) with stronger responses at higher frequencies (temporal colour code figure; pink). The line graphs display the results of one clone from two different individuals and represent the number of peaks recorded during the stimulation period, and its amplitude as readout of the area under the curve (AUC). Temporal colour code is displayed in seconds. Irresponsive cells are labelled in white.

3. PROJECT I

3. PROJECT I – All naturally occurring autoantibodies against the NMDA receptor subunit GluN1 have pathogenic potential irrespective of epitope and immunoglobulin class

Overview of Project I

The involvement of NMDAR-ABs in anti-NMDAR encephalitis has been mentioned in the introduction. Despite the pathogenic role attributed to NMDAR-AB in this context, circulating NMDAR-AB, along with other brain-reactive autoantibodies, have been detected in the serum of healthy individuals and with other conditions. These included Parkinson's and Alzheimer's disease, schizophrenia, affective disorders, stroke, amyotrophic lateral sclerosis and cancer (Levin *et al.* 2010, Brimberg *et al.* 2013, Busse *et al.* 2014, Dahm *et al.* 2014, Doss *et al.* 2014, Steiner *et al.* 2014, Schou *et al.* 2016, Finke *et al.* 2017, Jezequel *et al.* 2017). Indeed, seropositivity for NMDAR-AB has been reported with an overall seroprevalence of ~10%, where the isotypes IgM (~7%) and IgA (~5%) are more frequently detected than IgG (~1%) (Dahm *et al.* 2014, Finke *et al.* 2017). Effects of IgG NMDAR-AB have been assessed *in vitro* using rat hippocampal neurons and rodent brain sections or *in vivo* by intraventricular CSF IgG⁺ infusion in mice (Dalmau *et al.* 2007, Moscato *et al.* 2014, Planaguma *et al.* 2015). In both cases, effects of autoantibody exposure led to reduced surface expression of NMDAR1 synaptic clusters in both inhibitory and excitatory neurons (Moscato *et al.* 2014, Planaguma *et al.* 2015). Moreover, *in vivo* experiments demonstrated acquisition of progressive anhedonic/depressive-like behaviours and memory deficits upon exposure (Planaguma *et al.* 2015). Further studies confirmed the functional effect of NMDAR-AB of other isotypes *in vitro* and *in vivo* (Pruss *et al.* 2012, Hammer *et al.* 2014). Given the high seroprevalence of NMDAR-AB in healthy and diseased individuals, it is of outmost relevance to understand their potential pathogenic role. Therefore, this project aimed at a thorough characterization of NMDAR-AB at the functional and molecular level. To do so, a set of NMDAR-AB seropositive and seronegative human samples was selected to cover the immunoglobulin isotypes IgM, IgA and IgG and a spectrum of diseased and healthy individuals. These samples were part of a systematic screening of a large number of individuals for the presence of NMDAR-AB of IgG, IgA and IgM isotypes and determination of their seroprevalence (Dahm *et al.* 2014, Hammer *et al.* 2014, Zerche *et al.* 2015).

Two different approaches were employed to assess NMDAR-AB functionality *in vitro*: first the ability of all NMDAR-AB isotypes to internalize the NMDAR in human IPS cell-derived neurons was tested and secondly their ability to alter glutamate-evoked responses in *Xenopus laevis* transfected oocytes. Since all previous studies employed rodent cultures to

PROJECT I

assess functionality, a receptor endocytosis assay based on human IPS cells that underwent neuronal differentiation and express the GluN1 subunit of NMDAR was developed (for details see “*Establishing a cell culture system for translational studies*”). In this live cell-based assay, exposure to all NMDAR1-AB⁺ dialysed sera led to receptor endocytosis. A significant decrease in cell-surface fluorescence intensity ratio 37°C/4°C was detected as readout of a reduction in surface expression of NMDAR, while negative sera had no effect. This effect was also present when the impact of immunoglobulin isotypes was assessed separately (Castillo-Gomez&Oliveira *et al.* 2017). To investigate the impact of NMDAR1-AB on receptor activity, glutamate evoked responses were evaluated in *Xenopus laevis* oocytes co-expressing human GluN1-1/GluN2A subunits using two-electrode voltage clamp. After exposure of oocytes to human dialyzed sera, the area under the curve of the glutamate-evoked current was significantly lowered in seropositive compared with seronegative samples. This effect was sustained for at least 16 minutes in all seropositive samples regardless of their isotype, with no significant differences between isotypes (Castillo-Gomez&Oliveira *et al.* 2017). With these two experiments it was possible to demonstrate that (i) NMDAR-AB of IgG, IgA and IgM isotypes lead to receptor endocytosis and (ii) consequently reduce the cell response to glutamate.

After identifying the functional effect of NMDAR-AB, the interaction between these autoantibodies and NMDAR were characterized at the molecular level. Based on the concept of seropositivity detection using a cell based assay, HEK293 cells transfected with a series of mutated or chimeric GluN1-1b receptors using the GluN2B as backbone were used. The seven constructs generated allowed to test epitope recognition in the extracellular, transmembrane and intracellular regions of the NMDAR (Castillo-Gomez&Oliveira *et al.* 2017). Epitope mapping using different GluN1-1b constructs revealed binding to epitopes located in the extracellular ligand-binding domain and NTD, the intracellular CTD and extra-large pore domains (xlp) with no particular disease or isotype-related pattern. Overall, in both monospecific and polyspecific sera involvement of extracellular epitopes was more frequent (11/14). Monospecific and monoclonal sera reactive with intracellular epitopes (3/14) was less frequent and also reactive with GluN2A subunit. The NTD G7 glycosylation site, reported to be important for NMDAR-AB epitope recognition in anti-NMDAR encephalitis, was recognized in 2/10 sera binding to NTD. Targeting specifically the G7 site, seven additional sera from encephalitis patients were tested. All sera had NMDAR-AB of two immunoglobulin isotypes, challenging the previously described exclusivity for IgG associated with this condition and not all of them required the G7 site for binding (Castillo-Gomez&Oliveira *et al.* 2017). Moreover, autoantibodies targeting the GluN2A subunit were also present in these sera, while no positivity was detected regarding the GluN2B subunit. This result is in line with the postnatal developmental switch in NMDAR conformation, where

the GluN2A subunit becomes the preferential partner of the GluN1 subunit upon synaptic maturation leading to a decrease in expression of GluN2B in the adult brain (Gladding *et al.* 2011, Paoletti *et al.* 2013).

In this project, NMDAR-AB of three immunoglobulin isotypes (IgM, IgG and IgA) regarding *in vitro* functionality and epitope recognition has been analysed. Previous studies have focused on the IgG isotype and its role on the pathophysiology of anti-NMDAR encephalitis (Dalmau *et al.* 2008, Gleichman *et al.* 2012, Moscato *et al.* 2014). Thus, in this work the spectrum of NMDAR-AB effects has been broadened to other immunoglobulin isotypes by demonstrating their ability to promote receptor endocytosis and reduce glutamate-evoked responses. The diversity of epitopes recognized by NMDAR-AB demonstrated here, points to a more diverse interaction of these autoantibodies with NMDAR and overcomes the relevance credited exclusively to the G7 site of the NTD.

The presence of these autoantibodies in healthy individuals along with an increase in seroprevalence upon ageing points to the involvement of the BBB in their pathogenicity (Hammer *et al.* 2014). An intact BBB might pose as the ultimate obstacle for NMDAR-AB to exert their effects in the CNS. In this sense, the consequences of a compromised BBB in the context of NMDAR-AB are the focus of the next project.

Original publication

Castillo-Gómez E*, Oliveira B*, Tapken D*, Bertrand S, Klein-Schmidt C, Pan H, Zafeiriou P, Steiner J, Jurek B, Trippe R, Prüss H, Zimmermann WH, Bertrand D, Ehrenreich H, Hollmann M. *All naturally occurring autoantibodies against the NMDA receptor subunit NR1 have pathogenic potential irrespective of epitope and immunoglobulin class.* *Molecular Psychiatry*. 2017; 22(12):1776-1784

*Authors with equal contribution

Personal contribution: As one of the first authors of this manuscript I was involved in establishing the protocol to differentiate human IPS cells into cortical neurons and establishing and performing the NMDAR endocytosis assay to determine the functional effect of human NMDAR autoantibodies in all samples reported in this study. I have also contributed to the analysis and interpretation of the data. Additionally, I was involved in writing the methods and results sections of this paper, helped preparing the figures and figure legends and contributed to the overall preparation of the manuscript. Moreover, I was significantly involved on the study design, experiment planning, literature searches as well as rebuttal and revision.

ORIGINAL ARTICLE

All naturally occurring autoantibodies against the NMDA receptor subunit NR1 have pathogenic potential irrespective of epitope and immunoglobulin class

E Castillo-Gómez^{1,9}, B Oliveira^{1,9}, D Tapken^{2,9}, S Bertrand³, C Klein-Schmidt², H Pan¹, P Zafeiriou⁴, J Steiner⁵, B Jurek^{6,7}, R Trippe², H Prüss^{6,7}, W-H Zimmermann⁴, D Bertrand³, H Ehrenreich^{1,8,10} and M Hollmann^{2,10}

Autoantibodies of the IgG class against *N*-methyl-D-aspartate-receptor subunit NR1 (NMDAR1) were first described in anti-NMDAR encephalitis and seen as disease indicators. Recent work on together over 5000 individuals challenged this exclusive view by showing age-dependently up to >20% NMDAR1-autoantibody seroprevalence with comparable immunoglobulin class and titer distribution across health and disease. The key question therefore is to understand the properties of these autoantibodies, also in healthy carriers, in order to assess secondary complications and possible contributions to neuropsychiatric disease. Here, we believe we provide for human NMDAR1-autoantibodies the first comprehensive analysis of their target epitopes and functionality. We selected sera of representative carriers, healthy or diagnosed with very diverse conditions, that is, schizophrenia, age-related disorders like hypertension and diabetes, or anti-NMDAR encephalitis. We show that *all* positive sera investigated, regardless of source (ill or healthy donor) and immunoglobulin class, provoked NMDAR1 internalization in human-induced pluripotent stem cell-derived neurons and reduction of glutamate-evoked currents in NR1-1b/NR2A-expressing *Xenopus* oocytes. They displayed frequently polyclonal/polyspecific epitope recognition in the extracellular or intracellular NMDAR1 domains and some additionally in NR2A. We conclude that *all* circulating NMDAR1-autoantibodies have pathogenic potential regarding the whole spectrum of neuronal NMDAR-mediated effects upon access to the brain in situations of increased blood–brain–barrier permeability.

Molecular Psychiatry advance online publication, 9 August 2016; doi:10.1038/mp.2016.125

INTRODUCTION

Circulating autoantibodies (AB) directed against brain epitopes have long been documented, mainly in connection with classical autoimmune diseases or paraneoplastic syndromes.^{1–4} AB targeting the *N*-methyl-D-aspartate-receptor subunit NR1 (NMDAR1; *new nomenclature GluN1 disregarded here for consistency with the respective literature, except in the molecular biological section*) have attracted considerable attention lately. NMDAR1-AB of the IgG class were first described in connection with a condition named anti-NMDAR encephalitis⁵ and induced a flood of publications, among them many case reports. In several of them, immunosuppressive treatment of seropositive subjects is recommended.^{6–8} Anti-NMDAR encephalitis symptoms typically include psychosis, cognitive decline, seizures, dyskinesia, decreased consciousness and autonomic instability.⁵ These symptoms are reminiscent of those found upon NMDAR antagonism by ketamine, MK801, or related drugs, and have been explained by reduced surface expression of NMDAR1 upon exposure to NMDAR1-AB.⁵

Rendering the situation more complex, a high age-dependent seroprevalence of NMDAR1-AB has been recognized recently.^{9–14} According to these findings in meanwhile >5000 subjects, any 40-year-old person has an ~10%, any 80-year-old person an ~20%

chance of displaying NMDAR1-AB seropositivity.¹¹ Disease groups, ranging from schizophrenia and major depression, over multiple sclerosis, Parkinson's and Alzheimer's disease, to hypertension, diabetes and stroke, as well as healthy individuals, share not only similar NMDAR1-AB seroprevalence but also immunoglobulin (Ig) class distribution (IgM, IgA and IgG) and titer range.^{9–11,13} These unexpected results raised the question of functionality and relevance of the highly seroprevalent NMDAR1-AB. In translational mouse studies, similar effects of the different classes (IgG, IgM and IgA) of NMDAR1-AB on behavioral readouts were observed.⁹ Likewise, in a human study, an equivalent impact of circulating NMDAR1-AB of all three isotypes on evolution of lesion size after ischemic stroke was noticed.¹¹ Detectable neuropsychiatric consequences of circulating NMDAR1-AB of all three classes were restricted to individuals with compromised blood–brain–barrier, for example, *ApoE/APOE* carrier status, both clinically and experimentally.^{9,11,15} In studies using rodent hippocampal neurons, we found NMDAR1 internalization upon NMDAR1-AB (IgM, IgA, IgG) binding as explanation of its reduced surface expression.^{9,15} A comparable finding had previously been described only for IgG.^{5,16}

¹Clinical Neuroscience, Max Planck Institute of Experimental Medicine, Göttingen, Germany; ²Department of Biochemistry I – Receptor Biochemistry, Ruhr University, Bochum, Germany; ³HiQscreen, Geneva, Switzerland; ⁴Institute of Pharmacology and Toxicology, University Medical Center, Göttingen, Germany; ⁵Department of Psychiatry, University of Magdeburg, Magdeburg, Germany; ⁶Department of Neurology, Charité, University Medicine, Berlin, Germany; ⁷German Center for Neurodegenerative Disorders (DZNE), Berlin, Germany and ⁸DFG Research Center for Nanoscale Microscopy and Molecular Physiology of the Brain (CNMPB), Göttingen, Germany. Correspondence: Professor H Ehrenreich, Clinical Neuroscience, Max Planck Institute of Experimental Medicine, Hermann-Rein-Strasse 3, Göttingen 37075, Germany. E-mail: ehrenreich@em.mpg.de

⁹These authors share first authorship.

¹⁰These authors share last authorship.

Received 18 March 2016; revised 3 May 2016; accepted 1 June 2016

Considering the high seroprevalence of NMDAR1-AB across health and disease, the key question is to understand the properties of these AB, also in healthy carriers, in order to assess secondary complications and possible contributions to neuropsychiatric disease, for example, cognitive decline, psychotic symptoms or epileptic seizures. Are they like a 'ticking time bomb' once the blood barrier opens?

Here, we believe we provide for human NMDAR1-AB the first comprehensive analysis of their target epitopes and of functionality. We investigated whether NMDAR1-AB of different Ig classes, derived from sera of subjects with very diverse conditions, would (i) reveal functionality in an internalization assay using human induced pluripotent stem cell (iPSC)-derived cortical neurons; (ii) lead to electrophysiological consequences in NR1-1b/NR2A-expressing *Xenopus* oocytes; and (iii) be directed against the same or against different epitopes of NMDAR1.

We report as most important take-home message that, independent of any medical condition or Ig class, NMDAR1-AB are functional, leading to decreased NMDAR surface expression

and reduced glutamate-evoked currents. The AB recognize epitopes in the extracellular and/or intracellular NMDAR1 domains and, surprisingly, some positive sera also in the NR2A subunit of NMDAR. Thus, most intriguingly, they all have potentially (patho) physiological relevance regarding brain functions.

MATERIALS AND METHODS

All experiments were performed by researchers unaware of group assignment ('fully blinded').

Human samples

Serum specimens ($N=29$) from our phenotyping/biomarker trials^{8,10,11,17} were selected to (i) cover a spectrum of diseases and health, (ii) include all NMDAR1-AB Ig classes and (iii) build on enough material for extensive testing (Table 1). In addition, samples ($N=7$; few μ l available) for targeted epitope mapping were obtained from anti-NMDAR encephalitis patients (Charité, HP). Subject data/human materials (including iPSC) were collected according to ethical guidelines/Helsinki Declaration including subjects' informed consent.

Table 1. Overview of donors of NMDAR1-AB-positive and -negative serum samples

	Seropositive individuals (N = 14)	Seronegative individuals (N = 15)	P-value
Gender, No. (%), women ^a	10 (71.4)	7 (46.7)	0.176
Age at examination, mean \pm s.d., years ^b	62.87 \pm 24.44	65.24 \pm 10.99	0.234
<i>Diagnosis, No. (%)^a</i>			
Healthy	2 (14.3)	4 (26.7)	0.418
NMDAR1-AB encephalitis	2 (14.3)	0 (0.0)	
Psychiatric conditions ^c	1 (7.1)	1 (6.3)	
Diabetes	0 (0.0)	2 (13.3)	
Hypertension	7 (50.0)	6 (40.0)	
Diabetes and hypertension	2 (14.3)	1 (6.7)	
Other medical conditions ^d	0 (0.0)	1 (6.7)	
<i>NMDAR1-AB seroprevalence, titers, No.^e</i>			
IgA (1:10; 1:32; 1:100; 1:320; 1:1000; 1:3200)	2; 0; 0; 0; 4; 0		n/a
IgG (1:10; 1:32; 1:100; 1:320; 1:1000; 1:3200)	0; 0; 1; 1; 1; 1		
IgM (1:10; 1:32; 1:100; 1:320; 1:1000; 1:3200)	0; 0; 1; 1; 5; 1		

Abbreviations: AB, autoantibodies; IG, immunoglobulin; n/a, not applicable; NMDAR1, N-methyl-D-aspartate-receptor subunit NR1. ^aChi-square test. ^bMann-Whitney U-test. ^c'Psychiatric conditions' include two schizophrenia patients. ^d'Other medical conditions' include hypercholesterolemia, asthma bronchiale and glaucoma. ^eNote that of the total sample $N=4$ individuals were seropositive for both IgA and IgM.

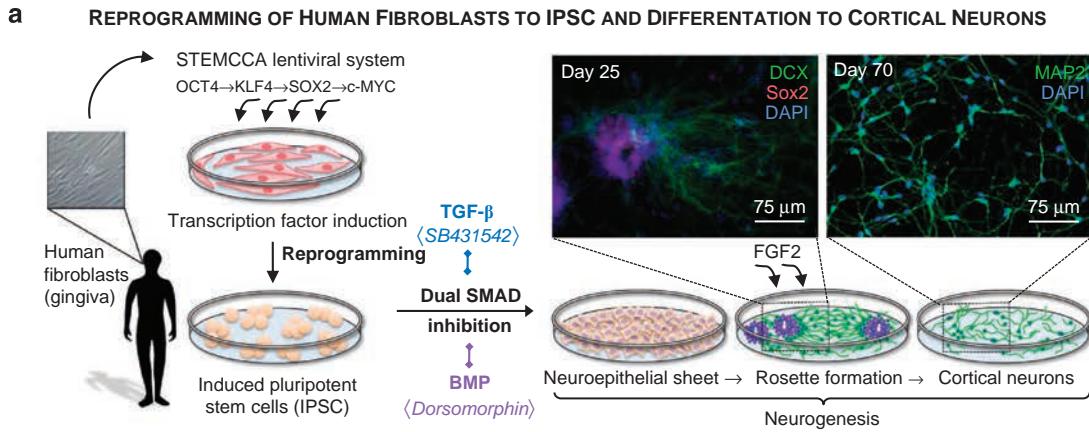
Figure 1. NMDAR1 endocytosis in human induced pluripotent stem cell (iPSC)-derived cortical neurons after autoantibodies (AB) exposure. **(a)** Reprogramming strategy: Human fibroblasts obtained from gingiva biopsies were transduced using a lentiviral system to simultaneously integrate the transcription factors OCT4, KLF4, SOX2 and c-MYC. Transcription factor expression leads to cell reprogramming and colony formation of iPSC, which are differentiated into cortical neurons using a dual SMAD inhibition strategy (selective blocking of TGF- β and BMP pathways). Cells acquire neuronal identity forming a neural stem cell monolayer. Dissociation of the neuroepithelial sheath leads to rearrangement of neural stem cells (SOX2+) in a rosette-like structure, further expanded by application of the mitogen FGF2. Immature neurons (DCX+) emerge from these structures during the neurogenesis period to give rise mainly to MAP2+ cortical excitatory neurons. **(b)** At day 70 of maturation, neurons are exposed to human sera. NMDAR1-AB binding to NMDAR1 (at 4 °C) leads to rapid endocytosis of the receptor-antibody complex at 37 °C. The remaining cell-surface NMDAR1 is detected by combining mouse anti-NMDAR1-AB (step 1) and secondary donkey anti-mouse Alexa 546-AB (step 2). Neurons are defined as NeuN+ cells. **(c)** Representative confocal images of neurons exposed to an IgG seropositive sample are shown on the left. Both pictures are Z-projections of three consecutive focal planes 0.5 μ m apart, taken at \times 100 magnification under confocal laser-scanning microscope. The upper picture depicts a neuron (NeuN+, labeled in green), kept at 4 °C (no endocytosis allowed—control condition) and the lower picture a neuron at 37 °C (endocytosis). For each serum sample, cell membrane NMDAR1 (labeled in red; arrow heads) is quantified. Degree of internalization is expressed as ratio of fluorescence intensity measured at both temperatures. Seropositive samples show reduced fluorescence intensity ratio (37 °C/4 °C) compared with seronegative samples (graph on the left; *unpaired Student's t-test*: $t_{16} = 11.16$; $P < 0.001$), consistent with a decrease in surface NMDAR1 after exposure to NMDAR1-AB. Right graph: Fluorescence intensity ratio is lower for all seropositive samples (separate analyses shown for samples with only IgG, IgM, IgA or IgM+IgA, in purple, orange, green and yellow columns, respectively) and the positive control (IgG M68-AB). *One-way ANOVA*: $F_{6,17} = 70.59$; $P < 0.001$; multiple comparisons with *Bonferroni's post hoc correction*, P -value < 0.05 ; results given as mean \pm s.e.m. BMP, bone morphogenetic pathway; c-MYC, avian myelocytomatosis virus oncogene cellular homolog; DAPI, 4',6'-diamidino-2-phenylindole; DCX, doublecortin; FGF2, fibroblast growth factor 2; KLF4, Krüppel-like factor 4; MAP2, microtubule-associated protein 2; NMDAR1, N-methyl-D-aspartate-receptor subunit NR1; NeuN, neuronal nuclear antigen; OCT4, octamer-binding transcription factor 4; SOX2, sex determining region Y-homeobox 2; STEMCCA, stem cell cassette; TGF- β , transforming growth factor- β .

NMDAR1-AB titer determination

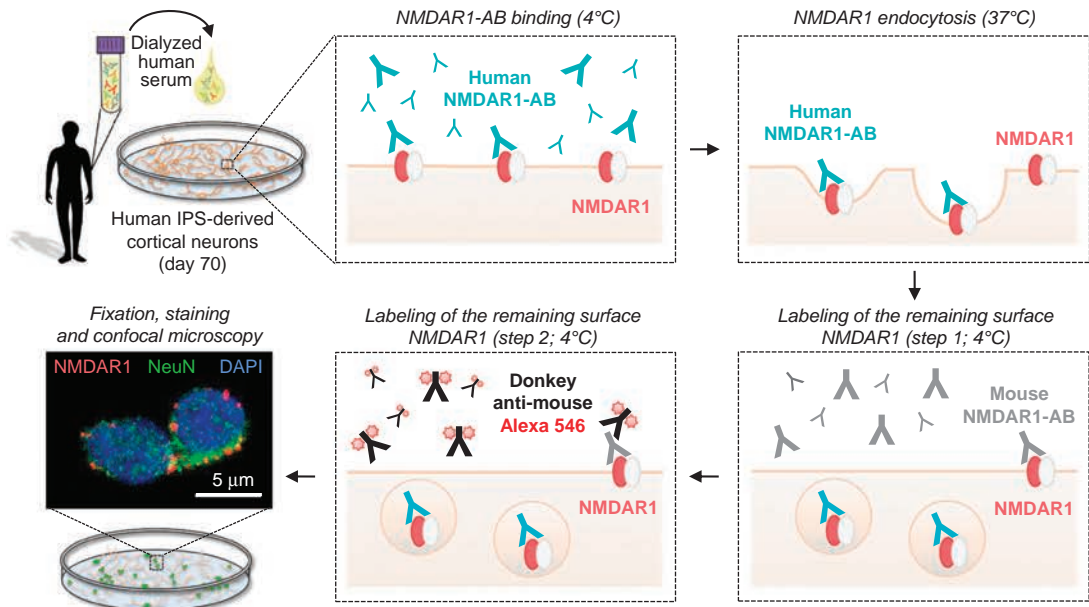
Recombinant immunofluorescence tests (Euroimmun, Lübeck, Germany), clinical standard procedures, were used to detect NMDAR1-AB, based on HEK293T cells transfected with NMDAR1,^{5,6} and secondary AB against human IgG, IgM or IgA. Results were independently assessed by three investigators.

Dialysis of serum samples

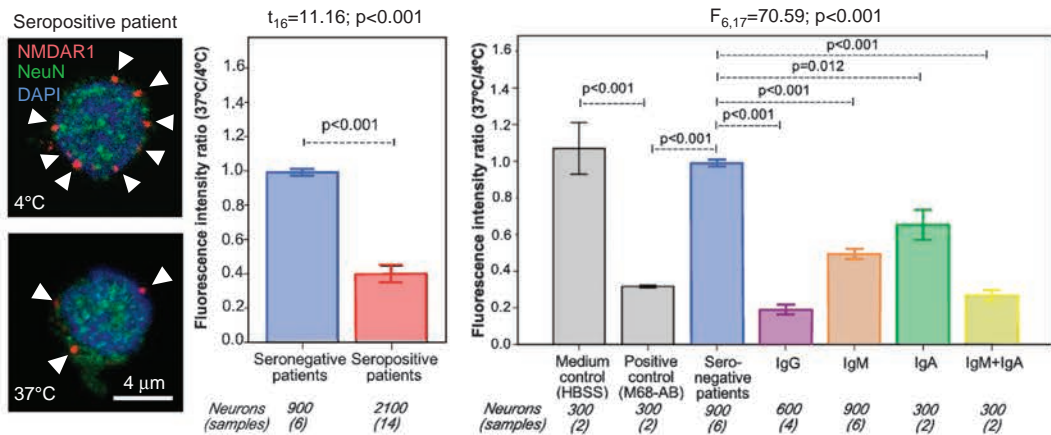
Functional studies were conducted with sera following ammonium sulfate precipitation of immunoglobulins¹⁸ and dialysis (Slide-A-Lyzer Mini-Dialysis-Units, 10 000 MWCO Plus Float, Thermo Fisher Scientific, Rockford, IL, USA).



b NMDAR1 ENDOCYTOSIS ASSAY



c EFFECT OF NMDAR1-AB ON NMDAR AVAILABILITY AT THE NEURONAL MEMBRANE



Reprogramming of human fibroblasts and differentiation into neurons

Human fibroblasts from gingiva biopsies were reprogrammed using STEMCCA system (Merck Millipore, Darmstadt, Germany) for introduction of OCT4, SOX2, KLF4 and c-MYC.¹⁹ Clones were tested for pluripotency markers following standard procedures.¹⁹ After reprogramming, iPSC was adapted to feeder-free culture system (Matrigel matrix, Corning, Wiesbaden, Germany) and TeSR™-E8™ medium (Stem Cell Technologies, Cologne, Germany). Neural induction was based on dual SMAD inhibition (Figure 1a).²⁰

Endocytosis assay

Human iPSC-derived cortical neurons grown on coverslips, 70 days post neural induction, were pre-cooled on ice (10 min), and washed 3 × with cold HBSS (Hank's balanced salt solution; Life Technologies, Darmstadt, Germany). Culture media were kept at 37 or 4 °C. Neurons were incubated (30 min) in cold HBSS with 1:100 diluted sera (14 seropositive; 6 seronegative), control NMDAR1-AB (M68, mouse IgG, SYSY, Göttingen, Germany) or HBSS alone (negative control). After three HBSS washes to remove unbound AB, neurons were returned to their media and incubated for 20 min at 37 °C (2 coverslips/sample, to allow endocytosis) or 4 °C (1 coverslip/sample, endocytosis control). After ice-cold HBSS wash, coverslips were kept on ice (5 min). Remaining surface NMDAR1 was exposed to a mouse NMDAR1-AB (N-terminal; Abcam, Cambridge, UK, 1:100), 10 min on ice, followed (after ice-cold HBSS wash) by secondary donkey anti-mouse IgG (Life Technologies, Alexa-Fluor546, 1:100) for 10 min on ice in dark, and finally three ice-cold HBSS washes to remove unbound AB. Neurons were fixed with ice-cold 4% paraformaldehyde (30 min) and washed 3 × (5 min) with 0.1 M phosphate-buffered saline (PBS). Then, cells were blocked and permeabilized for 1 h at RT (5% normal goat, 5% normal horse, 5% fetal calf serum, 0.5% Triton X in PBS), double-stained at 4 °C overnight with chicken anti-NeuN-AB (SYSY, 1:500) and secondary donkey anti-chicken AB (Life Technologies, Alexa Fluor 488, 1:250) for 1 h at RT (all dark) (Figure 1b). Nuclei were visualized using DAPI (Sigma-Aldrich, Munich, Germany, 0.01 µg ml⁻¹). After PBS wash, coverslips were mounted on Super-Frost slides with Mowiol-mounting-media (Sigma-Aldrich). Confocal laser-scanning microscopy was used to quantify cell-surface NMDAR1 density (×63 glycerol objective; TCS-SP5 Leica-Microsystems, Mannheim, Germany). From each coverslip, Z-series of optical sections (0.5 µm apart) covering the three-dimensional extension of neurons were acquired (sequential scanning mode, identical acquisition parameters). For analysis, 50 NeuN+ cells/coverslip were randomly selected using Fiji-ImageJ software.²¹ Soma profile including NMDAR1 surface expression was drawn and fluorescence intensity/cell surface area (Alexa-Fluor546) automatically measured. Background was subtracted, mean intensity for each coverslip determined and fluorescence intensity ratio (37 °C/4 °C) calculated.

Oocyte preparation and injection

Xenopus laevis oocytes were prepared, injected and tested using standard procedures. Briefly, ovaries were harvested from *Xenopus* females in deep anesthesia by hypothermia (4 °C) and MS-222 (Sigma-Aldrich, 150 mg l⁻¹). Animals were decapitated and pithed obeying animal rights (Geneva, Switzerland). A small piece of ovary was isolated for immediate preparation while the remaining part was placed at 4 °C in sterile Barth-solution containing [mm]: NaCl 88, KCl 1, NaHCO₃ 2.4, HEPES 10, MgSO₄·7H₂O 0.82, Ca(NO₃)₂·4H₂O 0.33, CaCl₂·6H₂O 0.41, at pH 7.4, supplemented with 100 U ml⁻¹ penicillin/100 µg ml⁻¹ streptomycin (Life Technologies). Automatic injection of mRNAs encoding for human NMDAR (NR1-1/NR2A) was performed in batches of 95 oocytes using Roboinject²² (Multi Channel Systems, Reutlingen, Germany) (Figure 2a). Optimal expression of NMDAR was obtained with injection of 15 nl containing 0.2 µg µl⁻¹ of RNAs, ratio NR1-1b:NR2A = 1:1; mRNA was prepared using mMessage mMachine SP6 transcription kit for NR1-1b and T7 for NR2A (Thermo Fisher Scientific).

Electrophysiological recordings and experimental protocol

NMDAR activity was validated 60 h after mRNA injection by 2-electrode voltage clamp (Figure 2a). All electrophysiological recordings were performed using an automated HiClamp system (Multi Channel Systems) at 18 °C and with cells superfused with OR2 medium (mm: NaCl 88, KCl 2.5, HEPES 5, CaCl₂·2H₂O 1.8, pH 7.85). To chelate zinc contaminant, 10 µM EDTA was added to all solutions. Unless otherwise indicated, cells were

maintained at holding potential of -80 mV and compounds/AB incubations conducted in 96-well-microtiter plates (Thermo Fisher Scientific). Only cells displaying low leak current and responses > 0.5 µA to a test pulse containing 0.3 µM glutamate/10 µM glycine (Sigma-Aldrich) were retained for successive testing (Figures 2a and b). Cells were then challenged with pre-incubation of 120 s in control medium (OR2 medium) followed by brief exposures to 0.3 µM glutamate/10 µM glycine (10 s) every 2 min for 10 min (Figure 2b, steps 1 and 2). The last 4 min was considered as control response-amplitude to glutamate (Figure 2c, right-side graphs, -4-0 min). Upon stabilization, cells were exposed for 16 min to dialyzed serum samples (titer dilution for seropositive and 1:1000 for seronegative samples) or to positive control (M68-AB, 1:1000). NMDAR activity was tested by brief exposure to 0.3 µM glutamate/10 µM glycine (10 s) every 2 min for 16 min in presence of the dialyzed serum (Figure 2b, steps 3 and 4). To evaluate the cellular response, area-under-the-curve (AUC) for each glutamate-evoked current was computed and normalized to AUC of control responses (-4-0 min). Data were analyzed using custom-made software (Matlab-Mathworks, Ismaning, Germany). For each sample, a mean of ≥ 3 oocytes was calculated (Figure 2c, left-side graphs).

Epitope mapping using NMDAR1 constructs

NMDAR1 constructs were generated based on the longest splice variant, GluN1-1b (GenBank accession #U08263; Figures 3a and b). All cDNAs (including GluN2A: #AF001423; GluN2B: #U11419) were cloned into pcDNA4.0/TO/myc-HisA (Invitrogen, Carlsbad, CA, USA) such that the encoded receptor had a myc-His-tag connected to its C-terminus by a short peptide linker (SRGPF). Chimeras and mutants for epitope analysis were constructed by overlap-extension-PCR using chimeric or mutagenic primers.^{23,24} To transiently express glutamate receptor subunits, HEK293T cells were cultured in high-glucose DMEM (Life Technologies). On a 35-mm dish, 50 000 cells were plated, grown for 3 days, transfected with receptor cDNA (3 µg) using Metafectene-Pro (Biontex, Munich, Germany) and, 24 h after transfection, seeded onto poly-D-lysine-coated coverslips (Sigma-Aldrich). At 2 days after transfection, cells were fixed with 5% paraformaldehyde (20 min), washed 5 × with 0.1 M PBS, permeabilized with 0.1% Triton X-100 (5 min), again washed 5 × with PBS, blocked for 1 h with 5% normal goat serum (Sigma-Aldrich). After 5 × PBS washes, cells were incubated with serum (1:10-1:200) or monoclonal mouse anti-myc antibody (transfection efficiency control; self-made, purified from mouse-clone-9E10) for 1 h, washed 10 × with PBS, incubated for 1 h with Alexa Fluor 488-labeled goat anti-human secondary AB (IgG: Southern Biotech, Birmingham, AL, USA; IgA: Jackson ImmunoResearch, West Grove, PA, USA; IgM: Thermo Fisher Scientific) or anti-mouse IgG (controls; Thermo Fisher Scientific), washed 5 × with PBS, incubated with TO-PRO-3 iodide nuclear-stain (Molecular Probes, Eugene, OR, USA) (15 min), and washed 5 × with PBS. Cells were mounted in Fluoromount-G (Southern Biotech) and analyzed by confocal microscopy (63 × oil objective, TCS SP2 AOBs, Leica-Microsystems). All results are consensus judgements from at least four independent investigators of two different laboratories.

Statistics

All statistical analyses were performed using SPSS for Windows version 17.0 (IBM-Deutschland, Munich, Germany). Group differences in categorical and continuous variables were assessed using Chi-square and Mann-Whitney *U*-test. One-way or repeated-measures ANOVA, followed by multiple pair-wise comparisons with Bonferroni's post hoc correction, was employed to determine the significance of fluorescence intensity or AUC; *P*-values < 0.05 were considered as significant; data in figures are mean ± s.e.m.

RESULTS

In human iPSC-derived cortical neurons, exposure to all NMDAR1-AB-positive sera tested, independent of Ig class and titer, led to receptor endocytosis, reflected by decreased cell-surface fluorescence intensity ratio 37 °C/4 °C (perikaryal labeling). Negative sera had no effect (*unpaired Student's t-test*: *t*₁₆ = 11.16; *P* < 0.001; seronegative samples: *n* = 6, neurons *n* = 900; seropositive samples: *n* = 14, neurons *n* = 2100) (Figure 1c). Analyzing the impact of Ig classes separately, significant results remained for all (one-way ANOVA: *F*_{6,17} = 70.59; *P* < 0.001 with Bonferroni post hoc

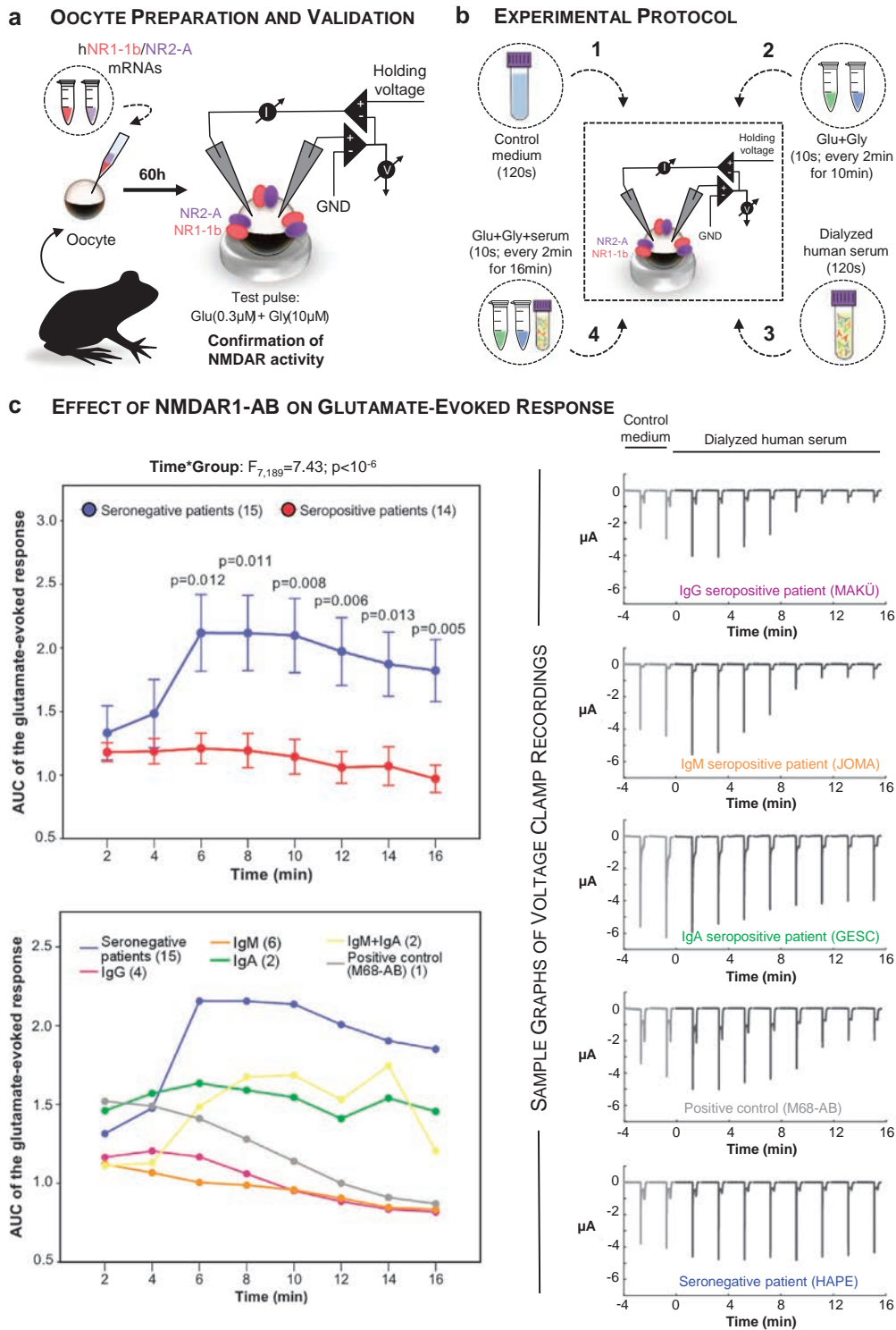
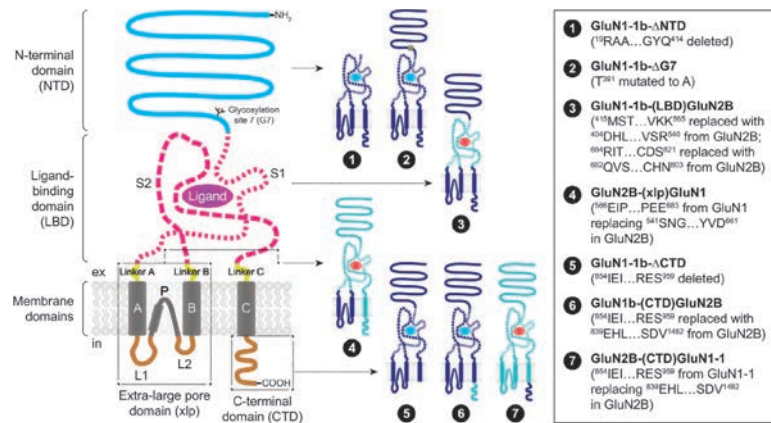
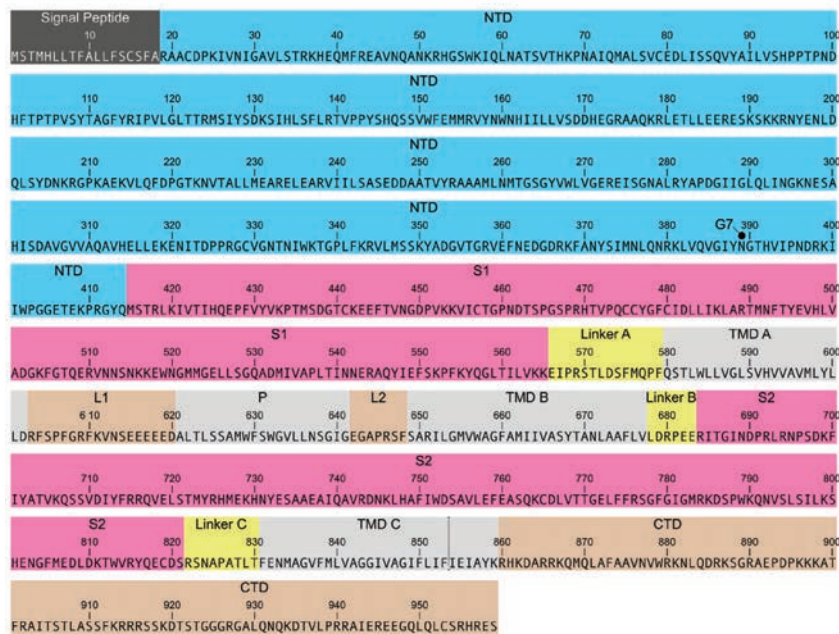


Figure 2. Decreased NMDAR activity after autoantibodies (AB) exposure. (a) NMDAR activity in *Xenopus laevis* oocytes expressing human NR1-1b/NR2A is confirmed using 2-electrode voltage clamp recordings. (b) Control glutamate response of each oocyte is tested after 120 s incubation in control medium followed by 10 s exposure to glutamate and glycine every 2 min for 10 min (steps 1 and 2). Cells are afterwards exposed for 120 s to dialyzed serum samples or to positive control (M68-AB), followed by 10 s exposures to glutamate and glycine every 2 min for 16 min (steps 3 and 4). (c) An increase in AUC of the glutamate-evoked response starting at 6 min and lasting for at least 16 min is observed in seronegative but not in seropositive samples (left upper graph; *one-way repeated-measures ANOVA*: time \times group interaction: $F_{7,189}=7.43$, $P<10^{-6}$; *Bonferroni's* post hoc correction for multiple comparison: only P -values <0.05 are shown). The left lower graph shows curves for Ig classes separately which all are below the seronegative curve (*one-way repeated-measures ANOVA*: time \times group interaction: $F_{35,168}=1.98$, $P=0.002$). On the right side, five representative recordings of cells exposed to IgG, IgM and IgA seropositive samples, positive control sample (M68-AB) and a seronegative sample are shown. The first two curves of every graph show the last 4 min of the control response to glutamate (see Materials and methods for detailed information). AUC, area-under-the-curve; Glu, glutamate; Gly, glycine; GND, signal ground; I, intensity; Ig, immunoglobulin; NMDAR, *N*-methyl-D-aspartate receptor; V, voltage.

a TOPOLOGY & DOMAIN STRUCTURE OF NMDAR1 (GluN1-1b) CONSTRUCTS



b AMINO ACID SEQUENCE & DOMAINS OF GluN1-1b

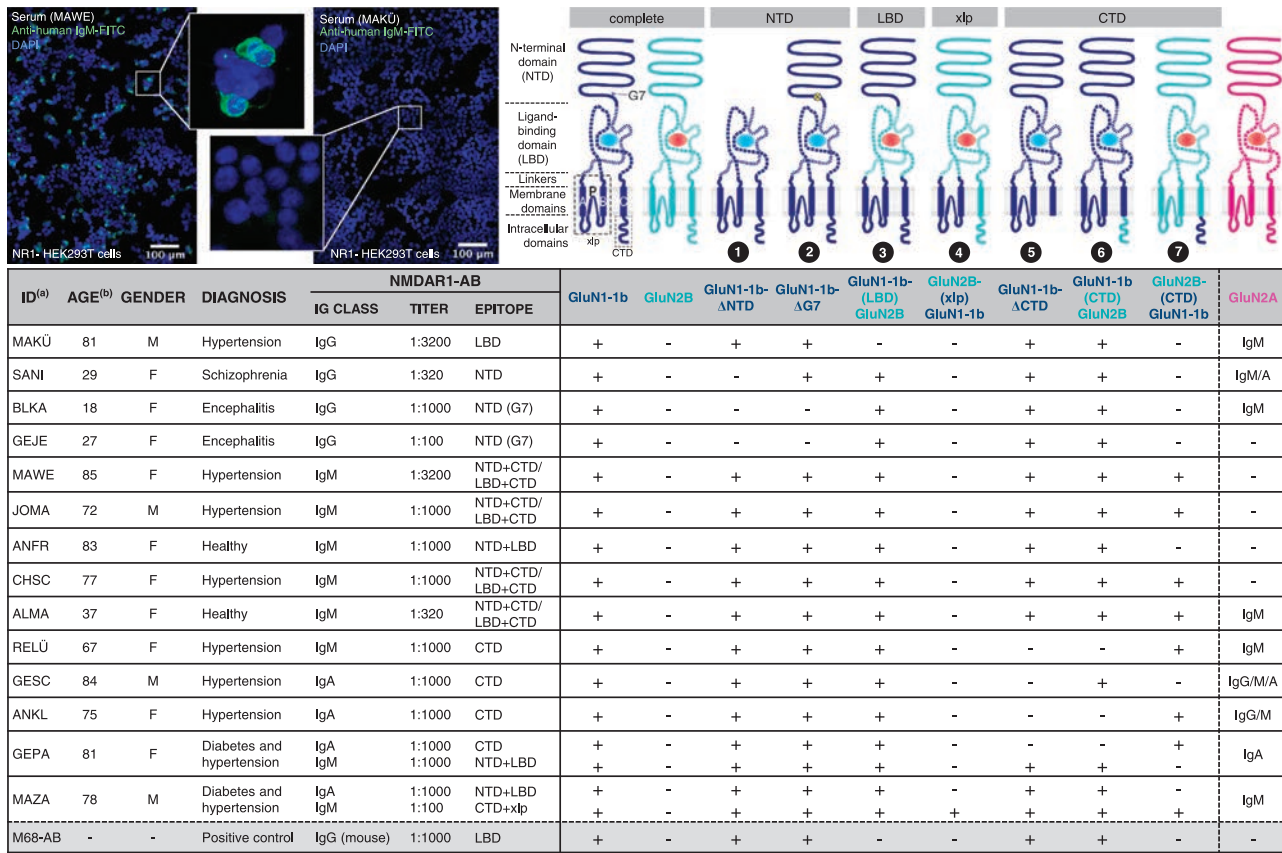


c NTD/G7 EPITOPES RECOGNIZED BY ANTI-NMDAR ENCEPHALITIS SERA

ID ^(a)	AGE ^(b)	GENDER	NMDAR1-AB		GluN1-1b	GluN1-1b-ΔNTD	GluN1-1b-ΔG7
			IG CLASS	TITER			
HP1	21	F	IgG	1:100	NTD (G7)	+	-
			IgM	1:10	Other	+	+
HP2	18	F	IgG	1:10	NTD (G7)	+	-
			IgM	1:100	Other	+	+
HP3	30	F*	IgG	1:100	NTD	+	-
			IgM	1:100	Other	+	+
HP4	19	F*	IgG	1:100	Other	+	+
			IgM	1:10	Other	+	+
HP5	27	F	IgG	1:10	NTD (G7)	+	-
			IgM	1:100	Other	+	+
HP6	22	F*	IgG	1:100	NTD (G7)	+	-
			IgA	1:1000	other	+	+
HP7	19	F*	IgG	1:100	Other	+	+
			IgA	1:10	Other	+	+

^(a) Scrambled identification code; ^(b) Age at examination (years); *cases with ovarian teratoma.

Figure 3. GluN1-1b constructs for epitope mapping of NMDAR1-AB. **(a)** Topology and domain structure of the GluN1-1b constructs used. The scheme on the left side shows the membrane topology of the GluN1-1b subunit, with domains colored as in **(b)**. Chimeras and mutagenic constructs targeting the different domains of GluN1 are explained on the right (all residue numbers include the signal peptide; GluN1 and GluN2B constructs were generated based on GenBank accession numbers U08263 and NM_012574, respectively). **(b)** Amino-acid sequence and domains of GluN1-1b. The position marked in the sequence as G7 (glycosylation site 7) is the residue to which the oligosaccharide is attached (N³⁸⁹). The recognition site for this type of glycosylation is N-X-S/T; therefore, mutation of T³⁹¹ to A in the construct number 2 (GluN1-1b-ΔG7) prevents glycosylation 2 residues upstream of it (N³⁸⁹). **(c)** NTD/G7 epitopes recognized by serum NMDAR1-AB of different Ig classes from seven female patients with diagnosed anti-NMDAR encephalitis. AB, antibodies; CTD, C-terminal domain; L1, intracellular loop 1; L2, intracellular loop 2; LBD, ligand-binding domain; NMDAR1, N-methyl-D-aspartate-receptor subunit NR1; NTD, N-terminal domain; P, ion channel pore; TMD, transmembrane domains; xlp, extra-large pore domain.



^(a) Scrambled identification code; ^(b) Age at examination (years).

Figure 4. NMDAR1-AB recognize several GluN1-1b epitopes. The figure-table, summarizing the results of NMDAR1-AB epitope mapping, includes only seropositive individuals. *Upper left:* Representative tilescan confocal images of HEK293T cells transfected with NMDAR1 as used for serum testing are shown. NMDAR1-AB seropositivity (left) and seronegativity (right) is illustrated for IgM as example (anti-human IgM FITC-labeled as secondary antibody). Insets are $\times 4$ magnifications of the squared areas in their respective images. All images are Z-projections of 10 consecutive focal planes located $0.5 \mu\text{m}$ apart and were taken under a confocal laser-scanning microscope using $\times 100$ oil objective (Leica TSC-SP5). *Upper right:* Schematic drawings of the different constructs used to transfected HEK293T cells (compare Figure 3). The first two constructs represent the complete version of the GluN1-1b and GluN2B subunits of NMDAR. The next seven constructs present deletions, mutations or replacements of defined regions, allowing identification of the epitopes recognized by NMDAR1-AB from healthy and ill individuals. Positivity (+) or negativity (-) for every construct in every sample is listed underneath. On the very right side, anti-GluN2A seropositivity/Ig class is listed (anti-GluN2A titers range from 1:10 up to 1:200). AB, autoantibodies; CTD, C-terminal domain; Ig, immunoglobulin; NMDAR1, N-methyl-D-aspartate-receptor subunit NR1; NTD, N-terminal domain.

test P -values: IgG: $P < 0.001$; IgM: $P < 0.001$; IgA: $P = 0.012$ and IgM + IgA: $P < 0.001$).

To investigate the impact of NMDAR1-AB on activity, glutamate-evoked responses were evaluated in *Xenopus laevis* oocytes co-expressing human NR1-1/NR2A subunits. Only 6 min after exposure of oocytes to human sera, the AUC of the glutamate-evoked response was significantly lower in seropositive compared with seronegative samples. This effect was sustained for at least 16 min (Figure 2c; one-way repeated-measures ANOVA: time \times group interaction: $F_{7,189} = 7.431$, $P < 10^{-6}$; Bonferroni *post hoc* correction for multiple comparison: only P -values < 0.05 are shown). Evaluating Ig classes separately, the significant global effect remained (one-way repeated-measures ANOVA: time \times group interaction: $F_{35,168} = 1.98$; $P = 0.002$; Figure 2c, left lower graph).

Epitope mapping using seven different NMDAR1 constructs (Figures 3a and b) revealed recognition by the NMDAR1-AB-positive sera of different epitopes, located in the extracellular ligand-binding domain and N-terminal domain (NTD) as well as the intracellular C-terminal domain (CTD) and extra-large pore domain (xlp). NMDAR1-AB seropositivity was polyclonal/polyspecific in 7/14 sera and likely mono- or oligoclonal/oligospecific (mainly IgG) in 7/14. Whereas no GluN2B-AB (0/14) was found,

GluN2A-AB (9/14) was frequently detected in the NMDAR1-AB-positive sera (Figure 4). Separate exploratory analyses of GluN2A-AB carrier versus non-carrier sera regarding internalization assay and electrophysiology results did not reveal differences. Overall, no particular disease-related pattern appeared.

The G7 site of the NTD, an epitope believed to be crucial for NMDAR1-AB found in encephalitis,²⁵ was recognized in 2/10 sera binding to NTD (Figure 4, negativity for construct 2). Since these sera were from two anti-NMDAR encephalitis cases reported previously (without epitope mapping),⁸ we tested another seven sera from anti-NMDAR encephalitis patients specifically for this epitope. All seven sera had NMDAR1-AB of two Ig classes. Epitope location in NTD was seen in 5/7 sera for IgG, with 4/7 recognizing G7. IgM and IgA recognized other epitopes, as did IgG in 2/7 sera (not further determined due to lack of material) (Figure 3c).

DISCUSSION

The present paper systematically analyzed for the first time NMDAR1-AB of three Ig classes (IgM, IgG and IgA), derived from randomly selected individuals of different age, gender and medical condition, regarding *in vitro* functionality and epitope location. All NMDAR1-AB-positive sera tested led to NMDAR1

internalization in IPSC-derived human cortical neurons and to reduced glutamate-evoked response in NR1-1b/NR2A-expressing oocytes. Several different epitopes were identified, located in the extracellular part of NMDAR1 (NTD, ligand-binding domain) or intracellular, CTD and in the xlp, which were recognized by NMDAR1-AB of the IgG, IgA and IgM class. Importantly, there was no consistent functional or epitope pattern detectable regarding Ig class or health/disease state.

In light of the comparable functionality of all NMDAR1-AB tested here, the high seroprevalence (up to > 20%) of NMDAR1-AB is even more puzzling and may indicate a previously unknown dimension of 'physiological autoimmunity' that increases with age.^{9–13} But what are the inducers of such abundant formation of NMDAR1-AB that potentially influence brain function? So far, associations were found with certain forms of cancer, mainly ovarian teratoma,⁵ influenza A and B,^{9–13} as well as with a genome-wide significant marker on chromosome 1, rs524991,⁹ close to *NFIA*, a transcription factor mediating neuroprotective effects of NMDAR.²⁶ There are certainly more hitherto unknown predisposing factors for carrying these AB. Broader significance of NMDAR1-AB is underscored by their presence in mammals other than humans.²⁷ This is less surprising in view of the substantial seroprevalence also of other brain-directed AB in species like rabbits, pigs and cows.²⁸

While irrespective of the epitope, all 14 NMDAR1-AB-positive sera investigated here (IgM, IgG, IgA) revealed similar AB functionality (internalization, electrophysiology), the AB-inducing factors may have determined the epitopes via mechanisms like molecular mimicry.^{29,30} Published work on NMDAR1-AB epitopes is scarce^{25,31,32} and focused on IgG recognizing NTD and the NTD-G7 domain (N³⁶⁸/G³⁶⁹), probably because this region and Ig class was first deemed pathognomonic for anti-NMDAR-encephalitis.^{5,25} Indeed, the sera investigated here of two young females with diagnosed anti-NMDAR-encephalitis, originally reported within a series of schizophrenia cases,⁸ also recognized this epitope, however, without sticking out functionally (that is, regarding internalization or electrophysiology). Therefore, we analyzed sera of seven additional young female patients, diagnosed with anti-NMDAR encephalitis (4/7 with ovarian teratoma), in an NTD-G7-targeted epitope screen. Interestingly, all 7 subjects carried NMDAR1-AB of 2 Ig classes, but only IgG recognized NTD or NTD-G7 in 5/7 sera. Similarly, in a recent study on young females with neuropsychiatric manifestation of systemic lupus erythematosus, two epitopes in the NTD (outside G7) were recognized by NMDAR1-AB (only IgG tested). Regrettably, NTD was the only mapped region, functionality was not evaluated, and instead of a cell-based assay, the accepted gold standard, an ELISA was used.³² Together, these data suggest that factors predisposing young women to neuropsychiatric manifestations of NMDAR-associated autoimmunity are connected with NTD or NTD-G7 epitopes. The accentuated role of IgG in this context is still a matter of speculation but may be related to inflammation-induced class-switch in the brain.³³ Regarding NMDAR1-AB of the IgA class, a single study, mapping epitopes of two female patients, found in one of them evidence of NTD/G7 as a target epitope (likely among other epitopes).³¹ Interestingly, the significance of AB for brain manifestation of lupus erythematosus seems still debatable. In a recent study, lack of B cells and autoantibodies in a murine model of systemic lupus did not prevent the development of key features of neuropsychiatric lupus.³⁴

To conclude, all naturally occurring serum NMDAR1-AB obviously have pathogenic potential. For still unexplored reasons, they are highly frequent and their prevalence increases with age. NMDAR-AB seropositivity alone definitely does not justify immunosuppressive treatment. Syndromal relevance of serum NMDAR1-AB depends on accessibility to the brain, that is, blood-brain-barrier permeability.^{9,11,13,15} This permeability might differ regionally, thereby explaining individually variable

symptomatic consequences.² Moreover, inflammation in the brain likely has a crucial role in determining syndrome acuteness and severity as contributed by circulating NMDAR1-AB and respective plasma cells, including boost in AB titers (upon epitope recognition) and class-switch to IgG.³³ Especially in individuals where an overt encephalitis diagnosis is unlikely, determination of blood-brain-barrier disruption, for example, by a novel magnetic resonance imaging method,³⁵ may prove helpful for estimating necessity and benefit of immunosuppressive therapeutic interventions.

CONFLICT OF INTEREST

The authors declare no conflict of interest.

ACKNOWLEDGMENTS

This work was supported by the Max Planck Society, the Deutsche Forschungsgemeinschaft (Center for Nanoscale Microscopy & Molecular Physiology of the Brain), EXTRABRAIN EU-FP7 and the Niedersachsen-Research Network on Neuroinfectiology (N-RENNT). The assistance by the UMG-Stem Cell Unit (S. Chen and L. Cyganek) is greatly appreciated.

AUTHOR CONTRIBUTIONS

HE, MH and DB contributed to concept and design of the study. ECG, BO, DT, SB, RT, PZ, JS, CK, HoP, BJ, HP, WHZ, DB, MH and HE contributed to data acquisition/analysis/interpretation. HE, ECG, BO, DT and MH contributed to drafting manuscript and figures. All authors read and approved the final version of the manuscript.

REFERENCES

- Sutton I, Winer JB. The immunopathogenesis of paraneoplastic neurological syndromes. *Clin Sci* 2002; **102**: 475–486.
- Diamond B, Huerta P, Mina-Osorio P, Kowal C, Volpe B. Losing your nerves? Maybe it's the antibodies. *Nat Rev Immunol* 2009; **9**: 449–456.
- Coutinho E, Harrison P, Vincent A. Do neuronal autoantibodies cause psychosis? A neuroimmunological perspective. *Biol Psychiatry* 2014; **75**: 269–275.
- Crisp SJ, Kullmann DM, Vincent A. Autoimmune synaptopathies. *Nat Rev Neurosci* 2016; **17**: 103–117.
- Dalmau J, Gleichman AJ, Hughes EG, Rossi JE, Peng X, Lai M *et al*. Anti-NMDA-receptor encephalitis: case series and analysis of the effects of antibodies. *Lancet Neurol* 2008; **7**: 1091–1098.
- Wandinger KP, Saschenbrecker S, Stoecker W, Dalmau J. Anti-NMDA-receptor encephalitis: a severe, multistage, treatable disorder presenting with psychosis. *J Neuroimmunol* 2011; **231**: 86–91.
- Zandi MS, Irani SR, Lang B, Waters P, Jones PB, McKenna P *et al*. Disease-relevant autoantibodies in first episode schizophrenia. *J Neurol* 2011; **258**: 686–688.
- Steiner J, Walter M, Glanz W, Sarnyai Z, Bernstein HG, Vielhaber S *et al*. Increased prevalence of diverse N-methyl-D-aspartate glutamate receptor antibodies in patients with an initial diagnosis of schizophrenia: specific relevance of IgG NR1a antibodies for distinction from N-methyl-D-aspartate glutamate receptor encephalitis. *JAMA Psychiatry* 2013; **70**: 271–278.
- Hammer C, Stepniak B, Schneider A, Papiol S, Tantra M, Begemann M *et al*. Neuropsychiatric disease relevance of circulating anti-NMDA receptor autoantibodies depends on blood-brain-barrier integrity. *Mol Psychiatry* 2013; **19**: 1143–1149.
- Dahm L, Ott C, Steiner J, Stepniak B, Teegen B, Saschenbrecker S *et al*. Seroprevalence of autoantibodies against brain antigens in health and disease. *Ann Neurol* 2014; **76**: 82–94.
- Zerche M, Weissenborn K, Ott C, Dere E, Asif AR, Worthmann H *et al*. Preexisting serum autoantibodies against the NMDAR subunit NR1 modulate evolution of lesion size in acute ischemic stroke. *Stroke* 2015; **46**: 1180–1186.
- Steiner J, Teegen B, Schiltz K, Bernstein H-G, Stoecker W, Bogerts B. Prevalence of N-methyl-D-aspartate receptor autoantibodies in the peripheral blood: healthy control samples revisited. *JAMA Psychiatry* 2014; **71**: 839.
- Castillo-Gomez E, Kastner A, Steiner J, Schneider A, Hettling B, Poggi G *et al*. The brain as 'immunoprecipitator' of serum autoantibodies against NMDAR1. *Ann Neurol* 2015; **79**: 144–151.
- Busse S, Busse M, Brix B, Probst C, Genz A, Bogerts B *et al*. Seroprevalence of N-methyl-D-aspartate glutamate receptor (NMDA-R) autoantibodies in aging

- subjects without neuropsychiatric disorders and in dementia patients. *Eur Arch Psychiatry Clin Neurosci* 2014; **264**: 545–550.
- 15 Hammer C, Zerche M, Schneider A, Begemann M, Nave KA, Ehrenreich H. Apolipoprotein E4 carrier status plus circulating anti-NMDAR1 autoantibodies: association with schizoaffective disorder. *Mol Psychiatry* 2014; **19**: 1054–1056.
- 16 Moscato EH, Peng X, Jain A, Parsons TD, Dalmau J, Balice-Gordon RJ. Acute mechanisms underlying antibody effects in anti-N-methyl-D-aspartate receptor encephalitis. *Ann Neurol* 2014; **76**: 108–119.
- 17 Begemann M, Grube S, Papiol S, Malzahn D, Krampe H, Ribbe K *et al*. Modification of cognitive performance in schizophrenia by complexin 2 gene polymorphisms. *Arch Gen Psychiatry* 2010; **67**: 879–888.
- 18 Toyka K, Brachman D, Pestronk A, Kao I. Myasthenia gravis: passive transfer from man to mouse. *Science* 1975; **190**: 397–399.
- 19 Streckfuss-Bomeke K, Wolf F, Azizian A, Stauske M, Tiburcy M, Wagner S *et al*. Comparative study of human-induced pluripotent stem cells derived from bone marrow cells, hair keratinocytes, and skin fibroblasts. *Eur Heart J* 2013; **34**: 2618–2629.
- 20 Shi Y, Kirwan P, Livesey FJ. Directed differentiation of human pluripotent stem cells to cerebral cortex neurons and neural networks. *Nat Protoc* 2012; **7**: 1836–1846.
- 21 Schindelin J, Arganda-Carreras I, Frise E, Kaynig V, Longair M, Pietzsch T *et al*. Fiji: an open-source platform for biological-image analysis. *Nat Methods* 2012; **9**: 676–682.
- 22 Hogg RC, Bandelier F, Benoit A, Dosch R, Bertrand D. An automated system for intracellular and intranuclear injection. *J Neurosci Methods* 2008; **169**: 65–75.
- 23 Ho S, Hunt H, Horton R, Pullen J, Pease L. Site-directed mutagenesis by overlap extension using the polymerase chain reaction. *Gene* 1989; **77**: 51–59.
- 24 Wurch T, Lestienne F, Pauwels P. A modified overlap extension PCR method to create chimeric genes in the absence of restriction enzymes. *Biotechnol Tech* 1998; **12**: 653–657.
- 25 Gleichman AJ, Spruce LA, Dalmau J, Seeholzer SH, Lynch DR. Anti-NMDA receptor encephalitis antibody binding is dependent on amino acid identity of a small region within the GluN1 amino terminal domain. *J Neurosci* 2012; **32**: 11082–11094.
- 26 Zheng S, Eacker SM, Hong SJ, Gronostajski RM, Dawson TM, Dawson VL. NMDA-induced neuronal survival is mediated through nuclear factor I-A in mice. *J Clin Invest* 2010; **120**: 2446–2456.
- 27 Pruss H, Leubner J, Wenke NK, Czirjak GA, Szentiks CA, Greenwood AD. Anti-NMDA receptor encephalitis in the polar bear (*Ursus maritimus*) Knut. *Sci Rep* 2015; **5**: 12805.
- 28 DeMarshall C, Sarkar A, Nagele EP, Goldwaser E, Godsey G, Acharya NK *et al*. Utility of autoantibodies as biomarkers for diagnosis and staging of neurodegenerative diseases. *Int Rev Neurobiol* 2015; **122**: 1–51.
- 29 Diamond B, Honig G, Mader S, Brimberg L, Volpe BT. Brain-reactive antibodies and disease. *Annu Rev Immunol* 2013; **31**: 345–385.
- 30 Bhat R, Steinman L. Innate and adaptive autoimmunity directed to the central nervous system. *Neuron* 2009; **1**: 123–132.
- 31 Doss S, Wandinger KP, Hyman BT, Panzer JA, Synofzik M, Dickerson B *et al*. High prevalence of NMDA receptor IgA/IgM antibodies in different dementia types. *Ann Clin Transl Neurol* 2014; **1**: 822–832.
- 32 Ogawa E, Nagai T, Sakuma Y, Arinuma Y, Hirohata S. Association of antibodies to the NR1 subunit of N-methyl-D-aspartate receptors with neuropsychiatric systemic lupus erythematosus. *Mod Rheumatol* 2015; **1**: 1–7.
- 33 Zhang J, Jacobi AM, Wang T, Berlin R, Volpe BT, Diamond B. Polyreactive autoantibodies in systemic lupus erythematosus have pathogenic potential. *J Autoimmun* 2009; **33**: 270–274.
- 34 Wen J, Doerner J, Chalmers S, Stock A, Wang H, Gullinello M *et al*. B cell and/or autoantibody deficiency do not prevent neuropsychiatric disease in murine systemic lupus erythematosus. *J Neuroinflammation* 2016; **13**: 73.
- 35 Montagne A, Barnes SR, Sweeney MD, Halliday MR, Sagare AP, Zhao Z *et al*. Blood-brain barrier breakdown in the aging human hippocampus. *Neuron* 2015; **85**: 296–302.



This work is licensed under a Creative Commons Attribution-NonCommercial-NoDerivs 4.0 International License. The images or other third party material in this article are included in the article's Creative Commons license, unless indicated otherwise in the credit line; if the material is not included under the Creative Commons license, users will need to obtain permission from the license holder to reproduce the material. To view a copy of this license, visit <http://creativecommons.org/licenses/by-nc-nd/4.0/>

© The Author(s) 2016

4. PROJECT II

4. PROJECT II – Uncoupling the widespread occurrence of anti-NMDAR1 autoantibodies from neuropsychiatric disease in a novel autoimmune model

Overview of Project II

The crosstalk between the brain and the immune system is a dynamic process where molecules of both systems can influence each other. Although the synergy between both systems is undeniable, when it comes to autoimmune events involving the brain several questions remain unanswered. Presence of serum autoantibodies does not necessarily correlate with CNS disease, and pathogenicity relies on direct contact between the brain antigen and its autoantibody (Nagele *et al.* 2013). The BBB limits interactions between the CNS and the systemic immune system. During gestation, maternal IgG can cross the placenta, reach the fetal bloodstream and gain access to the brain parenchyma. In mouse, the BBB is permeable to IgG until E17.5 and a similar period of vulnerability to IgG is presumed for the developing human brain (Simister 2003, Braniste *et al.* 2014). After this developmental period, the BBB is responsible for an almost immunoglobulin free brain parenchyma (Brimberg *et al.* 2015). In the adult brain, the access of immunoglobulins is restricted to less than 1% of the circulating levels, with the expected transfer over an intact BBB of IgG being 1/500, of IgA 1/600, and of IgM 1/3000 of the serum concentration (Hammer *et al.* 2014, Crisp *et al.* 2016).

To circumvent the protective effect of the BBB, the majority of rodent studies addressing the effects of NMDAR-AB *in vivo* employed brain injection of anti-NMDAR encephalitis patient-derived IgG or CSF in Wistar rats or infusion into the ventricular system of mice (Manto *et al.* 2010, 2011, Planaguma *et al.* 2015, Wright *et al.* 2015). Systemic injection of immunoglobulins (IgA, IgM and IgG) extracted from seropositive individuals in *ApoE*^{-/-}, presenting a compromised BBB, has also been performed (Hammer *et al.* 2014). Altogether, these studies highlighted the *in vivo* functional outcomes of exposure to NMDAR-AB beyond receptor internalization. Increased levels of extra-synaptic glutamate, excitability of the motor cortex and higher seizure propensity to the pro-convulsant pentylentetrazol emerged as direct consequences of exposure (Manto *et al.* 2011, Wright *et al.* 2015). Long-term effects included memory deficits and depressive-like behaviour (Planaguma *et al.* 2015). *In vivo* studies extending their focus beyond the IgG isotype, reported a hypersensitive response to MK-801 (Dizocilpine), a GluN1 antagonist, upon systemic application of NMDAR-AB in *ApoE*^{-/-} (Hammer *et al.* 2014). Additional experiments using *ApoE*^{-/-} mice also demonstrated that circulating NMDAR-AB upon accessing the brain parenchyma bind to prefrontal cortex, hippocampus, cerebellum, brain stem and spinal cord and are not detected in the CSF

PROJECT II

(Castillo-Gomez *et al.* 2016). Interestingly, several brain areas of wild type mice, with an intact BBB, were also positive for NMDAR-AB but at lower titres demonstrating that NMDAR-AB can cross the BBB, possibly by one of the mechanisms mentioned in Figure 2 of the introduction (Castillo-Gomez *et al.* 2016).

Determination of NMDAR-AB seroprevalence using large cohorts of healthy and diseased individuals pinpointed an increase in seroprevalence upon ageing in humans (Hammer *et al.* 2014). The presence of natural autoantibodies has been previously described in other species (Marchalonis *et al.* 1993, Avrameas *et al.* 2007, DeMarshall *et al.* 2015, Pruss *et al.* 2015). To further understand the role of NMDAR-AB, beyond pathogenicity, a systematic screening to determine for the first time its prevalence and age-dependence in dogs, rats, mice, cats, rhesus macaques and baboons has been conducted. Due to the lack of reliable secondary antibodies for some of the species tested, direct immunoglobulin labelling using fluorescein isothiocyanate (FITC) labelled Protein A (Protein A-FITC) was employed to screen cat, dog, rat and monkey sera (Pruss *et al.* 2015). Protein A is a bacterial Fc receptor present in *Staphylococcus aureus* and known to bind the Fc-portion of immunoglobulins of different species (Richman *et al.* 1982, Boyle *et al.* 1987). Mouse and human samples were screened using IgM, IgA and IgG species-specific secondary antibodies. This assay was cross validated using human serum samples in a two-step procedure: (1) screening with a commercial cell-based assay comprised of GluN1-transfected HEK293 cells and anti-human isotype-specific secondary antibodies (Dalmau *et al.* 2008) and (2) immunoglobulin labelling with Protein A-FITC followed by screening with GluN1-transfected HEK293 cells. Additionally, serum of both monkey species were tested in an independent lab using IgM species-specific secondary antibodies resulting in a 97% concordance of the results obtained in both laboratories. With this screening strategy seropositivity for NMDAR-AB in cats, dogs, rats, mice, rhesus macaques and baboons was detected, extending the list of species with reported NMDAR-AB seropositivity. Moreover, as described in humans, an age-dependent increase in seroprevalence for all species except for monkeys was found. Non-human primates kept in captivity are exposed to chronic life stress (Jacobson *et al.* 2016) and changes in serum immunoglobulins, particularly IgA, have been reported in individuals with high-stress perception when exposed to psychological stress (Maes *et al.* 1997). Hence, this inter-species difference might be related with an immunological response to captivity-related stress that leads to the presence of NMDAR-AB since young age in monkeys. Furthermore, in humans that underwent migration, a known stress factor, the previously reported age-dependent increase in seroprevalence is lost. Migrants show an increased seroprevalence of NMDAR-AB at young age when compared to non-migrant individuals of the same age, with IgA being the most frequent isotype.

Due to the high amino acid sequence homology between the human GluN1 and the species included in this study, the endocytosis assay previously established (see Project I), was applied to test the functionality of these NMDAR-AB. In line with the results obtained for human seropositive samples (Castillo-Gomez&Oliveira *et al.* 2017), exposure to NMDAR-AB⁺ sera from all species mentioned above promoted reduction of surface NMDAR demonstrating their functionality.

In anti-NMDAR encephalitis, the presence of NMDAR-AB and an inflammatory brain context mediate the pathophysiological events associated with the disease (Dalmau *et al.* 2008). Although some triggering events of NMDAR-AB production have been described, it is not clear if the production of these autoantibodies has a pro-inflammatory effect in the brain or if the encephalitic phenotype observed is the result of an additional pathological event (Ehrenreich 2017). Hence, a direct link between NMDAR-AB and inflammation in the brain is missing. The presence of NMDAR-AB in healthy individuals has been previously reported, pointing to the importance of the BBB in preventing them from exerting their pathological effect (Hammer *et al.* 2014). To clarify the role of the BBB in this context *ApoE*^{-/-} mice and wild type (*ApoE*^{+/+}) littermates were immunized with a mixture of four peptide sequences of the extracellular part of GluN1, which included the glycosylation site G7. *ApoE*^{-/-} mice have been previously described as having an open BBB and blood nerve barrier presenting extensive IgG extravasation in sciatic nerve, cerebellum, spinal cord and cortical and subcortical areas as the hippocampus (Fullerton *et al.* 2001). Here, the BBB integrity of *ApoE*^{-/-} mice was reassessed using two fluorescent tracers with different molecular weights: Evans blue (EB: 960.81) and sodium fluorescein (NaFl: 376.28). Increased extravasation of both tracers was detected in *ApoE*^{-/-} confirming the leakiness of the BBB in these mice. Increased permeability of the BBB does not seem to have an impact in anxiety levels, activity, exploratory behaviour, motor and sensory function, sensorimotor gating, pheromone-based social preference and cognitive performance as determined in a comprehensive behavioural assessment of *ApoE*^{-/-} and *ApoE*^{+/+}.

Reduced spontaneous activity in the open field and hyperlocomotion following application of the GluN1 antagonist MK-801 in *ApoE*^{-/-} mice injected with human serum immunoglobulin extracts of seropositive patients has been previously reported (Hammer *et al.* 2014). Aiming at assessing the effects of NMDAR-AB in a more physiological context *ApoE*^{-/-} and *ApoE*^{+/+} mice were immunized using a mixture of GluN1 peptides, ovalbumin and Freund's Adjuvant or ovalbumin and Freund's Adjuvant as immunization control. In a primary immune response naïve B cells and T cells are mobilized and antibody production peaks in 7 to 10 days upon contact with the antigen. Further B cell activation due to contact with the antigen stimulates naïve or memory B cells to proliferate and differentiate to antibody secreting plasma cells. Upon active immunization, the first antibody isotype produced by a developing B cell is IgM.

PROJECT II

Mature B cells eventually go through class switch recombination events and produce IgA and IgG antibodies (Alberts *et al.* 2002). Endogenous NMDAR1-AB production was monitored overtime using an ELISA essay. Serum anti-ovalbumin and anti-GluN1 IgG antibodies were first detected between day 5 and 10 after immunization and were present until day 28. The lag phase of antibody production for ovalbumin and GluN1 antibodies was comparable between genotypes pointing to a primary immune response in both groups. This makes the presence of pre-existing memory B cells and a secondary immune response to ovalbumin and GluN1 antigens unlikely and corroborates the negative results for NMDAR-AB obtained with the serum tested prior immunization (pre-immune serum) (Pan&Oliveira *et al.* 2018).

Immunized and immunization control mice of both genotypes were tested in the open field upon administration of MK-801, 27 days post immunization. MK-801 is a selective non-competitive antagonist of NMDAR known to induce hyperlocomotion (Irifune *et al.* 1995). In mice, systemic application leads to reduction of NMDAR-mediated neurotransmission and increased extracellular glutamate levels in limbic brain regions. Enhanced non-NMDAR glutamatergic signalling in cortico-striatal circuitry in response to increased glutamate levels is one of the currently accepted explanations for this phenotype (Chartoff *et al.* 2005). While no changes were detected in baseline locomotion (pre- and post-immunization) between genotype or immunization groups, administration of MK-801 in GluN1 immunized $ApoE^{-/-}$ lead to hyperactive behaviour in the open field. This effect was not found in $ApoE^{-/-}$ immunized with ovalbumin or in $ApoE^{+/+}$ of both immunization groups. Altogether, these results are in line with the effects of NMDAR-AB observed upon systemic injection in $ApoE^{-/-}$ and demonstrate that the behavioural effects of NMDAR-AB require diffusion of these antibodies to the brain parenchyma through a compromised BBB (Hammer *et al.* 2014). Thus, the increased hyperactive behaviour revealed in immunized $ApoE^{-/-}$ is a result of the combinatorial effect of NMDAR antagonism by MK-801 and lower NMDAR surface expression due to endocytosis by NMDAR-AB, only possible in the presence of a compromised BBB (Pan&Oliveira *et al.* 2018).

An inflammatory milieu *per se* can be detrimental for brain function. To address a potential contribution of NMDAR-AB and an open BBB to the development of an inflammatory reaction in the brain and untangle NMDAR-AB's contribution to the phenotype, immunohistochemical analysis was performed for both genotype and immunization groups. This analysis focused on the hippocampus as, despite the widespread expression of GluN1 in the CNS, a preferential binding of NMDAR-AB to hippocampal regions has been reported (Dalmau *et al.* 2008, Hughes *et al.* 2010). Therefore, the number of Iba1⁺, CD68⁺, MHC-II⁺, CD3⁺ cells was quantified and a densitometric analysis of GFAP⁺ was performed in the hippocampus. No significant differences between groups was observed for all markers assessed, pointing to no effect of the immunization with NMDAR-AB or presence of a leaky BBB in microglial cell

numbers and activation status as well as T cells or development of astrogliosis. Additionally, no difference in brain's water content between genotypes was observed, supporting the absence of inflammation in the presence of an open BBB. Altogether, this data suggests that the presence of these NMDAR1-AB alone does not trigger an inflammatory reaction and additional pro-inflammatory events are required to develop an encephalitic phenotype.

To conclude, several mammal species were systematically screened for NMDAR-AB seropositivity and seroprevalence, in young and old age, and for NMDAR-AB functionality. The results of this project broadened the number of species with reported seropositivity for NMDAR-AB and confirmed an age-dependent increase in seroprevalence in cats, dogs, rats and mice not present in monkeys or humans that underwent migration. Furthermore, by establishing a new autoimmune mouse model, with endogenous production of NMDAR-AB, the importance of an intact BBB in preventing NMDAR-AB of exerting its effects in the brain was confirmed and the development of an inflammatory reaction was uncoupled from the effects of NMDAR-AB in brain.

Original publication

Pan H*, **Oliveira B***, Saher G*, Dere E, Tapken D, Mitjans M, Seidel J, Wesolowski J, Wakhloo D, Klein-Schmidt C, Ronnenberg A, Schwabe K, Trippe R, Mätz-Rensing K, Berghoff S, Al-Krinawe Y, Martens H, Begemann M, Stöcker W, Kaup FJ, Mischke R, Boretius B, Nave KA, Krauss JK, Hollmann M, Lühder F, Ehrenreich H. *Uncoupling the widespread occurrence of anti-NMDAR1 autoantibodies from neuropsychiatric disease in a novel autoimmune model.* Molecular Psychiatry. 2018, *in press*.

*Authors with equal contribution

Personal contribution: As one of the first authors of this manuscript, I was involved in data acquisition and analysis of the experiments supporting the functionality of NMDAR autoantibodies in several mammalian species, including the preparation of human IPS cells derived neurons used to test functionality *in vitro*. I have analysed the open field data regarding the immunized mice injected with MK-801 and done the immunohistochemistry experiments to assess inflammation in the brain. I was responsible for all the experiments requested for the paper's revision, which included quantification of CD68⁺ and MHC-II⁺ cells in the hippocampus and densitometric analysis of GFAP expression in the CA1 and CA3 hippocampal areas (unpublished data). Additionally, I contributed to the study design and to the overall writing of the manuscript. I wrote the methods section of this paper, prepared the figures and figure legends. I contributed significantly to the revision and the rebuttal letter



Uncoupling the widespread occurrence of anti-NMDAR1 autoantibodies from neuropsychiatric disease in a novel autoimmune model

Hong Pan¹ · Bárbara Oliveira¹ · Gesine Saher² · Ekrem Dere¹ · Daniel Tapken³ · Marina Mitjans¹ · Jan Seidel¹ · Janina Wesolowski¹ · Debia Wakhloo¹ · Christina Klein-Schmidt³ · Anja Ronnenberg¹ · Kerstin Schwabe⁴ · Ralf Trippe³ · Kerstin Mätz-Rensing⁵ · Stefan Berghoff² · Yazeed Al-Krinawe⁴ · Henrik Martens⁶ · Martin Begemann¹ · Winfried Stöcker⁷ · Franz-Josef Kaup⁵ · Reinhard Mischke⁸ · Susann Boretius⁹ · Klaus-Armin Nave^{2,10} · Joachim K. Krauss⁴ · Michael Hollmann³ · Fred Lühder¹¹ · Hannelore Ehrenreich^{1,10}

Received: 29 August 2017 / Revised: 20 October 2017 / Accepted: 30 October 2017
© The Author(s) 2018. This article is published with open access

Abstract

Autoantibodies of the IgG class against N-methyl-D-aspartate-receptor subunit-NR1 (NMDAR1-AB) were considered pathognomonic for anti-NMDAR encephalitis. This view has been challenged by the age-dependent seroprevalence (up to >20%) of functional NMDAR1-AB of all immunoglobulin classes found in >5000 individuals, healthy or affected by different diseases. These findings question a merely encephalitogenic role of NMDAR1-AB. Here, we show that NMDAR1-AB belong to the normal autoimmune repertoire of dogs, cats, rats, mice, baboons, and rhesus macaques, and are functional in the NMDAR1 internalization assay based on human iPSC-derived cortical neurons. The age dependence of seroprevalence is lost in nonhuman primates in captivity and in human migrants, raising the intriguing possibility that chronic life stress may be related to NMDAR1-AB formation, predominantly of the IgA class. Active immunization of *ApoE^{-/-}* and *ApoE^{+/+}* mice against four peptides of the extracellular NMDAR1 domain or ovalbumin (control) leads to high circulating levels of specific AB. After 4 weeks, the endogenously formed NMDAR1-AB (IgG) induce psychosis-like symptoms upon MK-801 challenge in *ApoE^{-/-}* mice, characterized by an open blood–brain barrier, but not in their *ApoE^{+/+}* littermates, which are indistinguishable from ovalbumin controls. Importantly, NMDAR1-AB do not induce any sign of inflammation in the brain. Immunohistochemical staining for microglial activation markers and T lymphocytes in the hippocampus yields comparable results in *ApoE^{-/-}* and *ApoE^{+/+}* mice, irrespective of immunization against NMDAR1 or ovalbumin. These data suggest that NMDAR1-AB of the IgG class shape behavioral phenotypes upon access to the brain but do not cause brain inflammation on their own.

Introduction

Autoantibodies (AB) of the immunoglobulin G (IgG) class against the N-methyl-D-aspartate-receptor subunit-NR1 (NMDAR1) were originally interpreted as pathognomonic for a condition called “anti-NMDAR encephalitis”, characterized by high serum and cerebrospinal fluid (CSF) titers

of these AB, as well as a variably favorable response to immunosuppressive therapy. The reported syndrome, reflecting typical NMDAR1 antagonistic actions, consisted of psychosis, epileptic seizures, dyskinesia, cognitive decline, reduced consciousness, and autonomic dysregulation [1–4]. However, work on >5000 individuals, healthy or affected by different diseases, consistently revealed overall comparable age-dependent seroprevalence of functional NMDAR1-AB of all Ig classes, nurturing serious doubts regarding a purely pathological role of NMDAR1-AB of any Ig class [5–10].

NMDAR1-AB apparently belong to a pre-existing autoimmune repertoire [11–17], where Ig isotypes are determined by extracellular vs. intracellular antigen location [6]. This may explain the rarity of the IgG class among AB directed against extracellular epitopes, e.g., NMDAR1,

Hong Pan, Bárbara Oliveira, and Gesine Saher contributed equally to this work.

✉ Hannelore Ehrenreich
ehrenreich@em.mpg.de

Extended author information available on the last page of the article

MOG, and CASPR2. In contrast, AB that recognize intracellular antigens, e.g., amphiphysin, ARHGAP26, or GAD65, show predominance of IgG [6]. Despite this apparent “physiological autoimmunity”, no report exists that systematically screened mammals other than humans for the presence of NMDAR1-AB. In recent work, we found that all naturally occurring NMDAR1-AB are functional and thus have pathogenic potential irrespective of epitope and Ig class [10]. Pathophysiological significance may emerge in conditions of compromised blood–brain barrier (BBB), for instance, upon injury, infection, inflammation, or genetic predisposition (*APOE4* haplotype), which then allows substantial access of circulating NMDAR1-AB to the brain where they act as NMDAR antagonists [5, 9, 18–20]. Alternatively, AB-specific plasma cells may reside or settle in the brain and produce large amounts of AB intrathecally [14, 21]. The question whether abundant endogenously produced NMDAR1-AB of the IgG class can—upon access to the brain—induce inflammation and thus “anti-NMDAR1 encephalitis” has never been experimentally addressed.

The present paper has therefore been designed to (i) systematically screen mammals other than humans for seroprevalence of functional NMDAR1-AB and (ii) study mice with open BBB behavioral and morphological consequences of high circulating levels of endogenous NMDAR1-AB of the IgG class formed in response to immunization.

Materials and methods

Ethical approvals

Ethics committees of Georg-August University, Göttingen, and collaborating centers approved the Göttingen Research Association for Schizophrenia (GRAS) data collection and other studies “extended GRAS” acquiring human data, serum samples, and IPSC [5, 6, 8, 9, 22, 23]. Hannover Medical School Ethics Committee approved the neurosurgical specimen collection. Studies comply with Helsinki Declaration. Patients gave written informed consent. Mouse studies were approved by Animal Ethics (LAVES, Oldenburg) following German Animal Protection Law.

Notes: All experiments were performed by researchers unaware of group assignment. The new nomenclature GluN1 for NMDAR1 is mostly disregarded here for consistency with the respective literature.

Human samples

GRAS and “extended GRAS”

The GRAS [22, 23] subsample used here consists of deep-phenotyped patients ($N = 970$; age 39.29 ± 0.40 years; 66.3%

men), diagnosed with schizophrenia or schizoaffective disorder according to DSM-IV-TR [24]. Subjects of “extended GRAS” ($N = 4933$; age 43.29 ± 0.24 years; 56.9% men) comprise healthy individuals and patients with different neuropsychiatric diagnoses, including schizophrenia, affective disorders, multiple sclerosis, Parkinson, ALS, stroke, and personality disorders (detailed description in [5, 6, 8, 9]). For this study, subjects are dichotomously classified as nonmigrants or migrants comprising first (patient migrated) and second generation (parents migrated). Identified migrants ($N = 301/N = 4933$) are from Europe (49.8%), Asia (36.9%), Africa (9%), North America (2%), South America (0.7%), or mixed (1.6%).

Neurosurgical patients

A total of $N = 72$ paired samples of serum and ventricular CSF were available from patients ($N = 45$ women; age 55.9 ± 2.2 years; $N = 27$ men; age 60.2 ± 2.7 years) undergoing neurosurgery for various reasons: meningiomas, metastases, and other brain tumors ($N = 25$); intracerebral/subarachnoid hemorrhages ($N = 20$); hydrocephalus ($N = 12$); arterial aneurysms ($N = 7$); trigeminal neuralgia ($N = 4$); and others ($N = 4$). Most pairs were taken simultaneously at the time point of surgery, i.e., <5 min ($N = 64$) or <30 min ($N = 8$) apart.

Other mammals

Dogs and cats

Serum samples from dogs and cats of different breeds were prospectively collected during routine (health check/vaccination) or diagnostic (spectrum of different disorders) workup of outpatients in the Small Animal Clinic, University of Veterinary Medicine, Hannover.

Monkeys

Serum samples from healthy baboons and rhesus macaques were obtained through routine checkups at the Leibniz Institute for Primate Research, Göttingen.

Rodents

Serum samples from healthy rats and mice were obtained at the Max Planck Institute of Experimental Medicine and the Institute for Multiple Sclerosis Research, Göttingen.

Serological analyses

NMDAR1-AB determination by clinical standard procedures

Human serum and ventricular CSF were tested for NMDAR1-AB positivity using commercially available kits,

based on HEK293T cells transfected with NMDAR1 and secondary AB against human IgG, IgM, or IgA (Euroimmun, Lübeck, Germany) [2, 25]. Mouse serum was analyzed using the same assay with secondary AB against mouse IgG, IgM, or IgA (M31001, A-31570, A-21042; Thermo Fisher, Rockford, USA).

NMDAR1-AB IgM screening in monkey samples

HEK293T cells (50,000) cultured at 37 °C/8% CO₂ in DMEM (high glucose, Life Technologies, Carlsbad, USA) were seeded on a 35-mm dish, grown for 3 days, and transfected with 3 µg of myc-His-tagged GluN1-1b cloned into pcDNA4/TO/myc-His A (Invitrogen, Carlsbad, USA) using Metafectene-Pro (Biontex, Munich, Germany) [10]. One day post transfection, cells were split onto five poly-D-lysine-coated coverslips in a 35-mm dish and 1 day later, they were fixed with 5% paraformaldehyde (PFA) for 20 min, washed 5× (PBS), permeabilized with 0.1% Triton X-100 for 5 min, again washed 5× (PBS), and blocked with 5% normal goat serum (NGS; Sigma-Aldrich, Munich, Germany) for 1 h. After five PBS washes, cells were incubated with serum and monoclonal mouse anti-myc IgG (clone 9E10, Hollmann-Lab, Bochum) for 1 h, washed with 10× (PBS), incubated for 1 h with fluorescein-labeled goat anti-monkey IgM (072-11-031; KPL, Gaithersburg, USA) and AlexaFluor®594-labeled goat anti-mouse IgG (A11005; Thermo Fisher) secondary AB, and PBS washed 5×. Cells were mounted in Fluoromount-G (Southern Biotech, Birmingham, USA) and analyzed via TCS-SP2-AOBS confocal microscope (63× oil immersion objective; Leica-Microsystems, Wetzlar, Germany). The results were independently assessed by three investigators.

Protein-A assay

Human serum (for cross-validating clinical standard procedure and protein-A method), as well as dog, cat, rat, and monkey serum were labeled with protein-A from *Staphylococcus aureus*, binding the Fc portion of immunoglobulins of different species [26]. Plasma (50 µl) and 25 µg of FITC-conjugated protein-A (Sigma-Aldrich) were incubated for 2 h in the dark at room temperature (RT). The mixture was then diluted to 250 µl (PBS) and unbound FITC-Protein-A was removed using 100-kDa Amicon filter units (Sartorius, Göttingen, Germany), reconcentrating to ~50 µl [27]. NMDAR1-AB seropositivity was determined using Euroimmun assay combined with commercial monoclonal mouse NMDAR1-AB (114011; M68, SYSY, Göttingen, Germany). Samples showing distinct double labeling were rated “positive” (>98% consensus of three investigators).

Endocytosis assay

Functional studies were conducted with sera following ammonium-sulfate precipitation of immunoglobulins [28] and dialysis (Slide-A-Lyzer® Mini Dialysis Units, 10,000 MWCO Plus Float, Thermo Fisher). To assess AB functionality, human iPSC-derived neurons were exposed to dialyzed serum [10]. For each species, arbitrarily selected seronegative ($N = 1$) and seropositive samples ($N = 2-3$) were analyzed. Briefly, cells were precooled on ice and washed prior to incubation in cold HBSS with 1:50 diluted dialyzed sera, control NMDAR1-AB (M68-SYSY), or HBSS alone (negative control) for 30 min/4 °C. After washing to remove unbound AB, neurons were returned to their media and incubated for 20 min at 37 °C (three coverslips/sample, endocytosis) or 4 °C (one coverslip/sample, endocytosis control). The remaining surface NMDAR1 was exposed to mouse anti-human NMDAR1-AB (N-terminal; ab134308; Abcam, Cambridge, UK, 1:100), followed by labeling with secondary donkey anti-mouse IgG (A10036; Life Technologies, AlexaFluor®546, 1:100). Neurons were fixed with ice-cold 4% PFA and double stained with chicken anti-NeuN-AB (266006; SYSY, 1:500) and secondary donkey anti-chicken AB (703-546-155; Life Technologies, AlexaFluor®488, 1:250). Nuclei were visualized using DAPI (Sigma-Aldrich, 0.01 µg/ml). After PBS wash, coverslips were mounted on SuperFrost®-Plus slides with Mowiol mounting media (Sigma-Aldrich). Confocal laser-scanning microscopy was used to quantify NMDAR1 density at the membrane (63× glycerol objective; TCS-SP5 Leica-Microsystems, Mannheim, Germany). From each coverslip, Z series of optical sections (0.5 µm apart) covering the three-dimensional extension of neurons were acquired (sequential scanning mode, identical acquisition parameters). FIJI-ImageJ software [29] was used to randomly select NeuN⁺ cells and determine soma profile. Fluorescence intensity/cell surface area (AlexaFluor546) was automatically measured as readout of NMDAR1 surface expression. After background subtraction, the mean intensity for each coverslip was determined and fluorescence intensity ratio (37/4 °C) was calculated.

BBB-integrity testing

BBB integrity of 12-month-old *ApoE*^{-/-} ($N = 5$) and *ApoE*^{+/+} ($N = 5$) mice was determined using two different fluorescent tracers, Evans blue (50 mg/g body weight) [30] and sodium fluorescein (200 mg/g body weight). A detailed description of this method will be published elsewhere [31]. Briefly, for tracer quantification in the brain at 4 h after intravenous injection in the tail vein, animals were PBS perfused to remove the circulating tracer. Brains were dissected, immediately frozen on dry ice, weighed, and stored

at -80°C . Tissue was lyophilized at -56°C for 24 h under vacuum of 0.2 mBar (Christ LMC-1-BETA-1-16, Osterode, Germany). For tracer extraction, hemispheres were incubated with shaking in 10 ml formamide/mg brain at 57°C for 24 h. Integrated density of tracer fluorescence was determined in triplicates on a fluorescent microscope (Observer Z2, Zeiss, Germany), equipped with Axio-CamMRc3, 1×Camera-Adapter, and ZEN2012 blue-edition software, recorded at 10× magnification (Plan-Apochromat 10×/0.45M27). Tracer concentration was calculated using a standard curve and normalized to controls (set to 1).

Mouse immunization

Mice (12-month-old C57BL/6 littermates: $ApoE^{-/-}N = 20$ and $ApoE^{+/+}N = 23$; genders balanced) were immunized with a mixture of GluN1 extracellular peptides and/or chicken ovalbumin (Sigma-Aldrich), and emulsified in equal volume of complete Freund's Adjuvant (*Mycobacterium tuberculosis* H37RA plus incomplete Freund's Adjuvant; Becton-Dickinson, Sparks, USA) at a final concentration of 1 mg/ml [32]. At the tail base, 50 μg of GluN1 peptides and/or 20 μg of ovalbumin were injected subcutaneously (each side one).

Enzyme-linked immunosorbent assay (ELISA)

Orbital sinus blood of immunized mice was stored as EDTA plasma at -80°C . ELISA plates (96 well) were coated with 0.5 μg of GluN1 peptide mixture or 0.2 μg of chicken ovalbumin in 50 μl PBS/well overnight at 4°C and blocked with 5% BSA/PBS (Carl Roth, Karlsruhe, Germany). Mouse plasma (1:1000 or 1:50,000 5% BSA/PBS 50 μl /well) was added for 2 h at RT. The signal was amplified with horseradish peroxidase-linked anti-IgG (Sigma-Aldrich), and 3,3',5,5'-Tetramethylbenzidine as colorimetric substrate (BD Biosciences, San Jose, USA). Absorbance at 450 nm was measured by microplate reader (Tecan-Trading AG, Männedorf, Switzerland).

Basic behavioral screening

The behavioral test battery was performed as described previously [33–36]. Starting at age 5 months, experimentally naïve $ApoE^{-/-}$ and $ApoE^{+/+}$ littermates underwent (during light phase) tests of anxiety, activity and exploratory behavior (elevated plus-maze, open field, hole-board), motor (rotarod, grip strength) and sensory function (visual cliff, olfaction, hearing, hot plate), sensorimotor gating (prepulse inhibition), pheromone-based social preference, and cognitive performance (IntelliCage place/reversal learning). Males and females were tested separately.

Baseline and post MK-801 locomotion in the open field

The open-field apparatus consisted of a gray circular Perspex-arena (120 cm diameter; wall height 25 cm). Indirect white light illumination ensured constant light intensity of 120 lux in the center. Locomotion was measured using automated tracking software (Viewer2-Biobserve, Bonn, Germany). $ApoE^{-/-}$ and $ApoE^{+/+}$ littermates received four baseline measurements preimmunization and post immunization (15 min each), the last followed by intraperitoneal MK-801 (Dizocilpine-[5S,10R]-(+)-5-methyl-10,11-dihydro-5H-dibenzo[a,d]cyclohepten-5,10-imine hydrogen maleate; 0.3 $\mu\text{g}/10\ \mu\text{l}$ PBS/g Sigma-Aldrich). MK-801 is a noncompetitive NMDAR antagonist, acting as a use-dependent ion-channel blocker, and known to induce psychosis-like hyperactivity in the open field (loss of inhibition) [37]. Directly post injection, locomotor activity in open field was analyzed (4 min intervals), with the first 4 min defined as reference locomotion to express changes over 120 min as % reference.

Immunohistochemistry

Mice were anesthetized with Avertin (2,2,2-Tribromoethanol, Sigma-Aldrich), and transcardially perfused with 4% PFA/Ringer solution (Braun-Melsungen, Germany). Brains were removed, postfixed in 4% PFA overnight at 4°C , and incubated in 30% sucrose/PBS for 2 days at 4°C . Brains were cryosectioned coronally into 30 μm slices and stored in 25% ethylene glycol and 25% glycerol/PBS at -20°C . Frozen sections (three/mouse; rostral hippocampus), mounted on SuperFrost®-Plus slides (Thermo Fisher, Waltham, USA), were used for cell quantification. For CD3 staining, sections were microwaved 3× for 4 min in citrate buffer (1 mM, pH 6) and blocked with 5% normal horse serum (NHS), and 0.5% Triton X-100/PBS for 1 h at RT. Incubation with rat anti-mouse CD3 (MCA1477; BioRad, Hercules, USA; 1:100) diluted in 5% NHS, and 0.5% Triton X-100/PBS was performed for two nights/ 4°C , followed by incubation with goat anti-rat AlexaFluor®647 (A-21247; Thermo Fisher, Schwerte, Germany; 1:1000) diluted in 5% NHS, and 0.5% Triton X-100/PBS for 2 h at RT. For Iba1, GFAP, CD68, and MHC-II staining, sections were blocked with 5% NGS and/or 5% NHS in 0.5% Triton X-100/PBS for 1 h at RT. Incubation with rabbit anti-mouse Iba1 (019-19741; Wako-Chemicals GmbH, Neuss, Germany; 1:1000), or mouse anti-mouse GFAP (NCL-GFAP-GA5; Novocastra-Leica, Newcastle upon Tyne, UK; 1:500), diluted in 3% NGS or 3% NHS, and 0.5% Triton X-100/PBS, was performed overnight, and incubation with rat anti-mouse CD68 (MCA1957GA; BioRad GmbH, München, Germany, 1:400) and rat

anti-mouse MHC-II (14-5321; eBioscience, San Diego, USA, 1:100) diluted in 3% NGS and 3% NHS, and 0.5% Triton X-100/PBS, was performed over two nights, all at 4 °C. Incubation with secondary antibodies was performed with goat anti-rabbit AlexaFluor®555 (A-21428; Thermo Fisher; 1:500) diluted in 3% NGS, 0.5% Triton X-100/PBS, or donkey anti-rabbit AlexaFluor®488 (A-21206; Thermo Fisher, 1:500) or donkey anti-mouse AlexaFluor488 (A21202; Thermo Fisher, 1:500) or goat anti-rat AlexaFluor®647 (A-21247; Thermo Fisher, 1:500), diluted in 3% NGS or 3% NHS, and 0.5% Triton X-100/PBS for 1.5 h at RT. Nuclei were counterstained with DAPI (Sigma-Aldrich, 0.01 µg/ml) and sections were mounted using Aqua-Poly/Mount (Polysciences, Warrington, USA). Tile scans of hippocampus were acquired using Leica-DMI6000 epifluorescence microscope (20× objective; Leica) and Iba1⁺ and CD3⁺ cells were counted using cell counter plug-in of FIJI-ImageJ software [29]. GFAP⁺ cells in the hippocampus were quantified densitometrically upon uniform thresholding (expressed as % respective area).

Statistical analyses

Statistical analyses were performed using SPSSv.17 (IBM-Deutschland-GmbH, Munich, Germany) or Prism4 (GraphPad Software, San Diego, California, USA). Group differences in categorical and continuous variables were assessed using χ^2 , Mann–Whitney U, or Student's *t*-tests depending on data distribution/variance homogeneity. ANOVA was employed as indicated in display item legends. All *p*-values are two tailed; significance is set to *p* < 0.05; data are presented as mean ± S.E.M.

Results

Cross-validation of NMDAR1-AB detection methods

To determine NMDAR1-AB seropositivity in mammals other than humans, we had to validate the protein-A detection method [27]. For that, *N* = 72 paired human serum and ventricular CSF samples, prospectively collected from random neurosurgical patients, were analyzed by the usual cell-based assay, employing specific secondary AB for all Ig classes. A total of *N* = 5 sera turned out NMDAR1-AB positive (titers ≤ 1:100; 3 × IgM; 2 × IgA; 0 × IgG). Ventricular CSF samples were all negative. For cross-validation of NMDAR1-AB of the IgG class, we used serum of a seropositive stroke patient [8]. Application of protein-A method combined with double labeling for NMDAR1-AB M68 confirmed positive and negative results (Fig. 1a).

High seroprevalence of NMDAR1-AB across mammalian species

We next analyzed by protein-A method serum samples of dogs, cats, rats, baboons, and rhesus macaques. Strikingly, all mammalian species, independent of their respective life expectancy, show high NMDAR1-AB seropositivity (Fig. 1b). Mouse samples were analyzed using specific AB against murine IgA, IgM, and IgG. As known for humans [6], NMDAR1-AB of the IgG class were the rarest. For another cross-validation, all monkey samples (*N* = 100) were analyzed in blinded fashion by an independent lab (Bochum; using specific anti-monkey IgM). IgM-positive results coincided with the protein-A positivity by >97% (76 of 78). The fraction of protein-A positive but IgM-negative monkey samples (total 22%) likely presents NMDAR1-AB of IgA class and IgG class where specific AB were not available.

Age-dependent NMDAR1-AB seroprevalence except for nonhuman primates and human migrants

All species revealed age dependence of NMDAR1-AB seroprevalence (χ^2 test; dogs: $\chi^2(1) = 11.5$, *p* = 0.01; cats: $\chi^2(1) = 4.8$, *p* = 0.03; rats: $\chi^2(1) = 9.5$, *p* = 0.002; and mice: Fisher's exact test *p* = 0.032) as for humans [5, 8] with the exception of baboons ($\chi^2(1) = 1.0$, *p* = 0.3), where already >50% of young animals were seropositive. This surprising result made us investigate another monkey species, rhesus macaques, showing again high seroprevalence in old and young animals ($\chi^2(1) = 0.2$, *p* = 0.6) (Fig. 1b). We wondered what the difference between humans, dogs, cats, mice, and rats, on one hand, and monkeys, on the other hand, could be, leading to loss of the usual age pattern regarding seroprevalence. Postulating that captivity/non-domestication of young monkeys might induce chronic life stress due to maladaptation to the environment, we investigated in a hypothesis-driven way whether young human migrants would display a similar increase in NMDAR1-AB seropositivity. Of the GRAS data collection, detailed information on migration was available in a subsample of *N* = 970 individuals. While nonmigrants show the typical age association of NMDAR1-AB seroprevalence ($\chi^2(1) = 10.7$, *p* = 0.001), migrants do not ($\chi^2(1) = 0.6$, *p* = 0.4) (Fig. 1c). Seroprevalence in young migrants is significantly higher as compared to young nonmigrants ($\chi^2(1) = 5.381$, *p* = 0.020). In both monkey species and migrants, the IgM fraction still follows the expected age trend, while IgA seems to account for the early increase in NMDAR1-AB seroprevalence (Fig. 1c). Presentation of NMDAR1-AB by Ig class in the extended GRAS sample (*N* = 4933), with *N* = 4632 of likely nonmigrants (available information less detailed) and *N* = 301 known migrants, illustrates the

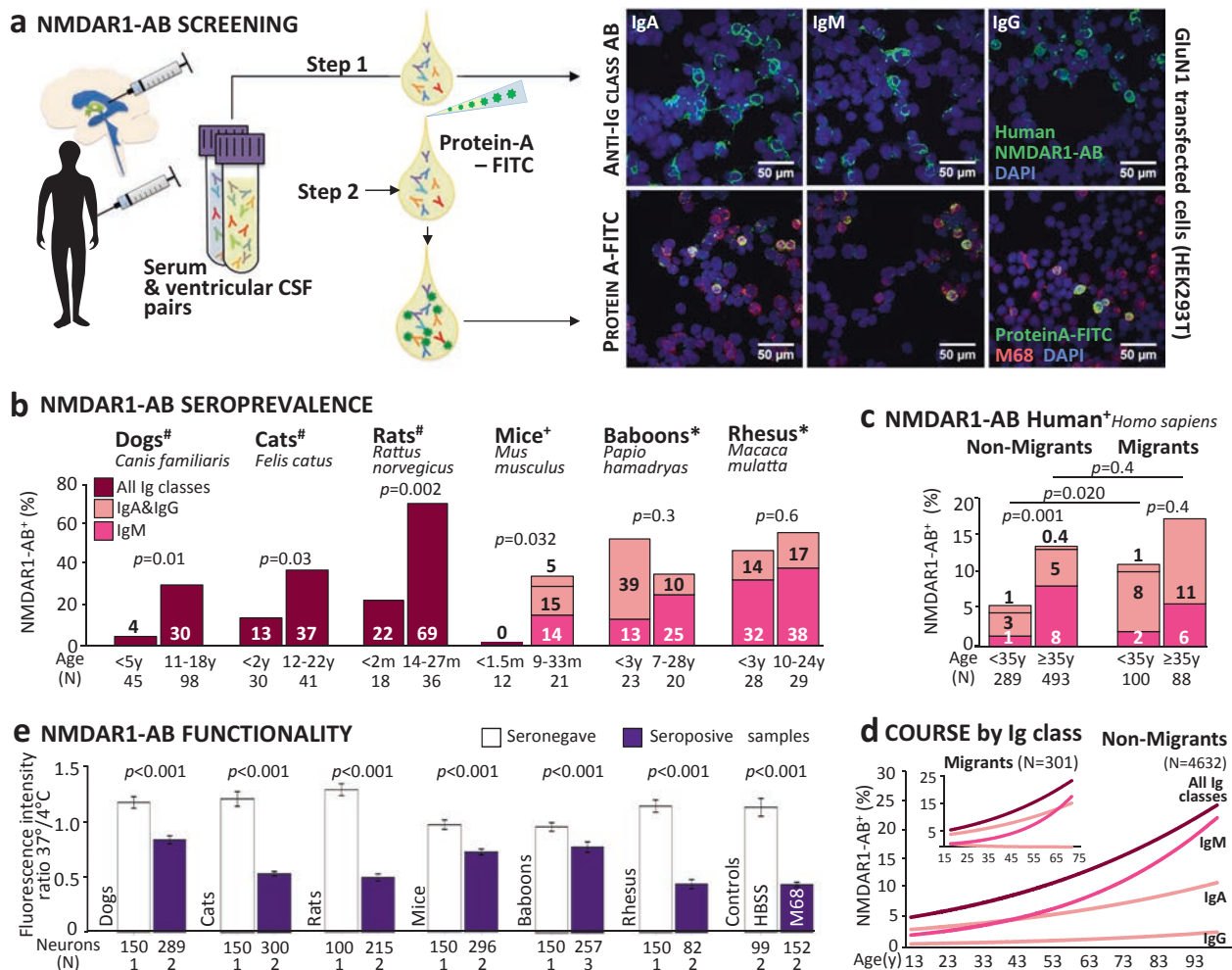


Fig. 1 NMDAR1-AB seropositivity and functionality across mammalian species. **a** Cross-validation of assays: paired serum and intraventricular CSF samples from neurosurgical patients were tested using a HEK293T cell-based clinical standard assay for NMDAR1-AB seropositivity (Euroimmun biochip). For step 1, fluorescently labeled IgA-specific, IgM-specific, and IgG-specific secondary AB were used; for method cross-validation (step 2), NMDAR1-AB seropositive and seronegative samples of each Ig class from step 1 were labeled with protein-A-FITC conjugate and tested for colocalization (yellow) of protein-A-FITC⁺ (green) and M68⁺ (monoclonal mouse NMDAR1-AB followed by Alexa555 donkey anti-mouse IgG red). Representative pictures of both methods using the same seropositive samples (IgA, IgM, and IgG) are displayed on the right: upper row step 1/lower row step 2. **b** NMDAR-AB seropositivity (%) of young and old

mammals for all Ig classes combined (#protein-A-FITC/Euroimmun) or for individual classes (+Euroimmun; *protein-A-FITC/Euroimmun and cross-validation with Euroimmun/monkey IgM) presented in the bars; color codes used for consistency and kept also in **c** and **d**; age given in months (m) or years (y); χ^2 or Fisher's exact test. **c** NMDAR-AB seropositivity of subjects with migration (first and second generation) vs. nonmigration history (GRAS data collection); all Ig classes presented; age split at 35 years; χ^2 test. **d** NMDAR1-AB course by Ig classes in serum over age groups in migrants vs. nonmigrants of the extended GRAS data collection. Note the different course particularly for IgA. **e** Functionality testing of NMDAR1-AB in human iPSC-derived cortical neurons: degree of internalization expressed as a ratio of fluorescence intensity measured at 37 and 4 °C; number of neurons and sera (N) given; Mann-Whitney U test

abnormal course of IgA vs. IgM/IgG seroprevalence over age in migrants (Fig. 1d).

Functionality of NMDAR1-AB from different mammalian species

To assess whether NMDAR1-AB of the tested species are functional, our endocytosis assay using iPSC-derived human cortical neurons [10] was employed. All positive

sera provoked NMDAR1 internalization, verifying functionality (Mann-Whitney U; all $p < 0.001$) (Fig. 1e).

BBB dysfunction but normal behavior of *ApoE*^{-/-} mice

We next induced endogenous NMDAR1-AB formation in a mouse model of BBB dysfunction, *ApoE*^{-/-} mice vs. WT littermates, *ApoE*^{+/+}. Before that, we confirmed in 12-

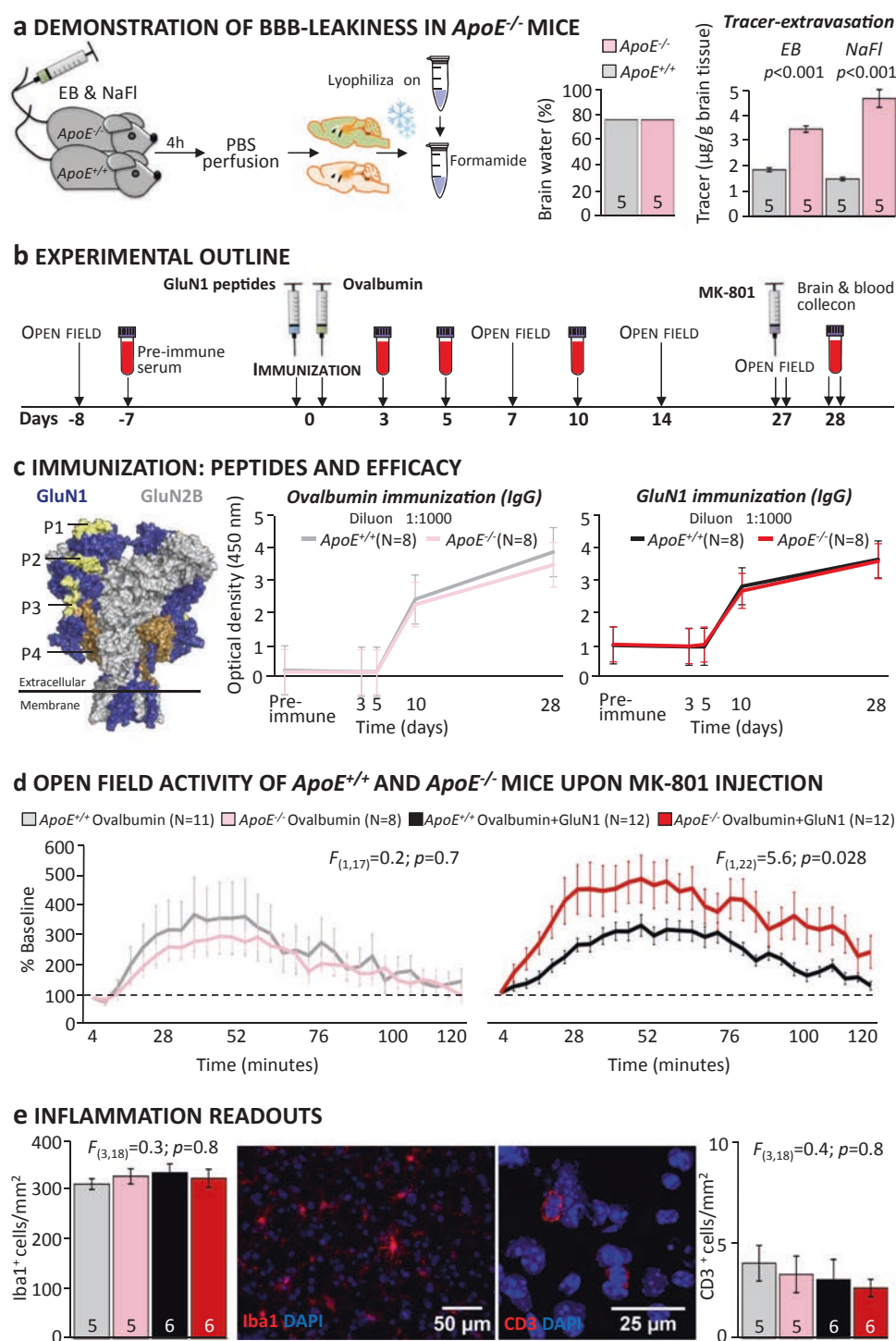


Fig. 2 Behavioral and morphological effects of endogenous NMDAR1-AB of the IgG class in a mouse model with open BBB. **a** Demonstration of BBB leakiness in *ApoE*^{-/-} mice using an intravenously injected mixture of Evans blue (EB) and sodium fluorescein (NaFl): After brain cryopreservation/lyophilization, tracers were extracted with formamide and quantified; Student's *t*-test; **b** Experimental outline; **c** Immunization: Left: GluN1 peptides (P1–P4) located in the extracellular part of the receptor were used for immunization (compare Fig. 3); middle and right: Time course of anti-ovalbumin and anti-GluN1-AB (IgG) upon immunization in *ApoE*^{-/-} and *ApoE*^{+/+} mice; optical density at dilution 1:1000 shown; titers after day 10 reach up to 1:50,000; **d** Effect of MK-

801 injection on activity in the open field; results presented as % change from baseline (first 4 min post MK-801 set to 100%); no difference in MK-801-induced hyperactivity between genotypes after ovalbumin immunization (one-way repeated measures ANOVA: treatment × group interaction: $F_{(1,17)} = 0.2$; $p = 0.7$); increase in hyperactivity (during rise, plateau, decline, and after-effect phases) upon MK-801 in *ApoE*^{-/-} but not *ApoE*^{+/+} mice immunized against GluN1 (one-way repeated measures ANOVA: treatment × group interaction: $F_{(1,22)} = 5.6$; $p = 0.028$). **e** Quantification of Iba1⁺ and CD3⁺ cells in the hippocampus to assess inflammation in the brain; one-way ANOVA; representative pictures of Iba1 (left) and CD3 (right) stainings in the middle

Table 1 Basic behavioral screening of male and female *ApoE^{+/+}* and *ApoE^{-/-}* mice

Behavioral paradigms	Males				Females			
	Age (month)	<i>ApoE^{+/+}</i> (N)	<i>ApoE^{-/-}</i> (N)	<i>p</i> -value	Age (month)	<i>ApoE^{+/+}</i> (N)	<i>ApoE^{-/-}</i> (N)	<i>p</i> -value
<i>Anxiety and activity</i>								
Elevated plus-maze (time open [%])	5	12.6±3.2 (10)	19.5±4.0 (10)	<i>p</i> = 0.14 <i>U</i> =30.0	5	17.5±2.9 (13)	14.8±1.3 (11)	<i>p</i> = 0.98 <i>U</i> =71.0
<i>Exploratory behavior</i>								
Hole-board (holes visited [#])	5	15.2±2.3 (10)	11.9±1.9 (10)	<i>p</i> = 0.30 <i>t</i> (18)=1.07	5	15.5±1.8 (13)	15.6±2.9 (13)	<i>p</i> = 0.96 <i>t</i> (22)=0.96
<i>Open-field</i>								
Locomotion [m]	5	31.8±1.7 (10)	32.7±1.5 (10)	<i>p</i> = 0.70 <i>t</i> (18)=0.39	5	42.7±1.3 (13)	43.7±3.2 (13)	<i>p</i> = 0.76 <i>t</i> (22)=0.31
<i>Motor learning and coordination</i>								
Rotarod day 1 (latency to fall [s])	6	89.3±11.6 (10)	130.0±15.3 (10)	<i>p</i> = 0.06 <i>t</i> (18)=2.01	5	130.9±14.0 (13)	133.3±16.0 (11)	<i>p</i> = 0.91 <i>t</i> (22)=0.11
Rotarod day 2 (latency to fall [s])	6	140.3±9.4 (10)	145.6±17.8 (10)	<i>p</i> = 0.81 <i>t</i> (18)=0.25	5	179.0±16.8 (13)	160.5±19.9 (11)	<i>p</i> = 0.5 <i>t</i> (22)=0.69
<i>Muscle strength</i>								
Grip-strength [au]	6	110.2±5.4 (10)	122.0±5.0 (10)	<i>p</i> = 0.15 <i>t</i> (18)=1.52	6	108.8±3.0 (13)	115.1±4.4 (11)	<i>p</i> = 0.26 <i>t</i> (22)=1.16
<i>Heat/pain perception</i>								
Hot-plate (latency to lick [s])	5	12.8±0.4 (10)	11.9±0.7 (10)	<i>p</i> = 0.22 <i>t</i> (18)=1.26	5	13.7±0.5 (12)	12.4±0.5 (10)	<i>p</i> = 0.15 <i>t</i> (20)=1.5
<i>Vision</i>								
Visual-cliff (time on "air" side [%])	5	26.5±7.2 (10)	22.0±5.6 (10)	<i>p</i> = 0.85 <i>U</i> =47.0	5	21.7±5.1 (13)	29.0±3.9 (11)	<i>p</i> = 0.13 <i>U</i> =45.0
<i>Olfaction</i>								
Buried food-test (latency to find cookie [s])	5	59.4±9.2 (10)	50.6±8.5 (9)	<i>p</i> = 0.52 <i>t</i> (17)=0.66	5	47.8±12.9 (12)	50.7±10.7 (11)	<i>p</i> = 0.87 <i>t</i> (21)=0.16
<i>Hearing</i>								
Acoustic startle at 65dB [AU]	6	0.5±0.04 (10)	0.5±0.04 (10)	<i>p</i> = 0.53 <i>F</i> (1,18)=0.42	8	0.4±0.1 (13)	0.5±0.04 (11)	<i>p</i> = 0.19 <i>F</i> (1,22)=1.82
Acoustic startle at 120dB [AU]		4.5±1.0 (10)	4.8±1.0 (10)			3.3±0.5 (13)	4.2±0.6 (11)	
<i>Sensorimotor gating</i>								
Mean pre-pulse inhibition [%]	6	44.8±6.7 (10)	40.6±7.4 (10)	<i>p</i> = 0.69 <i>F</i> (1,18)=0.16	8	57.7±4.1 (13)	50.4±6.3 (11)	<i>p</i> = 0.35 <i>F</i> (1,22)=0.91
<i>Pheromone-based social preference</i>								
Time spent in pheromone box [s]					15	1213±50.8 (12)	1115±83.7 (12)	<i>p</i> = 0.33 <i>t</i> (22)=1.0
Time spent in control box [s]						780.5±75.4 (12)	751.1±83.5 (12)	<i>p</i> = 0.84 <i>t</i> (22)=0.21
<i>Cognitive performance in IntelliCage</i>								
Place-learning [% target corner visits] ^a					15	34.2±1.3 (12)	34.2±1.8 (13)	<i>p</i> = 0.76 <i>U</i> =72.0
Reversal-learning [% target corner visits] ^a						34.2±1.3 (12)	34.2±1.8 (13)	<i>p</i> = 0.17 <i>U</i> =52.0

^aas previously described in *Netrakanti et al. 2015*

Note: All data in the table are mean ± S.E.M.

month-old mice (age of immunization) BBB leakiness using two fluorescent tracers. While brain water content was similar in both genotypes, pointing against inflammation, *ApoE^{-/-}* mice showed increased tracer extravasation, confirming BBB dysfunction (Student's *t*-test: EB: *t*(8) =

-10.66, *p* < 0.001; NaFl: *t*(8) = -8.97, *p* < 0.001) (Fig. 2a). We wondered whether this compromised BBB would by itself lead to behavioral abnormalities in *ApoE^{-/-}* mice. A comprehensive behavioral battery, including tests for anxiety, activity, exploratory behavior,

motor and sensory function, sensorimotor gating, pheromone-based social preference, and cognitive performance did not reveal any differences between genotypes (Table 1).

Immunization of *ApoE*^{-/-} and *ApoE*^{+/+} mice against NMDAR1-peptides

To explore whether endogenously formed NMDAR1-AB would lead to measurable behavioral and morphological effects, we immunized 12-month-old *ApoE*^{-/-} and *ApoE*^{+/+} littermates against four peptides of the extracellular NMDAR1/GluN1-domain (including NTD-G7; N368/G369) and ovalbumin or against ovalbumin alone as immunization control (Fig. 2b–c). GluN1 shows >99% sequence homology among all here-tested mammalian species, with immunizing peptides being 100% homologous (Fig. 3). Immunization led to high circulating levels of specific IgG (titers up to 1:50,000). Efficacy of immunization and time course of IgG appearance as determined by ELISA were comparable for NMDAR1-peptides and ovalbumin across genotypes, making a simple boosting effect of NMDAR1-peptides on pre-existing NMDAR1-specific B cell clones rather improbable (Fig. 2c).

Psychosis-related behavior of *ApoE*^{-/-} mice upon MK-801 challenge

Open-field tests measuring baseline preimmunization and postimmunization locomotion did not reveal any differences between genotypes and/or immunization groups (Fig. 2b; not shown). After 4 weeks, the endogenously formed NMDAR1-AB of the IgG class induced strong hyperactivity (psychosis-like symptoms [37]) upon MK-801 challenge in *ApoE*^{-/-} mice only. In contrast, *ApoE*^{+/+} mice behaved comparably to ovalbumin-only immunized mice of both genotypes (Fig. 2d; all $p > 0.5$). Thus, an open BBB together with sufficiently high titers of AB (to reach a threshold loss of NMDAR1 surface expression) is a prerequisite for the observed behavioral perturbation upon MK-801.

No inflammation in hippocampus of immunized *ApoE*^{-/-} and *ApoE*^{+/+} mice

Immunohistochemistry did not show any evidence of inflammation in either genotype and/or immunization group. Numbers of Iba1⁺ and CD3⁺ cells as markers of microglia and T cells, respectively, were comparable for total hippocampus (one-way ANOVA: Iba1: $F(3,18) = 0.3$; $p = 0.8$; CD3: $F(3,18) = 0.4$; $p = 0.8$) (Fig. 2e) and for all hippocampal subfields separately (all p -values > 0.2 ; not shown). Also, staining for microglial activity markers,

CD68 and MHCII, was essentially negative and identical across groups. Moreover, staining for GFAP did not reveal any appreciable density increase in the hippocampus, and thus no sign of astrogliosis (data not shown).

Discussion

The present work demonstrates high seroprevalence of functional NMDAR1-AB of all Ig classes across mammals, indicating that these AB are part of a pre-existing autoimmune repertoire [11–17]. As in humans, NMDAR1-AB of the IgG class are the least frequent [6, 20]. The age related up to >50% NMDAR1-AB seropositivity is independent of the respective species' life expectancy, indicating that the aging process itself rather than years of exposure to a certain environment triggers NMDAR1-AB formation. However, our knowledge on predisposing factors and inducing mechanisms is limited. Specific autoimmune-reactive B cells may get repeatedly boosted by, e.g., infections, neoplasms, or the microbiome, and less efficiently suppressed over a lifespan likely owing to a gradual loss of immune tolerance upon aging [14].

Unexpectedly, we find the age-dependence lost in non-human primates and in human migrants that all display an early-life rise in NMDAR1-AB seropositivity, mainly of IgA. The intriguing possibility that chronic life stress, known to be present in human migrants [38] and animals in captivity [39], acts as a trigger of early NMDAR1-AB formation is worth pursuing experimentally in the future. A large proportion of migrants in our human samples are suffering from neuropsychiatric illness. This may additionally support our chronic stress hypothesis since migration is recognized as an environmental stressor predisposing to mental disease [40]. Further studies should screen wild-life monkeys and species in zoos for NMDAR1-AB. Experimental confirmation of our findings provided, NMDAR1-AB (IgA) may even serve as stress markers. In fact, earlier reports show that total serum-Ig of all classes, most prominently IgA, respond to psychological stress [41]. NMDAR1-AB might thus belong to a set of stress-boosted AB. Interestingly, we also find accumulated seroprevalence of 23 other brain-directed AB [6] in young migrants vs. nonmigrants increased (data not shown), suggesting a global inducer role of chronic stress in humoral autoimmunity.

Earlier work has shown that AB against brain antigens in general are common among mammals [42], but no study has so far systematically screened nonhuman mammals for NMDAR1-AB. As an exception, a recent report described "anti-NMDAR1 encephalitis" in the young polar bear Knut [27]. Based on the present findings, Knut may have belonged to those nondomesticated species in captivity—

	Peptide 1	100
Homo sapiens	MSTMRLLLTALLFSCSVARAACDPKIVNIGAVLSTRKHEQMFREAVNQANKRHGWSKIQLNATSVTHKPNAIQMALSVCEDLISSQVYAILVSHPPPTPND	
Macaca mulatta	MSTMRLLLTALLFSCSVARAACDPKIVNIGAVLSTRKHEQMFREAVNQANKRHGWSKIQLNATSVTHKPNAIQMALSVCEDLISSQVYAILVSHPPPTPND	
Papio anubis	MSTMRLLLTALLFSCSVARAACDPKIVNIGAVLSTRKHEQMFREAVNQANKRHGWSKIQLNATSVTHKPNAIQMALSVCEDLISSQVYAILVSHPPPTPND	
Canis lupus fam.	MSTMRLLLTALLFSCSFAARAACDPKIVNIGAVLSTRKHEQMFREAVNQANKRHGWSKIQLNATSVTHKPNAIQMALSVCEDLISSQVYAILVSHPPPTPND	
Felis catus	MSTMRLLLTALLFSCSFAARAACDPKIVNIGAVLSTRKHEQMFREAVNQANKRHGWSKIQLNATSVTHKPNAIQMALSVCEDLISSQVYAILVSHPPPTPND	
Rattus norvegicus	MSTMHLLTFALLFSCSFAARAACDPKIVNIGAVLSTRKHEQMFREAVNQANKRHGWSKIQLNATSVTHKPNAIQMALSVCEDLISSQVYAILVSHPPPTPND	
Mus musculus	MSTMHLLTFALLFSCSFAARAACDPKIVNIGAVLSTRKHEQMFREAVNQANKRHGWSKIQLNATSVTHKPNAIQMALSVCEDLISSQVYAILVSHPPPTPND	
	—SP—	
		200
Homo sapiens	HFTPTPVSYTAGFYRIPVLGLTTRMSIYSDKSIHLSFLRTVPPYSHQSVVWFEMMRVYSWNHIIILLVSDDHGEGRAAQKRLETLLEERESKSKRNYENLD	
Macaca mulatta	HFTPTPVSYTAGFYRIPVLGLTTRMSIYSDKSIHLSFLRTVPPYSHQSVVWFEMMRVYSWNHIIILLVSDDHGEGRAAQKRLETLLEERESKSKRNYENLD	
Papio anubis	HFTPTPVSYTAGFYRIPVLGLTTRMSIYSDKSIHLSFLRTVPPYSHQSVVWFEMMRVYSWNHIIILLVSDDHGEGRAAQKRLETLLEERESKSKRNYENLD	
Canis lupus fam.	HFTPTPVSYTAGFYRIPVLGLTTRMSIYSDKSIHLSFLRTVPPYSHQSVVWFEMMRVYSWNHIIILLVSDDHGEGRAAQKRLETLLEERESKSKRNYENLD	
Felis catus	HFTPTPVSYTAGFYRIPVLGLTTRMSIYSDKSIHLSFLRTVPPYSHQSVVWFEMMRVYSWNHIIILLVSDDHGEGRAAQKRLETLLEERESKSKRNYENLD	
Rattus norvegicus	HFTPTPVSYTAGFYRIPVLGLTTRMSIYSDKSIHLSFLRTVPPYSHQSVVWFEMMRVYWNHIIILLVSDDHGEGRAAQKRLETLLEERESKSKRNYENLD	
Mus musculus	HFTPTPVSYTAGFYRIPVLGLTTRMSIYSDKSIHLSFLRTVPPYSHQSVVWFEMMRVYWNHIIILLVSDDHGEGRAAQKRLETLLEERESKSKRNYENLD	
		300
Homo sapiens	QLSYDNKRGPKAQKLVQDFDPTGKNTVALLMEAKELEARVILSASEDDAATVYRAAAMLNMTGSGYVWLVGEREISGNALRYAPDGIIGLQKINGKNESA	
Macaca mulatta	QLSYDNKRGPKAQKLVQDFDPTGKNTVALLMEAKELEARVILSASEDDAATVYRAAAMLNMTGSGYVWLVGEREISGNALRYAPDGIIGLQKINGKNESA	
Papio anubis	QLSYDNKRGPKAQKLVQDFDPTGKNTVALLMEAKELEARVILSASEDDAATVYRAAAMLNMTGSGYVWLVGEREISGNALRYAPDGIIGLQKINGKNESA	
Canis lupus fam.	QLSYDNKRGPKAQKLVQDFDPTGKNTVALLMEAKELEARVILSASEDDAATVYRAAAMLNMTGSGYVWLVGEREISGNALRYAPDGIIGLQKINGKNESA	
Felis catus	QLSYDNKRGPKAQKLVQDFDPTGKNTVALLMEAKELEARVILSASEDDAATVYRAAAMLNMTGSGYVWLVGEREISGNALRYAPDGIIGLQKINGKNESA	
Rattus norvegicus	QLSYDNKRGPKAQKLVQDFDPTGKNTVALLMEAKELEARVILSASEDDAATVYRAAAMLNMTGSGYVWLVGEREISGNALRYAPDGIIGLQKINGKNESA	
Mus musculus	QLSYDNKRGPKAQKLVQDFDPTGKNTVALLMEAKELEARVILSASEDDAATVYRAAAMLNMTGSGYVWLVGEREISGNALRYAPDGIIGLQKINGKNESA	
		400
		Peptide 2
Homo sapiens	HISDAVGVVAQVAVHELLEKENITDPPRGCVGNNTIWKTPGLFKRVLMSKAYADGVTGRVEFNEDGDRKFANYSIMLNQNRKLVQVGIYNGTHVIPNDRKI	
Macaca mulatta	HISDAVGVVAQVAVHELLEKENITDPPRGCVGNNTIWKTPGLFKRVLMSKAYADGVTGRVEFNEDGDRKFANYSIMLNQNRKLVQVGIYNGTHVIPNDRKI	
Papio anubis	HISDAVGVVAQVAVHELLEKENITDPPRGCVGNNTIWKTPGLFKRVLMSKAYADGVTGRVEFNEDGDRKFANYSIMLNQNRKLVQVGIYNGTHVIPNDRKI	
Canis lupus fam.	HISDAVGVVAQVAVHELLEKENITDPPRGCVGNNTIWKTPGLFKRVLMSKAYADGVTGRVEFNEDGDRKFANYSIMLNQNRKLVQVGIYNGTHVIPNDRKI	
Felis catus	HISDAVGVVAQVAVHELLEKENITDPPRGCVGNNTIWKTPGLFKRVLMSKAYADGVTGRVEFNEDGDRKFANYSIMLNQNRKLVQVGIYNGTHVIPNDRKI	
Rattus norvegicus	HISDAVGVVAQVAVHELLEKENITDPPRGCVGNNTIWKTPGLFKRVLMSKAYADGVTGRVEFNEDGDRKFANYSIMLNQNRKLVQVGIYNGTHVIPNDRKI	
Mus musculus	HISDAVGVVAQVAVHELLEKENITDPPRGCVGNNTIWKTPGLFKRVLMSKAYADGVTGRVEFNEDGDRKFANYSIMLNQNRKLVQVGIYNGTHVIPNDRKI	
		500
		Peptide 3
Homo sapiens	IWPGGETEKPRGYQMSTRLKIVTIHQEPPFVYKPTLSDGTCKEEFTVNGDPVKKVICITGPNDTSPGSRHTVPQCCYGCIDLLIKLARTMNFITYEVHLV	
Macaca mulatta	IWPGGETEKPRGYQMSTRLKIVTIHQEPPFVYKPTLSDGTCKEEFTVNGDPVKKVICITGPNDTSPGSRHTVPQCCYGCIDLLIKLARTMNFITYEVHLV	
Papio anubis	IWPGGETEKPRGYQMSTRLKIVTIHQEPPFVYKPTLSDGTCKEEFTVNGDPVKKVICITGPNDTSPGSRHTVPQCCYGCIDLLIKLARTMNFITYEVHLV	
Canis lupus fam.	IWPGGETEKPRGYQMSTRLKIVTIHQEPPFVYKPTLSDGTCKEEFTVNGDPVKKVICITGPNDTSPGSRHTVPQCCYGCIDLLIKLARTMNFITYEVHLV	
Felis catus	IWPGGETEKPRGYQMSTRLKIVTIHQEPPFVYKPTLSDGTCKEEFTVNGDPVKKVICITGPNDTSPGSRHTVPQCCYGCIDLLIKLARTMNFITYEVHLV	
Rattus norvegicus	IWPGGETEKPRGYQMSTRLKIVTIHQEPPFVYKPTLSDGTCKEEFTVNGDPVKKVICITGPNDTSPGSRHTVPQCCYGCIDLLIKLARTMNFITYEVHLV	
Mus musculus	IWPGGETEKPRGYQMSTRLKIVTIHQEPPFVYKPTLSDGTCKEEFTVNGDPVKKVICITGPNDTSPGSRHTVPQCCYGCIDLLIKLARTMNFITYEVHLV	
	—S1—	
		600
Homo sapiens	ADGKFGTQERVNNSNKKKEWNGMGGELLSGQADMIVAPLTINNERAQYIEFSKPFKYQGLTILVKKEIPRSTLDSFMQPFQSTLWLLVGLSVHVAVMMLYL	
Macaca mulatta	ADGKFGTQERVNNSNKKKEWNGMGGELLSGQADMIVAPLTINNERAQYIEFSKPFKYQGLTILVKKEIPRSTLDSFMQPFQSTLWLLVGLSVHVAVMMLYL	
Papio anubis	ADGKFGTQERVNNSNKKKEWNGMGGELLSGQADMIVAPLTINNERAQYIEFSKPFKYQGLTILVKKEIPRSTLDSFMQPFQSTLWLLVGLSVHVAVMMLYL	
Canis lupus fam.	ADGKFGTQERVNNSNKKKEWNGMGGELLSGQADMIVAPLTINNERAQYIEFSKPFKYQGLTILVKKEIPRSTLDSFMQPFQSTLWLLVGLSVHVAVMMLYL	
Felis catus	ADGKFGTQERVNNSNKKKEWNGMGGELLSGQADMIVAPLTINNERAQYIEFSKPFKYQGLTILVKKEIPRSTLDSFMQPFQSTLWLLVGLSVHVAVMMLYL	
Rattus norvegicus	ADGKFGTQERVNNSNKKKEWNGMGGELLSGQADMIVAPLTINNERAQYIEFSKPFKYQGLTILVKKEIPRSTLDSFMQPFQSTLWLLVGLSVHVAVMMLYL	
Mus musculus	ADGKFGTQERVNNSNKKKEWNGMGGELLSGQADMIVAPLTINNERAQYIEFSKPFKYQGLTILVKKEIPRSTLDSFMQPFQSTLWLLVGLSVHVAVMMLYL	
	—S1—	
		TMD A
		700
		Peptide 4
Homo sapiens	LDRFSPFGRFKVNSEEEEEEDALTLSSAMWFSWGLVLLNSGIGEGAPRSFARIILGMVWAGFAMIIVASYTANLAFLVLDLDRPEERITGINDPRLRNPDKKF	
Macaca mulatta	LDRFSPFGRFKVNSEEEEEEDALTLSSAMWFSWGLVLLNSGIGEGAPRSFARIILGMVWAGFAMIIVASYTANLAFLVLDLDRPEERITGINDPRLRNPDKKF	
Papio anubis	LDRFSPFGRFKVNSEEEEEEDALTLSSAMWFSWGLVLLNSGIGEGAPRSFARIILGMVWAGFAMIIVASYTANLAFLVLDLDRPEERITGINDPRLRNPDKKF	
Canis lupus fam.	LDRFSPFGRFKVNSEEEEEEDALTLSSAMWFSWGLVLLNSGIGEGAPRSFARIILGMVWAGFAMIIVASYTANLAFLVLDLDRPEERITGINDPRLRNPDKKF	
Felis catus	LDRFSPFGRFKVNSEEEEEEDALTLSSAMWFSWGLVLLNSGIGEGAPRSFARIILGMVWAGFAMIIVASYTANLAFLVLDLDRPEERITGINDPRLRNPDKKF	
Rattus norvegicus	LDRFSPFGRFKVNSEEEEEEDALTLSSAMWFSWGLVLLNSGIGEGAPRSFARIILGMVWAGFAMIIVASYTANLAFLVLDLDRPEERITGINDPRLRNPDKKF	
Mus musculus	LDRFSPFGRFKVNSEEEEEEDALTLSSAMWFSWGLVLLNSGIGEGAPRSFARIILGMVWAGFAMIIVASYTANLAFLVLDLDRPEERITGINDPRLRNPDKKF	
	—P—	
		TMD B
		S2
		800
		Peptide 4
Homo sapiens	IYATVKQSSVDIYFRROVELSTMYRHMEKHNYESAEEAIAQVRDNKHLHAFIWDVSAVLEFEASQKCDLVTGELFFRSFGFIMGMRKDSWPWKQNVSLILKS	
Macaca mulatta	IYATVKQSSVDIYFRROVELSTMYRHMEKHNYESAEEAIAQVRDNKHLHAFIWDVSAVLEFEASQKCDLVTGELFFRSFGFIMGMRKDSWPWKQNVSLILKS	
Papio anubis	IYATVKQSSVDIYFRROVELSTMYRHMEKHNYESAEEAIAQVRDNKHLHAFIWDVSAVLEFEASQKCDLVTGELFFRSFGFIMGMRKDSWPWKQNVSLILKS	
Canis lupus fam.	IYATVKQSSVDIYFRROVELSTMYRHMEKHNYESAEEAIAQVRDNKHLHAFIWDVSAVLEFEASQKCDLVTGELFFRSFGFIMGMRKDSWPWKQNVSLILKS	
Felis catus	IYATVKQSSVDIYFRROVELSTMYRHMEKHNYESAEEAIAQVRDNKHLHAFIWDVSAVLEFEASQKCDLVTGELFFRSFGFIMGMRKDSWPWKQNVSLILKS	
Rattus norvegicus	IYATVKQSSVDIYFRROVELSTMYRHMEKHNYESAEEAIAQVRDNKHLHAFIWDVSAVLEFEASQKCDLVTGELFFRSFGFIMGMRKDSWPWKQNVSLILKS	
Mus musculus	IYATVKQSSVDIYFRROVELSTMYRHMEKHNYESAEEAIAQVRDNKHLHAFIWDVSAVLEFEASQKCDLVTGELFFRSFGFIMGMRKDSWPWKQNVSLILKS	
	—S2—	
		900
		Peptide 4
Homo sapiens	HENGFMEDLTKTWRYQECDSRSNAPATLTFENMAGVFLVAGGIVAGIFLIFIEIAYKRHKDARRKQMLAFAAVNVWRKQLDQRKSGRAEPDPKKKAT	
Macaca mulatta	HENGFMEDLTKTWRYQECDSRSNAPATLTFENMAGVFLVAGGIVAGIFLIFIEIAYKRHKDARRKQMLAFAAVNVWRKQLDQRKSGRAEPDPKKKAT	
Papio anubis	HENGFMEDLTKTWRYQECDSRSNAPATLTFENMAGVFLVAGGIVAGIFLIFIEIAYKRHKDARRKQMLAFAAVNVWRKQLDQRKSGRAEPDPKKKAT	
Canis lupus fam.	HENGFMEDLTKTWRYQECDSRSNAPATLTFENMAGVFLVAGGIVAGIFLIFIEIAYKRHKDARRKQMLAFAAVNVWRKQLDQRKSGRAEPDPKKKAT	
Felis catus	HENGFMEDLTKTWRYQECDSRSNAPATLTFENMAGVFLVAGGIVAGIFLIFIEIAYKRHKDARRKQMLAFAAVNVWRKQLDQRKSGRAEPDPKKKAT	
Rattus norvegicus	HENGFMEDLTKTWRYQECDSRSNAPATLTFENMAGVFLVAGGIVAGIFLIFIEIAYKRHKDARRKQMLAFAAVNVWRKQLDQRKSGRAEPDPKKKAT	
Mus musculus	HENGFMEDLTKTWRYQECDSRSNAPATLTFENMAGVFLVAGGIVAGIFLIFIEIAYKRHKDARRKQMLAFAAVNVWRKQLDQRKSGRAEPDPKKKAT	
	—S2—	
		TMD C
		959
Homo sapiens	FRAITSTLASSFKRRRSKSDTSGGGRGALQNKQDVTLPRAIEREEGQLQCSRHRRES	XP_005266130
Macaca mulatta	FRAITSTLASSFKRRRSKSDTSGGGRGALQNKQDVTLPRAIEREEGQLQCSRHRRES	XP_014971750
Papio anubis	FRAITSTLASSFKRRRSKSDTSGGGRGALQNKQDVTLPRAIEREEGQLQCSRHRRES	XP_009186649
Canis lupus fam.	FRAITSTLASSFKRRRSKSDTSGGGRGALQNKQDVTLPRAIEREEGQLQCSRHRRES	AB195994/AB1959957NC_006591
Felis catus	FRAITSTLASSFKRRRSKSDTSGGGRGALQNKQDVTLPRAIEREEGQLQCSRHRRES	XP_011287050
Rattus norvegicus	FRAITSTLASSFKRRRSKSDTSGGGRGALQNKQDVTLPRAIEREEGQLQCSRHRRES	NP_001257531
Mus musculus	FRAITSTLASSFKRRRSKSDTSGGGRGALQNKQDVTLPRAIEREEGQLQCSRHRRES	XP_006497785

Fig. 3 Alignment of GluN1-1b receptor amino acid sequence across all mammalian species tested. Regions containing the four peptide sequences (peptides 1–4; P1: AA35–53, P2: AA361–376, P3: AA385–399, and P4: AA660–811) used in the immunization experiment are highlighted in yellow and light brown (compare three-

dimensional presentation in Fig. 2c) and nonhomologous amino acids in pink. SP signal peptide, S1, S2 segments of the ligand-binding domain, TMD A transmembrane domain A, TMD B transmembrane domain B, TMD C transmembrane domain C

comparable to monkey species investigated here—that are affected by chronic early-life stress, inducing NMDAR1-AB seropositivity. Pre-existing NMDAR1-AB of this bear may have ultimately shaped the clinical picture of an encephalitis of unexplained origin (likely infectious according to the zoo's pathology reports) where an epileptic seizure led to drowning [27].

This interpretation is supported by our novel auto-immune model, namely, mice immunized against NMDAR1-peptides. Even high titers of endogenously formed NMDAR1-AB (IgG; up to 1:50,000) that induce psychosis-like behavior upon MK-801 challenge in *ApoE^{-/-}* mice, with here-confirmed open BBB, do not lead to any appreciable signs of encephalitis. This dissociation of behavioral/symptomatic consequences and inflammation in the brain is of major importance for clinicians [14]. For instance, earlier studies reported an influence of NMDAR1-AB infusions into the hippocampus on learning and memory in mice [43], and others found increased NMDAR1-AB seroprevalence in patients with mild cognitive impairment and Alzheimer's disease [44, 45]. However, while all naturally occurring NMDAR1-AB that have pathogenic potential irrespective of epitope and Ig class [10], and upon entry to the brain (or via intrathecal production) can shape brain functions in the sense of NMDAR antagonism, only a fraction of individuals happens to have underlying encephalitis of various etiologies, which is then called anti-NMDAR encephalitis. The highly variable neuropathology and response to immunosuppression of this condition [2, 3, 46] may point to a broad range of possible encephalitogenic mechanisms (from infection to oncology or genetics) which need to be diagnosed and specifically treated [14].

Even though it is unclear how NMDAR1-AB are generated by chronic stress, it should be considered that NMDAR1 are not only expressed in the brain but also by peripheral organs and tissues, including adrenal glands and gut [47] which may be involved in triggering NMDAR1-AB formation but may also be functionally modulated by them. Since NMDAR antagonists are increasingly recognized as antidepressant, anxiolytic, and anti-inflammatory agents [48–52], we speculate that stress-induced NMDAR1-AB could serve as endogenous stress protectants. Remarkably, also in stroke, NMDAR1-AB can be protective [8].

In conclusion, the widespread occurrence of NMDAR1-AB across mammals, as well as the failure of even high titers of endogenously formed NMDAR1-AB of the IgG class to induce any signs of brain inflammation should lead to rethinking current concepts that link NMDAR1-AB to neuropsychiatric disease including encephalitis.

Acknowledgements This work was supported by the Max Planck Society, the Max Planck Förderstiftung, the DFG (CNMPB),

EXTRABRAIN EU-FP7, and the Niedersachsen-Research Network on Neuroinfectiology (N-RENNT). The authors thank all subjects for participating in the study, and the many colleagues who have contributed over the past decade to the extended GRAS data collection.

Author contributions Concept, design, and supervision of the study: HE; Data acquisition/analysis/interpretation: HP, BO, ED, DT, MM, JS, JW, DW, CKS, AR, KS, RT, KMR, StB, YAK, HM, MB, WS, GS, FJK, RM, SB, KAN, JKK, MH, FL, and HE; Drafting manuscript: HE, with the help of BO and HP; Drafting display items: HE and BO, with the help of HP, MM, DT, and JS. All authors read and approved the final version of the manuscript.

Compliance with ethical standards

Conflict of interest WS is a member of the board and holds stocks in Euroimmun AG. HM is a full-time employee of Synaptic Systems GmbH. The remaining authors declare that they have no conflict of interest.

Open Access This article is licensed under a Creative Commons Attribution-NonCommercial-NoDerivatives 4.0 International License, which permits any non-commercial use, sharing, distribution and reproduction in any medium or format, as long as you give appropriate credit to the original author(s) and the source, and provide a link to the Creative Commons license. You do not have permission under this license to share adapted material derived from this article or parts of it. The images or other third party material in this article are included in the article's Creative Commons license, unless indicated otherwise in a credit line to the material. If material is not included in the article's Creative Commons license and your intended use is not permitted by statutory regulation or exceeds the permitted use, you will need to obtain permission directly from the copyright holder. To view a copy of this license, visit <http://creativecommons.org/licenses/by-nc-sa/4.0/>.

References

- Dalmau J, Tuzun E, Wu HY, Masjuan J, Rossi JE, Voloschin A, et al. Paraneoplastic anti-N-methyl-D-aspartate receptor encephalitis associated with ovarian teratoma. *Ann Neurol*. 2007;61:25–36.
- Dalmau J, Gleichman AJ, Hughes EG, Rossi JE, Peng X, Lai M, et al. Anti-NMDA-receptor encephalitis: case series and analysis of the effects of antibodies. *Lancet Neurol*. 2008;7:1091–8.
- Dalmau J, Lancaster E, Martinez-Hernandez E, Rosenfeld MR, Balice-Gordon R. Clinical experience and laboratory investigations in patients with anti-NMDAR encephalitis. *Lancet Neurol*. 2011;10:63–74.
- Titulaer MJ, McCracken L, Gabilondo I, Armangue T, Glaser C, Iizuka T, et al. Treatment and prognostic factors for long-term outcome in patients with anti-NMDA receptor encephalitis: an observational cohort study. *Lancet Neurol*. 2013;12:157–65.
- Hammer C, Stepniak B, Schneider A, Papiol S, Tantra M, Begemann M, et al. Neuropsychiatric disease relevance of circulating anti-NMDA receptor autoantibodies depends on blood-brain barrier integrity. *Mol Psychiatry*. 2014;19:1143–9.
- Dahm L, Ott C, Steiner J, Stepniak B, Teegen B, Saschenbrecker S, et al. Seroprevalence of autoantibodies against brain antigens in health and disease. *Ann Neurol*. 2014;76:82–94.
- Steiner J, Teegen B, Schiltz K, Bernstein HG, Stoecker W, Bogerts B. Prevalence of N-methyl-D-aspartate receptor

- autoantibodies in the peripheral blood: healthy control samples revisited. *JAMA Psychiatry*. 2014;71:838–9.
8. Zerche M, Weissenborn K, Ott C, Dere E, Asif AR, Worthmann H, et al. Preexisting serum autoantibodies against the NMDAR subunit NR1 modulate evolution of lesion size in acute ischemic stroke. *Stroke*. 2015;46:1180–6.
 9. Castillo-Gomez E, Kastner A, Steiner J, Schneider A, Hettling B, Poggi G, et al. The brain as immunoprecipitator of serum autoantibodies against N-Methyl-D-aspartate receptor subunit NR1. *Ann Neurol*. 2016;79:144–51.
 10. Castillo-Gomez E, Oliveira B, Tapken D, Bertrand S, Klein-Schmidt C, Pan H et al. All naturally occurring autoantibodies against the NMDA receptor subunit NR1 have pathogenic potential irrespective of epitope and immunoglobulin class. *Mol Psychiatry*. 2016;22:1776–178.
 11. Abramson J, Husebye ES. Autoimmune regulator and self-tolerance—molecular and clinical aspects. *Immunol Rev*. 2016;271:127–40.
 12. Cohen I, Young D. Autoimmunity, microbial immunity and the immunological honunculus. *Immunol Today*. 1991;12:105–10.
 13. Coutinho A, Kazatchkine MD, Avrameas S. Natural autoantibodies. *Curr Opin Immunol*. 1995;7:812–8.
 14. Ehrenreich H. Autoantibodies against the N-methyl-d-aspartate receptor subunit NR1: untangling apparent inconsistencies for clinical practice. *Front Immunol*. 2017;8:181.
 15. Lobo PI. Role of natural autoantibodies and natural IgM anti-leucocyte autoantibodies in health and disease. *Front Immunol*. 2016;7:198.
 16. Mader S, Brimberg L, Diamond B. The role of brain-reactive autoantibodies in brain pathology and cognitive impairment. *Front Immunol*. 2017;8:1101.
 17. Nguyen TT, Baumgarth N. Natural IgM and the development of b cell-mediated autoimmune diseases. *Crit Rev Immunol*. 2016;36:163–77.
 18. Coutinho E, Harrison P, Vincent A. Do neuronal autoantibodies cause psychosis? A neuroimmunological perspective. *Biol Psychiatry*. 2014;75:269–75.
 19. Diamond B, Huerta P, Mina-Osorio P, Kowal C, Volpe B. Losing your nerves? Maybe it's the antibodies. *Nat Rev Immunol*. 2009;9:449–56.
 20. Hammer C, Zerche M, Schneider A, Begemann M, Nave KA, Ehrenreich H. Apolipoprotein E4 carrier status plus circulating anti-NMDAR1 autoantibodies: association with schizoaffective disorder. *Mol Psychiatry*. 2014;19:1054–6.
 21. Kreye J, Wenke NK, Chayka M, Leubner J, Murugan R, Maier N, et al. Human cerebrospinal fluid monoclonal N-methyl-D-aspartate receptor autoantibodies are sufficient for encephalitis pathogenesis. *Brain*. 2016;139:2641–52.
 22. Begemann MGS, Papiol S, Malzahn D, Krampe H, Ribbe K, et al. Modification of cognitive performance in schizophrenia by complexin 2 gene polymorphisms. *Arch Gen Psychiatry*. 2010;67:879–88.
 23. Ribbe K, Friedrichs H, Begemann M, Grube S, Papiol S, Kästner A, et al. The cross-sectional GRAS sample: a comprehensive phenotypical data collection of schizophrenic patients. *BMC Psychiatry*. 2010;10:0–20.
 24. American Psychiatric Association. (2000) Diagnostic and statistical manual of mental disorders. 4th edn American Psychiatric Press, Washington, DC. .
 25. Wandering KP, Saschenbrecker S, Stoecker W, Dalmau J. Anti-NMDA-receptor encephalitis: a severe, multistage, treafa disorder presenting with psychosis. *J Neuroimmunol*. 2011;231:86–91.
 26. Boyle MDP, Reis KJ. Bacterial Fc receptors. *Nat Biotechnol*. 1987;5:697–703.
 27. Pruss H, Leubner J, Wenke NK, Czirjak GA, Szentiks CA, Greenwood AD. Anti-NMDA receptor encephalitis in the polar bear (*Ursus maritimus*) Knut. *Sci Rep*. 2015;5:1–7.
 28. Toyka KBD, Pestronk A, Kao I. Myasthenia gravis: passive transfer from man to mouse. *Science*. 1975;190:397–9.
 29. Schindelin J, Arganda-Carreras I, Frise E, Kaynig V, Longair M, Pietzsch T, et al. Fiji: an open-source platform for biological-image analysis. *Nat Methods*. 2012;9:676–82.
 30. Berghoff SA, Gerndt N, Winchenbach J, Stumpf SK, Hosang L, Odoardi F, et al. Dietary cholesterol promotes repair of demyelinated lesions in the adult brain. *Nat Commun*. 2017;8:1–15.
 31. Berghoff SA, Düking T, Spieth L, Winchenbach J, Stumpf SK, Gerndt N, et al. Blood-brain barrier hyperpermeability precedes demyelination in the cuprizone model. *Acta Neuropathol Commun*. 2017;5:94.
 32. Wust S, van den Brandt J, Tischner D, Kleiman A, Tuckermann JP, Gold R, et al. Peripheral T cells are the therapeutic targets of glucocorticoids in experimental autoimmune encephalomyelitis. *J Immunol*. 2008;180:8434–43.
 33. Dere E, Dahm L, Lu D, Hammerschmidt K, Ju A, Tantra M, et al. Heterozygous ambral deficiency in mice: a genetic trait with autism-like behavior restricted to the female gender. *Front Behav Neurosci*. 2014;8:181.
 34. Dere E, Winkler D, Ritter C, Ronnenberg A, Poggi G, Patzig J, et al. Gpm6b deficiency impairs sensorimotor gating and modulates the behavioral response to a 5-HT2A/C receptor agonist. *Behav Brain Res*. 2015;277:254–63.
 35. Netrakanti PR, Cooper BH, Dere E, Poggi G, Winkler D, Brose N, et al. Fast cerebellar reflex circuitry requires synaptic vesicle priming by munc13-3. *Cerebellum*. 2015;14:264–83.
 36. Winkler D, Daher F, Wustefeld L, Hammerschmidt K, Poggi G, Seelbach A et al. Hypersocial behavior and biological redundancy in mice with reduced expression of PSD95 or PSD93. *Behav Brain Res*. 2017. <https://doi.org/10.1016/j.bbr.2017.02.011> (e-pub ahead of print).
 37. Radyushkin K, El-Kordi A, Boretius S, Castaneda S, Ronnenberg A, Reim K, et al. Complexin2 null mutation requires a 'second hit' for induction of phenotypic changes relevant to schizophrenia. *Genes Brain Behav*. 2010;9:592–602.
 38. Akdeniz C, Tost H, Streit F, Haddad L, Wust S, Schafer A, et al. Neuroimaging evidence for a role of neural social stress processing in ethnic minority-associated environmental risk. *JAMA Psychiatry*. 2014;71:672–80.
 39. Jacobson SL, Ross SR, Bloomsmith MA. Characterizing abnormal behavior in a large population of zoo-housed chimpanzees: prevalence and potential influencing factors. *PeerJ*. 2016;4:e2225.
 40. Stepiak B, Papiol S, Hammer C, Ramin A, Everts S, Hennig L, et al. Accumulated environmental risk determining age at schizophrenia onset: a deep phenotyping-based study. *Lancet Psychiatry*. 2014;1:444–53.
 41. Maes M, Hendriks D, Gastel AV, Demedts P, Wauters A, Neels H, et al. Effects of psychological stress on serum immunoglobulin, complement and acute phase protein concentrations in normal volunteers. *Psychoneuroendocrinology*. 1997;22:397–409.
 42. Nagele EP, Han M, Acharya NK, DeMarshall C, Kosciuk MC, Nagele RG. Natural IgG autoantibodies are abundant and ubiquitous in human sera, and their number is influenced by age, gender, and disease. *PLoS ONE*. 2013;8:4.
 43. Planaguma J, Leyboldt F, Mannara F, Gutierrez-Cuesta J, Martin-Garcia E, Aguilar E, et al. Human N-methyl D-aspartate receptor antibodies alter memory and behaviour in mice. *Brain*. 2015;138:94–109.
 44. Busse S, Brix B, Kunschmann R, Bogerts B, Stoecker W, Busse M. N-methyl-d-aspartate glutamate receptor (NMDA-R) antibodies in mild cognitive impairment and dementias. *Neurosci Res*. 2014;85:58–64.

45. Doss S, Wandinger KP, Hyman BT, Panzer JA, Synofzik M, Dickerson B, et al. High prevalence of NMDA receptor IgA/IgM antibodies in different dementia types. *Ann Clin Transl Neurol*. 2014;1:822–32.
46. Tuzun E, Zhou L, Baehring JM, Bannykh S, Rosenfeld MR, Dalmau J. Evidence for antibody-mediated pathogenesis in anti-NMDAR encephalitis associated with ovarian teratoma. *Acta Neuropathol*. 2009;118:737–43.
47. Du J, Li XH, Li YJ. Glutamate in peripheral organs: biology and pharmacology. *Eur J Pharmacol*. 2016;784:42–8.
48. Gerhard DM, Wohleb ES, Duman RS. Emerging treatment mechanisms for depression: focus on glutamate and synaptic plasticity. *Drug Discov Today*. 2016;21:454–64.
49. Abdallah CG, Adams TG, Kelmendi B, Esterlis I, Sanacora G, Krystal JH. Ketamine's mechanism of action: a path to rapid-acting antidepressants. *Depress Anxiety*. 2016;33:689–97.
50. Alexander JK, DeVries AC, Kigerl KA, Dahlman JM, Popovich PG. Stress exacerbates neuropathic pain via glucocorticoid and NMDA receptor activation. *Brain Behav Immun*. 2009;23:851–60.
51. Rubio-Casillas A, Fernandez-Guasti A. The dose makes the poison: from glutamate-mediated neurogenesis to neuronal atrophy and depression. *Rev Neurosci*. 2016;27:599–622.
52. Nair A, Hunzeker J, Bonneau RH. Modulation of microglia and CD8(+) T cell activation during the development of stress-induced herpes simplex virus type-1 encephalitis. *Brain Behav Immun*. 2007;21:791–806.

Affiliations

Hong Pan¹ · Bárbara Oliveira¹ · Gesine Saher² · Ekrem Dere¹ · Daniel Tapken³ · Marina Mitjans¹ · Jan Seidel¹ · Janina Wesolowski¹ · Debia Wakhloo¹ · Christina Klein-Schmidt³ · Anja Ronnenberg¹ · Kerstin Schwabe⁴ · Ralf Trippe³ · Kerstin Mätz-Rensing⁵ · Stefan Berghoff² · Yazeed Al-Krinawe⁴ · Henrik Martens⁶ · Martin Begemann¹ · Winfried Stöcker⁷ · Franz-Josef Kaup⁵ · Reinhard Mischke⁸ · Susann Boretius⁹ · Klaus-Armin Nave^{2,10} · Joachim K. Krauss⁴ · Michael Hollmann¹⁰ · Fred Lühder¹¹ · Hannelore Ehrenreich^{1,10}

¹ Clinical Neuroscience, Max Planck Institute of Experimental Medicine, Göttingen, Germany

² Department of Neurogenetics, Max Planck Institute of Experimental Medicine, Göttingen, Germany

³ Department of Biochemistry I—Receptor Biochemistry, Ruhr University, Bochum, Germany

⁴ Department of Neurosurgery, Hannover Medical School, Hannover, Germany

⁵ Department of Pathology, Leibniz Institute for Primate Research, Göttingen, Germany

⁶ Synaptic Systems GmbH, Göttingen, Germany

⁷ Institute for Experimental Immunology, affiliated to Euroimmun, Lübeck, Germany

⁸ Small Animal Clinic, University of Veterinary Medicine, Hannover, Germany

⁹ Functional Imaging Laboratory, Leibniz Institute for Primate Research, Göttingen, Germany

¹⁰ DFG Research Center for Nanoscale Microscopy and Molecular Physiology of the Brain (CNMPB), Göttingen, Germany

¹¹ Department of Neuroimmunology, Institute for Multiple Sclerosis Research and Hertie Foundation, University Medicine Göttingen, Göttingen, Germany

5. PROJECT III

5. PROJECT III – Excitation-inhibition dysbalance as predictor of autistic phenotypes

Overview of Project III

The phenotypic variability observed in autism defines it as a spectrum disorder with three main groups: autism, Asperger's syndrome and pervasive developmental disorder not otherwise specified, with all of them sharing deficits in social communication/interaction, restricted interests and stereotypic/repetitive behavior (Buxbaum *et al.* 2013). However, autistic phenotypes transcend diagnostic categories. Schizophrenia is among the many neurodevelopmental diseases with autistic symptoms contributing to disease severity (Kastner *et al.* 2015, Stepniak *et al.* 2015). Additionally, subthreshold deficits of the core phenotypic domains of autism spectrum disorders (ASD) can be found in the general population in different levels, supporting the continuous nature of autistic behaviors (Jones *et al.* 2013, Kastner *et al.* 2015).

Involvement of synaptic and synapse regulating genes is a constant observation across ASD genomic screenings as well as in monogenic forms of autism. This suggests a central role for defects in synaptic structure and function in the pathogenesis of ASD. Additionally, it has been postulated that hyperexcitability of cortical circuits, due to an increased ratio between excitation and inhibition (E/I), might be associated with ASD. This imbalance in E/I can be related with increased excitatory glutamatergic signalling, or with reduction in inhibition due to a reduction in GABAergic signalling (Rubenstein *et al.* 2003, Nelson *et al.* 2015). Furthermore, evidence of a reduced E/I ratio, as consequence of a shifted E/I ratio favouring inhibition over excitation, has also been reported in both mouse and *in vitro* human IPS neurons (Dani *et al.* 2005, Marchetto *et al.* 2010). Altogether, several genetic mouse models of ASD point to altered E/I ratio as a neural mechanism underlying the pathophysiology of ASD. Human studies also support the notion that an imbalanced E/I ratio represents a convergence point for many of the genetic causes associated with ASD. In fact, cellular abnormalities involving neural transmission might be associated with neurotransmitter generation, release, reception and re-uptake. Quantification of neurotransmitter levels provided some suggestive evidence supporting the involvement of altered E/I in ASD. Increased serum levels of glutamate and GABA have been reported in ASD when compared to neurotypical individuals. Magnetic resonance spectroscopy studies provided additional information by measuring the brain levels of GABA, glutamate and the glutamate precursor glutamine. Nevertheless, the results are very heterogeneous across studies and do not allow firm conclusions. Indirect evidence for imbalanced E/I ratio has been provided by

PROJECT III

electroencephalography and magnetoencephalography data. However, they do not point a clear direction of such imbalance (Dickinson *et al.* 2016).

Considering the transcending nature of autistic phenotypes, the severity of autistic traits in a population of schizophrenic patients was evaluated. To cover the ASD diagnostic domains of difficulties in social interaction, communication, and repetitive and stereotypic behaviour in the GRAS population, an autism severity score (PAUSS) based on specific items of the Positive and Negative Syndrome Scale (PANSS) was employed. The PANSS is a standardized clinical observation tool, applied to assess positive, negative and psychopathology symptom severity in schizophrenia (Kay *et al.* 1987, Kastner *et al.* 2015). By ranking individuals according to their PAUSS score it was possible to categorize them in two main groups: low and high PAUSS, in which higher scores represent a higher severity of autistic traits.

Male individuals of both groups were then selected and matched for age, handedness and antipsychotic medication to access their E/I ratio using TMS. Non-invasive brain stimulation techniques as TMS allow probing cortical excitability *in vivo* (Hallett 2007). An input-output (I/O) curve to assess excitability and a paired-pulse TMS protocol to monitor intracortical inhibition and facilitation were applied in schizophrenic patients presenting contrasting PAUSS scores. Threshold or suprathreshold stimulation of the motor cortex with TMS activates cortical neurons via the induction of electric currents, generating motor evoked potentials (MEP) in the respective target muscle. MEP amplitude serves as a measure of cortical excitability. Therefore, the minimum TMS intensity to elicit an MEP (motor threshold) and the I/O curve, in which the MEP response due to increasing stimulation intensity is monitored, are the global measures of corticospinal excitability. These readouts depend largely on the activation of voltage-gated ion channels, with the probable exception of MEPs resulting from high TMS intensities, in which the glutamatergic system is also involved (Paulus *et al.* 2008). In contrast, paired-pulse TMS protocols allow the relative specific determination of intracortical excitability. Here, a first sub-threshold TMS stimulus, which does not elicit an MEP and whose effects are consequently intracortical, is followed by a suprathreshold stimulus. The alteration of the MEP amplitude elicited by the second stimulus depends on the interstimulus interval and could serve as index of intracortical excitability. Short latency intracortical inhibition probes primarily inhibitory GABAergic interneurons, whereas intracortical facilitation probes glutamatergic excitatory connections (Kujirai *et al.* 1993, Paulus *et al.* 2008). While no differences in resting or active motor thresholds were observed between the two phenotypic groups, the group of schizophrenic patients with more severe autistic features showed higher cortico-spinal excitability and higher intracortical inhibition compared to the group with low autistic features. In contrast, intracortical facilitation

did not differ between groups. Additionally, the E/I ratio and the severity of autistic traits were positively correlated.

Our results suggest that the severity of autistic traits in these patients couples with altered GABAergic neurotransmission and activity of voltage-gated ion channels, with no clear changes in glutamatergic neurotransmission. Enhanced corticospinal excitability could have been driven by altered voltage-gated ion channel activity or glutamate signalling, particularly at high TMS intensities (Paulus *et al.* 2008). Since glutamate-driven intracortical facilitation did not differ between groups, a predominant impact on voltage-gated ion channels is more likely. Overall, the results of this study support the concept of a disturbed E/I balance in subjects with autistic features, which is based on altered GABAergic and voltage-gated ion channel functions.

These findings support the pathophysiological continuum of autistic traits and the convergence of the associated phenotypic and functional aspects in a common pathway that transcends diagnostic criteria.

Original publication

Oliveira B*, Mitjans M*, Nitsche MA, Kuo M-F and Ehrenreich H. *Excitation-inhibition dysbalance as predictor of autistic phenotypes.* *Under revision.*

*Authors with equal contribution

Personal contribution: I actively participated in outlining and writing the manuscript, together with my supervisor. I was significantly involved in the data analysis, prepared the figures and figure legends and contributed to the overall preparation of the manuscript. Additionally, I was responsible for the submission phase and will actively participate in the revision process.

The manuscript of Project III is currently under revision and is presented in the appendix section of the thesis.

6. SUMMARY AND CONCLUSIONS

6. SUMMARY AND CONCLUSIONS

The complexity of neuropsychiatric conditions reflects the heterogeneity of their etiological factors, in which a combination of genetic and environmental risk factors shapes phenotypes. However, one must dissect single contributors to disease and health status having in mind the possibility of overlapping phenotypes across diseases, and that an individual's biological repertoire influences their response to environmental triggers. The present thesis focused on the molecular and functional characterization of autoantibodies targeting the NMDAR and their role beyond its pathognomonic association with anti-NMDAR encephalitis (Project I and II); and how the severity of autistic traits in schizophrenic patients relates with imbalances in excitation and inhibition (Project III).

The nervous and immune systems integrate environmental cues that shape their function and influence the dynamic interaction between both systems. Alterations in this delicate balance are emerging as strong contributors to brain disease. Autoantibodies reactive with several brain expressed proteins have been associated with neurological conditions, either as an etiological factor or by contributing to disease severity (Crisp *et al.* 2016). The presence of different NMDAR-AB isotypes has been previously described in healthy individuals and individuals suffering from other conditions that do not include anti-NMDAR encephalitis (Dahm *et al.* 2014, Finke *et al.* 2017). However, the functional and molecular properties of these autoantibodies remained to be characterized. Projects I and II focused on understanding the molecular and functional underpinnings of NMDAR-AB and the role of the BBB in preventing the antagonizing effects of these autoantibodies in the brain.

In project I, a detailed characterization of different NMDAR-AB isotypes, that included IgM, IgA and IgG provided information regarding their functional effect on NMDAR cellular location and glutamate evoked-responses. Furthermore, a systematic mapping of the NMDAR epitopes recognized by these autoantibodies was performed. Altogether, this information broadened the spectrum of action of these autoantibodies. Anti-NMDAR encephalitis research has been focusing mainly on the effects of NMDAR-AB of IgG isotypes (Dalmau *et al.* 2008, Gleichman *et al.* 2012, Moscato *et al.* 2014). This work demonstrated that other isotypes can antagonize NMDAR activity and potentially impact brain function upon access to the brain. Beyond the pathogenic context of anti-NMDAR encephalitis, these NMDAR-AB can induce NMDAR antagonism and consequently alter glutamatergic signalling. *In vivo*, exposure to NMDAR-AB leads to extracellular accumulation of glutamate and the consequent hyperglutamatergic state might dysregulate the excitability of neuronal networks via excitotoxic neuronal dysfunction (Manto *et al.* 2010). *Post mortem* studies of anti-

SUMMARY AND CONCLUSIONS

NMDAR encephalitis patients did not reveal any pathological evidence of neuro-axonal injury (Bien *et al.* 2012). Thus, it is plausible to think that the NMDAR-AB glutamate-mediated excitotoxicity does not reach the necessary threshold to induce neurodegeneration but it is enough to alter glutamatergic neurotransmission. Indeed, in rat hippocampal neurons NMDAR-AB (IgG) from CSF of schizophrenic patients alter the surface dynamics and nanoscale organization of synaptic NMDAR, preventing long-term potentiation at glutamatergic synapses (Jezequel *et al.* 2017). The polyspecificity and polyclonality, of several of these NMDAR-AB, along with their functionality, contrasts with the relevance credited exclusively to one epitope (G7 site of the NTD) in the context of anti-NMDAR encephalitis and suggests a more diverse interaction of these autoantibodies with NMDAR.

Project II demonstrated that NMDAR-AB are also present in other mammal species and, as in humans, its seroprevalence increases with age (Hammer *et al.* 2014). However, of all the species tested two monkey species presented high seroprevalence in young age. This was also observed in humans that underwent migration. Altogether, this data broadened the number of species with reported seropositivity for NMDAR-AB and raised some interesting questions about the environmental triggers of antibody production such as chronic life stress, that warrant further clarification. Furthermore, using a novel autoimmune mouse model, with endogenous production of NMDAR-AB, the BBB emerged as a central player in avoiding the antagonizing effects of these autoantibodies in the brain. For the first time, in physiological conditions of NMDAR-AB production, it was shown that the BBB has a protective effect regarding the antagonizing action of these autoantibodies in the brain. NMDAR-AB are able to bind to several brain areas (Castillo-Gomez *et al.* 2016). An intact BBB prevents NMDAR-AB from reaching the brain parenchyma by restricting immunoglobulins influx and performing active efflux of the low levels of immunoglobulins that cross the BBB in physiological conditions. Additionally, it tightly controls the transendothelial migration of B cells, which once in the brain parenchyma could contact with NMDAR and, in the case of a secondary antigen encounter, be boosted to produce NMDAR-AB intrathecally (Diamond *et al.* 2009). In the presence of a compromised BBB, such as in *ApoE*^{-/-} mice, endogenous production of NMDAR-AB leads to an increased sensitivity to MK-801 treatment translated to an exaggerated hyperactive behaviour in the open field due to a cumulative antagonizing effect of these autoantibodies and MK-801. Moreover, the presence of NMDAR-AB in the brain *per se* does not trigger an inflammatory reaction which points to the necessity of other contributors for the development of an encephalitogenic phenotype.

The data gathered in Project I and II broadens the spectrum of action of these autoantibodies by attributing functional roles to other isotypes, and consolidates the protective role of the BBB in seropositive individuals. NMDAR-AB emerge as components of the immune repertoire with the potential to shape brain function and possibly contribute to psychiatric

phenotypes (Jezequel *et al.* 2017). It provides relevant information for the clinical management of asymptomatic individuals seropositive for NMDAR-AB and the importance of monitoring BBB integrity in these individuals (Ehrenreich 2017).

Project III addresses the continuous nature of autistic phenotypes in a sample of schizophrenic male individuals and demonstrates how imbalances in excitation and inhibition can correlate with the severity of autistic traits. By combining readouts of sociability, communication and stereotypic behaviour, in a single dimension, it was possible to classify schizophrenic patients regarding the severity of their autistic traits. Furthermore, non-invasive assessment of cortico-spinal excitability and intracortical inhibition using TMS provided information on excitation and inhibition levels in these individuals. The results of this project suggest a positive correlation between the severity of autistic traits and imbalances in E/I ratio in schizophrenic patients, mainly mediated by altered GABAergic and voltage-gated ion channel functions. It supports previous reports of altered GABAergic neurotransmission in schizophrenia, adding a new correlation with phenotypic readouts (Wobrock *et al.* 2008).

To conclude, this thesis comprises translational work in clinical neuroscience. It broadens the current knowledge on neuro-immune interactions, focusing on NMDAR-AB (patho)physiology, and on functional readouts associated with phenotypic differences within schizophrenia. Ultimately, it can contribute to improve clinical practices for diagnostics and disease management.

7. BIBLIOGRAPHY

7. BIBLIOGRAPHY

A

Alberts, B., Johnson, A., Lewis, J., Raff, M., Roberts, K. and Walter, P. (2002). Molecular biology of the cell. New York, *Garland Science*.

Alvarez, J. I., Dodelet-Devillers, A., Kebir, H., Ifergan, I., Fabre, P. J., Terouz, S., Sabbagh, M., Wosik, K., Bourbonniere, L., Bernard, M., *et al.* (2011). The Hedgehog pathway promotes blood-brain barrier integrity and CNS immune quiescence. *Science* 334(6063): 1727-1731.

Ang, C. W., Jacobs, B. C. and Laman, J. D. (2004). The Guillain-Barre syndrome: a true case of molecular mimicry. *Trends Immunol* 25(2): 61-66.

Argaw, A. T., Zhang, Y., Snyder, B. J., Zhao, M. L., Kopp, N., Lee, S. C., Raine, C. S., Brosnan, C. F. and John, G. R. (2006). IL-1 Regulates Blood-Brain Barrier Permeability via Reactivation of the Hypoxia-Angiogenesis Program. *J Immunol* 177(8): 5574-5584.

Armangue, T., Leypoldt, F., Malaga, I., Raspall-Chaure, M., Marti, I., Nichter, C., Pugh, J., Vicente-Rasoamalala, M., Lafuente-Hidalgo, M., Macaya, A., *et al.* (2014). Herpes simplex virus encephalitis is a trigger of brain autoimmunity. *Ann Neurol* 75(2): 317-323.

Atassi, M. Z. and Casali, P. (2008). Molecular mechanisms of autoimmunity. *Autoimmunity* 41(2): 123-132.

Avrameas, S., Ternynck, T., Tsonis, I. A. and Lymberi, P. (2007). Naturally occurring B-cell autoreactivity: a critical overview. *J Autoimmun* 29(4): 213-218.

Azevedo, F. A., Carvalho, L. R., Grinberg, L. T., Farfel, J. M., Ferretti, R. E., Leite, R. E., Jacob Filho, W., Lent, R. and Herculano-Houzel, S. (2009). Equal numbers of neuronal and nonneuronal cells make the human brain an isometrically scaled-up primate brain. *J Comp Neurol* 513(5): 532-541.

B

Barragan, A., Weidner, J. M., Jin, Z., Korpi, E. R. and Birnir, B. (2015). GABAergic signalling in the immune system. *Acta Physiol (Oxf)* 213(4): 819-827.

Bell, R. D., Winkler, E. A., Singh, I., Sagare, A. P., Deane, R., Wu, Z., Holtzman, D. M., Betsholtz, C., Armulik, A., Sallstrom, J., *et al.* (2012). Apolipoprotein E controls cerebrovascular integrity via cyclophilin A. *Nature* 485(7399): 512-516.

Bhat, R., Axtell, R., Mitra, A., Miranda, M., Lock, C., Tsien, R. W. and Steinman, L. (2010). Inhibitory role for GABA in autoimmune inflammation. *Proc Natl Acad Sci U S A* 107(6): 2580-2585.

Bhat, R. and Steinman, L. (2009). Innate and adaptive autoimmunity directed to the central nervous system. *Neuron* 64(1): 123-132.

Bialas, A. R., Presumey, J., Das, A., van der Poel, C. E., Lapchak, P. H., Mesin, L., Victora, G., Tsokos, G. C., Mawrin, C., Herbst, R., *et al.* (2017). Microglia-dependent synapse loss in type I interferon-mediated lupus. *Nature* 546(7659): 539-543.

Bien, C. G., Vincent, A., Barnett, M. H., Becker, A. J., Blumcke, I., Graus, F., Jellinger, K. A., Reuss, D. E., Ribalta, T., Schlegel, J., *et al.* (2012). Immunopathology of autoantibody-associated encephalitides: clues for pathogenesis. *Brain* 135(Pt 5): 1622-1638.

BIBLIOGRAPHY

Blanchette, M. and Daneman, R. (2015). Formation and maintenance of the BBB. *Mech Dev* 138 Pt 1: 8-16.

Borghese, L., Dolezalova, D., Opitz, T., Haupt, S., Leinhaas, A., Steinfarz, B., Koch, P., Edenhofer, F., Hampl, A. and Brustle, O. (2010). Inhibition of notch signaling in human embryonic stem cell-derived neural stem cells delays G1/S phase transition and accelerates neuronal differentiation in vitro and in vivo. *Stem Cells* 28(5): 955-964.

Boulanger, L. M. (2009). Immune proteins in brain development and synaptic plasticity. *Neuron* 64(1): 93-109.

Boyle, M. D. P. and Reis, K. J. (1987). Bacterial Fc-Receptors. *Bio-Technology* 5(7): 697-703.

Boyles, J. K., Pitas, R. E., Wilson, E., Mahley, R. W. and Taylor, J. M. (1985). Apolipoprotein E associated with astrocytic glia of the central nervous system and with nonmyelinating glia of the peripheral nervous system. *J Clin Invest* 76(4): 1501-1513.

Braniste, V., Al-Asmakh, M., Kowal, C., Anuar, F., Abbaspour, A., Toth, M., Korecka, A., Bakocevic, N., Ng, L. G., Kundu, P., *et al.* (2014). The gut microbiota influences blood-brain barrier permeability in mice. *Sci Transl Med* 6(263): 263ra158.

Brimberg, L., Mader, S., Fujieda, Y., Arinuma, Y., Kowal, C., Volpe, B. T. and Diamond, B. (2015). Antibodies as Mediators of Brain Pathology. *Trends Immunol* 36(11): 709-724.

Brimberg, L., Mader, S., Jeganathan, V., Berlin, R., Coleman, T. R., Gregersen, P. K., Huerta, P. T., Volpe, B. T. and Diamond, B. (2016). Caspr2-reactive antibody cloned from a mother of an ASD child mediates an ASD-like phenotype in mice. *Mol Psychiatry* 21(12): 1663-1671.

Brimberg, L., Sadiq, A., Gregersen, P. K. and Diamond, B. (2013). Brain-reactive IgG correlates with autoimmunity in mothers of a child with an autism spectrum disorder. *Mol Psychiatry* 18(11): 1171-1177.

Busse, S., Busse, M., Brix, B., Probst, C., Genz, A., Bogerts, B., Stoecker, W. and Steiner, J. (2014). Seroprevalence of N-methyl-D-aspartate glutamate receptor (NMDA-R) autoantibodies in aging subjects without neuropsychiatric disorders and in dementia patients. *Eur Arch Psychiatry Clin Neurosci* 264(6): 545-550.

Buxbaum, J. and Hof, P. (2013). The neuroscience of autism spectrum disorders. Amsterdam, *Academic press*.

C

Camdessanche, J. P., Streichenberger, N., Cavillon, G., Rogemond, V., Jousserand, G., Honnorat, J., Convers, P. and Antoine, J. C. (2011). Brain immunohistopathological study in a patient with anti-NMDAR encephalitis. *Eur J Neurol* 18(6): 929-931.

Castillo-Gomez, E., Kastner, A., Steiner, J., Schneider, A., Hettling, B., Poggi, G., Ostehr, K., Uhr, M., Asif, A. R., Matzke, M., *et al.* (2016). The brain as immunoprecipitator of serum autoantibodies against N-Methyl-D-aspartate receptor subunit NR1. *Ann Neurol* 79(1): 144-151.

Castillo-Gomez, E., Oliveira, B., Tapken, D., Bertrand, S., Klein-Schmidt, C., Pan, H., Zafeiriou, P., Steiner, J., Jurek, B., Trippe, R., *et al.* (2017). All naturally occurring

autoantibodies against the NMDA receptor subunit NR1 have pathogenic potential irrespective of epitope and immunoglobulin class. *Mol Psychiatry* 22(12): 1776-1784.

Chambers, S. M., Fasano, C. A., Papapetrou, E. P., Tomishima, M., Sadelain, M. and Studer, L. (2009). Highly efficient neural conversion of human ES and iPS cells by dual inhibition of SMAD signaling. *Nat Biotechnol* 27(3): 275-280.

Chartoff, E. H., Heusner, C. L. and Palmiter, R. D. (2005). Dopamine is not required for the hyperlocomotor response to NMDA receptor antagonists. *Neuropsychopharmacology* 30(7): 1324-1333.

Church, L. D., Cook, G. P. and McDermott, M. F. (2008). Primer: inflammasomes and interleukin 1beta in inflammatory disorders. *Nat Clin Pract Rheumatol* 4(1): 34-42.

Correale, J. and Villa, A. (2009). Cellular elements of the blood-brain barrier. *Neurochem Res* 34(12): 2067-2077.

Crisp, S. J., Kullmann, D. M. and Vincent, A. (2016). Autoimmune synaptopathies. *Nat Rev Neurosci* 17(2): 103-117.

Cunningham, M. W. (2012). Streptococcus and rheumatic fever. *Curr Opin Rheumatol* 24(4): 408-416.

D

Dahm, L., Ott, C., Steiner, J., Stepniak, B., Teegen, B., Saschenbrecker, S., Hammer, C., Borowski, K., Begemann, M., Lemke, S., *et al.* (2014). Seroprevalence of autoantibodies against brain antigens in health and disease. *Ann Neurol* 76(1): 82-94.

Dalmau, J. (2016). NMDA receptor encephalitis and other antibody-mediated disorders of the synapse: The 2016 Cotzias Lecture. *Neurology* 87(23): 2471-2482.

Dalmau, J., Gleichman, A. J., Hughes, E. G., Rossi, J. E., Peng, X., Lai, M., Dessain, S. K., Rosenfeld, M. R., Balice-Gordon, R. and Lynch, D. R. (2008). Anti-NMDA-receptor encephalitis: case series and analysis of the effects of antibodies. *Lancet Neurol* 7(12): 1091-1098.

Dalmau, J., Tuzun, E., Wu, H. Y., Masjuan, J., Rossi, J. E., Voloschin, A., Baehring, J. M., Shimazaki, H., Koide, R., King, D., *et al.* (2007). Paraneoplastic anti-N-methyl-D-aspartate receptor encephalitis associated with ovarian teratoma. *Ann Neurol* 61(1): 25-36.

Dani, V. S., Chang, Q., Maffei, A., Turrigiano, G. G., Jaenisch, R. and Nelson, S. B. (2005). Reduced cortical activity due to a shift in the balance between excitation and inhibition in a mouse model of Rett syndrome. *Proc Natl Acad Sci U S A* 102(35): 12560-12565.

DeGiorgio, L. A., Konstantinov, K. N., Lee, S. C., Hardin, J. A., Volpe, B. T. and Diamond, B. (2001). A subset of lupus anti-DNA antibodies cross-reacts with the NR2 glutamate receptor in systemic lupus erythematosus. *Nat Med* 7(11): 1189-1193.

DeMarshall, C., Sarkar, A., Nagele, E. P., Goldwaser, E., Godsey, G., Acharya, N. K. and Nagele, R. G. (2015). Utility of autoantibodies as biomarkers for diagnosis and staging of neurodegenerative diseases. *Int Rev Neurobiol* 122: 1-51.

Deverman, B. E. and Patterson, P. H. (2009). Cytokines and CNS development. *Neuron* 64(1): 61-78.

BIBLIOGRAPHY

Diamond, B., Honig, G., Mader, S., Brimberg, L. and Volpe, B. T. (2013). Brain-reactive antibodies and disease. *Annu Rev Immunol* 31: 345-385.

Diamond, B., Huerta, P. T., Mina-Osorio, P., Kowal, C. and Volpe, B. T. (2009). Losing your nerves? Maybe it's the antibodies. *Nat Rev Immunol* 9(6): 449-456.

Dickinson, A., Jones, M. and Milne, E. (2016). Measuring neural excitation and inhibition in autism: Different approaches, different findings and different interpretations. *Brain Res* 1648(Pt A): 277-289.

Dionisio, L., Jose De Rosa, M., Bouzat, C. and Esandi Mdel, C. (2011). An intrinsic GABAergic system in human lymphocytes. *Neuropharmacology* 60(2-3): 513-519.

Doss, S., Wandinger, K. P., Hyman, B. T., Panzer, J. A., Synofzik, M., Dickerson, B., Mollenhauer, B., Scherzer, C. R., Iverson, A. J., Finke, C., *et al.* (2014). High prevalence of NMDA receptor IgA/IgM antibodies in different dementia types. *Ann Clin Transl Neurol* 1(10): 822-832.

E

Ehrenreich, H. (2017). Autoantibodies against the N-Methyl-d-Aspartate Receptor Subunit NR1: Untangling Apparent Inconsistencies for Clinical Practice. *Front Immunol* 8: 181.

Engelhardt, B. and Liebner, S. (2014). Novel insights into the development and maintenance of the blood-brain barrier. *Cell Tissue Res* 355(3): 687-699.

F

Fabian, R. H. and Petroff, G. (1987). Intraneuronal IgG in the central nervous system: uptake by retrograde axonal transport. *Neurology* 37(11): 1780-1784.

Faust, T. W., Chang, E. H., Kowal, C., Berlin, R., Gazaryan, I. G., Bertini, E., Zhang, J., Sanchez-Guerrero, J., Fragoso-Loyo, H. E., Volpe, B. T., *et al.* (2010). Neurotoxic lupus autoantibodies alter brain function through two distinct mechanisms. *Proc Natl Acad Sci U S A* 107(43): 18569-18574.

Finke, C., Bartels, F., Lutt, A., Pruss, H. and Harms, L. (2017). High prevalence of neuronal surface autoantibodies associated with cognitive deficits in cancer patients. *J Neurol* 264(9): 1968-1977.

Finke, C., Kopp, U. A., Pruss, H., Dalmau, J., Wandinger, K. P. and Ploner, C. J. (2012). Cognitive deficits following anti-NMDA receptor encephalitis. *J Neurol Neurosurg Psychiatry* 83(2): 195-198.

Fujinami, R. S. and Oldstone, M. B. (1985). Amino acid homology between the encephalitogenic site of myelin basic protein and virus: mechanism for autoimmunity. *Science* 230(4729): 1043-1045.

Fuks, J. M., Arrighi, R. B., Weidner, J. M., Kumar Mendu, S., Jin, Z., Wallin, R. P., Rethi, B., Birnir, B. and Barragan, A. (2012). GABAergic signaling is linked to a hypermigratory phenotype in dendritic cells infected by *Toxoplasma gondii*. *PLoS Pathog* 8(12): e1003051.

Fullerton, S. M., Shirman, G. A., Strittmatter, W. J. and Matthew, W. D. (2001). Impairment of the blood-nerve and blood-brain barriers in apolipoprotein e knockout mice. *Exp Neurol* 169(1): 13-22.

Furukawa, H., Singh, S. K., Mancusso, R. and Gouaux, E. (2005). Subunit arrangement and function in NMDA receptors. *Nature* 438(7065): 185-192.

Fusaki, N., Ban, H., Nishiyama, A., Saeki, K. and Hasegawa, M. (2009). Efficient induction of transgene-free human pluripotent stem cells using a vector based on Sendai virus, an RNA virus that does not integrate into the host genome. *Proc Jpn Acad Ser B Phys Biol Sci* 85(8): 348-362.

G

Ge, S., Song, L., Serwanski, D. R., Kuziel, W. A. and Pachter, J. S. (2008). Transcellular transport of CCL2 across brain microvascular endothelial cells. *J Neurochem* 104(5): 1219-1232.

Germain, N., Banda, E. and Grabel, L. (2010). Embryonic stem cell neurogenesis and neural specification. *J Cell Biochem* 111(3): 535-542.

Gielen, M., Siegler Retchless, B., Mony, L., Johnson, J. W. and Paoletti, P. (2009). Mechanism of differential control of NMDA receptor activity by NR2 subunits. *Nature* 459(7247): 703-707.

Giulian, D., Young, D. G., Woodward, J., Brown, D. C. and Lachman, L. B. (1988). Interleukin-1 is an astroglial growth factor in the developing brain. *J Neurosci* 8(2): 709-714.

Gladding, C. M. and Raymond, L. A. (2011). Mechanisms underlying NMDA receptor synaptic/extrasynaptic distribution and function. *Mol Cell Neurosci* 48(4): 308-320.

Gleichman, A. J., Spruce, L. A., Dalmau, J., Seeholzer, S. H. and Lynch, D. R. (2012). Anti-NMDA receptor encephalitis antibody binding is dependent on amino acid identity of a small region within the GluN1 amino terminal domain. *J Neurosci* 32(32): 11082-11094.

H

Hallett, M. (2007). Transcranial magnetic stimulation: a primer. *Neuron* 55(2): 187-199.

Hammer, C., Stepniak, B., Schneider, A., Papiol, S., Tantra, M., Begemann, M., Siren, A. L., Pardo, L. A., Sperling, S., Mohd Jofry, S., *et al.* (2014). Neuropsychiatric disease relevance of circulating anti-NMDA receptor autoantibodies depends on blood-brain barrier integrity. *Mol Psychiatry* 19(10): 1143-1149.

Hatta, T., Moriyama, K., Nakashima, K., Taga, T. and Otani, H. (2002). The Role of gp130 in cerebral cortical development: in vivo functional analysis in a mouse exo utero system. *J Neurosci* 22(13): 5516-5524.

Hellstrom, M., Kalen, M., Lindahl, P., Abramsson, A. and Betsholtz, C. (1999). Role of PDGF-B and PDGFR-beta in recruitment of vascular smooth muscle cells and pericytes during embryonic blood vessel formation in the mouse. *Development* 126(14): 3047-3055.

Herculano-Houzel, S. (2009). The human brain in numbers: a linearly scaled-up primate brain. *Front Hum Neurosci* 3: 31.

Hogan-Cann, A. D. and Anderson, C. M. (2016). Physiological Roles of Non-Neuronal NMDA Receptors. *Trends Pharmacol Sci* 37(9): 750-767.

Horak, M., Petralia, R. S., Kaniakova, M. and Sans, N. (2014). ER to synapse trafficking of NMDA receptors. *Front Cell Neurosci* 8: 394.

BIBLIOGRAPHY

Huber, J. D., Egleton, R. D. and Davis, T. P. (2001). Molecular physiology and pathophysiology of tight junctions in the blood-brain barrier. *Trends Neurosci* 24(12): 719-725.

Hughes, E. G., Peng, X., Gleichman, A. J., Lai, M., Zhou, L., Tsou, R., Parsons, T. D., Lynch, D. R., Dalmau, J. and Balice-Gordon, R. J. (2010). Cellular and synaptic mechanisms of anti-NMDA receptor encephalitis. *J Neurosci* 30(17): 5866-5875.

Huh, G. S., Boulanger, L. M., Du, H., Riquelme, P. A., Brotz, T. M. and Shatz, C. J. (2000). Functional requirement for class I MHC in CNS development and plasticity. *Science* 290(5499): 2155-2159.

Hwang, J. K., Alt, F. W. and Yeap, L. S. (2015). Related Mechanisms of Antibody Somatic Hypermutation and Class Switch Recombination. *Microbiol Spectr* 3(1): MDNA3-0037-2014.

I

Iacobucci, G. J. and Popescu, G. K. (2017). NMDA receptors: linking physiological output to biophysical operation. *Nat Rev Neurosci* 18(4): 236-249.

Irifune, M., Shimizu, T., Nomoto, M. and Fukuda, T. (1995). Involvement of N-methyl-D-aspartate (NMDA) receptors in noncompetitive NMDA receptor antagonist-induced hyperlocomotion in mice. *Pharmacol Biochem Behav* 51(2-3): 291-296.

Isaacson, J. S. and Scanziani, M. (2011). How inhibition shapes cortical activity. *Neuron* 72(2): 231-243.

J

Jacobson, S. L., Ross, S. R. and Bloomsmith, M. A. (2016). Characterizing abnormal behavior in a large population of zoo-housed chimpanzees: prevalence and potential influencing factors. *PeerJ* 4: e2225.

Janeway, C., Travers, P., Walport, M. and Shlomchik, M. (2001). Immunobiology: The Immune System in Health and Disease. New York, *Garland Science*.

Jezequel, J., Johansson, E. M., Dupuis, J. P., Rogemond, V., Grea, H., Kellermayer, B., Hamdani, N., Le Guen, E., Rabu, C., Lepleux, M., *et al.* (2017). Dynamic disorganization of synaptic NMDA receptors triggered by autoantibodies from psychotic patients. *Nat Commun* 8(1): 1791.

Jones, R. M., Cadby, G., Melton, P. E., Abraham, L. J., Whitehouse, A. J. and Moses, E. K. (2013). Genome-wide association study of autistic-like traits in a general population study of young adults. *Front Hum Neurosci* 7: 658.

K

Kandel, E., Schwartz, J. and T., J. (2000). Principles of neural science. New York, *McGraw-Hill*.

Kastner, A., Begemann, M., Michel, T. M., Everts, S., Stepniak, B., Bach, C., Poustka, L., Becker, J., Banaschewski, T., Dose, M., *et al.* (2015). Autism beyond diagnostic categories: characterization of autistic phenotypes in schizophrenia. *BMC Psychiatry* 15: 115.

Kay, S. R., Fiszbein, A. and Opler, L. A. (1987). The positive and negative syndrome scale (PANSS) for schizophrenia. *Schizophr Bull* 13(2): 261-276.

Kohwi, M. and Doe, C. Q. (2013). Temporal fate specification and neural progenitor competence during development. *Nat Rev Neurosci* 14(12): 823-838.

Kracker, S. and Durandy, A. (2011). Insights into the B cell specific process of immunoglobulin class switch recombination. *Immunol Lett* 138(2): 97-103.

Kujirai, T., Caramia, M. D., Rothwell, J. C., Day, B. L., Thompson, P. D., Ferbert, A., Wroe, S., Asselman, P. and Marsden, C. D. (1993). Corticocortical inhibition in human motor cortex. *J Physiol* 471: 501-519.

L

Lau, C. G. and Zukin, R. S. (2007). NMDA receptor trafficking in synaptic plasticity and neuropsychiatric disorders. *Nat Rev Neurosci* 8(6): 413-426.

Lee, H., Brott, B. K., Kirkby, L. A., Adelson, J. D., Cheng, S., Feller, M. B., Datwani, A. and Shatz, C. J. (2014). Synapse elimination and learning rules co-regulated by MHC class I H2-Db. *Nature* 509(7499): 195-200.

Lee, S. W., Kim, W. J., Choi, Y. K., Song, H. S., Son, M. J., Gelman, I. H., Kim, Y. J. and Kim, K. W. (2003). SSeCKS regulates angiogenesis and tight junction formation in blood-brain barrier. *Nat Med* 9(7): 900-906.

Lefranc, M.-P. and Lefranc, G. (2001). The Immunoglobulin Factsbook. San Diego, *Academic Press*.

Lennon, V. A., Wingerchuk, D. M., Kryzer, T. J., Pittock, S. J., Lucchinetti, C. F., Fujihara, K., Nakashima, I. and Weinshenker, B. G. (2004). A serum autoantibody marker of neuromyelitis optica: distinction from multiple sclerosis. *The Lancet* 364(9451): 2106-2112.

Levin, E. C., Acharya, N. K., Han, M., Zavareh, S. B., Sedeyn, J. C., Venkataraman, V. and Nagele, R. G. (2010). Brain-reactive autoantibodies are nearly ubiquitous in human sera and may be linked to pathology in the context of blood-brain barrier breakdown. *Brain Res* 1345: 221-232.

Levite, M. (2008). Neurotransmitters activate T-cells and elicit crucial functions via neurotransmitter receptors. *Curr Opin Pharmacol* 8(4): 460-471.

Lu, M., Grove, E. A. and Miller, R. J. (2002). Abnormal development of the hippocampal dentate gyrus in mice lacking the CXCR4 chemokine receptor. *Proc Natl Acad Sci U S A* 99(10): 7090-7095.

Lussier, M. P., Sanz-Clemente, A. and Roche, K. W. (2015). Dynamic Regulation of N-Methyl-d-aspartate (NMDA) and alpha-Amino-3-hydroxy-5-methyl-4-isoxazolepropionic Acid (AMPA) Receptors by Posttranslational Modifications. *J Biol Chem* 290(48): 28596-28603.

M

Mader, S., Brimberg, L. and Diamond, B. (2017). The Role of Brain-Reactive Autoantibodies in Brain Pathology and Cognitive Impairment. *Front Immunol* 8: 1101.

Maes, M., Hendriks, D., Van Gastel, A., Demedts, P., Wauters, A., Neels, H., Janca, A. and Scharpe, S. (1997). Effects of psychological stress on serum immunoglobulin, complement and acute phase protein concentrations in normal volunteers. *Psychoneuroendocrinology* 22(6): 397-409.

BIBLIOGRAPHY

Manto, M., Dalmau, J., Didelot, A., Rogemond, V. and Honnorat, J. (2010). In vivo effects of antibodies from patients with anti-NMDA receptor encephalitis: further evidence of synaptic glutamatergic dysfunction. *Orphanet J Rare Dis* 5: 31.

Manto, M., Dalmau, J., Didelot, A., Rogemond, V. and Honnorat, J. (2011). Afferent facilitation of corticomotor responses is increased by IgGs of patients with NMDA-receptor antibodies. *J Neurol* 258(1): 27-33.

Marchalonis, J. J., Hohman, V. S., Thomas, C. and Schluter, S. F. (1993). Antibody production in sharks and humans: a role for natural antibodies. *Dev Comp Immunol* 17(1): 41-53.

Marchetto, M. C., Carromeu, C., Acab, A., Yu, D., Yeo, G. W., Mu, Y., Chen, G., Gage, F. H. and Muotri, A. R. (2010). A model for neural development and treatment of Rett syndrome using human induced pluripotent stem cells. *Cell* 143(4): 527-539.

Marchiando, A. M., Shen, L., Graham, W. V., Weber, C. R., Schwarz, B. T., Austin, J. R., 2nd, Raleigh, D. R., Guan, Y., Watson, A. J., Montrose, M. H., *et al.* (2010). Caveolin-1-dependent occludin endocytosis is required for TNF-induced tight junction regulation in vivo. *J Cell Biol* 189(1): 111-126.

Martinez-Hernandez, E., Horvath, J., Shiloh-Malawsky, Y., Sangha, N., Martinez-Lage, M. and Dalmau, J. (2011). Analysis of complement and plasma cells in the brain of patients with anti-NMDAR encephalitis. *Neurology* 77(6): 589-593.

Mason, D. (1998). A very high level of crossreactivity is an essential feature of the T-cell receptor. *Immunol Today* 19(9): 395-404.

Mason, H. A., Rakowiecki, S. M., Gridley, T. and Fishell, G. (2006). Loss of notch activity in the developing central nervous system leads to increased cell death. *Dev Neurosci* 28(1-2): 49-57.

Mayer, M. L. (2011). Emerging models of glutamate receptor ion channel structure and function. *Structure* 19(10): 1370-1380.

Mehta, A., Prabhakar, M., Kumar, P., Deshmukh, R. and Sharma, P. L. (2013). Excitotoxicity: bridge to various triggers in neurodegenerative disorders. *Eur J Pharmacol* 698(1-3): 6-18.

Molyneaux, B. J., Arlotta, P., Menezes, J. R. and Macklis, J. D. (2007). Neuronal subtype specification in the cerebral cortex. *Nat Rev Neurosci* 8(6): 427-437.

Moscato, E. H., Peng, X., Jain, A., Parsons, T. D., Dalmau, J. and Balice-Gordon, R. J. (2014). Acute mechanisms underlying antibody effects in anti-N-methyl-D-aspartate receptor encephalitis. *Ann Neurol* 76(1): 108-119.

Munoz-Sanjuan, I. and Brivanlou, A. H. (2002). Neural induction, the default model and embryonic stem cells. *Nat Rev Neurosci* 3(4): 271-280.

N

Nagele, E. P., Han, M., Acharya, N. K., DeMarshall, C., Kosciuk, M. C. and Nagele, R. G. (2013). Natural IgG autoantibodies are abundant and ubiquitous in human sera, and their number is influenced by age, gender, and disease. *PLoS One* 8(4): e60726.

Nelson, B. R., Hartman, B. H., Georgi, S. A., Lan, M. S. and Reh, T. A. (2007). Transient inactivation of Notch signaling synchronizes differentiation of neural progenitor cells. *Dev Biol* 304(2): 479-498.

Nelson, S. B. and Valakh, V. (2015). Excitatory/Inhibitory Balance and Circuit Homeostasis in Autism Spectrum Disorders. *Neuron* 87(4): 684-698.

Neuwelt, E., Abbott, N. J., Abrey, L., Banks, W. A., Blakley, B., Davis, T., Engelhardt, B., Grammas, P., Nedergaard, M., Nutt, J., *et al.* (2008). Strategies to advance translational research into brain barriers. *Lancet Neurol* 7(1): 84-96.

Neuwelt, E. A., Bauer, B., Fahlke, C., Fricker, G., Iadecola, C., Janigro, D., Leybaert, L., Molnar, Z., O'Donnell, M. E., Povlishock, J. T., *et al.* (2011). Engaging neuroscience to advance translational research in brain barrier biology. *Nat Rev Neurosci* 12(3): 169-182.

Nishitsuji, K., Hosono, T., Nakamura, T., Bu, G. and Michikawa, M. (2011). Apolipoprotein E regulates the integrity of tight junctions in an isoform-dependent manner in an in vitro blood-brain barrier model. *J Biol Chem* 286(20): 17536-17542.

O

Orihara, K., Odemuyiwa, S. O., Stefura, W. P., Ilarraza, R., HayGlass, K. T. and Moqbel, R. (2018). Neurotransmitter signalling via NMDA receptors leads to decreased T helper type 1-like and enhanced T helper type 2-like immune balance in humans. *Immunology* 153(3): 368-379.

P

Pacheco, R., Gallart, T., Lluís, C. and Franco, R. (2007). Role of glutamate on T-cell mediated immunity. *J Neuroimmunol* 185(1-2): 9-19.

Pacheco, R., Oliva, H., Martínez-Navio, J. M., Climent, N., Ciruela, F., Gatell, J. M., Gallart, T., Mallol, J., Lluís, C. and Franco, R. (2006). Glutamate Released by Dendritic Cells as a Novel Modulator of T Cell Activation. *J Immunol* 177(10): 6695-6704.

Pan, H., Oliveira, B., Saher, G., Dere, E., Tapken, D., Mitjans, M., Seidel, J., Wesolowski, J., Wakhloo, D., Klein-Schmidt, C., *et al.* (2018). Uncoupling the widespread occurrence of anti-NMDAR1 autoantibodies from neuropsychiatric disease in a novel autoimmune model. *Mol Psychiatry*.

Paoletti, P. (2011). Molecular basis of NMDA receptor functional diversity. *Eur J Neurosci* 33(8): 1351-1365.

Paoletti, P., Bellone, C. and Zhou, Q. (2013). NMDA receptor subunit diversity: impact on receptor properties, synaptic plasticity and disease. *Nat Rev Neurosci* 14(6): 383-400.

Paulus, W., Classen, J., Cohen, L. G., Large, C. H., Di Lazzaro, V., Nitsche, M., Pascual-Leone, A., Rosenow, F., Rothwell, J. C. and Ziemann, U. (2008). State of the art: Pharmacologic effects on cortical excitability measures tested by transcranial magnetic stimulation. *Brain Stimul* 1(3): 151-163.

Planaguma, J., Leypoldt, F., Mannara, F., Gutierrez-Cuesta, J., Martín-García, E., Aguilar, E., Titulaer, M. J., Petit-Pedrol, M., Jain, A., Balice-Gordon, R., *et al.* (2015). Human N-methyl D-aspartate receptor antibodies alter memory and behaviour in mice. *Brain* 138(Pt 1): 94-109.

BIBLIOGRAPHY

Platt, M. P., Agalliu, D. and Cutforth, T. (2017). Hello from the Other Side: How Autoantibodies Circumvent the Blood-Brain Barrier in Autoimmune Encephalitis. *Front Immunol* 8: 442.

Pruss, H., Finke, C., Holtje, M., Hofmann, J., Klingbeil, C., Probst, C., Borowski, K., Ahnert-Hilger, G., Harms, L., Schwab, J. M., *et al.* (2012). N-methyl-D-aspartate receptor antibodies in herpes simplex encephalitis. *Ann Neurol* 72(6): 902-911.

Pruss, H., Leubner, J., Wenke, N. K., Czirjak, G. A., Szentiks, C. A. and Greenwood, A. D. (2015). Anti-NMDA Receptor Encephalitis in the Polar Bear (*Ursus maritimus*) Knut. *Sci Rep* 5: 12805.

R

Rajewsky, K. (1996). Clonal selection and learning in the antibody system. *Nature* 381(6585): 751-758.

Ransohoff, R. M. (2009). Immunology: In the beginning. *Nature* 462(7269): 41-42.

Richman, D. D., Cleveland, P. H., Oxman, M. N. and Johnson, K. M. (1982). The binding of staphylococcal protein A by the sera of different animal species. *J Immunol* 128(5): 2300-2305.

Rogers, S. W., Andrews, P. I., Gahring, L. C., Whisenand, T., Cauley, K., Crain, B., Hughes, T. E., Heinemann, S. F. and McNamara, J. O. (1994). Autoantibodies to glutamate receptor GluR3 in Rasmussen's encephalitis. *Science* 265(5172): 648-651.

Rose, N. R. (2015). Molecular mimicry and clonal deletion: A fresh look. *J Theor Biol* 375: 71-76.

Roth, J., Harre, E. M., Rummel, C., Gerstberger, R. and Hubschle, T. (2004). Signaling the brain in systemic inflammation: role of sensory circumventricular organs. *Front Biosci* 9: 290-300.

Rubenstein, J. L. and Merzenich, M. M. (2003). Model of autism: increased ratio of excitation/inhibition in key neural systems. *Genes Brain Behav* 2(5): 255-267.

S

Schafer, D. P., Lehrman, E. K., Kautzman, A. G., Koyama, R., Mardinly, A. R., Yamasaki, R., Ransohoff, R. M., Greenberg, M. E., Barres, B. A. and Stevens, B. (2012). Microglia sculpt postnatal neural circuits in an activity and complement-dependent manner. *Neuron* 74(4): 691-705.

Schou, M., Saether, S. G., Borowski, K., Teegen, B., Kondziella, D., Stoecker, W., Vaaler, A. and Reitan, S. K. (2016). Prevalence of serum anti-neuronal autoantibodies in patients admitted to acute psychiatric care. *Psychol Med* 46(16): 3303-3313.

Schuermans, C. and Guillemot, F. (2002). Molecular mechanisms underlying cell fate specification in the developing telencephalon. *Curr Opin Neurobiol* 12(1): 26-34.

Selsing, E. (2006). Ig class switching: targeting the recombinational mechanism. *Curr Opin Immunol* 18(3): 249-254.

Sheikh, K. A., Zhang, G., Gong, Y., Schnaar, R. L. and Griffin, J. W. (2004). An anti-ganglioside antibody-secreting hybridoma induces neuropathy in mice. *Ann Neurol* 56(2): 228-239.

- Sheng, M., Cummings, J., Roldan, L. A., Jan, Y. N. and Jan, L. Y. (1994). Changing subunit composition of heteromeric NMDA receptors during development of rat cortex. *Nature* 368(6467): 144-147.
- Shi, Y., Kirwan, P. and Livesey, F. J. (2012). Directed differentiation of human pluripotent stem cells to cerebral cortex neurons and neural networks. *Nat Protoc* 7(10): 1836-1846.
- Silbereis, J. C., Pochareddy, S., Zhu, Y., Li, M. and Sestan, N. (2016). The Cellular and Molecular Landscapes of the Developing Human Central Nervous System. *Neuron* 89(2): 248-268.
- Simister, N. (2003). Placental transport of immunoglobulin G. *Vaccine* 21(24): 3365-3369.
- Skerry, T. M. and Genever, P. G. (2001). Glutamate signalling in non-neuronal tissues. *Trends Pharmacol Sci* 22(4): 174-181.
- Sommer, C. A., Sommer, A. G., Longmire, T. A., Christodoulou, C., Thomas, D. D., Gostissa, M., Alt, F. W., Murphy, G. J., Kotton, D. N. and Mostoslavsky, G. (2010). Excision of reprogramming transgenes improves the differentiation potential of iPS cells generated with a single excisable vector. *Stem Cells* 28(1): 64-74.
- Sommer, C. A., Stadtfeld, M., Murphy, G. J., Hochedlinger, K., Kotton, D. N. and Mostoslavsky, G. (2009). Induced pluripotent stem cell generation using a single lentiviral stem cell cassette. *Stem Cells* 27(3): 543-549.
- Stamatovic, S. M., Keep, R. F., Wang, M. M., Jankovic, I. and Andjelkovic, A. V. (2009). Caveolae-mediated internalization of occludin and claudin-5 during CCL2-induced tight junction remodeling in brain endothelial cells. *J Biol Chem* 284(28): 19053-19066.
- Steiner, J., Teegen, B., Schiltz, K., Bernstein, H. G., Stoecker, W. and Bogerts, B. (2014). Prevalence of N-methyl-D-aspartate receptor autoantibodies in the peripheral blood: healthy control samples revisited. *JAMA Psychiatry* 71(7): 838-839.
- Stenman, J. M., Rajagopal, J., Carroll, T. J., Ishibashi, M., McMahon, J. and McMahon, A. P. (2008). Canonical Wnt signaling regulates organ-specific assembly and differentiation of CNS vasculature. *Science* 322(5905): 1247-1250.
- Stepniak, B., Kastner, A., Poggi, G., Mitjans, M., Begemann, M., Hartmann, A., Van der Auwera, S., Sananbenesi, F., Krueger-Burg, D., Matuszko, G., *et al.* (2015). Accumulated common variants in the broader fragile X gene family modulate autistic phenotypes. *EMBO Mol Med* 7(12): 1565-1579.
- Stevens, B., Allen, N. J., Vazquez, L. E., Howell, G. R., Christopherson, K. S., Nouri, N., Micheva, K. D., Mehalow, A. K., Huberman, A. D., Stafford, B., *et al.* (2007). The classical complement cascade mediates CNS synapse elimination. *Cell* 131(6): 1164-1178.
- Streckfuss-Bomeke, K., Wolf, F., Azizian, A., Stauske, M., Tiburcy, M., Wagner, S., Hubscher, D., Dressel, R., Chen, S., Jende, J., *et al.* (2013). Comparative study of human-induced pluripotent stem cells derived from bone marrow cells, hair keratinocytes, and skin fibroblasts. *Eur Heart J* 34(33): 2618-2629.
- Stumm, R. K., Zhou, C., Ara, T., Lazarini, F., Dubois-Dalcq, M., Nagasawa, T., Holtt, V. and Schulz, S. (2003). CXCR4 regulates interneuron migration in the developing neocortex. *J Neurosci* 23(12): 5123-5130.

BIBLIOGRAPHY

T

Tao, H. W., Li, Y. T. and Zhang, L. I. (2014). Formation of excitation-inhibition balance: inhibition listens and changes its tune. *Trends Neurosci* 37(10): 528-530.

Teixeira, A. R., Hecht, M. M., Guimaro, M. C., Sousa, A. O. and Nitz, N. (2011). Pathogenesis of chagas' disease: parasite persistence and autoimmunity. *Clin Microbiol Rev* 24(3): 592-630.

Tian, J., Lu, Y., Zhang, H., Chau, C. H., Dang, H. N. and Kaufman, D. L. (2004). - Aminobutyric Acid Inhibits T Cell Autoimmunity and the Development of Inflammatory Responses in a Mouse Type 1 Diabetes Model. *J Immunol* 173(8): 5298-5304.

V

van den Heuvel, M. P., Bullmore, E. T. and Sporns, O. (2016). Comparative Connectomics. *Trends Cogn Sci* 20(5): 345-361.

W

Wake, H., Moorhouse, A. J., Jinno, S., Kohsaka, S. and Nabekura, J. (2009). Resting microglia directly monitor the functional state of synapses in vivo and determine the fate of ischemic terminals. *J Neurosci* 29(13): 3974-3980.

Wobrock, T., Schneider, M., Kadovic, D., Schneider-Axmann, T., Ecker, U. K., Retz, W., Rosler, M. and Falkai, P. (2008). Reduced cortical inhibition in first-episode schizophrenia. *Schizophr Res* 105(1-3): 252-261.

Wosik, K., Cayrol, R., Dodelet-Devillers, A., Berthelet, F., Bernard, M., Moundjian, R., Bouthillier, A., Reudelhuber, T. L. and Prat, A. (2007). Angiotensin II controls occludin function and is required for blood brain barrier maintenance: relevance to multiple sclerosis. *J Neurosci* 27(34): 9032-9042.

Wright, S., Hashemi, K., Stasiak, L., Bartram, J., Lang, B., Vincent, A. and Upton, A. L. (2015). Epileptogenic effects of NMDAR antibodies in a passive transfer mouse model. *Brain* 138(Pt 11): 3159-3167.

Y

Yaron, O., Farhy, C., Marquardt, T., Applebury, M. and Ashery-Padan, R. (2006). Notch1 functions to suppress cone-photoreceptor fate specification in the developing mouse retina. *Development* 133(7): 1367-1378.

Z

Zerche, M., Weissenborn, K., Ott, C., Dere, E., Asif, A. R., Worthmann, H., Hassouna, I., Rentzsch, K., Tryc, A. B., Dahm, L., *et al.* (2015). Preexisting Serum Autoantibodies Against the NMDAR Subunit NR1 Modulate Evolution of Lesion Size in Acute Ischemic Stroke. *Stroke* 46(5): 1180-1186.

Zhang, Q., Tanaka, K., Sun, P., Nakata, M., Yamamoto, R., Sakimura, K., Matsui, M. and Kato, N. (2012). Suppression of synaptic plasticity by cerebrospinal fluid from anti-NMDA receptor encephalitis patients. *Neurobiol Dis* 45(1): 610-615.

Zhang, Y. and Pardridge, W. M. (2001). Mediated efflux of IgG molecules from brain to blood across the blood-brain barrier. *J Neuroimmunol* 114(1-2): 168-172.

Zheng, S., Eacker, S. M., Hong, S. J., Gronostajski, R. M., Dawson, T. M. and Dawson, V. L. (2010). NMDA-induced neuronal survival is mediated through nuclear factor I-A in mice. *J Clin Invest* 120(7): 2446-2456.

Zhou, J., Su, P., Li, D., Tsang, S., Duan, E. and Wang, F. (2010). High-efficiency induction of neural conversion in human ESCs and human induced pluripotent stem cells with a single chemical inhibitor of transforming growth factor beta superfamily receptors. *Stem Cells* 28(10): 1741-1750.

8. APPENDIX

8. APPENDIX

Accepted co-author publications

Manuscript 1

Oliveira B & Ehrenreich H. *Pursuing functional connectivity in NMDAR1 autoantibody carriers.* Letter to Lancet Psychiatry. 2018; 5(1):21-22

Personal contribution: I actively participated in the discussion of the original publication that this letter refers to, after presenting the paper in the context of a lab journal club. I wrote the manuscript together with my supervisor, Prof. Dr. Dr. Hannelore Ehrenreich.

Manuscript 2

Mitjans M*, Begemann M*, Ju A*, Dere E, Wüstefeld L, Hofer S, Hassouna I, Balkenhol J, **Oliveira B**, Van der Auwera S, Tammer R, Hammerschmidt K, Völzke H, Homuth G, Cecconi F, Chowdhury K, Grabe H, Frahm J, Boretius S, Dandekar T, Ehrenreich H. *Sexual dimorphism of AMBRA1 related autistic features in human and mouse.* Translational Psychiatry. 2017; 10;7(10):e1247.

Personal contribution: I contributed to the design and execution of the experiments to determine *AMBRA1* expression levels in individuals with different genotypes of interest. Additionally, I prepared and analysed brain sections of aged-matched mice regarding the MRI experiments for quantification of inhibitory cells in the hippocampus (unpublished data). I was involved in the preparation of the manuscript.

Manuscript 3

Ehrenreich H, Castillo-Gomez E, **Oliveira B**, Ott C, Steiner J, Weissenborn K. *Circulating NMDAR1 autoantibodies of different immunoglobulin classes modulates evolution of lesion size in acute ischemic stroke.* Neurology Psychiatry and Brain Research. 2016; 22(1).

Personal contribution: I differentiated the human IPS cell-derived neurons from patient fibroblasts, standardized and performed the NMDAR1 internalization assay to test functionality of human autoantibodies targeting the NR1 subunit of the aforementioned receptor. Additionally, I contributed to the study design and the overall writing of the manuscript.

Manuscript 4

Ott C, Martens H, Hassouna I, **Oliveira B**, Erck C, Zafeiriou MP, Peteri UK, Hesse D, Gerhart S, Altas B, Kolbow T, Stadler H, Kawabe H, Zimmermann WH, Nave KA, Schulz-Schaeffer W, Jahn O, Ehrenreich H. Widespread expression of erythropoietin receptor in brain and its induction by injury. Molecular Medicine. 2015; 21:803-815.

Personal contribution: I prepared the human IPS cell lines used to test EPOR antibody and performed the immunocytochemistry experiments. Additionally, I validated the detection of EPOR in UT-7 cells using the same antibody by flow cytometry. I contributed to the overall preparation of the manuscript.

[https://doi.org/10.1016/2215-0366\(17\)30465-0](https://doi.org/10.1016/2215-0366(17)30465-0)

a gambling disorder is confronted with EGMs. A more detailed understanding of the interactions between these machine design features and aspects of human decision-making and behaviours, including their interactions within vulnerable groups (adolescents, those with a mental illness, or under substantial psychosocial distress), will provide valuable insights for producing safer gambling products. The use of virtual reality and computational or decision neuroscience approaches can provide ecologically valid and real-time investigations of affective, cognitive, and physiological changes while gambling.

Urgent reform of EGM regulations to limit the impact of structural characteristics on gambling-related harm is needed. Opportunities abound for regulatory attention to reduce the prevalence and harm of gambling, including venue and machine accessibility, modification of EGM structural characteristics, enhanced user understanding and information, and use of systems to assist users to make and observe limits to gambling.² The time has come to prevent further damage associated with gambling and protect our communities.

No funding was received in relation to the present article. MY reports grants from the National Health and Medical Research Council, Australian Research Council, The David Winston Turner Endowment Fund, from Monash University, and from law firms in relation to expert witness report or statement. AC reports grants from the National Health and Medical Research Council, during the conduct of the study. CL reports grants from the Victorian Responsible Gambling Foundation, Australian Research Council, City of Melbourne, Maribyrnong City Council, City of Whittlesea, Alliance for Gambling Reform, outside the submitted work. RJvH and KH declare no competing interests.

*Murat Yücel, Adrian Carter, Kevin Harrigan, Ruth J van Holst, Charles Livingstone
murat.yucel@monash.edu

Brain and Mental Health Laboratory, Monash Institute of Cognitive and Clinical Neurosciences and School of Psychological Sciences, Monash University, Melbourne, VIC, Australia (MY, AC); Gambling Research Laboratory, University of Waterloo, ONT, Canada (KH); Department of

Psychiatry, Academic Medical Center, University of Amsterdam, Amsterdam, Netherlands (RJvH); and Gambling and Social Determinants Unit, School of Public Health and Preventive Medicine, Monash University, Melbourne, VIC, Australia (CL)

- Schull ND. *Addiction by design: machine gambling in Las Vegas*. Princeton: Princeton University Press, 2012.
- Harris A, Griffiths MD. A critical review of the harm-minimisation tools available for electronic gambling. *J Gambling Stud* 2017; **33**: 187–221.
- Harrigan KA, Dixon M. PAR sheets, probabilities, and slot machine play: implications for problem and non-problem gambling. *J Gambling Issues* 2009; **23**: 81–110.
- Breen RB, Zimmerman M. Rapid onset of pathological gambling in machine gamblers. *J Gambling Studies* 2002; **18**: 31–43.
- Robinson TE, Berridge KC. The neural basis of drug craving: an incentive-sensitization theory of addiction. *Brain Res Brain Res Rev* 1993; **18**: 247–91.

Pursuing functional connectivity in NMDAR1 autoantibody carriers

We read with interest the article by Michael Peer and colleagues.¹ The authors investigated by resting-state functional MRI (fMRI) a reasonable number of patients (n=43; 24 of which were reported previously) who were diagnosed earlier with so-called anti-NMDAR encephalitis (treatment regimens were not mentioned). It is acknowledged that a collection of patients with encephalitis who are also NMDAR1 autoantibody-positive is not easy to obtain. Of this collection, a large proportion had, on the day of fMRI, negative NMDAR1 autoantibody titres. In fact, only 17 of 43 patients were CSF positive and 27 of 43 were seropositive, if we consider a titre of 1:10 as a reasonable cut-off. Resting-state fMRI was done at highly variable timepoints after the initial diagnosis and led to the authors' conclusion of a "characteristic pattern of whole-brain functional connectivity alterations in anti-NMDAR encephalitis that is well suited to explain the major clinical symptoms of the disorder".

Undoubtedly, a sexy new method was applied to a hot topic. However,

any conclusion linking the described connectivity disturbance to NMDAR1 autoantibodies is difficult based on these data which lack the adequate control. Only a well-matched control group of patients with encephalitis without history of NMDAR1 autoantibody positivity could allow any speculation in this direction. Healthy individuals are not a proper control. Although information on functional connectivity in age-matched and gender-matched healthy individuals provides some baseline for comparison, they do not allow dissecting the effects of NMDAR1 autoantibodies on brain connectivity. A proper control population would require the underlying inflammatory context of an encephalitic brain without NMDAR1 autoantibodies. A dysconnectivity syndrome can be expected in any kind of encephalitis.²⁻⁴ In addition, the absence of NMDAR1 autoantibodies at the time of fMRI in a considerable number of individuals questions an ongoing influence of them on functional connectivity. Long-term persisting effects of NMDAR1 autoantibodies in their absence (ie, once they are eliminated by immunosuppression, plasmapheresis, or other means) have not yet been documented anywhere. They would also be difficult to prove non-experimentally. On a side note, catatonia is still classified as a positive symptom.

Future studies evaluating the importance of autoantibodies for brain functions should employ resting-state fMRI for standardised comparative assessment of different forms of acute and chronic encephalitides, including encephalitis with autoantibodies directed against brain epitopes, like NMDAR1 autoantibodies. In addition, NMDAR1 autoantibody carriers (all Ig classes)⁵ with a compromised blood-brain barrier should be investigated using this method.

We declare no competing interests.

Bárbara Oliveira,*Hannelore Ehrenreich ehrenreich@em.mpg.de

Clinical Neuroscience, Max Planck Institute of Experimental Medicine, Hermann-Rein-Strasse 3, 37075 Goettingen, Germany

- Peer M, Prüss H, Ben-Dayan I, Paul F, Arzy S, Finke C. Functional connectivity of large-scale brain networks in patients with anti-NMDA receptor encephalitis: an observational study. *Lancet Psychiatry* 2017; **4**: 768–74.
- Kharabian Masouleh S, Herzig S, Klose L, et al. Functional connectivity alterations in patients with chronic hepatitis C virus infection: a multimodal MRI study. *J Viral Hepat* 2017; **24**: 216–25.
- Lin Y, Zou QH, Wang J, et al. Localization of cerebral functional deficits in patients with non-neuropsychiatric systemic lupus erythematosus. *Hum Brain Mapp* 2011; **32**: 1847–55.
- Liu Y, Wang H, Duan Y, et al. Functional brain network alterations in clinically isolated syndrome and multiple sclerosis: a graph-based connectome study. *Radiology* 2017; **282**: 534–41.
- Castillo-Gomez E, Oliveira B, Tapken D, et al. All naturally occurring autoantibodies against the NMDA receptor subunit NR1 have pathogenic potential irrespective of epitope and immunoglobulin class. *Mol Psychiatry* 2016; published online Aug 9. DOI:10.1038/mp.2016.125.

Authors' reply

We thank Bárbara Oliveira and Hannelore Ehrenreich for their comments on our work.¹ Resting-state functional MRI (fMRI) is indeed a promising new imaging tool that already provided substantial insight into the pathophysiology of several neuropsychiatric disorders, including major depressive disorder, schizophrenia, and Alzheimer's disease.^{2,3} Using resting-state fMRI, we identified a characteristic pattern of functional connectivity alterations in the largest cohort of anti-NMDA receptor encephalitis examined with MRI so far. These connectivity disturbances correlated with symptoms of psychosis and memory impairment and extend recent observations of hippocampal damage and white matter alterations.⁴

Additionally, machine learning analyses based on resting-state fMRI data reliably distinguished patients from controls.

Notably, 86% of our patients were positive for IgG NMDAR antibodies at the time of imaging and all patients had CSF IgG NMDAR antibodies at diagnosis, the well-accepted hallmark of anti-NMDAR encephalitis. The significant resting-state fMRI connectivity disturbances, irrespective of antibody persistence or disease duration, indicate that the observed changes reflect long-term effects on brain activity. Long-term persisting deficits in meanwhile antibody-negative NMDAR encephalitis are rather the well-documented rule than the exception in the literature⁵ and our clinical experience.

We respectfully disagree that healthy controls are not an adequate control group. A comparison with carefully matched healthy individuals is not only common practice in computational neuropsychiatry and functional neuroimaging, it is essential to identify disturbances of brain activity. Other autoimmune CNS disorders differ in their level of inflammation, the pathophysiological mechanisms, and affected brain regions, and therefore cannot provide a meaningful "inflammatory baseline". By contrast, preliminary analyses show that resting-state fMRI can distinguish characteristic connectivity alterations between anti-NMDAR encephalitis and other autoimmune encephalitides such as anti-LGI1 encephalitis. We therefore believe that resting-state fMRI can become a highly useful tool in the work-up of neuropsychiatric patients, potentially able to facilitate the differential diagnosis,

treatment response, and follow-up. Indeed, this should include NMDAR antibody carriers of IgG, IgA, and IgM antibodies, given their association with cognitive impairments.⁶

We declare no competing interests.

Michael Peer, Harald Prüss, Inbal Ben-Dayan, Friedemann Paul, Shahar Arzy, *Carsten Finke
carsten.finke@charite.de

Computational Neuropsychiatry Laboratory, Department of Medical Neurosciences, Hebrew University of Jerusalem Medical School, Jerusalem, Israel (MP, IB-D, SA); Department of Neurology, Hadassah Medical Center, Jerusalem, Israel (MP, IB-D, SA); Department of Neurology (HP, FP, CF), Berlin Center for Advanced Neuroimaging Analyses (CF), and NeuroCure Clinical Research Center (FP), Charité-Universitätsmedizin Berlin, Berlin, Germany; German Center for Neurodegenerative Diseases, Berlin, Germany (HP); The Rachel and Selim Benin, School of Computer Science and Engineering, Hebrew University of Jerusalem, Jerusalem, Israel (IB-D); Experimental and Clinical Research Center, Max Delbrück Center for Molecular Medicine and Charité-Universitätsmedizin Berlin, Berlin, Germany (FP); and Berlin School of Mind and Brain, Humboldt-Universität zu Berlin, Berlin, Germany (CF)

- Peer M, Prüss H, Ben-Dayan I, Paul F, Arzy S, Finke C. Functional connectivity of large-scale brain networks in patients with anti-NMDA receptor encephalitis: an observational study. *Lancet Psychiatry* 2017; **4**: 768–74.
- Stam CJ. Modern network science of neurological disorders. *Nat Rev Neurosci* 2014; **15**: 683–95.
- Woodward ND, Cascio CJ. Resting-state functional connectivity in psychiatric disorders. *JAMA Psychiatry* 2015; **72**: 743–44.
- Finke C, Kopp U a, Pajkert A, et al. Structural hippocampal damage following anti-N-methyl-D-aspartate receptor encephalitis. *Biol Psychiatry* 2016; **79**: 727–34.
- Titulaer MJ, McCracken L, Gabilondo I, et al. Treatment and prognostic factors for long-term outcome in patients with anti-NMDA receptor encephalitis: an observational cohort study. *Lancet Neurol* 2013; **12**: 157–65.
- Finke C, Bartels F, Lütt A, Prüss H, Harms L. High prevalence of neuronal surface autoantibodies associated with cognitive deficits in cancer patients. *J Neurol* 2017; **264**: 1968–77.

ORIGINAL ARTICLE

Sexual dimorphism of *AMBRA1*-related autistic features in human and mouse

M Mitjans^{1,2,14}, M Begemann^{1,2,3,14}, A Ju^{1,14}, E Dere^{1,2}, L Wüstefeld¹, S Hofer⁴, I Hassouna¹, J Balkenhol⁵, B Oliveira¹, S van der Auwera⁶, R Tammer⁴, K Hammerschmidt⁷, H Völzke⁸, G Homuth⁹, F Cecconi^{10,11}, K Chowdhury¹², H Grabe⁶, J Frahm⁴, S Boretius¹³, T Dandekar⁵ and H Ehrenreich^{1,2}

Ambra1 is linked to autophagy and neurodevelopment. Heterozygous *Ambra1* deficiency induces autism-like behavior in a sexually dimorphic manner. Extraordinarily, autistic features are seen in female mice only, combined with stronger *Ambra1* protein reduction in brain compared to males. However, significance of *AMBRA1* for autistic phenotypes in humans and, apart from behavior, for other autism-typical features, namely early brain enlargement or increased seizure propensity, has remained unexplored. Here we show in two independent human samples that a single normal *AMBRA1* genotype, the intronic SNP rs3802890-AA, is associated with autistic features in women, who also display lower *AMBRA1* mRNA expression in peripheral blood mononuclear cells relative to female GG carriers. Located within a non-coding RNA, likely relevant for mRNA and protein interaction, rs3802890 (A versus G allele) may affect its stability through modification of folding, as predicted by *in silico* analysis. Searching for further autism-relevant characteristics in *Ambra1*^{+/-} mice, we observe reduced interest of female but not male mutants regarding pheromone signals of the respective other gender in the social intelligence set-up. Moreover, altered pentylentetrazol-induced seizure propensity, an *in vivo* readout of neuronal excitation–inhibition dysbalance, becomes obvious exclusively in female mutants. Magnetic resonance imaging reveals mild prepubertal brain enlargement in both genders, uncoupling enhanced brain dimensions from the primarily female expression of all other autistic phenotypes investigated here. These data support a role of *AMBRA1*/*Ambra1* partial loss-of-function genotypes for female autistic traits. Moreover, they suggest *Ambra1* heterozygous mice as a novel multifaceted and construct-valid genetic mouse model for female autism.

Translational Psychiatry (2017) 7, e1247; doi:10.1038/tp.2017.213; published online 10 October 2017

INTRODUCTION

Autism spectrum disorders (ASD) are extremely heterogeneous neurodevelopmental conditions, affecting ~1% of the population. Typical, shared symptoms range from social communication and interaction deficits, including decreased attraction by and compromised reading of social signals, restricted interests, repetitive behaviors or pronounced routines, to reduced cognitive flexibility.^{1–4} Early brain enlargement^{5–8} and predisposition to epileptic seizures^{9,10} are among the reported non-behavioral characteristics found in this disorder category. Causes likely converge at the synapse, as indicated by mutations of synaptic genes or by mutations causing quantitative alterations in synaptic protein expression, half-life or degradation, and are reflected by a virtually autism-pathognomonic neuronal excitation–inhibition dysbalance.^{4,11–15} Neuroligin-4 mutations, for instance, belong to the most common causes of monogenetic heritable autism.¹⁶ Construct-valid and face-valid mouse models of autism, building

on monogenetic grounds, have helped in approaching the underlying common biology.^{17,18}

The estimated heritability of autism approximates 90%. We note, however, that monogenetic forms including copy number variations altogether account for <20%, leaving ~80% of cases unexplained, which also enter the final common pathway of disease expression.^{1–3} Importantly, normal genetic variants, mainly single nucleotide polymorphisms (SNPs), likely contribute to the manifestation of autistic phenotypes. This is indicated by the results of genome-wide association (GWAS) and respective polygenic-risk studies on autism,^{2,19,20} but even more so by phenotype-based genetic association studies (PGAS), reporting an accumulation of ‘unfortunate’ normal variants, so-called pro-autistic genotypes, to be associated with increasing severity of autistic traits.^{21–23} In fact, phenotypical continua of autistic features from health to disease suggest underlying mechanisms of quantitative rather than qualitative nature.^{21,24} Genetic modifiers, like protective genes and environmental (co-)factors,

¹Department of Clinical Neuroscience, Max Planck Institute of Experimental Medicine, Göttingen, Germany; ²DFG Research Center for Nanoscale Microscopy and Molecular Physiology of the Brain (CNMPB), Göttingen, Germany; ³Department of Psychiatry and Psychotherapy, UMG, Georg-August-University, Göttingen, Germany; ⁴Biomedizinische NMR Forschungs GmbH, Max Planck Institute for Biophysical Chemistry, Göttingen, Germany; ⁵Department of Bioinformatics, Biocenter, University of Würzburg, Würzburg, Germany; ⁶Department of Psychiatry and Psychotherapy, University Medicine, and German Center for Neurodegenerative Diseases (DZNE) Greifswald, Greifswald, Germany; ⁷Cognitive Ethology Laboratory, German Primate Center, Göttingen, Germany; ⁸Institute for Community Medicine, University Medicine Greifswald, Greifswald, Germany; ⁹Interfaculty Institute for Genetics and Functional Genomics, University of Greifswald, Greifswald, Germany; ¹⁰IRCCS Fondazione Santa Lucia and Department of Biology, University of Rome Tor Vergata, Rome, Italy; ¹¹Unit of Cell Stress and Survival, Danish Cancer Society Research Center, Copenhagen, Denmark; ¹²Department of Molecular Cell Biology, Max Planck Institute of Biophysical Chemistry, Göttingen, Germany and ¹³Department of Functional Imaging, German Primate Center, Leibniz Institute of Primate Research, Göttingen, Germany. Correspondence: Professor H Ehrenreich, Clinical Neuroscience, Max Planck Institute of Experimental Medicine, Hermann-Rein-Str. 3, Göttingen 37075, Germany.

E-mail: ehrenreich@em.mpg.de

¹⁴These authors contributed equally to this work.

Received 13 June 2017; revised 1 August 2017; accepted 17 August 2017

mainly those acting during uterine and early postnatal development may also modulate autism severity.^{25,26}

ASD has an overall gender distribution of ~4:1 males/females.^{1,2,27} Remarkably, little research has focused on the reasons for this disparity. Better understanding of this difference, however, could lead to major advancements in the prevention or treatment of ASD in both genders.²⁸ We previously reported that an *Ambra1* (activating molecule in Beclin1-regulated autophagy) partial loss-of-function genotype is associated with the autism-like behavior in female mice. The restriction to the female gender of autism generation by a defined genetic trait has thus far remained unique.²⁹ *Ambra1* is a positive regulator of a principal player in autophagosome formation, Beclin1. Importantly, autophagy has already been linked to autism in recent work.^{30,31} Moreover, *Ambra1* is involved in other developmentally relevant processes in the nervous system and in neuronal function.^{32,33} Although homozygosity of the *Ambra1* null mutation causes embryonic lethality, heterozygous mice with reduced *Ambra1* expression appear completely normal at first view.³³ Only upon comprehensive behavioral characterization, a striking autism-like phenotype of *Ambra1*^{+/-} females emerges. This trait is quantifiable by the autism severity composite score, which even allows a behavior-based genotype predictability of >90%.^{29,34} As first mechanistic hint explaining the prominent gender difference, stronger reduction of *Ambra1* protein in the cortex of *Ambra1*^{+/-} females was found.²⁹

Until now, no association of *AMBRA1* genotypes with autistic features has been described in humans, therefore still questioning the construct-validity of our mouse model.²⁹ However, a recent GWAS on schizophrenia identified a genetic risk variation on chromosome 11 (11p11.2) in a region containing *AMBRA1*.³⁵ Schizophrenia and ASD show considerable syndromic overlap, including deficits in social cognition and communication,^{24,36} and at least a subgroup of schizophrenia is also regarded as a disorder of the synapse.³⁷

The present study has therefore been designed to explore whether any autism-relevant phenotype association with normal *AMBRA1* genotypes would emerge in humans, thereby supporting the construct-validity of our *Ambra1*^{+/-} mouse model. In addition, we aimed at defining potential further characteristics of ASD in *Ambra1*^{+/-} mice, namely (1) decreased interest in social odors, as highly relevant social signals in mice, (2) increased epileptic predisposition as *in vivo* readout of neuronal excitation–inhibition dysbalance and (3) early brain enlargement, as recognized in human autism. Indeed, we show here that also in humans, an *AMBRA1* genotype, the intronic SNP rs3802890-AA, located in a long non-coding (lnc) RNA, is linked to autistic features and characterized by partial loss-of-function in females. Moreover, we demonstrate in *Ambra1*^{+/-} mice prepubertal brain enlargement. Only in female mutants, we see loss of interest in sex pheromones and altered seizure propensity.

MATERIALS AND METHODS

In all experiments, the experimenters were unaware of genotypes ('fully blinded').

Human studies

Discovery: schizophrenia subjects and healthy controls (GRAS). The Göttingen Research Association for Schizophrenia (GRAS) data collection consists of >1200 deep-phenotyped patients, diagnosed with schizophrenia or schizoaffective disorder (DSM-IV-TR³⁸), recruited across Germany since 2005.^{39,40} Diagnosis is based on a comprehensive examination, lasting for at least 4 h (the examination often took much longer, with breaks in between, dependent on the patient's condition). It is guided by the GRAS manual, which contains standardized interviews, psychopathology and neuropsychology testing. Moreover, careful study of all the medical discharge letters and charts of every single individual aids in assessing

longitudinal aspects of the diagnosis as well.^{39,40} GRAS, complying with Helsinki Declaration, was approved by Ethics Committees of Georg-August-University, Göttingen, Germany, and participating centers. All study participants (European-Caucasian 95.6%; other 1.8%; unknown 2.6%) and, if applicable, legal representatives gave written informed consent. Of the 1105 successfully genotyped patients, 66.7% were male ($N=737$), 33.3% female ($N=368$), aged 39.46 ± 12.58 years (range: 17–79). For genetic case-control analysis, healthy GRAS blood donors were employed,³⁹ in total $N=1258$ (European-Caucasian 97.8%; other 2%; unknown 0.2%), 61.6% male ($N=775$), 38.4% female ($N=483$), aged 37.45 ± 13.21 (range: 18–69) years. Voluntary blood donors widely fulfill health criteria according to the national guidelines for blood donation, ensured by a broad pre-donation screening process containing standardized questionnaires, interviews, hemoglobin, blood pressure, pulse and body temperature determinations.³⁹

Replication: population-based cohort (SHIP-O). The general population sample comprises $N=2359$ homozygous subjects, mean age 49.8 ± 16 (range=20–81) years, $N=1144$ males, $N=1215$ females, from baseline examinations of Study of Health in Pomerania (SHIP), approved by the Ethics Committee, University Greifswald, and conducted in North-East Germany.⁴¹

Phenotyping. For quantification of autistic phenotypes, we used the Positive and Negative Syndrome Scale (PANSS)⁴²-based autism severity score (PAUSS)²⁴ with slight modifications (Figure 1a), available for 1067 patients. For the replication sample, the Instrumental Support Index (ISI) was taken as proxy, indicating quality of instrumental and emotional support,⁴³ expected to be low in autistic individuals.²³ It was cross-validated with PAUSS in GRAS subjects, with social support operationalized as self-reported number of individuals a person can rely on in case of emergency.²³ For both measures of social support (intercorrelation 0.77), higher score values (z-transformed; range: 1.5–9) represent higher social support, that is, lower autistic features.

Genotyping. GRAS subjects were genotyped using semi-custom Axiom MyDesign Genotyping Array (Affymetrix, Santa Clara, CA, USA), based on a CEU (Caucasian residents of European ancestry from UT, USA) marker backbone, including 518 722 SNPs, plus custom marker-set of 102 537 SNPs. Genotyping was performed by Affymetrix on a GeneTitan platform with high quality (SNP call rate >97%, Fisher's linear-discriminant, heterozygous cluster-strength offset, homozygote-ratio offset).^{23,44,45} Markers were selected according to our SOP for PGAS²³ using following selection criteria: (1) SNPs in Hardy–Weinberg equilibrium; (2) SNPs with minor allele frequency (MAF ≥ 0.2) allowing for statistical analyses; (3) SNPs not in high linkage disequilibrium (LD) with other selected SNPs ($r^2 < 0.8$). Based hereon, only rs3802890-A/G remained for analysis.

SHIP-O subjects were genotyped using Affymetrix Genome-Wide SNP Array-6.0 (genotyping efficiency 98.6%). Imputation of genotypes was performed with software IMPUTE v0.5.0⁴⁶ against 1000-Genomes (phase1v3) reference-panel using 869 224 genotyped SNPs.⁴¹ Rs3802890 was imputed with IQ=1.

In silico analyses. Genome sequences were established according to latest available releases (human-genome vs32–2015; mouse-genome 2016). Iterative sensitive sequence comparisons were conducted⁴⁷ and evaluated including detailed genome and transcriptome mapping. Expression of the rs3802890-containing RNA region was derived from latest largest collection of ESTs available at NIH.⁴⁸ lncRNA matches were also established according to latest human lncRNA release at NCBI. RNA folding used RNAfold.⁴⁹ For demonstrating rs3802890-A/G differences, thermodynamic ensemble structures drawing encoded base-pair probabilities were used. Protein binding regions were calculated using RNAanalyzer⁵⁰ and CatRapid,⁵¹ coding potential was calculated using Genscan.⁵²

***AMBRA1* and EST TCAAP2E6309 mRNA expression.** Peripheral blood mononuclear cells (PBMC) were isolated from morning blood, obtained via phlebotomy into CPDA-vials (Citrate-Phosphate-Dextrose-Adenine, Sarstedt, Germany), applying standard Ficoll-Paque-Plus isolation procedure (GE-Healthcare, Munich, Germany). Total RNA extraction was done using miRNeasy Mini-kit (Qiagen, Hilden, Germany). For reverse transcription, 1 μ g of cDNA was applied using a mixture of oligo(dT)/hexamers, dNTPs, DTT and 200U SuperscriptIII (Life Technologies, Darmstadt,

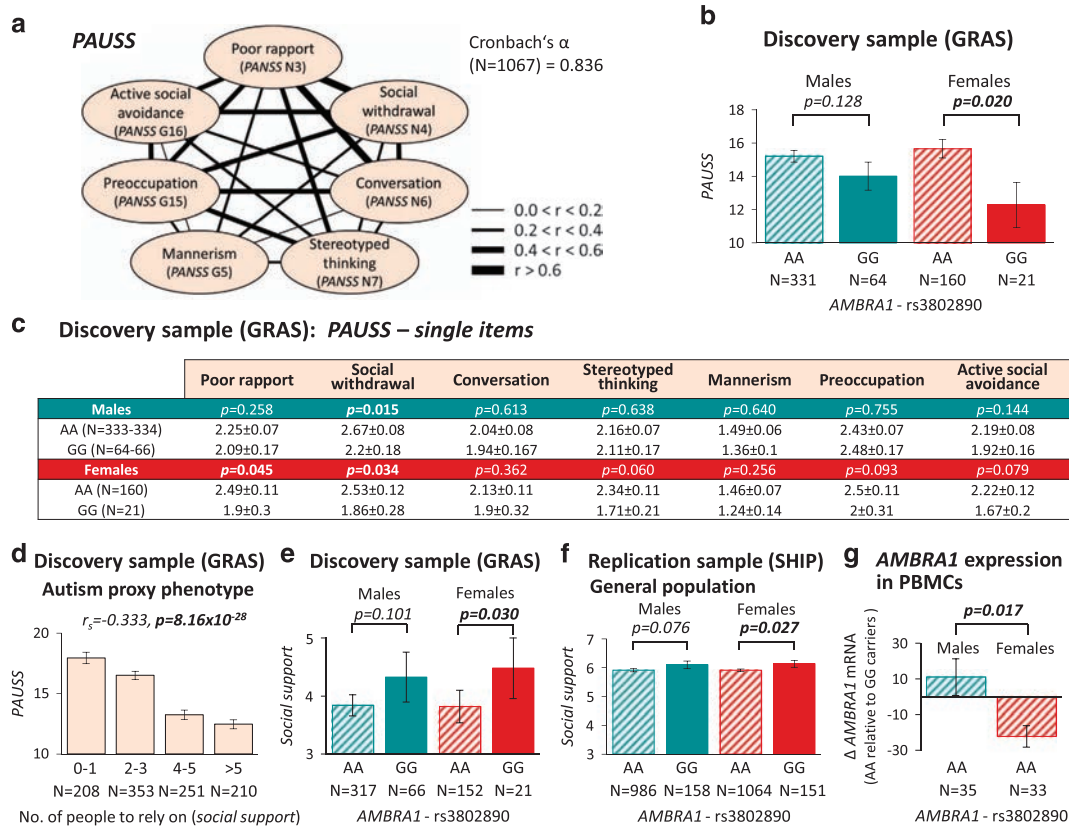


Figure 1. Human *AMBRA1*-rs3802890 G/A: association with autistic features. **(a)** Quantification of autistic symptoms using *PAUSS* (PANSS Autism Severity Score).²⁴ Note the high intercorrelation of *PAUSS* items and the high internal consistency of the scale (Spearman rank correlation coefficients; Cronbach's α). **(b)** PGAS using *AMBRA1*-rs3802890 and *PAUSS* score: female AA subjects display a higher *PAUSS* score than GG subjects in the discovery sample; mean \pm s.e.m.; two-tailed Mann-Whitney *U*-test (data-corrected by linear regression analysis for age). **(c)** Trends of positive association between rs3802890-AA genotype and sub-items of *PAUSS*, more pronounced in females; mean \pm s.e.m.; two-tailed Mann-Whitney *U*-test. **(d)** The highly significant correlation of *PAUSS* and social support underlines the validity of social support as an autism proxy phenotype; mean \pm s.e.m. **(e)** Genotype effect of *AMBRA1*-rs3802890 on degree of social support in the discovery sample, again significant in females; mean \pm s.e.m.; Mann-Whitney *U*-test. **(f)** Replication of the genotype and gender effect of *AMBRA1*-rs3802890 using social support as proxy in the general population; linear regression analyses (bootstrap; data-corrected for age); mean \pm s.e.m. **(g)** Relative *AMBRA1* mRNA expression in peripheral blood mononuclear cells (PBMC) is reduced in female AA (risk SNP) carriers: shown is the *AMBRA1* mRNA expression in AA carriers, given as mean Δ -value compared to GG carriers (GG males $N=33$; GG females, $N=14$). Values of individual AA males ($N=35$) and AA females ($N=33$) are expressed in %GG (mean) of the respective gender. The Δ -value is calculated as: $\Delta = \%GG - 100\%$; mean \pm s.e.m.; two-tailed Mann-Whitney *U*-test.

Germany). *AMBRA1* RNA expression was measured using quantitative real-time PCR. The cDNA was diluted 1:25 in 10 μ l reaction-mix, containing 5 μ l of SYBR-green (Life Technologies) and 1pmol/primer:

AMBRA1-Fw: 5'-GACCACCAATTTACCCAGA-3'
AMBRA1-Rv: 5'-GATCATCCTCTGGCGTAGTA-3'
GAPDH-Fw: 5'-CTGACTTCAACAGCGACACC-3'
GAPDH-Rv: 5'-TGCTGTAGCCAAATTCGTTGT-3'

Technical replicates were run on LightCycler480 (Roche-Diagnostics, Mannheim, Germany). Relative *AMBRA1* expression was calculated using the threshold-cycle method (LightCycler480 Software1.5.0SP3-Roche) and normalization to *GAPDH*. EST TCAAP2E6309 RNA expression was measured using traditional PCR. Extracted RNA, cDNA synthesized with oligo-dT primers with/without hexamers, or genomic DNA were used as template with the following primers:

EST TCAAP2E6309-Fw: 5'-GGCAGAGCAGAATGGATAGACA-3'
 EST TCAAP2E6309-Rv: 5'-AACGCTGTTATCTGGGATCA-3'

Mouse studies

Investigations were carried out in agreement with guidelines for welfare of experimental animals, issued by the Federal Government of Germany and Max Planck Society, approved by local animal care and use committee (Niedersächsisches Landesamt für Verbraucherschutz und Lebensmittelsicherheit, Oldenburg, Germany).

Mouse line and housing. *Ambra1* mutation in mice is caused by a truncated, non-functional *Ambra1* protein via insertion of a gene-trapping vector into the murine *Ambra1* gene.³³ *Ambra1* wild-type (WT, *Ambra1*^{+/+}) and heterozygous (*Ambra1*^{+/-}) littermates of both genders with >99% C57BL/6 N background were used (male *Ambra1*^{+/-} \times female WT-C57BL/6N). Genotyping was performed as described.²⁹ Males and females were kept in separate ventilated cabinets (Scantainers; Scanbur Karlslunde, Denmark), group-housed, with woodchip bedding and nesting material, 12 h-light-dark cycle, 20–22 °C, food/water *ad libitum*.

Social intelligence paradigm. For pheromone-based social preference test, *Ambra1*^{+/+} and *Ambra1*^{+/-} mice were separately group-housed in large type4 cages after weaning until age 8 weeks. After transponder implantation, they were put into intelligences (IntelliCage; TSE-Systems, Bad Homburg, Germany), placed inside standard laboratory rodent cages (height 20.5 cm, length 55 cm, width 38.5 cm; Techniplast-Model-2000, Germany) with floor covered by sawdust bedding.⁵³ Each intelligence contains four housing shelters beneath the food hopper. Left and right of the intelligence, two social boxes are connected via plastic tubes, each equipped with two ring RFID-antennas to track individual mice. IntelliCage software records time spent in social boxes. Experiments are performed during the light phase. After habituation for 1 h to social boxes containing fresh bedding, mice undergo the pheromone-based social preference test: for 1 h they can freely choose between a social box with used bedding of

C3H mice of opposite gender and another box with only fresh bedding. WT mice typically prefer used bedding containing pheromones.

Magnetic resonance imaging for morphometry. Mice were anesthetized (5% isoflurane), intubated and kept at 1.75% isoflurane/5% oxygen by active ventilation with constant respiratory frequency (85 breaths per minute; Animal-Respirator-Advanced, TSE-Systems). Magnetic resonance imaging (MRI) was performed at 7 and 9.4T (Bruker Biospin MRI, Ettlingen, Germany). Radiofrequency excitation and signal reception were accomplished with use of a birdcage resonator (inner diameter, 72 mm) and a four-channel phased-array surface-coil, respectively. T2-weighted MRI data were acquired with three-dimensional fast spin-echo MRI sequence (repetition-time TR = 3.5 s, effective echo-time TE_{eff} = 55 ms, 12 differently phase-encoded echoes, 56 min measuring time) at isotropic spatial resolution of 100 μm. From these datasets, polygonal surface models of selected brain structures were generated by importing DICOM images into AMIRA (Visage-Imaging, Berlin, Germany). Structures of interest (whole brain, hippocampus, cerebellum, olfactory bulb, ventricles) were manually and semi-automatically labeled with segmentation editor on three-dimensional label fields (80 horizontal, 192 coronal, 144 sagittal slices).

Pentylenetetrazol-induced seizures. Mouse groups were tested during the light phase at postnatal day 23 or at 13 months. Seizures were induced by single intraperitoneal injection of pentylenetetrazol (PTZ) (50 mg kg⁻¹; Sigma-Aldrich, Taufkirchen, Germany). After injection, mice are observed for 30 min in their home cage.⁵⁴ Response to PTZ injection is quantified: (1) hypoactivity: decrease in mobility until rest in crouched or prone position, abdomen at bottom; (2) partial clonus (PC): clonic seizure in face, head or forelimbs; (3) generalized clonus (GC): sudden loss of upright posture, whole-body clonus including all limbs and tail, rearing and autonomic signs; and (4) tonic-clonic seizure (TC): generalized seizure up to tonic hind-limb extension and death. Latencies to (2)–(4) are used to calculate individual seizure scores (ISS), where factors weight relative severity: ISS = 1000/(0.2 × PC-latency + 0.3 × GC-latency + 0.5 × TC-latency).^{55–57}

Statistical methods

Case-control analysis and test for deviation from Hardy–Weinberg equilibrium was performed using PLINK1.07.⁵⁸ Statistics for human phenotype–genotype associations and mouse studies were conducted with SPSS v.17.0 (IBM-Deutschland, Munich, Germany), STATA MP-v.13.1 (StataCorp, College Station, TX, USA) and Prism4 (GraphPad-Software, San Diego, CA, USA). Statistical tests used are always given in figure legends. Data are presented as mean ± s.e.m., statistical significance was set to $P = 0.05$.

RESULTS

A normal *AMBRA1* genotype, rs3802890-AA, is associated with autistic traits predominantly in female schizophrenic individuals. Only one directly genotyped and—according to our PGAS SOP²³—suitable SNP, *AMBRA1*-rs3802890-A/G, was available in our array. Case–control analysis (1105 schizophrenic versus 1258 healthy GRAS subjects) yielded comparable genotypic and allelic chi-square comparison (MAF = 0.31; controls: AA = 607, AG = 532, GG = 119; cases: AA = 507, AG = 505, GG = 93; genotypic: $\chi^2 = 2.974$, df = 2, $P = 0.226$; allelic: $\chi^2 = 0.242$, df = 1, $P = 0.623$). Thus, rs3802890 is not associated with the schizophrenia diagnosis.

Next, PGAS was performed with rs3802890-AA/GG and PAUSS²⁴ as quantitative measure of autistic traits (Figure 1a). In previous work, we have demonstrated that autistic features cross diagnostic borders and can be quantified not only in ASD, but also in schizophrenia and other diseases as well as in healthy individuals.^{21,23,24} For quantification, we developed the PAUSS, a dimensional instrument based on PANSS,⁴² capturing the continuous nature of autistic behaviors.²⁴ PGAS revealed an association: AA carriers display higher PAUSS scores than GG subjects ($P = 0.039$). Interestingly, when separating genders, the PAUSS association remains significant only for females and,

likewise, most PAUSS sub-items show this trend in females but not males (Figures 1b and c).

A role of *AMBRA1*-rs3802890-AA for female autistic features is confirmed in a general population sample

Even though this highly targeted approach to an association of only one available *AMBRA1* SNP with autistic traits in schizophrenic individuals was already encouraging, we aimed at replication of this finding in a general population sample. For this, a social support score, derived from ISI,⁴³ was used as proxy phenotype, expected to be low in individuals with autistic features.²³ Cross-validation of social support (operationalized as the self-reported number of individuals a person can rely on in case of emergency) with PAUSS in the discovery sample (GRAS) yielded a high negative Spearman rank correlation (Figure 1d), underlining the relevance of this proxy for autistic features. Again, the social support score disclosed a genotype effect (rs3802890-AA/GG) in both discovery and replication sample, more pronounced in females (Figures 1e and f). Thus, in two independent human cohorts, a single normal variant in the *AMBRA1* gene, rs3802890, is associated with autism-related behaviors predominantly in females.

Consequence of *AMBRA1*-rs3802890-A versus G on mRNA expression in human PBMC and *in silico* prediction of potential underlying mechanisms

In some subjects, PBMCs were available for *AMBRA1* mRNA analysis. Although female GG ($N = 14$) versus male GG ($N = 33$) carriers had higher expression levels (0.0059 versus 0.0045 *AMBRA1*/*GAPDH*; $P = 0.05$), AA carriers of both genders (males $N = 35$; females $N = 33$) did not differ in their level (males 0.0049; females 0.0046; $P = 0.62$), which was comparable to that of male GG carriers. Comparing both genders, *AMBRA1* mRNA expression in PBMC of AA (risk SNP) relative to GG carriers is reduced in females but not males ($P = 0.017$; Figure 1g), possibly indicating partial loss-of-function of *AMBRA1* in AA females. This relative reduction found in PBMC of women resembles the situation in cortex of female mice: normal WT females have higher *Ambra1* expression than WT males, whereas *Ambra1*^{+/-} females show stronger relative *Ambra1* reduction compared to *Ambra1*^{+/-} males.²⁹

A detailed map of human *AMBRA1* gene is explained in Figure 2a. Exploring the location of the intronic rs3802890, a similarity to expressed sequence tags (EST) from NCBI database arises (Figure 2a). The predicted RNA folding of the transcribed EST TCAAP2E6309, covering the SNP region, is remarkably influenced by the presence in rs3802890 of G versus A (Figure 2b). As we find EST TCAAP2E6309 RNA expressed in PBMC and other human tissues (Figure 2c), relevance of this lncRNA for *AMBRA1* mRNA or protein levels may be assumed.

Together, these data suggest that *AMBRA1* likely shapes autistic behavior also in humans in a sexually dimorphic way. This across-species unique female autism generation by a defined genetic trait that appears to cause partial loss-of-function encouraged us to continue searching for further autism-specific readouts in our *Ambra1*^{+/-} mouse model.

Pheromone-based social preference is reduced in *Ambra1*^{+/-} females

Sex pheromones have an important role in social behavior throughout the animal kingdom.^{59–62} Mice typically favor a social context that contains pheromones of the opposite gender. In autistic phenotypes, social interest, approach and communication as well as understanding of social signals are compromised.^{1–4,62} We therefore designed a novel intelligage set-up to test pheromone preference as potential autism-relevant readout in

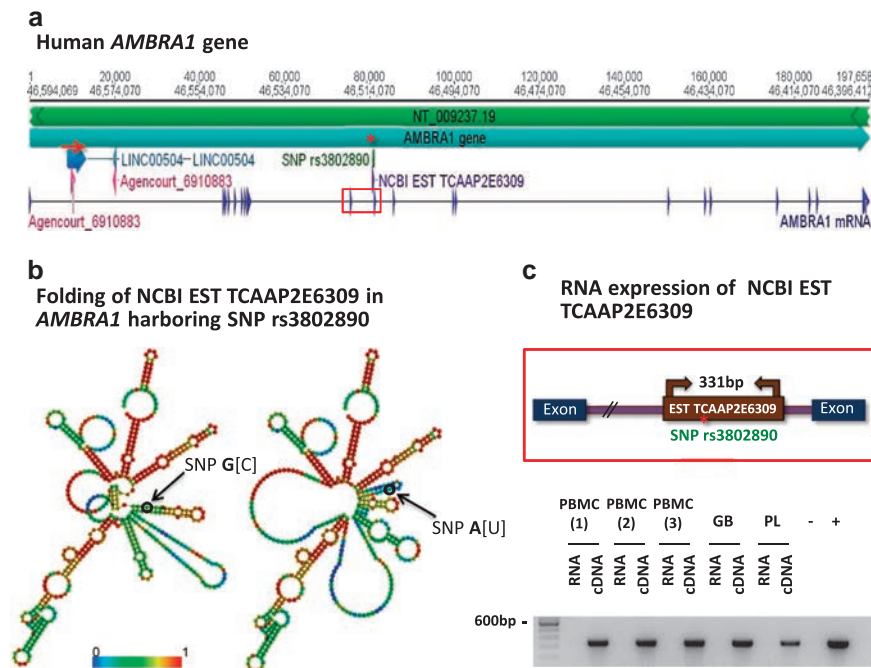


Figure 2. *AMBRA1*-rs3802890 G/A: *in silico* approach to mechanistic insight. (a) Detailed map showing the human *AMBRA1* gene (NCBI accession: 55626; chromosomal location: Chr.11: 46 396 412–46 594 069). The *AMBRA1* mRNA (21 exons) is mapped at the bottom. The location of *AMBRA1*-rs3802890 is indicated by a red asterisk. The region shared between all chromosomes (nucleotides from around 9530 to 11 030 on *AMBRA1*; red arrow) is indicated. Similar to man, the murine *Ambra1* gene region matches on all chromosomes (nucleotides from around 68 110–69 940 on murine *Ambra1*). However, the chromosomal match region of *AMBRA1/Ambra1* is different between both species. Both match regions show similarities to expressed sequence tags (EST) from NCBI database (best match EST gil22688027 in human and gil44663783 in mice; both with full-length alignment) and to specific lncRNAs in Refseq database (best match human: Refseq Accession NR_126435.1 named LINC00504; best match in mice: Refseq Accession NR_131899.1 named Mrqpra6). (b) RNA folding of human *AMBRA1* transcribed EST comparing the G allele with the A allele. The presentation of thermodynamic ensemble folding stresses differences in the obtained structure. The color code indicates pairing propensities. The fold is further supported by reoccurring similar differences comparing several foldings and also lengths using software mFold. As template for folding, the full RNA sequence of EST from myelogenous leukemia cells (496 nucleotides long, 98% identity; full-length alignment; genbank accession BM149074.1; pediatric acute myelogenous leukemia cell (FAB M1) EST TCAAP2E6309) is shown. This RNA encodes no protein, has no introns/exons and has no complementary match in any other chromosomal region. (c) EST TCAAP2E6309 expression in all tested tissues: RNA was isolated from peripheral blood mononuclear cells (PBMC), human glioblastoma tissue (GB), and human placenta (PL). PCR was performed from cDNA. To exclude false positive results by genomic DNA contamination, several controls were performed (DNase digestion; respective RNA amplification). Genomic DNA from whole blood was used as positive control (+) and ddH₂O as negative control (–).

Ambra1^{+/-} mice. Upon free choice between a social box containing used bedding from mice of the opposite gender and another social box with fresh bedding only, WT male and female and *Ambra1*^{+/-} male mice behave as expected, namely choose to stay longer in the respective ‘pheromone box’. In contrast, *Ambra1*^{+/-} females fail to show this preference (Figure 3).

MRI analysis reveals brain enlargement in *Ambra1*^{+/-} mice

Brain enlargement has been described both in children and adults with ASD.^{5–8} Recently, brain volume overgrowth in children was linked to the emergence and severity of autistic social deficits.⁷ We measured by high-resolution MRI (T2-weighted) brain dimensions in *Ambra1*^{+/-} versus WT mice. Whole brain and hippocampus were enlarged in male and female mutants at postnatal day 23 (around puberty). Cerebellum was increased in female *Ambra1*^{+/-} mice only (Figure 4). Sizes of olfactory bulb and ventricles in *Ambra1*^{+/-} mice were similar to WT. Repeated examination of females at age 13 months revealed persistence of the increased brain dimensions (Figure 5a). We note that *Ambra1*^{+/-} mice are the first autism model showing autism-typical brain enlargement. Regarding this particular readout, genders were comparable, uncoupling in this model autism-like behavior (only females) from brain dimensions.

Female *Ambra1*^{+/-} mice show altered seizure propensity

Another frequently observed trait, connected with autistic behaviors, not only in syndromic forms of autism, is epileptic seizures.^{9,10} Most likely, seizure predisposition reflects the autism-pathognomonic neuronal excitation–inhibition dysbalance.^{4,11–15} In our *Ambra1*^{+/-} model, prepubertal female mutants displayed reduced response to PTZ, namely longer latency to the first whole-body seizure and decreased seizure score compared to female WT (Figure 5b). This early resistance turned into the opposite response at older age: Number of tonic-clonic seizures and duration of whole-body seizures were enhanced in 3-months (data not shown) and 13-months-old *Ambra1*^{+/-} females versus WT, also resulting in reduced survival (Figures 5c and d). Male mutants did not differ from WT at any time point investigated. Together, these data support *Ambra1*^{+/-} mice as multidimensional model of human autism.

DISCUSSION

We previously reported in female *Ambra1*^{+/-} mice a discrete behavioral trait, reminiscent of human ASD.²⁹ In the present study, we extend this finding, showing for the first time that *AMBRA1* may—in likewise sexually dimorphic manner—be relevant also in humans for the expression of a female autistic

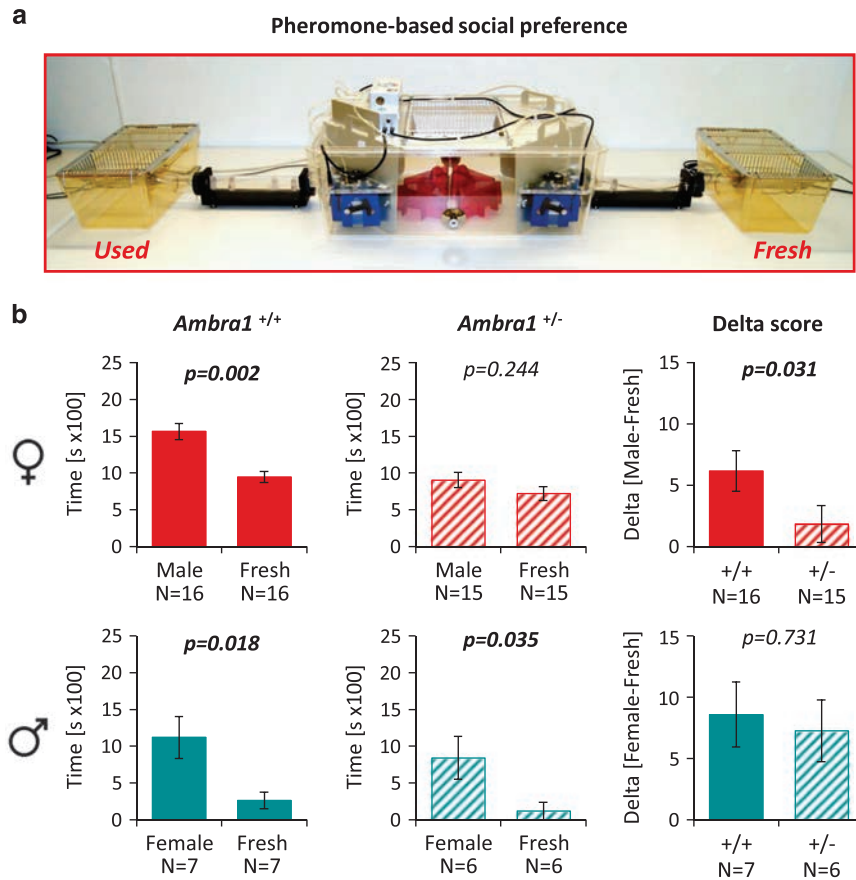


Figure 3. Impaired pheromone preference in female *Ambra1* mutants. (a) Intelligence apparatus with connected social boxes. (b) Time spent in social boxes with used or fresh bedding or delta difference scores for the indicated genotypes. Upper row females; lower row males; mean \pm s.e.m. presented. Within-group comparisons performed with paired *t*-tests, between-group with Mann-Whitney *U*-tests; all tests two-tailed.

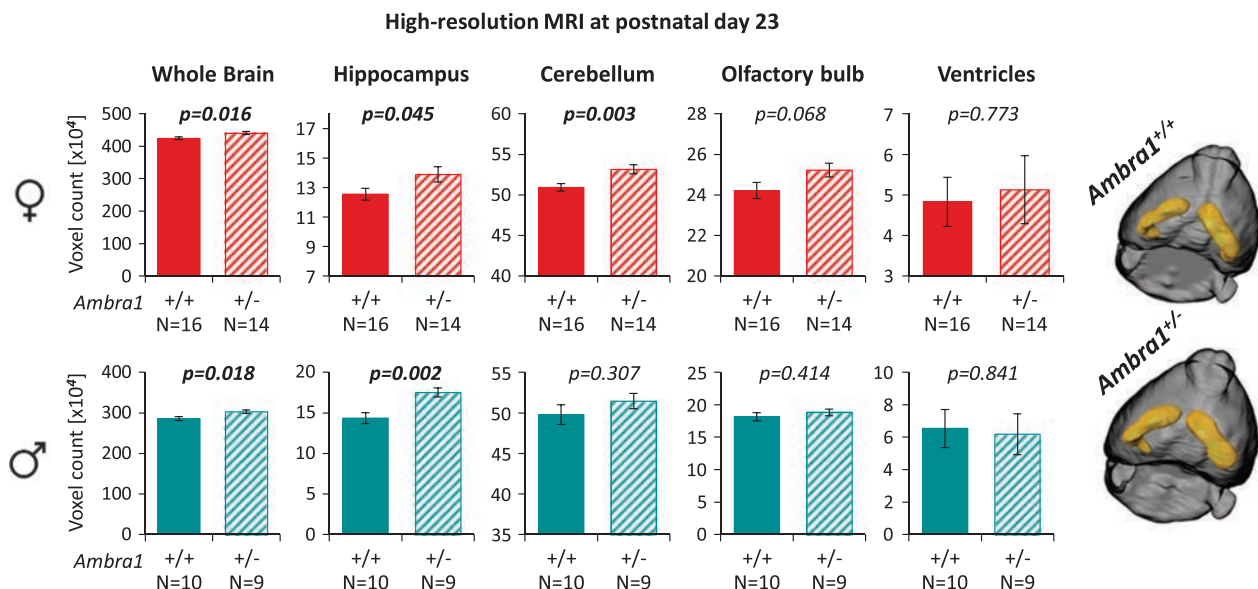


Figure 4. Brain enlargement in prepubertal *Ambra1* mutants of both genders. Shown are results of high-resolution magnetic resonance imaging (MRI) (T2-weighted). Brain regions of interest (whole brain, hippocampus, cerebellum, olfactory bulb, ventricles) in 23day-old female (upper row) and male (lower row) mice of both genotypes are presented; mean \pm s.e.m.; two-tailed unpaired *t*-tests. Right side: Representative pictures of 3D-reconstructed brains of both genotypes illustrate brain enlargement in mutants.

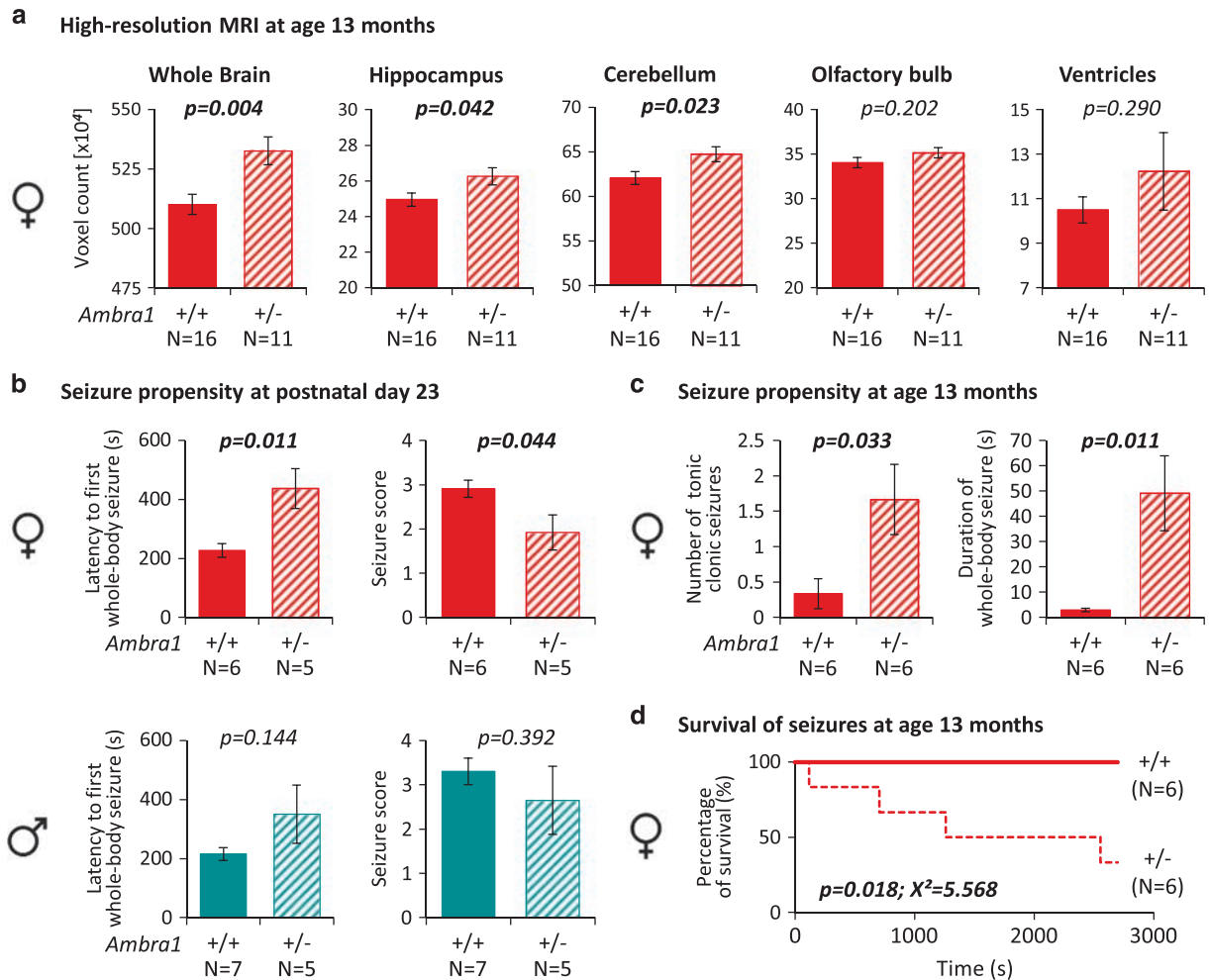


Figure 5. Persistent brain enlargement and altered pentylentetrazol (PTZ)-induced seizure propensity in female *Ambra1* mutants. **(a)** Brain regions of interest (whole brain, hippocampus, cerebellum, olfactory bulb, ventricles) were analyzed by high-resolution magnetic resonance imaging (MRI) in 13-months-old female *Ambra1*^{+/-} and WT mice; mean \pm s.e.m.; two-tailed unpaired *t*-tests. **(b)** PTZ-induced seizure propensity (intraperitoneal injection of 50 mg kg⁻¹) in 23-day-old WT and *Ambra1*^{+/-} mice of both genders; mean \pm s.e.m. presented; two-tailed unpaired *t*-tests. **(c)** PTZ-induced seizure propensity (intraperitoneal injection of 50 mg kg⁻¹) in 13-months-old female WT and *Ambra1*^{+/-} mice; mean \pm s.e.m. presented; two-tailed unpaired *t*-tests. **(d)** Survival of PTZ-induced seizures (intraperitoneal injection of 50 mg kg⁻¹) in 13-months-old female WT and *Ambra1*^{+/-} mice; Kaplan–Meier survival analysis.

phenotype. The female preponderance, unique thus far in autism genetics, may even help illuminating some general molecular underpinnings of gender susceptibility to brain disease. Remarkably, in a highly targeted association approach, using the only *AMBRA1* SNP available for analysis, rs3802890-A/G, we find in two independent populations, the GRAS sample of schizophrenic individuals and the SHIP sample of general population subjects, relevance for this marker regarding autistic traits in women. Partial loss-of-function, reflected by a relative decrease in *AMBRA1* mRNA levels in PBMC of female risk genotype (AA) carriers, may suggest an underlying autism-causing mechanism similar to that in heterozygous mice where *Ambra1* reduction was stronger in female than male mutant cortex.²⁹

The question of how *AMBRA1*/*Ambra1* reduction may influence synaptic function, thereby causing the autism-pathognomonic neuronal excitation–inhibition dysbalance,^{4,11–15} still remains unanswered. We may, however, speculate that reduced autophagy at synaptic terminals,^{30,31,63} likely more pronounced in *Ambra1*^{+/-} females,²⁹ influences synaptic protein turnover and function in a gender-specific manner. In fact, females may be particularly sensitive to reduced autophagy as suggested also by a recent paper reporting higher basal autophagy activity in the

brain of neonatal female as compared to male rats.⁶⁴ In this sense, *AMBRA1*/*Ambra1* adds to the number of proteins shown to underlie sexually dimorphic effects on the brain.^{65,66}

In a first *in silico* search for mechanisms, we saw that the lncRNA, covering the SNP region, shows highly diverse folding upon presence of G versus A allele. This pronounced structural effect may influence *AMBRA1* mRNA and/or protein stability and will be subject for further investigation.

Returning to the *Ambra1*^{+/-} mouse model, we extend our earlier findings²⁹ to crucial, additional autistic features, so far not systematically addressed in genetic models of autism, namely early brain enlargement, altered propensity towards epileptic seizures and reduced pheromone preference.

Brain enlargement is a consistently reported feature in human autism, both in adults and children.^{5–8} Already upon first description of autism, increased size of the head was observed in affected children.⁶⁷ The substrate underlying the enlarged brain has remained obscure, and the *Ambra1*^{+/-} mouse model may now help to approach this question. Interestingly, we found *Ambra1*^{+/-}-associated brain enlargement in both genders, thus uncoupled from the predominantly female behavioral phenotype. This finding may be important in connection with recent

suggestions, based on genetically undefined autistic children, where brain volume overgrowth was linked to the emergence and severity of autistic social deficits, predicting a later autism diagnosis based on MRI deep-learning algorithms.⁷ This obvious discrepancy should stimulate further investigations considering gender, genetics and biological ASD subgroups.

Epileptic seizures are frequently observed, not only in syndromic autism, where they are often intractable,^{9,10} and mirror neuronal excitation/inhibition dysbalance.^{4,11–15} Also here, *Ambra1*^{+/-} mice revealed a striking sexual dimorphism and may serve as future model to study and treat autism-associated epilepsy.

Olfactory deficits in human autism have been reported, even though the literature is scarce, heterogeneous and inconsistent, likely reflecting subject selection and assessment biases or other methodological limitations, including statistical power issues.⁶⁸ We note, however, that compared to humans, pheromone preference in mice represents a more prominent component of their social behavioral repertoire, thus more vulnerable to be disturbed in autism-like phenotypes of this species.

To conclude, our data suggest a fascinating sexual dimorphism regarding the role of the autosomal *AMBRA1/Ambra1* gene for autistic traits across species. In humans, it will for instance be interesting to systematically screen ASD patients for *AMBRA1* mutations, particularly female autists. *Ambra1*^{+/-} mice may serve as a novel multilayered construct-valid genetic model of human autistic phenotypes.

CONFLICT OF INTEREST

The authors declare no conflict of interest.

ACKNOWLEDGMENTS

This work was supported by the Max Planck Society, the Max Planck Förderstiftung, the DFG (CNMPB), EXTRABRAIN EU-FP7, the Niedersachsen-Research Network on Neuroinfectiology (N-RENNT) and EU-AIMS. The research of EU-AIMS receives support from the Innovative Medicines Initiative Joint Undertaking under grant agreement n 115300, resources of which are composed of financial contribution from the European Union's Seventh Framework Program (FP7/2007–2013), from the EFPIA companies and from Autism Speaks. SHIP is part of the Community Medicine Research net of the University Medicine Greifswald, which is funded by the Federal State of Mecklenburg-West Pomerania. Genome-wide data in SHIP have been supported by a joint grant from Siemens Healthineers, Erlangen, and the Federal State of Mecklenburg-West Pomerania. We thank all subjects for participating in the study, and all the many colleagues who have contributed over the past decade to the GRAS data collection.

AUTHOR CONTRIBUTIONS

Concept, design and supervision of the study: HE. Data acquisition/analysis/interpretation: MM, MB, AJ, ED, SH, LW, JB, Svda, RT, IH, KH, BO, HV, GH, FC, KC, HG, JF, TD, SB, HE. Drafting manuscript and figures: HE, MM, MB, AJ, ED, TD. All authors read and approved the final version of the manuscript.

REFERENCES

- Bourgeron T. From the genetic architecture to synaptic plasticity in autism spectrum disorder. *Nat Rev Neurosci* 2015; **16**: 551–563.
- de la Torre-Ubieta L, Won H, Stein JL, Geschwind DH. Advancing the understanding of autism disease mechanisms through genetics. *Nat Med* 2016; **22**: 345–361.
- Delorme R, Ey E, Toro R, Leboyer M, Gillberg C, Bourgeron T. Progress toward treatments for synaptic defects in autism. *Nat Med* 2013; **19**: 685–694.
- Mullins C, Fishell G, Tsien RW. Unifying views of autism spectrum disorders: a consideration of autoregulatory feedback loops. *Neuron* 2016; **89**: 1131–1156.
- Courchesne E, Carper R, Akshoomoff N. Evidence of brain overgrowth in the first year of life in autism. *JAMA* 2003; **290**: 337–344.
- Courchesne E, Mouton PR, Calhoun ME, Semendeferi K, Ahrens-Barbeau C, Hallet MJ et al. Neuron number and size in prefrontal cortex of children with autism. *JAMA* 2011; **306**: 2001–2010.

- Hazlett HC, Gu H, Munsell BC, Kim SH, Styner M, Wolff JJ et al. Early brain development in infants at high risk for autism spectrum disorder. *Nature* 2017; **542**: 348–351.
- Piven J, Arndt S, Bailey J, Havercamp S, Andreasen NC, Palmer P. An MRI study of brain size in autism. *Am J Psychiatry* 1995; **152**: 1145–1149.
- Keller R, Basta R, Salerno L, Elia M. Autism, epilepsy, and synaptopathies: a not rare association. *Neurol Sci* 2017; **38**: 1353–1361.
- Tuchman R, Rapin I. Epilepsy in autism. *Lancet Neurol* 2002; **1**: 352–358.
- Nelson SB, Valakh V. Excitatory/inhibitory balance and circuit homeostasis in autism spectrum disorders. *Neuron* 2015; **87**: 684–698.
- Ramocki MB, Zoghbi HY. Failure of neuronal homeostasis results in common neuropsychiatric phenotypes. *Nature* 2008; **455**: 912–918.
- Sudhof TC. Neuroligins and neuroligins link synaptic function to cognitive disease. *Nature* 2008; **455**: 903–911.
- Uhlhaas PJ, Singer W. Neural synchrony in brain disorders: relevance for cognitive dysfunctions and pathophysiology. *Neuron* 2006; **52**: 155–168.
- Uhlhaas PJ, Singer W. Neuronal dynamics and neuropsychiatric disorders: toward a translational paradigm for dysfunctional large-scale networks. *Neuron* 2012; **75**: 963–980.
- Jamain S, Quach H, Betancur C, Rastam M, Colineaux C, Gillberg IC et al. Mutations of the X-linked genes encoding neuroligins NLGN3 and NLGN4 are associated with autism. *Nat Genet* 2003; **34**: 27–29.
- Jamain S, Radyushkin K, Hammerschmidt K, Granon S, Boretius S, Varoquaux F et al. Reduced social interaction and ultrasonic communication in a mouse model of monogenic heritable autism. *Proc Natl Acad Sci USA* 2008; **105**: 1710–1715.
- Schroeder JC, Reim D, Boeckers TM, Schmeisser MJ. Genetic animal models for autism spectrum disorder. *Curr Top Behav Neurosci* 2017; 30311–30324.
- Clarke TK, Lupton MK, Fernandez-Pujals AM, Starr J, Davies G, Cox S et al. Common polygenic risk for autism spectrum disorder (ASD) is associated with cognitive ability in the general population. *Mol Psychiatry* 2016; **21**: 419–425.
- Gaugler T, Klei L, Sanders SJ, Bodea CA, Goldberg AP, Lee AB et al. Most genetic risk for autism resides with common variation. *Nat Genet* 2014; **46**: 881–885.
- Ehrenreich H, Mitjans M, Van der Auwera S, Centeno TP, Begemann M, Grabe HJ et al. OTTO: a new strategy to extract mental disease-relevant combinations of GWAS hits from individuals. *Mol Psychiatry* 2016.
- Ehrenreich H, Nave KA. Phenotype-based genetic association studies (PGAS)-towards understanding the contribution of common genetic variants to schizophrenia subphenotypes. *Genes* 2014; **5**: 97–105.
- Stepniak B, Kastner A, Poggi G, Mitjans M, Begemann M, Hartmann A et al. Accumulated common variants in the broader fragile X gene family modulate autistic phenotypes. *EMBO Mol Med* 2015; **7**: 1565–1579.
- Kastner A, Begemann M, Michel TM, Everts S, Stepniak B, Bach C et al. Autism beyond diagnostic categories: characterization of autistic phenotypes in schizophrenia. *BMC Psychiatry* 2015; **15**: 115.
- Careaga M, Murai T, Bauman MD. Maternal immune activation and autism spectrum disorder: from rodents to nonhuman and human primates. *Biol Psychiatry* 2017; **81**: 391–401.
- Ehrenreich H. The impact of environment on abnormal behavior and mental disease: to alleviate the prevalence of mental disorders, we need to phenotype the environment for risk factors. *EMBO Rep* 2017; **18**: 661–665.
- Baron-Cohen S, Cassidy S, Auyeung B, Allison C, Achoukhi M, Robertson S et al. Attenuation of typical sex differences in 800 adults with autism vs. 3,900 controls. *PLoS ONE* 2014; **9**: e102251.
- Halladay AK, Bishop S, Constantino JN, Daniels AM, Koenig K, Palmer K et al. Sex and gender differences in autism spectrum disorder: summarizing evidence gaps and identifying emerging areas of priority. *Mol Autism* 2015; **6**: 36.
- Dere E, Dahm L, Lu D, Hammerschmidt K, Ju A, Tantra M et al. Heterozygous *Ambra1* deficiency in mice: a genetic trait with autism-like behavior restricted to the female gender. *Front Behav Neurosci* 2014; **8**: 181.
- Shen DN, Zhang LH, Wei EQ, Yang Y. Autophagy in synaptic development, function, and pathology. *Neurosci Bull* 2015; **31**: 416–426.
- Tang G, Gudsruk K, Kuo SH, Cotrina ML, Rosoklija G, Sosunov A et al. Loss of mTOR-dependent macroautophagy causes autistic-like synaptic pruning deficits. *Neuron* 2014; **83**: 1131–1143.
- Cianfanelli V, De Zio D, Di Bartolomeo S, Nazio F, Strappazon F, Cecconi F. *Ambra1* at a glance. *J Cell Sci* 2015; **128**: 2003–2008.
- Fimia GM, Stoykova A, Romagnoli A, Giunta L, Di Bartolomeo S, Nardacci R et al. *Ambra1* regulates autophagy and development of the nervous system. *Nature* 2007; **447**: 1121–1125.
- El-Kordi A, Winkler D, Hammerschmidt K, Kastner A, Krueger D, Ronnenberg A et al. Development of an autism severity score for mice using *Nlgn4* null mutants as a construct-valid model of heritable monogenic autism. *Behav Brain Res* 2013; **251**: 41–49.
- Rietschel M, Mattheisen M, Degenhardt F, Genetic R, Outcome in P, Muhleisen TW et al. Association between genetic variation in a region on chromosome 11 and schizophrenia in large samples from Europe. *Mol Psychiatry* 2012; **17**: 906–917.

- 36 Parnas J, Bovet P. Autism in schizophrenia revisited. *Compr Psychiatry* 1991; **32**: 7–21.
- 37 Eack SM, Bahorik AL, McKnight SA, Hogarty SS, Greenwald DP, Newhill CE *et al*. Commonalities in social and non-social cognitive impairments in adults with autism spectrum disorder and schizophrenia. *Schizophr Res* 2013; **148**: 24–28.
- 38 American Psychiatric Association. *Diagnostic and Statistical Manual of Mental Disorders*, 4th edn. American Psychiatric Press: Washington, DC, 2000.
- 39 Begemann M, Grube S, Papiol S, Malzahn D, Krampe H, Ribbe K *et al*. Modification of cognitive performance in schizophrenia by complexin 2 gene polymorphisms. *Arch Gen Psychiatry* 2010; **67**: 879–888.
- 40 Ribbe K, Friedrichs H, Begemann M, Grube S, Papiol S, Kastner A *et al*. The cross-sectional GRAS sample: a comprehensive phenotypical data collection of schizophrenic patients. *BMC Psychiatry* 2010; **10**: 91.
- 41 Volzke H, Alte D, Schmidt CO, Radke D, Lorbeer R, Friedrich N *et al*. Cohort profile: the study of health in Pomerania. *Int J Epidemiol* 2011; **40**: 294–307.
- 42 Kay SR, Fiszbein A, Opler LA. The positive and negative syndrome scale (Pans) for schizophrenia. *Schizophr Bull* 1987; **13**: 261–276.
- 43 Klein J, Vonnellich N, Baumeister SE, Kohlmann T, von dem Knesebeck O. Do social relations explain health inequalities? Evidence from a longitudinal survey in a changing eastern German region. *Int J Public Health* 2012; **57**: 619–627.
- 44 Hammer C, Stepniak B, Schneider A, Papiol S, Tantra M, Begemann M *et al*. Neuropsychiatric disease relevance of circulating anti-NMDA receptor auto-antibodies depends on blood-brain barrier integrity. *Mol Psychiatry* 2014; **19**: 1143–1149.
- 45 Stepniak B, Papiol S, Hammer C, Ramin A, Everts S, Hennig L *et al*. Accumulated environmental risk determining age at schizophrenia onset: a deep phenotyping-based study. *Lancet Psychiatry* 2014; **1**: 444–453.
- 46 Howie BN, Donnelly P, Marchini J. A flexible and accurate genotype imputation method for the next generation of genome-wide association studies. *PLoS Genetics* 2009; **5**: e1000529.
- 47 Altschul SF, Gertz EM, Agarwala R, Schaffer AA, Yu YK. PSI-BLAST pseudocounts and the minimum description length principle. *Nucleic Acids Res* 2009; **37**: 815–824.
- 48 Boguski MS, Lowe TM, Tolstoshev CM. dbEST—database for "expressed sequence tags". *Nat Genet* 1993; **4**: 332–333.
- 49 Zuker M. Mfold web server for nucleic acid folding and hybridization prediction. *Nucleic Acids Res* 2003; **31**: 3406–3415.
- 50 Bengert P, Dandekar T. A software tool-box for analysis of regulatory RNA elements. *Nucleic Acids Res* 2003; **31**: 3441–3445.
- 51 Agostini F, Zanzoni A, Klus P, Marchese D, Cirillo D, Tartaglia GG. catRAPID omics: a web server for large-scale prediction of protein–RNA interactions. *Bioinformatics* 2013; **29**: 2928–2930.
- 52 Burge C, Karlin S. Prediction of complete gene structures in human genomic DNA. *J Mol Biol* 1997; **268**: 78–94.
- 53 Netrakanti PR, Cooper BH, Dere E, Poggi G, Winkler D, Brose N *et al*. Fast cerebellar reflex circuitry requires synaptic vesicle priming by munc13-3. *Cerebellum* 2015; **14**: 264–283.
- 54 Ju A, Hammerschmidt K, Tantra M, Krueger D, Brose N, Ehrenreich H. Juvenile manifestation of ultrasound communication deficits in the neuroigin-4 null mutant mouse model of autism. *Behav Brain Res* 2014; **270**: 159–164.
- 55 Bodda C, Tantra M, Mollajew R, Arunachalam JP, Laccone FA, Can K *et al*. Mild overexpression of *Mecp2* in mice causes a higher susceptibility toward seizures. *Am J Pathol* 2013; **183**: 195–210.
- 56 Ferraro TN, Golden GT, Smith GG St, Jean P, Schork NJ, Mulholland N *et al*. Mapping loci for pentylenetetrazol-induced seizure susceptibility in mice. *J Neurosci* 1999; **19**: 6733–6739.
- 57 Wojcik SM, Tantra M, Stepniak B, Man KN, Muller-Ribbe K, Begemann M *et al*. Genetic markers of a Munc13 protein family member, BAIAP3, are gender specifically associated with anxiety and benzodiazepine abuse in mice and humans. *Mol Med* 2013; **19**: 135–148.
- 58 Purcell S, Neale B, Todd-Brown K, Thomas L, Ferreira MAR, Bender D *et al*. PLINK: A tool set for whole-genome association and population-based linkage analyses. *Am J Hum Genet* 2007; **81**: 559–575.
- 59 Chang YC, Cole TB, Costa LG. Behavioral phenotyping for autism spectrum disorders in mice. *Curr Protoc Toxicol* 2017; **72**: 11 22 11–11 22 21.
- 60 Lubke KT, Pause BM. Always follow your nose: the functional significance of social chemosignals in human reproduction and survival. *Hormones Behav* 2015; **68**: 134–144.
- 61 Stowers L, Kuo TH. Mammalian pheromones: emerging properties and mechanisms of detection. *Curr Opin Neurobiol* 2015; **34**: 103–109.
- 62 Wohr M, Roulet FI, Hung AY, Sheng M, Crawley JN. Communication impairments in mice lacking Shank1: reduced levels of ultrasonic vocalizations and scent marking behavior. *PLoS ONE* 2011; **6**: e20631.
- 63 Vijayan V, Verstreken P. Autophagy in the presynaptic compartment in health and disease. *J Cell Biol* 2017; **216**: 1895–1906.
- 64 Weis SN, Toniazzo AP, Ander BP, Zhan X, Careaga M, Ashwood P *et al*. Autophagy in the brain of neonates following hypoxia-ischemia shows sex- and region-specific effects. *Neuroscience* 2014; **256**: 201–209.
- 65 Li K, Nakajima M, Ibanez-Tallon I, Heintz N. A cortical circuit for sexually dimorphic oxytocin-dependent anxiety behaviors. *Cell* 2016; **167**: 60–72.
- 66 Malishkevich A, Amram N, Hacoheh-Kleiman G, Magen I, Giladi E, Gozes I. Activity-dependent neuroprotective protein (ADNP) exhibits striking sexual dichotomy impacting on autistic and Alzheimer's pathologies. *Transl Psychiatry* 2015; **5**: e501.
- 67 Asperger H. The "autistic psychopathy" in childhood. *Archiv Fur Psychiatrie Und Nervenkrankheiten* 1944; **117**: 76–136.
- 68 Boudjarane MA, Grandgeorge M, Marianowski R, Misery L, Lemonnier E. Perception of odors and tastes in autism spectrum disorders: a systematic review of assessments. *Autism Res* 2017; **10**: 1045–1057.



This work is licensed under a Creative Commons Attribution 4.0 International License. The images or other third party material in this article are included in the article's Creative Commons license, unless indicated otherwise in the credit line; if the material is not included under the Creative Commons license, users will need to obtain permission from the license holder to reproduce the material. To view a copy of this license, visit <http://creativecommons.org/licenses/by/4.0/>

© The Author(s) 2017

needed to ameliorate inflammatory pathology caused by bacterial infections of the CNS. MicroRNA (miR) are short, non-coding RNA that regulate inflammation in bone marrow (BM)-derived myeloid cells as well as in brain parenchymal cells, e.g. microglia. Among these, miR-155 is an important regulator of brain inflammation in autoimmune conditions but little is known about its expression and role during bacterial infection. Experiments presented here analyzed expression and function of miR-155 in the brain during experimental *Listeria monocytogenes* (*Lm*) infection of mice. Infection of C57BL/6 mice with of 2-5LD50 *Lm* upregulated miR-155 measured in whole brain by 24 h following i.p. injection. Similarly, using a model in which lethally infected mice were rescued with antibiotics given 48 h post-infection (PI), miR-155 expression increased at day 3PI, peaked at day 7PI, then declined slowly despite brain infection being eliminated by day 7 PI. Analysis of mRNA expression in antibiotic treated mice showed maximal expression of *Il1b* and *Tnfa* coincided with maximal miR-155 expression. In isolated CD11b^{pos} brain cells, miR-155 expression increased at day 7PI but not at day 3 PI suggesting it may have a measurable role regulating inflammatory responses in microglia at that time point. Functional studies measured cytokine expression in brain cells isolated from C57BL/6 and miR-155^{-/-} mice after overnight culture with heat-killed *Lm*. Cells from miR-155^{-/-} mice isolated at day 6 & 7PI produced greater concentrations of IL-1 α , IL-1 β , TNF- α , CCL3, and CCL4 than did cells from normal mice. Similarly, a higher percentage of TNF- α ^{pos} microglia was found by intracellular flow cytometry in miR-155^{-/-} mice compared with normal animals. In contrast, cytokine production and intracellular TNF- α expression in microglia did not differ between genotypes at steady state or day 3PI. These data suggest miR-155 upregulated in the brain by *Lm* infection dampens inflammatory responses in microglia. Thus, enhancing its expression could be a novel form of adjunctive therapy during bacterial meningitis.

<http://dx.doi.org/10.1016/j.npbr.2015.12.018>

Two different immune pathogenesis models for bipolar disorder and major depressive disorder



Hemmo A. Drexhage on behalf of all MOODINFLAM, PSYCHAID investigators

Erasmus MC, Dr. Molewaterplein 50, Rotterdam, The Netherlands

Two integrated models 2015 for the immune pathogenesis of the two severe mood disorders are proposed. These models are based on the observations of a dynamic course of T cell and monocyte abnormalities in patients with either bipolar disorder or major depression as obtained in the MOODINFLAME and PSYCHAID EU projects. The observations are:

For bipolar disorder (BD)

1. In “early” pre-stages of bipolar disorder (prior to symptoms, i.e. in adolescent children of a bipolar parent) partial T cell defects are observed in FACS analysis, i.e. slightly lower numbers of circulating CD3+ and/or CD4+ T cells. These T cell defects do in particular involve CD4+ CD25+ FoxP3+ T regulatory cells. In bipolar twin studies these CD4+ CD25+ FoxP3+ T regulatory cell defects were almost entirely determined by the genetic background of the individual.
2. Lymphoid and myeloid growth factors are *increased* in serum of pre-stage bipolar disorder and also in established bipolar disorder, such as increases in IL-7, IGF-BP2, sCD25 and SCF.
3. In established bipolar disorder (and also in older children of a bipolar parent) defects in T regulatory cells do not determine the

picture anymore, but T regulatory cells are normalized or increased and inflammatory type T helper subsets (Th1 and Th17 cells) increased.

4. In stages of T regulatory T cell defects, i.e. in early pre-stage bipolar disorder (adolescent children of a bipolar parent) the expression of inflammatory genes is enhanced in circulating monocytes. This is also the case in active disease in later stages of bipolar disorder.

For major depressive disorder (MDD):

5. In all stages of major depressive disorder partial T cell defects are observed in FACS analysis, i.e. slightly lower numbers of circulating CD3+ and/or CD4+ T cells. These T cell defects again involve in particular CD4+ CD25+ FoxP3+ T regulatory cells and are most prominent in MDD of over 28 years.
6. Lymphoid and myeloid growth factors are *decreased* in the serum of MDD cases.
7. In MDD patients of <28 years there is a *reduced* expression of immune activation genes in monocytes
8. In late stage MDD (> 28 years) the expression of inflammatory and immune activation genes is *enhanced* in circulating monocytes. This enhanced expression correlates to the T regulatory cell defects occurring at that time. A course of 7 weeks anti-depressive drug treatment increases the number of circulating CD4+ CD25+ FoxP3+ T regulatory cells almost two fold, but does not (yet) have significant effects on inflammatory gene expression in monocytes.

In summary:

Major depressive disorder is characterized by defects in lymphoid and myeloid growth factors, relatively low numbers of T regulator and effector T helper cells, and a reduced monocyte function, apart from a high inflammatory function of monocytes at older age (i.e. >28 years).

Bipolar disorder is characterized by *increases* in lymphoid and myeloid growth factors (compensating initial T cell and myeloid cell defects?), and in later stages of the disease normal T regulatory cells, relatively high numbers of effector T helper cells and a high inflammatory function of monocytes related to the activity of the disease.

<http://dx.doi.org/10.1016/j.npbr.2015.12.019>

Circulating NMDAR1 autoantibodies of different immunoglobulin classes modulate evolution of lesion size in acute ischemic stroke



Hannelore Ehrenreich^{1,*}, Esther Castillo-Gomez¹, Barbara Oliveira¹, Christoph Ott¹, Johann Steiner², Karin Weissenborn³

¹ *Clinical Neuroscience, Max Planck Institute of Experimental Medicine, and DFG Research Center for Nanoscale Microscopy & Molecular Physiology of the Brain (CNMPB), Göttingen, Germany*

² *Department of Psychiatry, University of Magdeburg, Magdeburg, Germany*

³ *Department of Neurology, Hannover Medical School, Hannover, Germany*

*Corresponding author.

Building on the high seroprevalence of autoantibodies (AB) directed against the N-methyl-D-aspartate-receptor subunit NR1 (NMDAR1) across health and disease, we provide here examples where circulating NMDAR1-AB may be of (patho) physiological relevance. Dependent on acute or chronic dysfunction of the blood-brain-barrier (BBB), they may play the role of a ‘double-edged sword’. We further report that NMDAR1-AB not only bind to

neurons, but also to other cell types in the brain, and that their immunoglobulin class does not seem to affect their function in an internalization assay using human cortical neurons or in modulating stroke outcome of human patients.

We previously reported high seroprevalence (age-dependent up to >20%) of N-methyl-D-aspartate-receptor subunit NR1 (NMDAR1) autoantibodies (AB) in healthy and neuropsychiatrically ill subjects ($N=4236$) (Dahm et al., 2014). Neuropsychiatric syndrome relevance was restricted to individuals with compromised blood-brain-barrier (BBB), e.g. *APOE4* carrier status, both clinically and experimentally (Hammer et al., 2013; Hammer et al., 2014). Considering earlier data in rats (During et al., 2000), and the fact that excessive NMDAR-stimulation is regarded as a lead mechanism mediating stroke-associated brain damage, we hypothesized that NMDAR1-AB may modulate stroke outcome. We further hypothesized that in ischemic stroke patients the Ig class of serum NMDAR1-AB would not matter regarding their effects on stroke outcome. This latter hypothesis was based on our previous studies, using IgG, IgA and IgM NMDAR1-AB derived from human serum in the *ApoE*^{-/-} mouse model of BBB dysfunction with comparable behavioral consequences (Hammer et al., 2014).

Patients with acute ischemic stroke in the middle cerebral artery territory ($N=464$) were prospectively enrolled for a biomarker study with treatment as usual. Blood for NMDAR1-AB measurements was collected within 3–5 hours after stroke. *APOE4* carrier status was determined as indicator of a pre-existing leaky BBB. Evolution of lesion size (delta day7-1) in diffusion weighted magnetic resonance imaging (MRI) was primary outcome parameter. In subgroups, NMDAR1-AB measurements were repeated on days 2 and 7 (Zerche, Weissenborn, & Ott, 2015). For further mechanistic insight, wildtype and transgenic mouse brain sections, *ApoE*^{-/-} mice and human IPS-derived cortical neurons were employed.

Of 464 patients (mean age 68 years), 21.6% were NMDAR1-AB positive (IgM, A, or G), 21% were *APOE4* carriers. Patients with MRI data available on days1 and 7 were divided into 4 groups: (1) AB-/APOE4- ($N=236$); (2) AB+/APOE4- ($N=64$); (3) AB-/APOE4+ ($N=64$) and (4) AB+/APOE4+ ($N=20$). Groups were comparable in stroke-relevant presenting characteristics. The AB+/APOE4- group had a smaller mean delta lesion size, compared to the AB-/APOE4- group, suggesting a protective effect of circulating NMDAR1-AB. Conversely, the AB+/APOE4+ group had the largest mean delta lesion area, indicating a damaging influence of NMDAR1-AB in *APOE4* carriers. Hence, dependent on BBB integrity before an acute ischemic stroke, pre-existing NMDAR1-AB appear to be beneficial or detrimental. NMDAR1-AB effects on outcome were comparable in carriers of all 3 Ig classes (Zerche et al., 2015).

NMDAR1-AB titers in serum dropped on day2 and remounted by day7 after stroke (Zerche et al., 2015), consistent with the brain acting as immunoprecipitating trap for brain antigen-directed AB in conditions of BBB breakdown, later followed by boosting of AB production by plasma cells. This boosting likely occurs as a consequence of the abrupt exposure of the immune system to brain antigens upon major BBB disruption. The serum titer drop observed after stroke was reproducible in the *ApoE*^{-/-} mouse model of BBB disturbance (still unpublished). Since in the stroke study we had essentially comparable results for carriers of IgM, IgA and IgG (5), we employed human IPS-derived cortical neurons to compare Ig class effects in vitro using a receptor internalization assay (3). We found comparable internalization of NMDAR1 by all NMDAR1-AB isotypes (still unpublished).

Many NMDAR1 expressing cell types in the brain apart from neurons likely contribute to short-term and/or long-term outcome after stroke and may be functionally modulated by circulating NMDAR1-AB that suddenly gain access to the brain in larger amounts. In fact, endothelial cells, oligodendrocytes and astrocytes

express NMDAR1 which may influence their neuron/axon supporting, detoxifying, metabolic and protection/defense properties. Blocking these NMDAR1 functions by AB might variably contribute to the modulation of brain functions in these conditions and ultimately co-determine stroke outcome.

To substantiate these considerations, we provide here a first composite figure of our *work in progress* which illustrates scattered binding of a human NMDAR1-AB (IgG; 1:1000) positive serum of a stroke patient to endothelial cells (CD13), NG2 cells and astrocytes (GFAP), but not to microglia (Iba1) in healthy mouse hippocampus. Expectedly, also neurons are specifically labeled by this human AB (data not shown). In conditions of hypoxia/ischemia, inflammation, demyelination or degeneration, but also during normal pre- and postnatal development, aging, and perhaps even during learning processes, binding of NMDAR1-AB to the different cell types may be increased or altered (Fig. 1).

In conclusion, much more work will have to go into understanding consequences of circulating NMDAR1-AB in disease states with accompanying BBB breakdown, where these AB may possibly play the role of a double-edged sword. Reduction of lesion size during acute ischemia may be followed by an increased risk of cognitive decline, epilepsy or psychosis upon extended AB exposure of the brain, due to a lastingly compromised BBB after stroke (5). Further studies will be necessary to evaluate potential benefits of passive (rather than active) immunization under carefully controlled conditions.

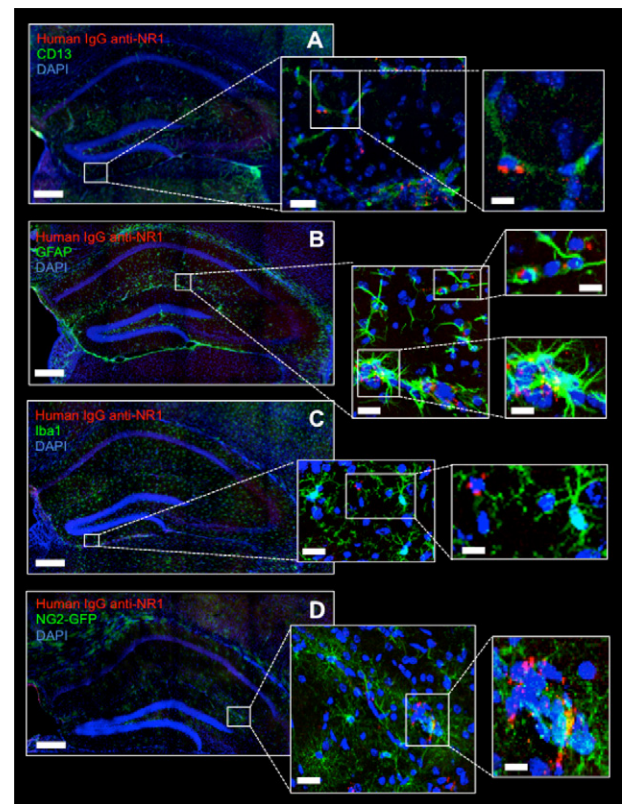


Fig. 1. Representative tilescan confocal images showing a panoramic view of the hippocampus of 4-week old mice, immunostained with dialyzed serum of a stroke patient, seropositive (IgG) for NMDAR1-AB (secondary AB: goat anti-human IgG-Cy3 = red, Jackson Immuno Research; A–D). Nuclei in all images are stained with DAPI (blue). Endothelial cells (green; A), astrocytes (green, B) and microglia (green; C) are stained with commercial primary AB [rat anti-CD13, BD Biosciences; mouse anti-GFAP, Boehringer Mannheim; rabbit anti-Iba1, WaKo], followed by the respective secondary AB, in a wild-type mouse hippocampus. D: NG2-GFP positive cells (green) in the brain of an NG2-CreERT2 transgenic mouse (tamoxifen injections at postnatal days 26 and 27). Scale bar: 250 μm (left panel), 25 μm (middle panel), 65 μm (right panel).

References

- Dahm, L., Ott, C., Steiner, J., Stepniak, B., Teegen, B., Saschenbrecker, S., et al. (2014). Seroprevalence of autoantibodies against brain antigens in health and disease. *Annals of Neurology*, 76(1), 82–94.
- During, M. J., Symes, C. W., Lawlor, P. A., Lin, J., Dunning, J., Fitzsimons, H. L., et al. (2000). An oral vaccine against NMDAR1 with efficacy in experimental stroke and epilepsy. *Science*, 287, 1453–1460.
- Hammer, C., Stepniak, B., Schneider, A., Papiol, S., Tantra, M., Begemann, M., et al. (2013). Neuropsychiatric disease relevance of circulating anti-NMDA receptor autoantibodies depends on blood-brain barrier integrity. *Molecular Psychiatry*, 19(10), 1143–1149.
- Hammer, C., Zerche, M., Schneider, A., Begemann, M., Nave, K. A., & Ehrenreich, H. (2014). Apolipoprotein E4 carrier status plus circulating anti-NMDAR1 autoantibodies: association with schizoaffective disorder. *Molecular Psychiatry*, 19(10), 1054–1056.
- Zerche, M., Weissenborn, K., Ott, C., Dere, E., Asif, A. R., Worthmann, H., et al. (2015). Preexisting serum autoantibodies against the NMDAR subunit NR1 modulate evolution of lesion size in acute ischemic stroke. *Stroke*, 46(5), 1180–1186.

<http://dx.doi.org/10.1016/j.npbr.2015.12.020>

Prenatal immune challenge induces changes of microglial surface markers in an animal model of schizophrenia

Manuela Eßlinger^{1,*}, Simone Wachholz¹,
Marie-Pierre Manitz¹, Rainer Sommer¹,
Jennifer Plümper¹, Awatef Esshili¹,
Alexandra Gerhard^{1,2}, Georg Juckel^{1,2},
Astrid Friebe^{1,2}

¹ Workgroup of Psychoneuroimmunology, Department of Psychiatry, ZKF1 2.052 Ruhr University Bochum, Universitätsstr. 150, 44801 Bochum, Germany

² LWL University Hospital, Alexandrinenstr. 1-3, 44791 Bochum, Germany

*Corresponding author.

Epidemiological studies indicate that maternal infection during pregnancy is associated with a higher incidence of schizophrenia in the offspring. It is hypothesized that an inflammatory immune response interferes with normal fetal brain development. Long-lasting changes of this developmental disruption might provide a neural basis for enhanced vulnerability which might manifest in schizophrenia in the adult descendants. We suggest microglia as possible initiator for this enhanced vulnerability. In previous studies we showed a significant alteration of microglial cell numbers in the adolescent offspring of Poly(I:C) injected mice compared to controls. Here we suggest a long term effect on microglia properties manifested in an altered expression pattern of pro- and anti-inflammatory surface markers due to prenatal immune challenge.

We used the Poly(I:C) mouse model of maternal immune activation to analyze pro- and anti-inflammatory surface markers on microglia of descendants from Poly(I:C) vs. saline exposed BALB/c mice at postnatal days 30 (puberty) and 100 (adulthood) by flow cytometric analysis. Analysis showed clear sex dependent differences in microglia surface marker expression between treatment groups. At day 30, female offspring from Poly(I:C) exposed mice showed significant microglia activation by up-regulation of M1 related activation markers and down-regulation of M2 associated markers. Microglia activation was not detected in adult female mice. In contrast, male descendants did not show signs of activation neither in puberty nor in adulthood. The alteration of microglia surface marker expression corresponds with our prior study, in which we showed an increased microglial cell number in the brains of the adolescent offspring from Poly(I:C) exposed mice. Here we show

significant changes in M1 and M2 associated surface markers which indicate modified activation patterns of microglia populations based on prenatal infection. The shift towards a M1 phenotype of the microglial cells of Poly(I:C) descendants points to the significance of immunological processes in schizophrenia.

<http://dx.doi.org/10.1016/j.npbr.2015.12.021>

Anti-inflammatory characteristics of acetylcholine esterase inhibitor Physostigmine and its potential role in preventing postoperative cognitive dysfunction



Lea Fritzenschaft^{*}, Simon Zolg, Benedikt Zujalovic,
E. Marion Schneider, Eberhard Barth

Department Anesthesiology, University Hospital Ulm, Albert-Einstein-Allee 23, Ulm 89081, Germany

*Corresponding author.

Postoperative cognitive dysfunction (POCD) is a complication affecting cognitive and locomotor functions in patients suffering from brain trauma as well as severe sepsis and intensive care treatment. Symptoms include clouding of consciousness and memory loss as well as impairment of attention, language and locomotor abilities.

Various possible pathologic causes for POCD have been proposed, but the most popular hypothesis is a central cholinergic deficiency caused by dysregulation of cholinergic anti-inflammatory pathways, leading to increased and chronic inflammation. Acetylcholine, the main mediator of the cholinergic anti-inflammatory pathway, suppresses NF- κ B activation and inhibits the release of pro-inflammatory cytokines (e.g. tumor necrosis factor, interleukin (IL)-1 β , IL-6, and IL-18) by macrophages. The anti-inflammatory properties of acetylcholine are mediated through the nicotinic acetylcholine receptors, especially the alpha-7 subunit is crucial for the anti-inflammatory effect. Available acetylcholine is degraded by acetylcholinesterase. As pretested with healthy donors, we are going to establish whole blood assays to determine the acetylcholine and butyrylcholinesterase activities from patients treated by intensive care and a high risk to manifest POCD. So far, ex vivo whole blood stimulation assays have been applied to test whether inflammation and/or enzyme activities can be modulated by exogenous Physostigmine.

Physostigmine is a reversible acetylcholinesterase inhibitor and therefore a cholinergic stimulant.

We hypothesize that Physostigmine can activate the cholinergic anti-inflammatory pathway and prevent the activation of macrophages via stimulation of the alpha-subunit of the nicotinic acetylcholine receptor.

Blood samples from volunteer donors and from ICU patients will be collected into the TruCulture whole blood culture system. As a stimulant, LPS will be added to mimic postoperative infection. The anti-inflammatory properties of Physostigmine will be determined by flow cytometry and cytokine quantification using the Immulite 1000 ELISA.

We expect that the application of Physostigmine significantly reduces the amount of activated macrophages and cytokines. Our results will contribute to our understanding of the complex molecular pathology in POCD.

<http://dx.doi.org/10.1016/j.npbr.2015.12.022>

Widespread Expression of Erythropoietin Receptor in Brain and Its Induction by Injury

Christoph Ott,¹ Henrik Martens,² Imam Hassouna,^{1,3} Bárbara Oliveira,¹ Christian Erck,² Maria-Patapia Zafeiriou,⁴ Ulla-Kaisa Peteri,¹ Dörte Hesse,⁵ Simone Gerhart,¹ Bekir Altas,⁶ Tekla Kolbow,² Herbert Stadler,² Hiroshi Kawabe,⁶ Wolfram-Hubertus Zimmermann,⁴ Klaus-Armin Nave,^{7,8} Walter Schulz-Schaeffer,⁹ Olaf Jahn,^{5,8} and Hannelore Ehrenreich^{1,8}

¹Clinical Neuroscience, Max Planck Institute of Experimental Medicine, Göttingen, Germany; ²Synaptic Systems GmbH, Göttingen, Germany; ³Physiology Unit, Zoology Department, Faculty of Science, Menoufia University, Egypt; ⁴Institute of Pharmacology, University Medicine Göttingen, Göttingen, Germany; ⁵Proteomics Group, ⁶Molecular Neurobiology, and ⁷Neurogenetics, Max Planck Institute of Experimental Medicine, Göttingen, Germany; ⁸DFG Center for Nanoscale Microscopy and Molecular Physiology of the Brain (CNMPB), Göttingen, Germany; and ⁹Department of Neuropathology, University Medicine Göttingen, Göttingen, Germany

Erythropoietin (EPO) exerts potent neuroprotective, neuroregenerative and procognitive functions. However, unequivocal demonstration of erythropoietin receptor (EPOR) expression in brain cells has remained difficult since previously available anti-EPOR antibodies (EPOR-AB) were unspecific. We report here a new, highly specific, polyclonal rabbit EPOR-AB directed against different epitopes in the cytoplasmic tail of human and murine EPOR and its characterization by mass spectrometric analysis of immunoprecipitated endogenous EPOR, Western blotting, immunostaining and flow cytometry. Among others, we applied genetic strategies including overexpression, Lentivirus-mediated conditional knockout of *EpoR* and tagged proteins, both on cultured cells and tissue sections, as well as intracortical implantation of *EPOR*-transduced cells to verify specificity. We show examples of EPOR expression in neurons, oligodendroglia, astrocytes and microglia. Employing this new EPOR-AB with double-labeling strategies, we demonstrate membrane expression of EPOR as well as its localization in intracellular compartments such as the Golgi apparatus. Moreover, we show injury-induced expression of EPOR. In mice, a stereotactically applied stab wound to the motor cortex leads to distinct *EpoR* expression by reactive GFAP-expressing cells in the lesion vicinity. In a patient suffering from epilepsy, neurons and oligodendrocytes of the hippocampus strongly express EPOR. To conclude, this new analytical tool will allow neuroscientists to pinpoint EPOR expression in cells of the nervous system and to better understand its role in healthy conditions, including brain development, as well as under pathological circumstances, such as upregulation upon distress and injury.

Online address: <http://www.molmed.org>

doi: 10.2119/molmed.2015.00192

INTRODUCTION

The growth factor erythropoietin (EPO) was named based on its first discovered effects on cells of the hematopoietic system. For >20 years it has been shown to act on other tissues, including the brain (1–5). Its remarkable neuroprotective, neuroregenerative and procogni-

tive effects make EPO an attractive candidate for treating human brain disease (6–7), and an important target of neuroscience research. In 1989, the EPO receptor (*EpoR*) was first cloned in mice (8), soon followed by cloning and characterization of the human *EPOR* gene (9–10). A single EPO molecule binds to two spe-

cific cytokine-type-1 transmembrane receptor molecules, each with a calculated molecular mass of 59 kDa, that together form the classical homodimeric EPOR (2,11). Binding of EPO to its receptor induces a conformational change, initiating EPOR-associated JAK2 transphosphorylation and multiple, cell-type-specific, downstream signal transduction cascades. These cascades include signal transducers and activators of transcription (STATs), phosphatidylinositol-3 kinase (PI3K)/AKT, RAS/extracellular signal-regulated kinase (ERK1/2), nuclear factor κ B (NF- κ B). Activation of these signaling cascades leads to further activation of antiapoptotic factors and pathways, stimulation of cell differentiation, including induction of cellular

Address correspondence to Hannelore Ehrenreich, Clinical Neuroscience, Max Planck Institute of Experimental Medicine, Göttingen, Germany. Phone: +49-551-3899615; Fax: +49-551-3899670; E-mail: ehrenreich@em.mpg.de.

Submitted August 25, 2015; Accepted for publication September 1, 2015; Published Online (www.molmed.org) September 1, 2015.

The Feinstein Institute
for Medical Research 

Empowering Imagination. Pioneering Discovery.®

EPOR IN BRAIN

shape-change and growth, or modulation of plasticity, in a cell-type and stimulation-dependent manner (5,12–13).

Antibodies against EPOR (EPOR-AB) have been widely used to characterize EPOR expression and localization, but cell surface EPOR expression is low, even in stimulated states, and, most importantly, all commercially available EPOR-AB have been hampered by non-specific cross-reactivities, calling into question the literature based exclusively on them. This, in turn, raised discussions within the scientific community, questioning the expression of EPOR in extrahematopoietic tissues (14–16). These discussions were likely nurtured by conflicts of interest, trying to restrict the effects of EPO, a highly attractive compound commercially for the anemia market, to hematopoiesis. Nevertheless, they made it very obvious that the existing EPOR-AB were essentially unreliable, and that the production and thorough characterization of new and more specific EPOR-AB had to be seen as a major challenge for the future (14,17–18).

Independent of work based on EPOR-AB, genetically altered mice helped to demonstrate that EPOR signaling is necessary for normal brain development (19) and that it has a distinct function in neurogenesis (20). In addition, EPO and EPOR mRNA are expressed in brain tissue (21), and specific binding sites for EPO in the brain have been demonstrated in mouse and humans by means of radio-labeled EPO (22–23). In cell culture, mRNA expression combined with functional assays, for example, altered phosphorylation of second messenger pathways induced by EPO in microglia, served to prove specific EPOR expression in the absence of reliable EPOR-AB (24).

The fact that cellular EPOR protein expression has been difficult to assess strongly limited the in-depth investigation of the EPO/EPOR system. Particularly in the human brain, the study of its (patho-) physiological role has been highly constrained since additional means of verification as used in experimental animals and cell cultures are naturally ex-

cluded. Recognizing this critical issue in EPO/EPOR research, we aimed at generating reliable EPOR-AB. We present here the comprehensive characterization of a novel, highly specific EPOR-AB, using an array of state-of-the-art technologies. This new AB tool may help overcome the described obstacles and lead to revisiting some of the reported data.

MATERIALS AND METHODS

Generation of EPOR-AB

Polyclonal AB. Two rabbits were immunized with a purified recombinant protein corresponding to amino acids (AA) 273-508 (intracellular C-terminus) of the unprocessed human EPOR. The coding sequence was generated by gene synthesis (Geneart, Regensburg, Germany) and ligated via EcoRI and HindIII into the bacterial expression vector pASK-IBA37+ (IBA-Lifescience, Göttingen, Germany). The recombinant His-Tag fusion protein was expressed and purified by Ni-NTA affinity chromatography according to the manufacturer's manual. Crude antiserum SA7378 was affinity purified with the immunogen coupled to CNBr Sepharose (GE-Healthcare, Freiburg, Germany). The AB is called "ctEPOR-AB" in this article.

Monoclonal AB. AB producing hybridomas were generated by Synaptic Systems (Göttingen, Germany; see also <http://sysy.com/services/index.php>) as follows: Three 8–10 wks old BALB/c female mice were subcutaneously immunized with a synthetic peptide corresponding to AA 25-39 (extracellular N-terminus) of unprocessed human EPOR precursor coupled to KLH via a C-terminal cysteine over a period of 75 d. Cells from the knee lymph nodes were fused with the mouse myeloma cell line P3X63Ag8.653 (ATCC CRL-1580). Resulting hybridomas were screened by direct enzyme-linked immunosorbent assay (ELISA) against the immunogen and immunofluorescence on 3T3 NIH fibroblasts overexpressing full-length human EPOR. Clone 45A3, used in this study, was recloned two times by limiting dilu-

tion and the immunoglobulin subclass was determined (IgG2b). The AB is called "ntEPOR-AB" in this article.

Cell Culture

Cell lines. The following human cell lines were used: The EPO-dependent megakaryoblastic leukemia UT-7 cell line, the erythroleukemia cell line OCIM-1, the mouse microglia cell line EOC-20 and HEK293 FT cells. The EPO-dependent megakaryoblastic leukemia UT-7 cell line was from Drorit Neumann of Tel Aviv University in Israel. This cell line was cultured in IMDM with 1% GlutaMAX supplement (Invitrogen, Darmstadt, Germany), 10% FBS, 100 U/mL penicillin and 100 µg/mL streptomycin (all Life Technologies GmbH, Darmstadt, Germany) and 2 IU/mL EPO (NeoRecormon, Roche, Welwyn Garden City, UK). The erythroleukemia cell line OCIM-1 (DSMZ GmbH, Braunschweig, Germany) was cultured in IMDM with 1% GlutaMAX supplement, 10% FBS and 100 U/mL penicillin and 100 µg/mL streptomycin (all Life Technologies GmbH).

The mouse microglia cell line EOC-20 (ATTC LGC Standards, Wesel, Germany) was cultured in DMEM with 1 mmol/L sodium pyruvate, 0.15% sodium bicarbonate, 10% FBS, 100 U/mL penicillin, 100 µg/mL streptomycin (all Life Technologies GmbH) and 0.01 µg/mL murine M-CSF (PAN-Biotech, Aidenbach, Germany). HEK293 FT cells (Sigma-Aldrich, Taufkirchen, Germany) were cultured in DMEM with 5% FBS and 100 U/mL penicillin and 100 µg/mL streptomycin (all Life Technologies GmbH).

Human IPS cells. Human material was used in accordance with ethical guidelines and the Helsinki Declaration. Subjects gave informed consent regarding generation and use of IPS cells or scientific investigation of brain samples. Human fibroblasts were reprogrammed using a nonintegrative RNA-based virus to induce the expression of four reprogramming factors: OCT4, SOX2, KLF4 and c-MYC (CytoTune-iPS 2.0 Sendai Reprogramming Kit, Life Technologies

GmbH). After transduction, IPS cells (clones isAu1-3; isAu3-2) were adapted to a feeder-free culture system (Matrigel matrix, Corning, Wiesbaden, Germany) and cultured in TeSR-E8 medium (STEMCELL Technologies SARL, Cologne, Germany).

Primary mouse cell culture. The preparation and culture conditions of primary mouse oligodendrocytes and microglia are described in detail elsewhere (24–25). In brief, oligodendrocytes were prepared from the forebrains of newborn P1-2 NMRI mice. After differentiation, oligodendrocyte precursors were shaken off from a bottom layer of astrocytes and seeded in Super-Sato medium (DMEM with high glucose supplemented with B-27 supplement, 2 mmol/L GlutaMAX, 1 mmol/L sodium pyruvate, 1% horse serum [HS], 50 U/mL penicillin and 50 µg/mL streptomycin [all from Life Technologies GmbH] and 0.5 mmol/L triiodothyronine, and 0.52 mmol/L L-thyroxine [both Merck, Darmstadt, Germany]). For primary microglia, newborn C57BL6 mice (P0-P1) were used. The cell suspension derived from their forebrains was seeded in high glucose DMEM medium with 10% HS, 1% GlutaMAX supplement, 50 U/mL penicillin and 50 µg/mL streptomycin (all from Life Technologies GmbH). Half of the microglia-conditioned medium was exchanged by fresh medium 3–4 d later, and at d 7 the medium was partially replaced by L929-conditioned medium. Primary microglia were detached by shaking of flasks and seeded in serum-free microglial growth medium (high glucose DMEM with 1 mmol/L sodium pyruvate, 1.5 g/L sodium bicarbonate, 100 U/mL penicillin and 100 µg/mL streptomycin [all from Life Technologies GmbH]).

Lentiviral Transduction of Primary Cells

EpoR conditional mouse mutants with floxed exons 3–6 were generated on the C57BL/6 background by standard procedures using mutant ES cells (EPD0316_5_A03) from the International Mouse Phenotyping Consortium. Details will be published elsewhere and are

available upon request. Primary mouse astrocytes prepared from P0-2 forebrains of *EpoR-fl/fl* mice were used. The preparation and culture conditions of these cells are described in detail elsewhere (26). The cells were infected with lentiviruses at d 1 *in vitro*. The viral constructs contained either a cassette for GFP-only (control) or a cassette for GFP and Cre-recombinase. Protein was extracted on d 10 *in vitro*.

EOC-20 Cell Transduction

For viral transduction, 100,000 EOC-20 cells were seeded in 12-well plates overnight. The next day, the medium was partially exchanged by DMEM (Life Technologies GmbH) containing viral supernatant and 8 µg/mL polybrene (Sigma-Aldrich). The ecotropic virus particles used were derived from a pMOWS vector encoding N-terminally HA-tagged full-length human *EPOR* and puromycin-resistant cassette (gift from Ursula Klingmüller, DKFZ Heidelberg, Germany) (27). Next, the 12-well plates were centrifuged for 3 h at 330g at room temperature. The medium was exchanged again to DMEM with 1 mmol/L sodium pyruvate, 0.15% sodium bicarbonate, 10% FBS, 100 U/mL penicillin, 100 µg/mL streptomycin (all Life Technologies GmbH) and 0.01 µg/mL murine M-CSF (PAN-Biotech). The medium was supplemented 1 d later with 6 µg/mL puromycin (Sigma-Aldrich) for selection of successfully transduced EOC-20 cells. After successful transduction, cells were constantly cultured in the presence of 6 µg/mL puromycin.

HEK293 FT Cell Transfection

HEK293 FT cells were transfected with Lipofectamine 2000 reagent (Life Technologies GmbH) according to the manufacturer's instructions. The pEuExpress-hEPOR vector (Synaptic Systems, Göttingen, Germany) was used to transfect the cells with full-length human *EPOR* (~60 kDa), full-length murine *EpoR* (~60 kDa), an N-terminally HA-tagged and C-terminally truncated human *EPOR* (lacks the intracellular do-

main, ~40 kDa) and an anchored human *EPOR* (lacks the N-terminus and the C-terminus, ~12 kDa).

STAT5 Phosphorylation Assay

This assay is described in detail elsewhere (17). In brief, UT-7 or OCIM-1 cells were serum- and EPO-deprived overnight (1% FBS in IMDM, both Life Technologies GmbH). On the next day, they were incubated with different concentrations of recombinant human EPO (rhEPO, NeoRecormon, Roche) or control solution for 15 min, followed by protein extraction for Western blotting. Immunodetection was done with antiphosphorylated STAT5 (1:500, Cell Signaling, Danvers, MA, USA) and GAPDH (1:5000, Enzo Life Sciences, Farmingdale, NY, USA); 20 µg of protein was loaded for SDS-PAGE.

MAPK Phosphorylation Assay

Transduced EOC-20 cells were kept in serum-free DMEM (Life Technologies GmbH) overnight. Then, cells were incubated with different concentrations of rhEPO (NeoRecormon, Roche) or the respective control solution for 10 min, followed by protein extraction for Western blotting. Immunodetection was done with antiphosphorylated MAPK (1:1000), anti-MAPK (1:5000) and anti- α -tubulin (1:5000, all Sigma-Aldrich); 15 µg of protein was loaded for SDS-PAGE.

Animal Experiments

All experiments were approved by and conducted in accordance with the regulations of the local Animal Care and Use Committee (Niedersächsisches Landesamt für Verbraucherschutz und Lebensmittelsicherheit [LAVES]).

Stereotactic cell implantation. Male C57BL/6N mice, 8 wks old, were used. Animals were injected intraperitoneally (i.p.) with carprofen (5 mg/kg Rimadyl, Pfizer, Berlin, Germany) 2 h before surgery. Under anesthesia (0.276 mg/g tribromoethanol, Sigma-Aldrich, St. Louis, MO, USA), mice were positioned in a stereotactic frame and a small, midline scalp incision was made. A hole was drilled over the left cranial hemisphere at

EPOR IN BRAIN

a position 1.5 mm anterior and 1.0 mm lateral to the bregma. Using a sterile 10-mL Hamilton syringe with a 26-gauge needle, 15,000 transduced EOC-20 cells (description see above) or medium only (DMEM without phenol-red, Life Technologies GmbH) were slowly (over 2 min) implanted 2 mm deep into the left M2 motor cortex. After implantation, the needle was left in place for 2 min, then slowly withdrawn from the brain and the skin incision closed with sterile suture. Directly after the skin incision was closed, the animals received carprofen i.p. for pain treatment, which was repeated every 6-8 h (5 mg/kg Rimadyl, Pfizer). At 24 h after surgery, animals were anesthetized i.p. (0.276 mg/g tribromoethanol, Sigma-Aldrich) and perfused transcardially with 0.9% saline followed by 4% formaldehyde in PBS.

Labeling of oligodendrocyte precursor cells *in vivo*. For induction of CreERT2-activity in NG2-Cre-ERT2:R26R-td-tomato-mEGFP mice (28–29), 100 mg/kg tamoxifen (dissolved in corn oil; Sigma-Aldrich, Taufkirchen, Germany) was injected i.p. at postnatal d 26 and 27. Animals were anesthetized i.p. (0.276 mg/g tribromoethanol, Sigma-Aldrich) 72 h later and perfused transcardially with 0.9% saline followed by 4% formaldehyde in PBS.

Detection of EPOR

Immunoprecipitation (IP). UT-7 protein lysates were obtained using an IP buffer (150 mmol/L NaCl, 20 mmol/L Tris, 1 mmol/L EDTA, 10% glycerol, pH = 7.4) containing 1% Triton X-100. Before IP, lysates were diluted 1:1 with IP buffer to obtain 0.5% Triton X-100. For the EPOR IP, protein-G sepharose beads were covalently linked to ctEPOR-AB (Synaptic Systems) with 40 mmol/L dimethyl-pimelimidate (Sigma-Aldrich). Bead slurry (200 μ L; Thermo Scientific, Waltham, MA, USA) was cross-linked with 400 μ g ctEPOR-AB or 400 μ g of the IgG fraction from the same rabbit before immunization. For EPOR IP from UT-7 protein lysates, 9 μ g of ctEPOR-AB coupled to protein-G sepharose per 1 mg protein

lysate were incubated for 2 h at 4°C. Afterward, beads were centrifuged and washed. For immunoblot analysis, EPOR was eluted from the beads by repeated boiling in Laemmli buffer at 95°C. For mass spectrometric protein identification, EPOR was eluted as before but with a nonreducing SDS-buffer (without β -mercaptoethanol) to prevent masking of the EPOR by excess AB heavy chains in the subsequent gel electrophoresis. To increase the efficiency of EPOR capture from UT-7 protein lysates, two consecutive IPs with fresh beads were performed in a way that the flow-through of the first IP was used as input for the second. Eluted proteins were precipitated by methanol/chloroform treatment (30). Pellets were solubilized in reducing sample buffer and pooled prior to electrophoresis. As starting material for mass spectrometry, 4 mg protein lysate from UT-7 cells was used.

SDS-PAGE and Western blots. SDS-PAGE was performed with self-made 10% SDS-polyacrylamide gels. As a protein ladder we used PageRuler Plus prestained and SeeBlue Plus2 prestained in this gel system (both Life Technologies GmbH). For all Western blotting, the following protein amounts were loaded: 15 μ g for lysates derived from cell lines; 20 μ g for lysates derived from primary cultures; 50 μ g for lysates derived from tissue. Afterward, proteins were transferred to a nitrocellulose membrane and blocked with 4% milk powder and 4% HS in Tris buffered saline with 0.05% Tween 20. Membranes were incubated with ctEPOR-AB (1:2000, Synaptic Systems) at 4°C overnight. For all EPOR immunoblots, membranes were washed, blocked again and incubated with donkey anti-rabbit IRDye 800 AB (1:10000, Rockland, Limerick, PA, USA) for 1 h at room temperature. Primary mouse AB were detected with donkey anti-mouse IRDye 800 AB (1:10000, Rockland) for 1 h at room temperature. After washing, the membranes were scanned with Odyssey imager (LI-COR Biosciences, Lincoln, NE, USA) and analyzed with the Image Studio software. Gel electrophoresis for mass

spectrometric protein identification were performed in parallel on precast Nu-PAGE 4% to 12% Bis-Tris gradient gels using a 3-(*N*-morpholino)propanesulfonic acid (MOPS) buffer system according to the manufacturer (Invitrogen). As a protein ladder we used SeeBlue Plus2 prestained in this gel system (Life Technologies GmbH). Proteins were either visualized by colloidal Coomassie staining (gel 1) or transferred on PVDF membranes and immunodetected as described above (gel 2).

Protein identification. Gel regions of interest were identified by overlaying images from colloidal Coomassie staining and immunodetection in the Delta 2D image analysis software (Decodon, Greifswald, Germany). Gel bands were excised manually and subjected to automated in-gel digestion with trypsin as described previously (31). Tryptic peptides were dried down in a vacuum centrifuge, redissolved 0.1% trifluoro-acetic acid and spiked with 2.5 fmol/ μ L of yeast enolase1 tryptic digest standard (Waters Corporation, Milford, MA, USA) for quantification purposes (32). Nanoscale reversed-phase UPLC separation of tryptic peptides was performed with a nanoAcquity UPLC system equipped with a Symmetry C18 trap column (5 μ m, 180 μ m \times 20 mm) and a BEH C18 analytical column (1.7 μ m, 75 μ m \times 100 mm) (Waters Corporation). Peptides were separated over 60 min at a flow rate of 300 nL/min with a linear gradient of 1% to 45% mobile phase B (acetonitrile containing 0.1% formic acid) while mobile phase A was water containing 0.1% formic acid. Mass spectrometric analysis of tryptic peptides was performed using a Synapt G2-S quadrupole time-of-flight mass spectrometer equipped with ion mobility option (Waters Corporation). Positive ions in the mass range m/z 50 to 2000 were acquired with a typical resolution of at least 20,000 FWHM (full width at half maximum) and data were lock mass corrected after acquisition. With the aim of increasing the sequence coverage of the identified proteins, analyses were performed in the ion mobility-enhanced

data-independent acquisition mode (33–34) with drift time-specific collision energies (35). For protein identification, continuum LC-MS data were processed and searched using Waters ProteinLynx Global Server version 3.0.2 (36). A custom database was compiled by adding the sequence information for yeast enolase 1 and porcine trypsin to the UniProtKB/Swiss-Prot human proteome (UniProtKB release 2015_06, 20,206 entries) and by appending the reversed sequence of each entry to enable the determination of false discovery rate (FDR). Precursor and fragment ion mass tolerances were automatically determined by PLGS 3.0.2 and were typically below 5 ppm for precursor ions and below 10 ppm (root mean square) for fragment ions. Carbamidomethylation of cysteine was specified as fixed and oxidation of methionine as variable modification. One missed trypsin cleavage was allowed. The FDR for protein identification was set to 1% threshold.

Flow cytometry. UT-7 cells were fixed with 4% Histofix solution (Carl Roth, Karlsruhe, Germany). For EPOR staining, cells were blocked, permeabilized with 5% normal horse serum (NHS) and 0.5% Triton X-100, and incubated with ctEPOR-AB (1:500, Synaptic Systems) and Hoechst (5 µg/mL Invitrogen) or for control only Hoechst for 30 min on ice. After washing, cell suspensions were incubated with Alexa Fluor 488 donkey anti-rabbit (1:250, Life Technologies GmbH) for 30 min on ice, followed by FACS analysis (FACSaria III, BD Biosciences, Heidelberg, Germany).

Immunocytochemistry. Cells were fixed with 4% formaldehyde in PBS for 20 min, permeabilized and blocked in 0.2% Triton X-100 with 10% NHS in PBS for 20 min. After washing with 1% NHS in PBS, cells were incubated overnight at 4°C with the primary AB in 0.2% Triton X-100 with 1% NHS in PBS. The following primary AB were used: rabbit ctEPOR-AB (1:1000, Synaptic Systems), mouse ntEPOR-AB (1:1000, Synaptic Systems), mouse anti-HA (1:500, Covance Inc., Princeton, NJ, USA), mouse anti-GM130

(1:100, BD Biosciences, Heidelberg, Germany), rat anti-NG2 (1:250, gift from Jacqueline Trotter, University of Mainz, Germany), goat anti-human Oct-3/4 (1:40, R&D Systems, Minneapolis, MN, USA). After washing, cells were incubated with the following secondary AB in 0.2% Triton X-100 with 1% NHS in PBS for 1 h at room temperature: donkey anti-rabbit Alexa Fluor 488 and anti-goat Alexa Fluor 488, donkey anti-mouse Alexa Fluor 568, donkey anti-rabbit Alexa Fluor 594 (all 1:500, Life Technologies GmbH) and goat anti-rat Alexa Fluor 488 (1:250, Jackson ImmunoResearch, West Grove, PA, USA). Primary microglia were counterstained with tomato lectin Alexa Fluor 488 (1:250, Vector Laboratories, Burlingame, CA, USA). Cell nuclei were visualized with DAPI dissolved in H₂O (0.01 µg/mL, Sigma-Aldrich). Afterward, the coverslips were dried and mounted with Aqua-Poly/Mount (Polysciences, Warrington, PA, USA). All stainings were scanned by confocal microscopy (TCS SP5-II, Leica, Wetzlar, Germany). Illustration was done using Imaris 7.5.1 (www.bitplane.com [Bitplane AG, Zurich, Switzerland]).

Immunohistochemistry on frozen mouse sections. C57BL/6N mice, 5 wks old, were anesthetized by i.p. injection (0.276 mg/g tribromoethanol, Sigma-Aldrich) and perfused transcardially with 0.9% saline followed by 4% formaldehyde in PBS. Brains were removed, postfixed overnight at 4°C with 4% formaldehyde in PBS and placed in 30% sucrose in PBS for cryoprotection and stored at –20°C. Whole mouse brains were cut into 30 µm-thick coronal sections on a cryostat (Leica). Frozen sections were permeabilized and blocked with 0.5% Triton X-100 and 5% NHS in PBS for 1 h at room temperature. Then, sections were incubated with the following primary AB in 3% NHS, 0.5% Triton X-100 in PBS for 48 h at 4°C: Rabbit ctEPOR-AB (1:200), chicken anti-NeuN (266 006; 1:500), guinea pig anti-GFAP (173 004; 1:500, all Synaptic Systems) and mouse anti-APC (clone CC-1, 1:100, Merck). After washing in PBS, sections were incubated with the following secondary AB in 3% NHS, 0.5% Triton

X-100 in PBS for 1.5 h at room temperature: donkey anti-rabbit Alexa Fluor 594, donkey anti-mouse Alexa Fluor 488 (both 1:500; Life Technologies GmbH), donkey anti-chicken Alexa Fluor 488 (1:250), goat anti-guinea pig Cy5 (1:300, both Jackson ImmunoResearch). Cell nuclei were visualized with DAPI dissolved in H₂O (0.01 µg/mL, Sigma-Aldrich). After washing in PBS, sections were mounted on Super Frost microscopic slides, dried and covered with Aqua-Poly/Mount (Polysciences). All stainings were scanned by confocal microscopy (TCS SP5-II, Leica). Illustration was done using Imaris 7.5.1 (www.bitplane.com [Bitplane AG, Zurich, Switzerland]).

Immunohistochemistry on paraffin-embedded human brain sections. Brain slices of 1–3 µm thickness from formalin-fixed and paraffin-embedded tissue blocks were deparaffinized. Endogenous peroxidases were blocked with 3% H₂O₂ in PBS for 20 min followed by epitope blocking with 0.02% casein in PBS for 15 min. Immunoreaction was performed by incubation with ctEPOR-AB (1:500, Synaptic Systems) overnight at room temperature, followed by the addition of the secondary biotinylated donkey anti-rabbit AB (1:500; Amersham Biosciences, Freiburg, Germany) and an extravidin-peroxidase enzyme complex (1:1000; Sigma-Aldrich), each for 1 h at room temperature. The AB reaction was visualized with the chromogen AEC: 4 mL 4% 3-amino-9-ethylcarbazole (Sigma-Aldrich) in *N,N*-dimethylformamide (Merck) were dissolved in 56 mL 0.1 mol/L sodium-acetate buffer adjusted to pH 5.2 with acetic acid and 1% H₂O₂. The brain slices were counterstained with hemalum. Coverslips were mounted with Aquatex (Merck).

RESULTS

Generation of EPOR-AB

The aim of this work was to generate specific and sensitive EPOR-AB and to investigate EPOR expression in the central nervous system (CNS). Therefore, polyclonal rabbit EPOR-AB and mono-

EPOR IN BRAIN

clonal mouse EPOR-AB were produced and tested. After extensive characterization of a whole panel of AB (data not shown), two highly promising candidates were selected and validated for several research purposes: The polyclonal rabbit EPOR-AB SA7378, directed against the C-terminus (here always called “ctEPOR-AB”) and the monoclonal mouse EPOR-AB 45A3, directed against the N-terminus (here called “ntEPOR-AB”). The present study is mainly built on ctEPOR-AB because of its high specificity and broad spectrum of applications in human and mouse.

Functional EPOR Validation in the Test Systems

As a prerequisite of testing EPOR-AB in the cell lines used here, we functionally validated their EPOR expression. In the EPO-dependent megakaryoblastic leukemia cell line UT-7, incubation with different concentrations of rhEPO led to STAT-5 phosphorylation (Figure 1A). Also, in the erythroleukemia cell line OCIM-1, incubation with rhEPO induced STAT-5 phosphorylation (Figure 1B). UT-7 cells only proliferated and survived in the presence of rhEPO in the medium (Figures 1C, D). In the mouse microglia cell line EOC-20, stably transduced with N-terminally HA-tagged human *EPOR*, rhEPO administration activated MAPK phosphorylation in a concentration-dependent manner (Figure 1E). We also confirmed *EPOR* mRNA expression in all of these cell lines by qPCR (normalized to GAPDH as housekeeping gene, data not shown).

Detection of EPOR/EpoR by Western Blotting

To confirm reliable detection of EPOR by Western blotting, we transfected HEK293 FT cells with different *EPOR* expression vectors. The polyclonal rabbit ctEPOR-AB detected full-length human EPOR and its degradation product specifically while the C-terminally truncated mutant of EPOR was not detected by this AB (Figures 1F, G). Immunoblots of lysates from transduced

EOC-20 cells (N-terminally HA-tagged human EPOR) and respective controls showed specific detection of full-length human EPOR by ctEPOR-AB (Figure 1H). This was validated with an HA immunoblot of the same lysates (Figure 1I). In protein lysates from UT-7 and OCIM-1 cells, ctEPOR-AB detected bands of the same molecular weight (Figure 1J). As shown in Figures 1F and J, in UT-7 cells and HEK293 FT cells (only when transfected with the full length human EPOR) a specific degradation product was additionally detected at ~40kDa by the ctEPOR-AB. This degradation product of EPOR has been described earlier (11). Fixed UT-7 cells were successfully used for flow cytometric analysis after staining with ctEPOR-AB (Figure 1K). EPOR was further recognized by ctEPOR-AB in human placenta and fetal brain extracts (Figure 1L). In addition to human EPOR, ctEPOR-AB detected murine EpoR in transfected HEK293 FT cells, mouse fetal liver and lysates from cultured primary mouse oligodendrocytes (Figure 1M). To validate the specificity of murine EpoR detection, *EpoR* was knocked out in primary astrocytes derived from *EpoR^{-fl/fl}* mice. In fact, ctEPOR-AB recognized a doublet of bands (EPOR with or without N-glycosylation, resulting in a difference of ~3kDa) with a molecular weight of around 65 kDa (Figure 1N, control transduction). Shown is a clear reduction upon expression of Cre-recombinase. The residual expression of the protein is likely due to a slow turnover of EpoR, slow kinetics of Cre-recombination of the floxed *EpoR* allele or incomplete infection of the lentivirus. In any case, Cre-dependent reduction of the signal led us to conclude that ctEPOR-AB specifically detects EpoR. Together, these results indicate specific EPOR/EpoR detection with ctEPOR-AB in human and murine cell and tissue extracts.

EPOR Protein Identification

To test whether the specific band detected in Western blots is indeed EPOR,

we performed IPs from UT-7 lysates and subsequent mass spectrometric protein identification. We used covalently immobilized ctEPOR-AB in combination with nonreducing elution conditions to minimize the masking effect of excess antibody heavy chains, which have an apparent electrophoretic mobility similar to the EPOR. After IP with ctEPOR-AB, eluted proteins from ctEPOR-AB protein-G sepharose beads and respective control beads were separated by SDS-PAGE and visualized by colloidal Coomassie staining or immunoblotting. The overlay of the two gel images (Figure 2A) was used to identify the region of the Coomassie-stained gel potentially containing the EPOR protein. Identical gel regions from ctEPOR-AB IP and the control IP were excised and subjected to tryptic digestion followed by liquid chromatography coupled to mass spectrometry (LC-MS). Against a common background mainly consisting of chaperone proteins, human EPOR protein was detected in eluates from ctEPOR-AB beads, but not from control beads. The identification of 11 EPOR-derived peptides with high mass accuracy at both precursor and fragment ion level resulted in sequence coverage of 22.6% (Figures 2B, C), basically in line with recent LC-MS data on EPOR immunoprecipitates (37). Taken together, our results show that ctEPOR-AB indeed binds specifically to full-length EPOR. Also, in reducing conditions we could effectively elute EPOR after IP (Figure 2D). Noteworthy, we detected the EPOR protein in Western blots between 59 and 68 kDa, depending on the gel system and protein molecular weight marker used (Figures 1, 2A, D; also see Materials and Methods).

EPOR/EpoR Detection by Immunocytochemistry

To validate the specificity of ctEPOR-AB on formaldehyde fixed cells, we stained the same antigen with AB directed against different epitopes (38). In EOC-20 cells transduced with an N-terminally HA-tagged human *EPOR*, anti-HA and ctEPOR-AB double-staining

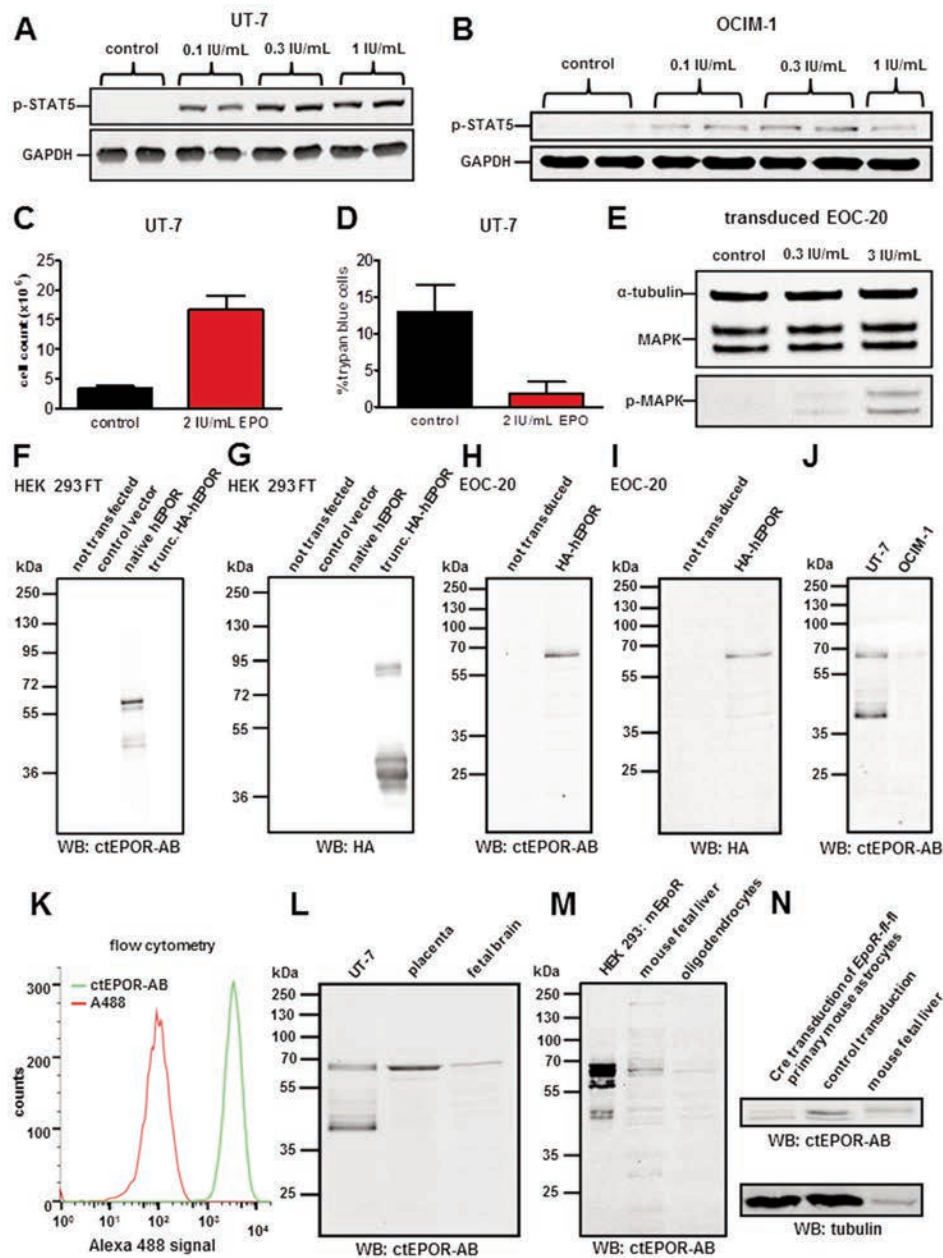


Figure 1. Functional EPOR validation and EPOR/EpoR detection using ctEPOR-AB in Western blots. (A) Incubation of EPO-dependent UT-7 cells (after 12 h of EPO deprivation) for 15 min with increasing EPO concentrations inducing STAT5 phosphorylation. (B) Incubation of OCIM-1 cells for 15 min with increasing EPO concentrations inducing STAT5 phosphorylation. (C) Cell counts of EPO-dependent UT-7 cultures 72 h after seeding in the presence and absence of EPO ($n = 6$, mean \pm SEM; $p < 0.0001$). (D) Cell death in EPO-dependent UT-7 cultures 72 h after seeding in presence and absence of EPO ($n = 5$, mean \pm SEM; $p < 0.03$). (E) Incubation of EOC-20 cells transduced with HA-tagged human EPOR for 10 min with increasing EPO concentrations inducing MAPK phosphorylation. (F) EPOR Western blot using ctEPOR-AB on transfected HEK293 FT cell lysates (truncated HA-EPOR: human EPOR lacking the C-terminus, HA-tag at the N-terminus; control vector: anchored human EPOR without N-terminus and C-terminus). (G) HA Western blot of the same transfected HEK293 FT cell lysates used in (F). (H) EPOR Western blot using ctEPOR-AB on EOC-20 cell lysates transduced with N-terminally HA-tagged human EPOR and respective controls. (I) HA Western blot of the same EOC-20 cell lysates used in (H). (J) EPOR Western blot using ctEPOR-AB on UT-7 and OCIM-1 cell lysates. (K) Flow cytometry of fixed UT-7 cells stained with ctEPOR-AB and Alexa Fluor 488 donkey anti-rabbit secondary AB; as control secondary AB only. (L) EPOR detection in human placenta and human fetal brain using ctEPOR-AB. (M) Detection of murine EpoR in transfected HEK293 FT cells overexpressing murine *EpoR*, mouse fetal liver and mouse primary oligodendrocytes using ctEPOR-AB. (N) Lentivirus-mediated conditional *EpoR* knockout in primary *EpoR-fl/fl* mouse astrocytes; anti- α tubulin as stably expressed comparator.

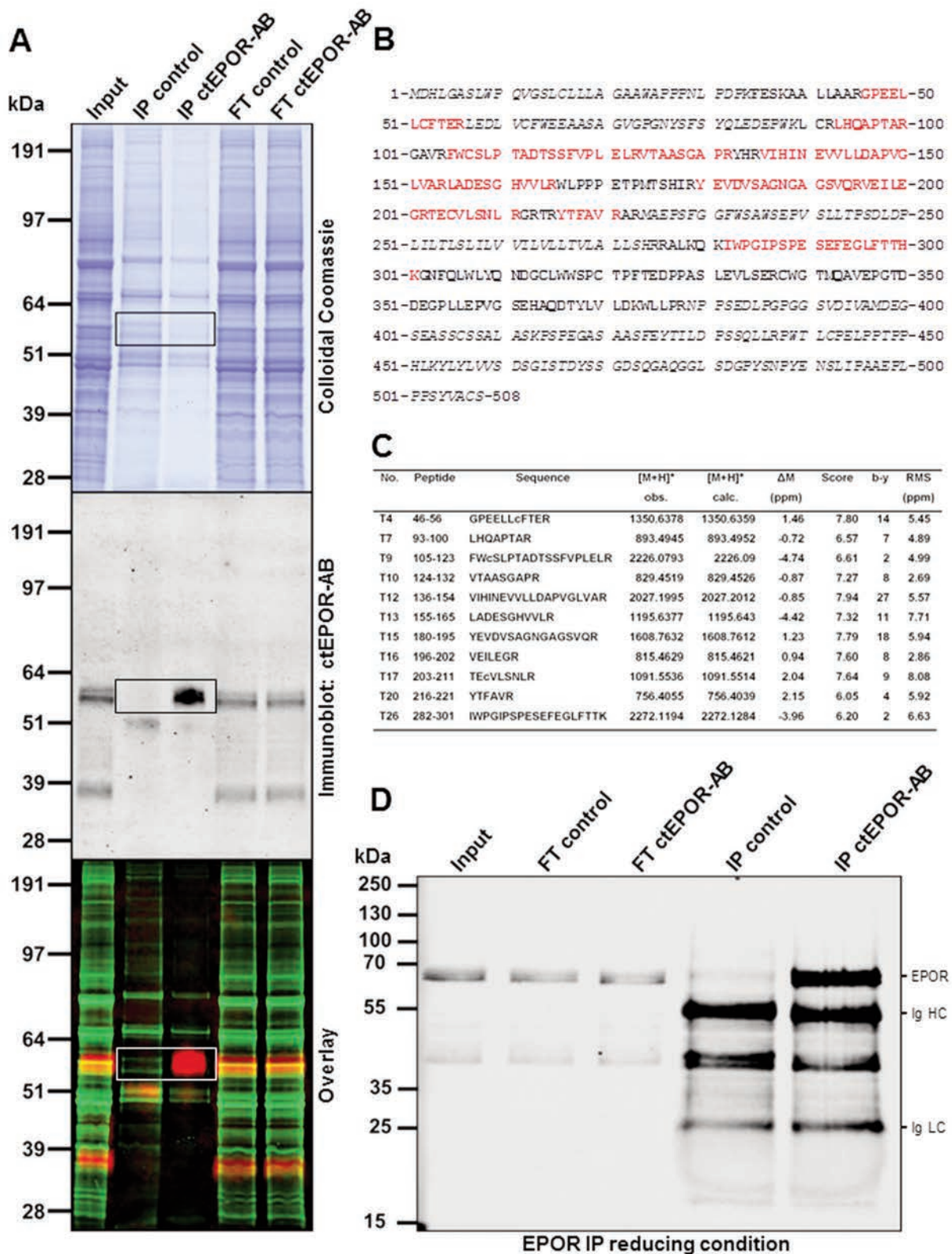


Figure 2. EPOR IP using ctEPOR-AB and protein identification by mass spectrometry.

Continued on next page

Figure 2. Continued. (A) Colloidal Coomassie staining and immunoblot of the same EPOR IP using ctEPOR-AB from UT-7 protein lysates. The overlay was used to determine the region to be excised from the Coomassie gel for subsequent mass spectrometric protein identification (area indicated by rectangles; abbreviations: FT = flow-through, IP = immunoprecipitation). (B) Amino acid sequence of EPOR (UniProtKB/Swiss-Prot P19235). Peptides identified by mass spectrometry are indicated in red. Note that large parts of the EPOR precursor sequence (indicated in italics) cannot be covered in a standard proteomic experiment with tryptic cleavage as they are either modified (amino acids 1–34, signal peptide; 57–89, N-glycosylation site), attached to the transmembrane domain (224–275) or too large (>5 kDa) to reveal useful information by mass spectrometric sequencing (379–453, 454–508). (C) Table with details on peptide identification. Columns show from left to right: numbering of tryptic peptides; numbering of amino acids according to the sequence in B; peptide sequence (c, carboxamidomethyl-Cys); observed and calculated mass of the singly protonated peptide; peptide mass deviation in ppm; PLGS score; number of b–y fragment ions; root mean square fragment mass deviation in ppm. (D) Immunoblot of EPOR IP using ctEPOR-AB from UT-7 lysates. In contrast to the IP used for mass spectrometry, EPOR was eluted from the beads in reducing conditions (Laemmli buffer with β -mercaptoethanol; abbreviations: FT = flow-through, IP = immunoprecipitation, Ig HC = immunoglobulin heavy chains, Ig LC = immunoglobulin light chains). The prominent band at around 40 kDa in both IP conditions has to be an immunoglobulin fragment eluted from the beads in the reducing condition only, since it was not eluted without β -mercaptoethanol (see subpanel 2A immunoblot).

showed almost complete colocalization with most of the signal located intracellularly (Figure 3A). Control EOC-20 cells were negative (Figure 3A). In UT-7 cells, ctEPOR-AB revealed a similar staining pattern (Figure 3B). EPOR staining was colocalized with Golgi staining, indicating detection of a membrane protein (Figure 3C). In addition, ntEPOR-AB and ctEPOR-AB double-stained EPOR in UT-7 cells (Figure 3D). In OCIM-1 cells, ctEPOR-AB also yielded intracellular staining, even though less pronounced compared with UT-7 cells (Figure 3E). Using ctEPOR-AB, we also detected EPOR in human IPS cells (Figure 3F). Moreover, ctEPOR-AB specifically stained HEK293 FT cells transfected with full-length murine *EpoR* (Figure 3G). When tested on cultured primary murine brain cells, ctEPOR-AB stained oligodendrocyte precursor cells (Figure 3H), oligodendrocytes (Figure 3I) and microglia (Figure 3J). These results indicate specific staining of human and mouse EPOR/EpoR by the ctEPOR-AB in cell lines and primary cells.

EpoR Detection in the Brain of Healthy Mice

Using ctEPOR-AB on frozen brain sections of healthy young mice, we found EpoR expression mainly in a subpopulation of cells of the oligodendrocyte lineage (Figure 4A). To get better insight at which stages cells of the oligodendrocyte lineage express EpoR, we labeled oligodendrocyte precursor cells by tamoxifen

injections in NG2-CreERT2 mice (28). At 72 h after the second tamoxifen injection, we identified precursors double-stained for GFP and ctEPOR-AB (GFP+/EpoR+), as well as GFP+/EpoR+ cells with clear morphology (processes with parallel myelin bundles) of already differentiated oligodendrocytes (Figures 4B–B’). Moreover, GFAP+/EpoR+ cells were seen in postnatal neurogenesis areas such as dentate gyrus (Figure 4C) or subventricular zone (data not shown). These results indicate EpoR expression in differentiating oligodendrocytes and stem cells in the adult neurogenic niches of healthy young mice.

EPOR/EpoR Detection in the Injured CNS of Mice

Next, we stereotactically injected EPOR-transduced EOC-20 cells or medium only (stab wound analogue) in the motor cortex of adult mice (Figure 4D). This experiment served two purposes: to recover defined cells that carry human EPOR in brain sections and to confirm injury-induced endogenous *EpoR* expression, since in earlier work, we had proposed upregulation of EPOR upon injury (6). At 24 h after injection of medium only (stab wound), we saw cells with strong ctEPOR-AB signal near the injection site (Figure 4E). Many of these cells were GFAP+/EpoR+ (Figure 4F). On the contralateral site, no GFAP+/EpoR+ cells were seen (Figure 4G). In the motor cortex of mice injected with transduced EOC-20 cells (murine microglia cell line),

double labeling with HA-AB and ctEPOR-AB confirmed specific recovery of these cells in frozen sections of paraformaldehyde-perfused mice. Also in this condition, endogenous cells with high EpoR expression were observed in close proximity of the injection site (Figures 4H–H’). These results confirm the pronounced upregulation of EpoR in cells reacting to injury, provoked here by an experimental stab wound.

Upregulation of EPOR in the Hippocampal Formation of a Patient Suffering from Temporomesial Complex-Focal Epilepsy

Formalin-fixed, paraffin-embedded tissue from a patient who underwent selective unilateral hippocampectomy, was used for immunohistochemical detection of EPOR upregulation under these conditions (Figure 5A). The patient had been suffering from pharmacoresistant complex-focal seizures of temporomesial origin for more than 10 years. Neuropathological analysis of the surgery material revealed hippocampal sclerosis stage Wyler III. EPOR was upregulated in several but not all remaining neurons of CA1 (Figure 5B), of CA4 (Figure 5C) and of the dentate gyrus (Figure 5D), as well as in oligodendrocytes and endothelial cells of capillaries in the adjacent white matter (Figure 5E). Without primary AB, no staining could be detected (Figure 5F). This suggests upregulation of EPOR upon severe chronic distress in different cell types of the human CNS.

EPOR IN BRAIN

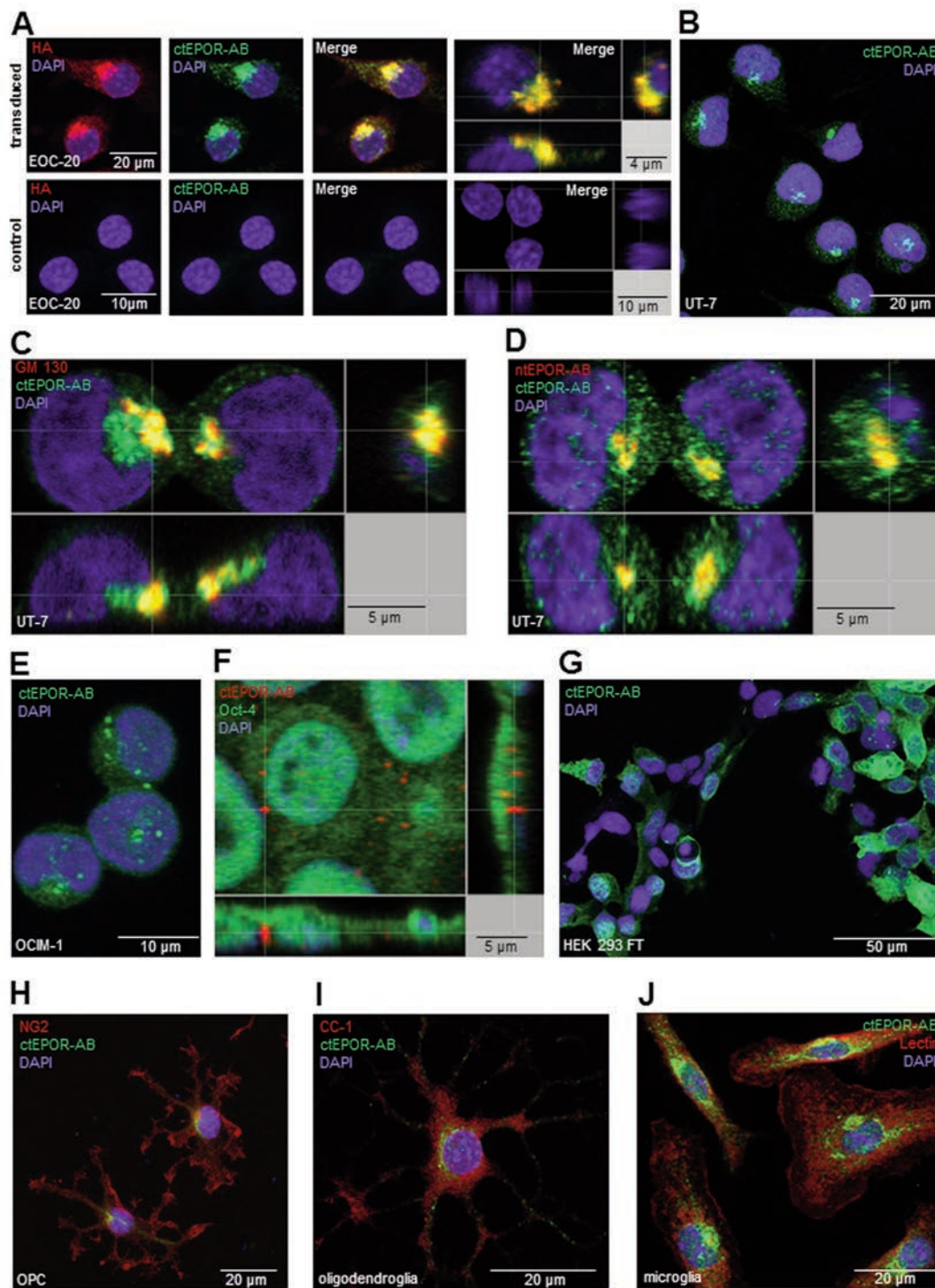


Figure 3. Detection of EPOR by immunocytochemistry: (A) EPOR detection using ctEPOR-AB and monoclonal HA-AB on transduced (N-terminally HA-tagged human EPOR, upper row) and control (lower row) EOC-20 cells. (B) EPOR staining with ctEPOR-AB on EPO-dependent UT-7 cells. (C) Double-immunostaining of UT-7 cells with anti-GM130 AB as marker for the Golgi apparatus and ctEPOR-AB. (D) EPOR double staining of UT-7 cells with nEPOR AB and ctEPOR-AB. (E) EPOR staining with ctEPOR-AB on OCM-1 cells. (F) Distinct EPOR staining in human Oct-4 + IPS cells using ctEPOR-AB. (G) EpoR staining with ctEPOR-AB of HEK293 FT cells transfected with full-length murine *EpoR*. Neighboring nontransfected cells show no immunofluorescence. (H) EpoR and NG2 double-staining with ctEPOR-AB in primary mouse oligodendrocyte precursor cells. (I) EpoR and CC-1 double-staining of primary mouse oligodendrocytes with ctEPOR-AB. (J) Detection of EPOR in primary mouse microglia using ctEPOR-AB and lectin as counterstain.

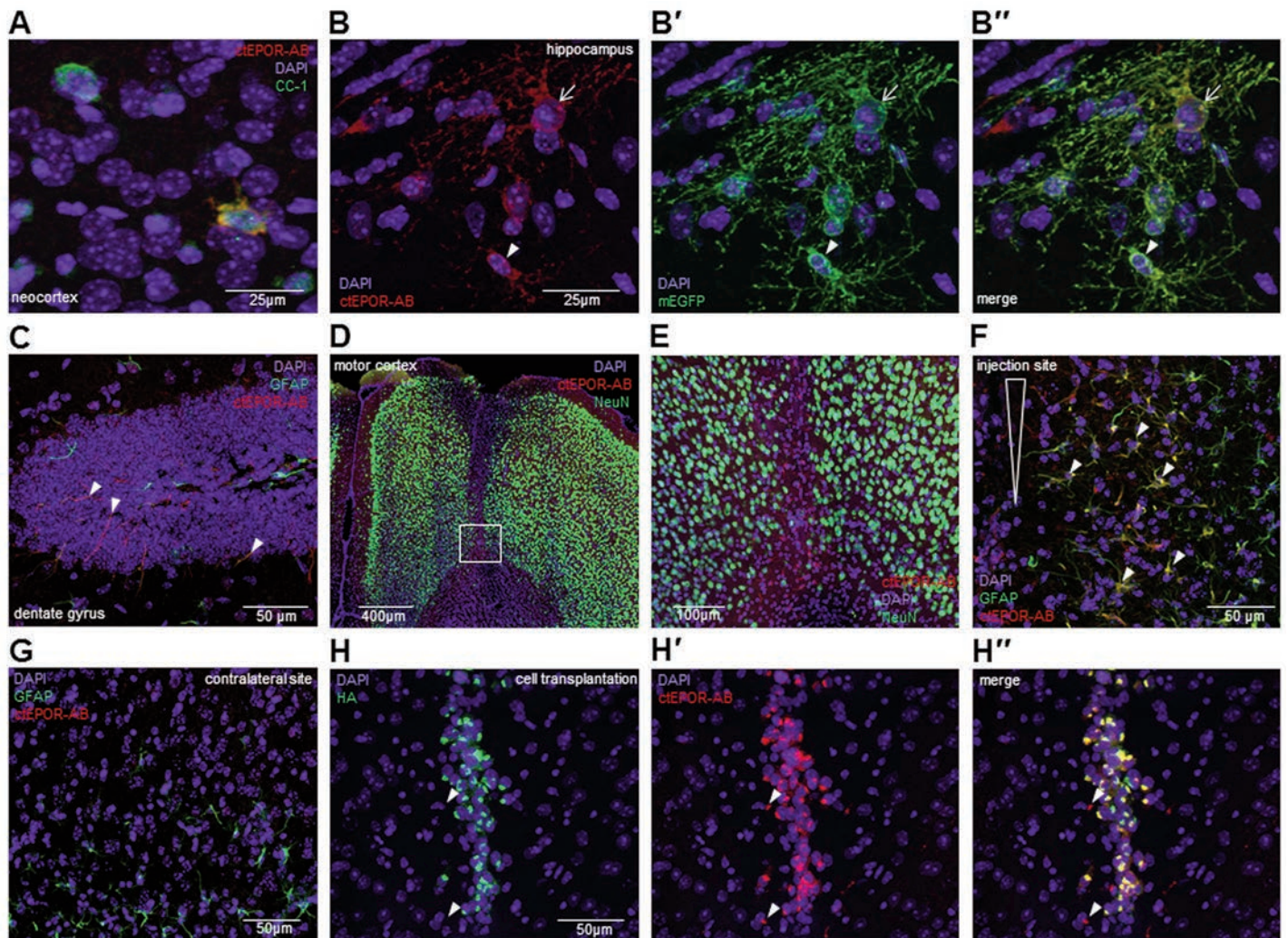


Figure 4. EPOR detection using cEPOR-AB in healthy and injured mouse brain by immunohistochemistry: (A) EpoR staining in a subpopulation of CC-1 positive mature oligodendrocytes in the neocortex of a 5-wk-old healthy mouse. (B, B', B'') EpoR staining in the hippocampus of a 5-wk-old NG2-CreERT2;R26-td-tomato-mEGFP mouse. Some oligodendrocyte precursor cells (arrow head) and newly differentiated oligodendrocytes (arrow) express EpoR. Both cell types are endogenously labeled with membrane-tagged EGFP. (C) EpoR staining of GFAP+ cellular processes in the dentate gyrus of a 5-wk-old mouse (arrow heads). (D) Overview of the injection site in the motor cortex of an 8-wk-old mouse injected with medium only (stab wound analogue). The section was stained for neuronal nuclei with NeuN and for EpoR with cEPOR-AB. (E) Close-up of the white-rectangle region in (D) shows reactive cells with upregulated EpoR expression. (F) Many of the cells at the injection site with upregulated EpoR expression are GFAP+ (arrow heads). (G) Contralateral to the injection site, GFAP+ cells show no EpoR expression at 24 h after lesion. (H, H', H'') Shown is EPOR and HA double-labeling of injected EOC-20 microglial cells transduced with an HA-tagged human EPOR. In addition, HA-negative cells at the injection site show strong EpoR expression (arrow heads).

DISCUSSION

In the present work, we took the challenge requested for a long time by the scientific community (14,17–18) to generate a specific AB for valid detection of EPOR in human and murine cells and tissues, with particular focus on the brain. We present here a highly specific

polyclonal rabbit AB directed against the intracellular C-terminus of the human EPOR. This AB, referred to as “cEPOR-AB,” specifically recognizes EPOR, as proven by mass spectrometry, and has a broad range of documented applications in both human and murine cells and tissues, ranging from Western blotting,

flow cytometry and IP to immunocytochemistry and immunohistochemistry on frozen as well as paraffin-embedded sections. Importantly, by employing this AB, we were able to confirm expression of EPOR in brain cells and its upregulation upon injury (39). Our comprehensive *in vitro* and *in vivo* data clearly reject earlier

EPOR IN BRAIN

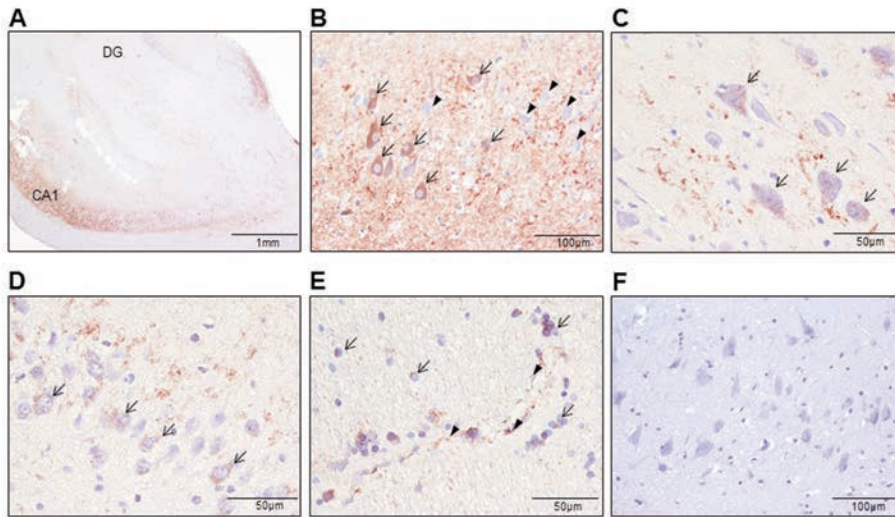


Figure 5. EPOR upregulation in neurons and oligodendrocytes of the hippocampal formation of a patient suffering from temporomesial complex-focal epilepsy as demonstrated by immunohistochemistry using ctEPOR-AB. (A) Overview of the surgical sample stained with ctEPOR-AB. (B) Upregulation of EPOR, visualized by brown color of the AEC-chromogen, in some (arrows) but not all (arrow heads) neurons of the CA1 region. (C) EPOR positive neurons in the CA4 region (arrows). (D) Dentate gyrus neurons (arrows) expressing EPOR. (E) EPOR positive oligodendrocytes (arrows) as well as endothelial cells of capillaries (arrow heads) in the adjacent white matter. (F) No staining was observed when omitting the primary antibody.

claims, solely based on *in vitro* studies, that EPOR expression and EPO function outside the hematopoietic system does not exist (15).

The great need for specific EPOR-AB in the field is also reflected by a very recent study of Drorit Neumann and colleagues (37). This group of authors published specific mouse and rat monoclonal EPOR-AB that detect EPOR expression in human cancer cells and tissues (37). Complementary to this approach and with particular focus on the brain, we have developed a highly specific and sensitive polyclonal rabbit AB, ctEPOR-AB, suitable for applications not only in human but also in murine material. Since the polyclonal nature of this AB has limitations, not only due to the restricted lifetime of a rabbit, we are currently working on further exploitation of the herewith acquired knowledge. Preliminary results of epitope mapping with this polyclonal ctEPOR-AB revealed only few strongly recognized epitopes. These epitopes are presently used

for generating specific mouse monoclonal AB. They will be tested alone or in the form of potentially more sensitive cocktails, with collective properties similar to ctEPOR-AB.

With the examples of EPOR expression in the brain shown here, we confirmed earlier work of our own and of others, which in the past needed additional methods for validation and still left doubts in the scientific community due to the nonspecificity of previous EPOR-AB. For instance, GFAP-positive stem cells in the adult neurogenic niches showed EpoR immunoreactivity here, which is in line with reports demonstrating distinct effects of EPO on adult neural stem cells (40–41). Also, studies identifying EPO as an inducer of oligodendrocyte precursor cell differentiation (42–43) are now further supported by the detection of specific EPOR-binding sites in culture and brain sections. Importantly, the role of the EPO/EPOR system in response to brain injury (5–6) is confirmed with our stab wound approach.

CONCLUSION

On the basis of the novel tool reported here, it will now be possible to investigate the role of EPOR in the intact and injured human and murine brain in more detail. This, in turn, will facilitate the development of EPO for therapeutic use outside the hematopoietic system.

ACKNOWLEDGMENTS

This work was supported by ZIM-BWMI, the Max Planck Society, the Deutsche Forschungsgemeinschaft (Center for Nanoscale Microscopy and Molecular Physiology of the Brain, SFB-TRR43), EXTRABRAIN EU-FP7 and the Niedersachsen-Research Network on Neuroinfectiology (N-RENNT). The EPO-dependent megakaryoblastic leukemia UT-7 cell line was a kind gift from Drorit Neumann of Tel Aviv University in Israel. The pMOWS vector, encoding N-terminally HA-tagged full-length human *EPOR* plus puromycin-resistant cassette, was a kind gift from Ursula Klingmüller, DKFZ, Heidelberg, Germany. The rat anti-NG2 was a kind gift from Jacqueline Trotter, University of Mainz, Germany. We thank Marina Uecker and Thomas Liepold for their expert technical help.

DISCLOSURE

H Stadler is member of the board of and holds stocks in Synaptic Systems GmbH. H Martens, C Erck and T Kolbow are full-time employees of Synaptic Systems GmbH.

REFERENCES

1. Brines M, Cerami A. (2005) Emerging biological roles for erythropoietin in the nervous system. *Nat. Rev. Neurosci.* 6:484–94.
2. Jelkmann W. (2007) Erythropoietin after a century of research: younger than ever. *Eur. J. Haematol.* 78:183–205.
3. Jelkmann W. (2013) Physiology and pharmacology of erythropoietin. *Transfus. Med. Hemother.* 40:302–9.
4. Arcasoy MO. (2008) The non-haematopoietic biological effects of erythropoietin. *Br. J. Haematol.* 141:14–31.
5. Sargin D, Friedrichs H, El-Kordi A, Ehrenreich H. (2010) Erythropoietin as neuroprotective and neu-

- roregenerative treatment strategy: comprehensive overview of 12 years of preclinical and clinical research. *Best Pract. Res. Clin. Anaesthesiol.* 24:573–94.
6. Siren AL, Fasshauer T, Bartels C, Ehrenreich H. (2009) Therapeutic potential of erythropoietin and its structural or functional variants in the nervous system. *Neurotherapeutics.* 6:108–27.
 7. Miskowiak KW, Vinberg M, Harmer CJ, Ehrenreich H, Kessing LV. (2012) Erythropoietin: a candidate treatment for mood symptoms and memory dysfunction in depression. *Psychopharmacology (Berl.)*. 219:687–98.
 8. D'Andrea AD, Lodish HF, Wong GG. (1989) Expression cloning of the murine erythropoietin receptor. *Cell.* 57:277–85.
 9. Jones SS, D'Andrea AD, Haines LL, Wong GG. (1990) Human erythropoietin receptor: cloning, expression, and biologic characterization. *Blood.* 76:31–5.
 10. Noguchi CT, et al. (1991) Cloning of the human erythropoietin receptor gene. *Blood.* 78:2548–56.
 11. Elliott S, et al. (2010) Identification of a sensitive anti-erythropoietin receptor monoclonal antibody allows detection of low levels of EpoR in cells. *J. Immunol. Methods* 352:126–39.
 12. Noguchi CT, Wang L, Rogers HM, Teng R, Jia Y. (2008) Survival and proliferative roles of erythropoietin beyond the erythroid lineage. *Expert Rev. Mol. Med.* 10:e36.
 13. Siren AL, et al. (2001) Erythropoietin prevents neuronal apoptosis after cerebral ischemia and metabolic stress. *Proc. Natl. Acad. Sci. U. S. A.* 98:4044–9.
 14. Elliott S, et al. (2006) Anti-Epo receptor antibodies do not predict Epo receptor expression. *Blood.* 107:1892–5.
 15. Sinclair AM, et al. (2010) Functional erythropoietin receptor is undetectable in endothelial, cardiac, neuronal, and renal cells. *Blood.* 115:4264–72.
 16. Ghezzi P, et al. (2010) Erythropoietin: not just about erythropoiesis. *Lancet.* 375:2142.
 17. Kirkeby A, van Beek J, Nielsen J, Leist M, Helboe L. (2007) Functional and immunochemical characterisation of different antibodies against the erythropoietin receptor. *J. Neurosci. Methods.* 164:50–8.
 18. Brown WM, et al. (2007) Erythropoietin receptor expression in non-small cell lung carcinoma: a question of antibody specificity. *Stem Cells.* 25:718–22.
 19. Yu X, et al. (2002) Erythropoietin receptor signalling is required for normal brain development. *Development.* 129:505–16.
 20. Tsai PT, et al. (2006) A critical role of erythropoietin receptor in neurogenesis and post-stroke recovery. *J. Neurosci.* 26:1269–74.
 21. Ehrenreich H, et al. (2005) A hematopoietic growth factor, thrombopoietin, has a proapoptotic role in the brain. *Proc. Natl. Acad. Sci. U. S. A.* 102:862–7.
 22. Digicaylioglu M, et al. (1995) Localization of specific erythropoietin binding sites in defined areas of the mouse brain. *Proc. Natl. Acad. Sci. U. S. A.* 92:3717–20.
 23. Ehrenreich H, et al. (2004) Erythropoietin: a candidate compound for neuroprotection in schizophrenia. *Mol. Psychiatry.* 9:42–54.
 24. Mitkovski M, et al. (2015) Erythropoietin dampens injury-induced microglial motility. *J. Cereb. Blood Flow Metab.* 35:1233–6.
 25. Aggarwal S, et al. (2013) Myelin membrane assembly is driven by a phase transition of myelin basic proteins into a cohesive protein meshwork. *PLoS Biol.* 11:e1001577.
 26. Pyott SJ, Rosenmund C. (2002) The effects of temperature on vesicular supply and release in autaptic cultures of rat and mouse hippocampal neurons. *J. Physiol.* 539:523–5.
 27. Becker V, et al. (2010) Covering a broad dynamic range: information processing at the erythropoietin receptor. *Science.* 328:1404–8.
 28. Huang W, et al. (2014) Novel NG2-CreERT2 knock-in mice demonstrate heterogeneous differentiation potential of NG2 glia during development. *Glia.* 62:896–913.
 29. Muzumdar MD, Tasic B, Miyamichi K, Li L, Luo L. (2007) A global double-fluorescent Cre reporter mouse. *Genesis.* 45:593–605.
 30. Wessel D, Flugge UI. (1984) A method for the quantitative recovery of protein in dilute solution in the presence of detergents and lipids. *Anal. Biochem.* 138:141–3.
 31. Schmidt C, Hesse D, Raabe M, Urlaub H, Jahn O. (2013) An automated in-gel digestion/iTRAQ-labeling workflow for robust quantification of gel-separated proteins. *Proteomics.* 13:1417–22.
 32. Silva JC, Gorenstein MV, Li GZ, Vissers JP, Geromanos SJ. (2006) Absolute quantification of proteins by LCMSE: a virtue of parallel MS acquisition. *Mol. Cell Proteomics.* 5:144–56.
 33. Silva JC, et al. (2005) Quantitative proteomic analysis by accurate mass retention time pairs. *Anal. Chem.* 77:2187–200.
 34. Geromanos SJ, Hughes C, Ciavarini S, Vissers JP, Langridge JI. (2012) Using ion purity scores for enhancing quantitative accuracy and precision in complex proteomics samples. *Anal. Bioanal. Chem.* 404:1127–39.
 35. Distler U, et al. (2014) Drift time-specific collision energies enable deep-coverage data-independent acquisition proteomics. *Nat. Methods.* 11:167–70.
 36. Li GZ, et al. (2009) Database searching and accounting of multiplexed precursor and product ion spectra from the data independent analysis of simple and complex peptide mixtures. *Proteomics.* 9:1696–719.
 37. Maxwell P, et al. (2015) Novel antibodies directed against the human erythropoietin receptor: creating a basis for clinical implementation. *Br. J. Haematol.* 168:429–42.
 38. Saper CB. (2005) An open letter to our readers on the use of antibodies. *J. Comp. Neurol.* 493:477–8.
 39. Siren AL, et al. (2001) Erythropoietin and erythropoietin receptor in human ischemic/hypoxic brain. *Acta Neuropathol.* 101:271–6.
 40. Shingo T, Sorokan ST, Shimazaki T, Weiss S. (2001) Erythropoietin regulates the in vitro and in vivo production of neuronal progenitors by mammalian forebrain neural stem cells. *J. Neurosci.* 21:9733–43.
 41. Ransome MI, Turnley AM. (2007) Systemically delivered Erythropoietin transiently enhances adult hippocampal neurogenesis. *J. Neurochem.* 102:1953–65.
 42. Jantzie LL, Miller RH, Robinson S. (2013) Erythropoietin signaling promotes oligodendrocyte development following prenatal systemic hypoxic-ischemic brain injury. *Pediatr. Res.* 74:658–67.
 43. Kako E, et al. (2012) Subventricular zone-derived oligodendrogenesis in injured neonatal white matter in mice enhanced by a nonerythropoietic erythropoietin derivative. *Stem Cells.* 30:2234–47.

Cite this article as: Ott C, et al. (2015) Widespread expression of erythropoietin receptor in brain and its induction by injury. *Mol. Med.* 21:803–15.

Manuscript under revision**Manuscript 1**

Oliveira B*, Mitjans M*, Nitsche MA, Kuo M-F and Ehrenreich H. *Excitation-inhibition dysbalance as predictor of autistic phenotypes. Under revision*

*Authors with equal contribution

Personal contribution: I actively participated in outlining and writing the manuscript, together with my supervisor. I was significantly involved in the data analysis, prepared the figures and figure legends and contributed to the overall preparation of the manuscript. Additionally, I was responsible for the submission phase and will actively participate in the revision process.

Excitation-inhibition dysbalance as predictor of autistic phenotypes

Bárbara Oliveira, MSc^{1§}, Marina Mitjans, PhD^{1§}, Michael A. Nitsche, MD²,
Min-Fang Kuo, MD, PhD^{2*} and Hannelore Ehrenreich, MD, DVM^{1*}

§Equal contributing first authors

**Equal contributing last authors*

¹Clinical Neuroscience, Max Planck Institute of Experimental Medicine, Göttingen, Germany

²Department of Psychology and Neurosciences, Leibniz Research Centre for Working
Environment and Human Factors, Dortmund, Germany

Word count: Abstract 250; Text body 1204; 1 Figure; 1 Table

Running head: E/I dysbalance and autistic traits

Key words: TMS, transcranial magnetic stimulation, behavioral continua, severity rating, *PAUSS*, autistic traits

Corresponding Author:

Prof. Hannelore Ehrenreich, MD, DVM
Clinical Neuroscience
Max Planck Institute of Experimental Medicine
Hermann-Rein-Str.3
37075 Göttingen, GERMANY
Tel: 49-551-3899 628
E-Mail: ehrenreich@em.mpg.de

Abstract

Autistic traits are normally distributed across health and disease, with autism spectrum disorders (ASD) at the extreme end. As we learned from mutations of synaptic or synapse regulating genes, leading to monogenetic forms of autism, the heterogeneous etiologies of ASD converge at the synapse. They result in a mild synaptic dysfunction as the final common pathway, also addressed as synaptopathy. Based on genetic rodent models and EEG/MEG findings in autists, a neuronal excitation-inhibition dysbalance is considered autism-pathognomonic. We hypothesized that this objectively measurable consequence is not restricted to the diagnosis of ASD but transcends disease borders and is of quantitative rather than qualitative nature. For proof-of-principle, we conducted a transcranial magnetic stimulation (TMS) study, monitoring corticospinal excitability and intracortical inhibition of the motor cortex. Employing the GRAS data collection of N>1800 deep-phenotyped schizophrenic subjects, we had the chance to select for this study N=20 perfectly matched men. They differed only by autistic trait severity, as assessed using *PANSS autism severity score (PAUSS)*, capturing the continuum of autistic behaviors. Applying TMS to these men, we provide intriguing hints of a positive correlation of autistic phenotype severity with functional cortical correlates, mainly alterations in GABAergic system and ion channels. This 'dose-response relationship' between severity of autistic traits and excitation-inhibition ratio in non-ASD subjects underlines the biological basis of this continuous trait. Based on these data, TMS may serve as new *add-on* biomarker of autistic traits across disease groups. Moreover, potential common treatment strategies targeting the excitation-inhibition dysbalance in humans may now evolve.

Introduction

Most neuropsychiatric disease-relevant behavioral phenotypes are continua, with a certain severity threshold defining the starting point of a clinical diagnosis. As typical example, autistic traits are normally distributed across health and disease, including at the extreme end autism spectrum disorders (ASD). Shared features are variably pronounced deficits in social communication, reading of social signals, theory-of-mind abilities, and cognitive flexibility, typically together with restricted interests, repetitive behaviors and prominent routines (Mitjans et al., 2017; Stepniak et al., 2015).

Causes of autistic phenotypes likely converge at the synapse, as indicated by mutations of genes influencing synaptic function, and are reflected by circuit-level disturbances, aberrant synaptic plasticity, and a virtually autism-pathognomonic neuronal excitation-inhibition dysbalance (Mitjans et al., 2017; Mullins et al., 2016; Nelson and Valakh, 2015; Ramocki and Zoghbi, 2008; Sudhof, 2008; Uhlhaas and Singer, 2006; Uzunova et al., 2016). This dysbalance was consolidated experimentally using construct-valid genetic rodent models and has likewise been suspected in humans, mainly based on EEG and MEG findings, including the frequently seen predisposition to epileptic seizures. Importantly, not only mutations, but normal genetic variants contribute to the manifestation of autistic traits as indicated by genome-wide association studies (GWAS), but even more so by phenotype-based genetic association studies (PGAS), finding an accumulation of 'unfortunate' normal variants associated with increasing severity of autistic phenotypes (Ehrenreich et al., 2016; Stepniak et al., 2015).

We hypothesize that measurable consequences of the heterogeneous causes underlying autistic traits, which characterize the final common pathway to the phenotype, are of quantitative rather than qualitative nature. Thus, we wondered whether very well-matched individuals, differing only with regard to the clinical severity of autistic features, would show respective differences in excitation-inhibition as an overarching functional consequence of diverse causalities. To address this question in humans, we applied transcranial magnetic stimulation (TMS) (Nitsche et al., 2005). TMS, presently discussed as ASD biomarker tool, allows noninvasive focal brain stimulation, where localized intracranial electrical currents, large enough to depolarize a small population of neurons, are generated by extracranial magnetic fields (Oberman et al., 2016). Translating this paradigm to the autistic continuum, we provide intriguing

evidence of a connection between phenotype severity and functional cortical correlates in humans.

Materials and methods

Subjects

For proof-of-principle, carefully selected male schizophrenic subjects (N=20) of the GRAS (Göttingen Research Association for Schizophrenia) data collection agreed to participate in a TMS study, approved by the Ethical Committee of the University of Göttingen, Germany. Subjects were matched for age, handedness and medication and asked not to smoke or drink coffee prior to TMS (Table1). For comparing deeply phenotyped schizophrenic individuals, based on autistic trait severity, we used the *PANSS autism severity score (PAUSS)*, capturing the continuum of autistic behaviors.¹²

Transcranial magnetic stimulation (TMS) protocol

Motor cortex excitability measures

Motor cortical excitability was monitored by generating motor evoked potentials (MEP) via TMS applied with a figure-of-eight coil (diameter of one winding: 70mm; peak magnetic field: 2.2Tesla) connected to a Magstim-200 magnetic stimulator (Magstim, Whiteland, Dyfed, UK). The coil was held with the handle pointing backwards and laterally at 45°. Surface electromyography (EMG) was recorded from the right first dorsal interosseous (FDI) muscle by Ag/AgCl electrodes in a belly tendon montage. The signals were filtered with a low-pass filter of 2.0kHz, then digitized at an analogue-to-digital rate of 5kHz and further relayed into a laboratory computer using the Signal software and CED1401 hardware (Cambridge Electronic Design, Cambridge, UK).

Motor threshold

The resting motor threshold (RMT) was defined as the minimum TMS intensity which elicited a peak-to-peak MEP amplitude of 50 μ V or larger in the resting FDI in at least 3 out of 6 measurements. The active motor threshold (AMT) was the minimum intensity eliciting a MEP of a superior size compared to moderate spontaneous muscular background activity (~15% of the maximum muscle strength) in at least 3 out of 6 trials.

Input-output (I/O) curve

The recruitment curve was generated with TMS-intensities of 100, 110, 130, and 150% RMT; 15 stimuli were obtained for each intensity. TMS stimuli were applied with a frequency of 0.25Hz.

Intracortical inhibition and facilitation

Intracortical inhibition and facilitation were obtained by a paired-pulse TMS protocol (Kujirai et al., 1993), with a test pulse eliciting MEP amplitude of about 1mV. MEP was preceded by a subthreshold (70% AMT) conditioning stimulus with inter-stimuli-intervals (ISI) of 2, 3, 5, 10, and 15ms. The first three ISIs monitor intracortical inhibition and the last two monitor facilitation. The protocol consisted of 15 blocks, where each block contained the 5 pairs of different ISIs together with a single test pulse applied in randomized order. TMS stimuli were applied with an interval of 4 seconds.

Experimental procedures

Subjects were seated in a reclining chair with head and arm rests to guarantee optimal relaxation. After mounting the EMG electrodes, the TMS coil position over the left motor cortex resulting consistently in the largest MEP in the right FDI was identified and marked to keep constant coil position throughout the course of the experiment. The intensity of the TMS stimulus was adjusted to elicit MEPs with a peak-to-peak amplitude of average 1 mV. RMT and AMT were then determined accordingly, followed by a 5-min break to allow muscle relaxation after the AMT determination procedure. Afterwards, the I/O curve, and intracortical inhibition/facilitation were obtained as outlined above. The duration of this experimental block was about 60 minutes per individual.

Results

RMT and AMT did not differ between groups (low *PAUSS*: 42.50 ± 5.33 versus high *PAUSS*: 44.00 ± 9.16 ; $p=0.909$ and low *PAUSS*: 32.90 ± 4.43 versus high *PAUSS*: 34.90 ± 7.38 ; $p=0.622$, respectively; Mann-Whitney test, two-tailed). Individual excitation and inhibition curves are presented in Fig 1A-B. The group of schizophrenic men with more severe autistic features ($PAUSS \geq 20$) showed higher cortico-spinal excitability and higher intracortical inhibition compared to the group with low autistic features ($PAUSS < 20$). In contrast, intracortical facilitation did not differ between groups (Fig 1A-

B; Table1). Importantly, the ratio between excitation and inhibition (each calculated as area under the curve for each individual) correlated positively with the severity of autistic traits ($r=0.511$, $p=0.021$; Pearson's Correlation, two-tailed) (Fig 1C).

Discussion

Even though only 20 male schizophrenic subjects with different *PAUSS* scores were included, we obtained a surprisingly clear separation of TMS-derived individual excitation and inhibition readouts based on *PAUSS* and, importantly, a positive correlation of the E/I ratio with *PAUSS*. These findings provide for the first time a 'dose-response relationship' between severity of autistic traits and degree of excitation-inhibition dysbalance. The clarity of these results is certainly owed to an optimal matching of deep-phenotyped individuals regarding all main clinical characteristics, based on selection from the large GRAS data collection, which allows widely excluding potential confounders (Oberman et al., 2016).

We interpret these data as indication of effects on GABAergic transmission and ion channels, and no clear effect on glutamate, since intracortical inhibition is primarily driven by GABA (Paulus et al., 2008). The enhanced corticospinal excitability shown in the group with high autistic features could principally have been driven by an impact on ion channels, but also by glutamate, especially for the high TMS intensities (Paulus et al., 2008). Since glutamate-driven intracortical facilitation did, however, not differ between groups, a predominant impact on ion channels is more probable. Taken together, the results of this study support the concept of a disturbed excitation-inhibition balance in subjects with autistic features, which is based on altered GABAergic and ion channel functions.

These findings support the disease-independent pathophysiological continuum of autistic traits and the etiology-independent final common pathway leading to an autistic phenotype. Not only the diagnostic use of TMS as a new add-on biomarker of autistic traits across disease groups, but also potential common treatment strategies targeting the E/I ratio in humans should now be encouraged.

Acknowledgements

This work was supported by the Max Planck Society, the Max Planck Förderstiftung, the DFG (CNMPB), EXTRABRAIN EU-FP7, the Niedersachsen-Research Network on Neuroinfectiology (N-RENNT) and EU-AIMS. The research of EU-AIMS receives support from the Innovative Medicines Initiative Joint Undertaking under grant agreement n°115300, resources of which are composed of financial contribution from the European Union's Seventh Framework Programme (FP7/2007-2013), from the EFPIA companies, and from Autism Speaks. The authors thank all subjects for participating in the study, and the many colleagues who have contributed over the past decade to the extended GRAS data collection.

AUTHOR CONTRIBUTIONS

Concept and design of the study: HE, MFK

Data acquisition and analysis: BO, MM, MFK, MAN, HE

Drafting manuscript and figures: HE, BO, MM, with help of all authors

All authors read and approved the final version of the manuscript.

Competing interests

The authors declare no conflict of interest.

References

- Ehrenreich, H., Mitjans, M., Van der Auwera, S., Centeno, T.P., Begemann, M., Grabe, H.J., Bonn, S., Nave, K.A., 2016. OTTO: a new strategy to extract mental disease-relevant combinations of GWAS hits from individuals. *Mol Psychiatry*.
- Kujirai, T., Caramia, M.D., Rothwell, J.C., Day, B.L., Thompson, P.D., Ferbert, A., Wroe, S., Asselman, P., Marsden, C.D., 1993. Corticocortical inhibition in human motor cortex. *J Physiol* 471, 501-519.
- Mitjans, M., Begemann, M., Ju, A., Dere, E., Wustefeld, L., Hofer, S., Hassouna, I., Balkenhol, J., Oliveira, B., van der Auwera, S., Tammer, R., Hammerschmidt, K., Volzke, H., Homuth, G., Cecconi, F., Chowdhury, K., Grabe, H., Frahm, J., Boretius, S., Dandekar, T., Ehrenreich, H., 2017. Sexual dimorphism of AMBRA1-related autistic features in human and mouse. *Transl Psychiatry* 7(10), e1247.
- Mullins, C., Fishell, G., Tsien, R.W., 2016. Unifying Views of Autism Spectrum Disorders: A Consideration of Autoregulatory Feedback Loops. *Neuron* 89(6), 1131-1156.
- Nelson, S.B., Valakh, V., 2015. Excitatory/Inhibitory Balance and Circuit Homeostasis in Autism Spectrum Disorders. *Neuron* 87(4), 684-698.
- Nitsche, M.A., Seeber, A., Frommann, K., Klein, C.C., Rochford, C., Nitsche, M.S., Fricke, K., Liebetanz, D., Lang, N., Antal, A., Paulus, W., Tergau, F., 2005. Modulating parameters of excitability during and after transcranial direct current stimulation of the human motor cortex. *J Physiol* 568(Pt 1), 291-303.
- Oberman, L.M., Enticott, P.G., Casanova, M.F., Rotenberg, A., Pascual-Leone, A., McCracken, J.T., Group, T.M.S.i.A.C., 2016. Transcranial magnetic stimulation in autism spectrum disorder: Challenges, promise, and roadmap for future research. *Autism Res* 9(2), 184-203.
- Paulus, W., Classen, J., Cohen, L.G., Large, C.H., Di Lazzaro, V., Nitsche, M., Pascual-Leone, A., Rosenow, F., Rothwell, J.C., Ziemann, U., 2008. State of the art: Pharmacologic effects on cortical excitability measures tested by transcranial magnetic stimulation. *Brain Stimul* 1(3), 151-163.
- Ramocki, M.B., Zoghbi, H.Y., 2008. Failure of neuronal homeostasis results in common neuropsychiatric phenotypes. *Nature* 455(7215), 912-918.
- Stepniak, B., Kastner, A., Poggi, G., Mitjans, M., Begemann, M., Hartmann, A., Van der Auwera, S., Sananbenesi, F., Krueger-Burg, D., Matuszko, G., Brosi, C., Homuth, G., Volzke, H., Bensele, F., Bagni, C., Fischer, U., Dityatev, A., Grabe, H.J., Rujescu, D., Fischer, A., Ehrenreich, H., 2015. Accumulated common variants in the broader fragile X gene family modulate autistic phenotypes. *EMBO Mol Med* 7(12), 1565-1579.
- Sudhof, T.C., 2008. Neuroligins and neurexins link synaptic function to cognitive disease. *Nature* 455(7215), 903-911.
- Uhlhaas, P.J., Singer, W., 2006. Neural synchrony in brain disorders: relevance for cognitive dysfunctions and pathophysiology. *Neuron* 52(1), 155-168.
- Uzunova, G., Pallanti, S., Hollander, E., 2016. Excitatory/inhibitory imbalance in autism spectrum disorders: Implications for interventions and therapeutics. *World J Biol Psychiatry* 17(3), 174-186.

Figure Legend

Excitation and inhibition dysbalance dependent on autistic phenotype severity

(A) Input-output curves as a readout of cortico-spinal excitability are presented for each individual, obtained with TMS-intensities of 100, 110, 130, and 150% RMT (15 stimuli for each intensity with a frequency of 0.25Hz). The severity of autistic traits determined by *PAUSS* is dichotomously classified for illustration in the figure. **(B)** Individual intracortical inhibition curves presented analogously to (A). Intracortical inhibition was obtained by a paired-pulse TMS protocol, MEP was preceded by a subthreshold (70% AMT) conditioning stimulus with ISI of 2, 3 and 5ms. **(C)** Individual E or I values were determined as areas under the curve (of individual data shown in A and B) and used to calculate the individual excitation/inhibition (E/I) ratios. Dysbalance is visualized in individuals with higher *PAUSS* scores. TMS, Transcranial Magnetic Stimulation; RMT, Resting Motor Threshold; MEP, Motor-Evoked Potential; AMT, Active Motor Threshold; ISI, Inter-Stimuli-Intervals; *PAUSS*, *PANSS autism severity score* (Mitjans et al., 2017; Stepniak et al., 2015); AU, Arbitrary Units; Pearson's correlation, two-tailed p-value (SPSS version-17.0 IBM-Deutschland GmbH, Munich, Germany).

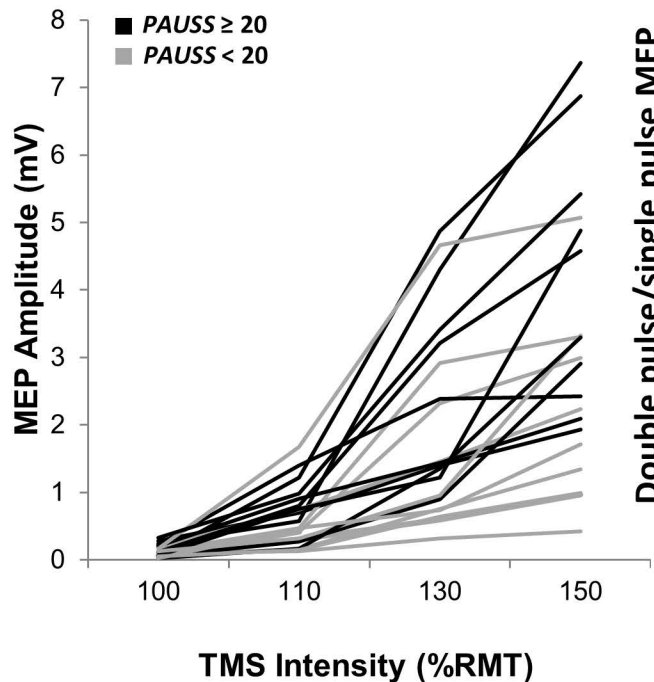
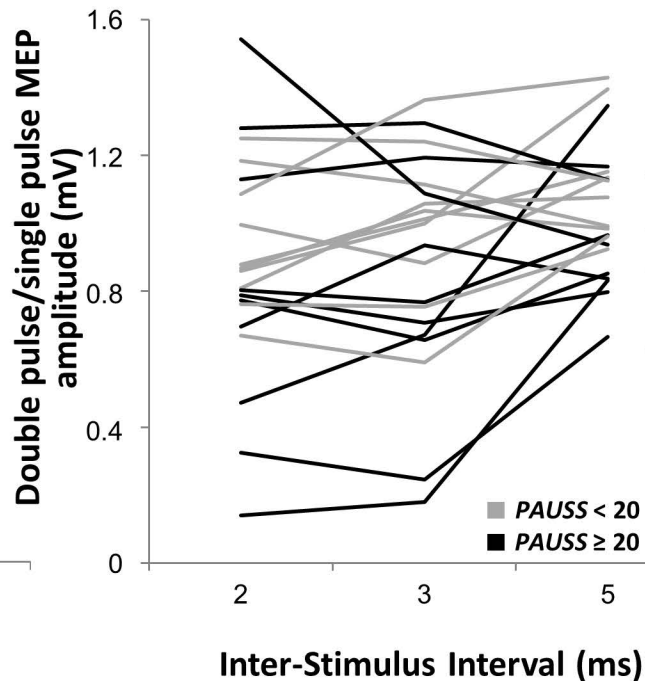
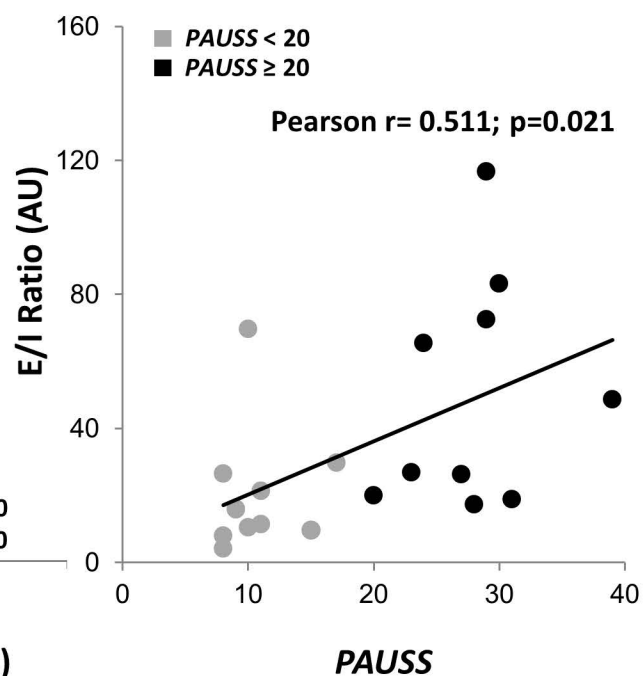
A**Excitation (E)****B****Inhibition (I)****C****E/I Dysbalance**

Table 1: SUBJECT CHARACTERIZATION

Subject ID*	PAUSS	Age at TMS (y)	Type of medication	CPZE	Smoker (cig/day)	Age of disease onset (y)	Duration of disease (y)	Premorbid IQ (MWTB)	Excitation (AUC, AU)	Inhibition (AUC, AU)	Facilitation (AUC, AU)
Low PAUSS (<20)											
COFO	8	37	Atypical	600	Yes (40)	20	16	143	82.91	3.11	5.42
SEKO	8	31	Atypical	200	No	22	10	95	26.36	3.26	5.86
JOKR	8	38	Atypical	4	Yes (20)	32	6	85	12.99	3.07	6.62
JORI	9	29	Atypical	450	Yes (20)	17	12	107	57.68	3.61	9.48
CLLA	10	29	Atypical	375	No	23	6	130	31.08	2.96	5.96
KARI	10	31	Atypical	133	Yes (20)	22	9	112	169.86	2.44	3.65
BEZI	11	32	Atypical	1200	Yes (20)	19	13	92	63.48	2.97	5.55
MAMA	11	43	Atypical & typical	163	Yes (20)	31	12	92	25.01	2.18	6.12
SEBO	15	32	Atypical & typical	1956	Yes (15)	18	14	97	38.92	4.02	7.16
MIBO	17	31	No neuroleptics	-	Yes (20)	14	16	97	99.07	3.33	4.57
Mean	10.70	33.20	-	564.53	-	21.69	11.51	105.00	60.73	3.09	6.03
±SD	±3.06	±4.45	-	±630.97	-	±5.58	±3.64	±18.52	±47.12	±0.53	±1.56
High PAUSS (≥20)											
MASC	20	28	Atypical	150	No	19	8	78	51.36	2.59	5.28
RERE	23	55	Atypical	67	Yes (2)	49	6	124	94.11	3.52	5.16
JURU	24	30	No neuroleptics	-	No	17	12	97	169.55	2.59	5.52
HAKA	27	30	Atypical & typical	1631	Yes (20)	18	12	91	59.10	2.25	4.83
GEFA	28	33	Atypical & typical	2491	Yes (20)	21	13	100	64.26	3.71	4.67
TYBA	29	31	Atypical	1067	Yes (20)	18	13	94	84.87	1.17	3.79
THFI	29	45	Atypical & typical	1110	Yes (40)	36	9	100	138.75	1.19	6.64
BJWA	30	35	Atypical	267	Yes (26)	23	12	92	184.80	2.22	5.70
MASI	31	32	Typical	168	No	25	7	93	62.50	3.34	7.73
MAGU	39	53	Atypical	300	No	19	34	130	122.49	2.52	4.31
Mean	28.00	37.26	-	805.55	-	24.62	12.64	99.90	103.18	2.51	5.36
±SD	±5.19	±10.23	-	±837.51	-	±10.33	±7.97	±15.63	±48.21	±0.87	±1.14
Low versus high PAUSS p-values	0.00001°	0.529°	0.620#	0.730°	0.628#	0.684°	0.684°	0.579°	0.031§	0.044§	0.143§

Notes: *Subject ID scrambled; °Mann-Whitney U-Test (two-tailed); #Fisher's exact test (two-tailed); §Student t-test (one-tailed); PAUSS, PANSS autism severity score,^{1,2} TMS, Transcranial Magnetic Stimulation; MWTB, Mehrfachwahl-Intelligenztest-B; CPZE, Chlorpromazine Equivalent; AUC, Area Under the Curve; AU, Arbitrary Units; cig, cigarettes; y, year

List of abbreviations

<i>Abbreviation</i>	<i>Extended name</i>
AMPA	α -amino-3-hydroxy-5-methyl-4-isoxazolepropionic acid
APC	Antigen Presenting Cells
ApoE	Apolipoprotein E
ASD	Autism Spectrum Disorders
BBB	Blood Brain Barrier
BCR	B Cell Receptor
BMP	Bone Morphogenic Protein
Caspr2	Anti-Contactin-Associated Protein-like 2
CCL-2	CC-chemokine Ligand
c-MYC	MYC Proto-oncogene
CNS	Central Nervous System
CSF	Cerebrospinal Fluid
CTD	Carboxy-Terminal Domain
CXCR4	C-X-C Chemokine Receptor Type 4
DAPT	N-[N-3,5-Difluorophenacetyl-L-alanyl]-S-phenylglycine t-butyl ester
DCX⁺	Doublecortin
DNA	Deoxyribonucleic Acid
EMX1	Empty Spiracles Homeobox 1
E/I	Excitation/Inhibition
Fc	Fragment Crystallisable
FGF2	Fibroblast Growth Factor 2
FGF8	Fibroblast Growth Factor 8
FITC	Fluorescein Isothiocyanate
FoxA2	Forkhead Box Protein A2
GABA	γ -Aminobutyric Acid
GABA_AR	GABA Type A Receptor
GABA_BR	GABA Type B Receptor
GRAS	Göttingen Research Association for Schizophrenia
HLA	Human Leukocyte Antigen
Ig	Immunoglobulins
IgG	Immunoglobulin G
IL-1β	Interleukin-1 β

APPENDIX

IL-17A	Interleukin-17A
IPS	Induced Pluripotent Stem Cell
KA	Kainate
KLF4	Kruppel-Like Factor 4
LBD	Ligand-Binding Domain
LIN28	Zinc Finger CCHC Domain-containing Protein 1
LIM1	LIM homeobox 1
MEP	Motor Evoked Potentials
mGluR	Metabotropic Glutamate Receptors
MHC	Histocompatibility Complex
MK-801	Dizocilpine
NFIA	Nuclear Factor I A
NMDA	N-methyl-D-aspartate
NMDAR	NMDA Receptors
NMDAR-AB	NMDA Receptors Autoantibodies
NTD	Amino-Terminal Domain
OTX1	Orthodenticle Homeobox 1
OCT4	Octamer-binding Transcription Factor 4
PANSS	Positive and Negative Syndrome Scale
PAUSS	PANSS Autism Severity Score
PAX6	Paired Box 6
qPCR	Quantitative Real Time Polymerase Chain Reaction
RNA	Ribonucleic Acid
SDF-1	Stromal Cell-derived Factor 1
SeV	Sendai Virus
SSEA4	Stage-Specific Embryonic Antigen-4
SOX2	Sex Determining Region Y-box 2
TCR	T Cell Receptors
TGF-β	Transforming Growth Factor β
TLR4	Toll-like Receptor 4
TMD	Transmembrane Domain
TMS	Transcranial Magnetic Stimulation
TNF-α	Tumour Necrosis Factor α

Curriculum vitae

Bárbara Oliveira

Phone number: +49 17661488577
email: oliveira@em.mpg.de

EDUCATION

PHD IN SYSTEMS NEUROSCIENCE

Institution: Göttingen Graduate School for Neurosciences, Biophysics and Molecular Biosciences GGNB; PhD program 'Systems Neuroscience'

Thesis topic: "Genetic and autoimmune modulators of brain function in neuropsychiatric illness and health"

Since 2014

MSC IN MOLECULAR BIOLOGY AND CYTOMICS IN HEALTH SCIENCES

Institution: Northern Polytechnic Institute of Health, Porto, Portugal

Thesis topic: "X-linked Intellectual Disability: Retrospective study of risk populations resorting to a set of genes implicated in intellectual disability"

Grade: Excellent

2008-2011

BSC IN ANATOMICAL PATHOLOGY

Institution: Northern Polytechnic Institute of Health, Porto, Portugal

Grade: 16 in a scale of 0-20

2004-2008

PROFESSIONAL ACTIVITIES

PhD candidate at Clinical Neuroscience

Institution: Max Planck Institute for Experimental Medicine, Göttingen, Germany

Since 2014

PhD candidate at Neurogenetics and Mental Health Unit

Institution: National Institute of Health Dr. Ricardo Jorge, Lisbon, Portugal

2012-2014

Research assistant at Neurogenetics and Mental Health Unit

Institution: National Institute of Health Dr. Ricardo Jorge, Lisbon, Portugal

2011

Master student at Molecular Genetics Unit

Institution: Center for Medical Genetics Jacinto de Magalhães, Porto, Portugal

2010-2011

Teaching assistant at Anatomical Pathology Department

Institution: Northern Polytechnic Institute of Health, Porto, Portugal

2010

Anatomical Pathology technician at IPATIMUP

Institution: Institute of Molecular Pathology and Immunology of the University of Porto, Porto, Portugal

2009

AWARDS AND FELLOWSHIPS

- Early Stage Researcher fellowship, Marie Skłodowska Curie actions 2014
- PhD fellowship, Fundação para a Ciência e Tecnologia SFRH/BD/79081/2011 2012
- Research assistant fellowship: "Autism Genome Project Consortium" 2011
- CIBEME'2010 awards for personal communication – Research in Health Sciences 2010

List of publications

1. **Oliveira B***, Mitjans M*, Nitsche MA, Kuo M-F and Ehrenreich H. *Excitation-inhibition dysbalance as predictor of autistic phenotypes. Under revision*
2. **Oliveira B** & Ehrenreich H. *Pursuing functional connectivity in NMDAR1 autoantibody carriers.* Letter to Lancet Psychiatry. 2018; 51:21-22
3. Pan H*, **Oliveira B***, Dere E, Tapken D, Mitjans M, Seidel J, Wesolowski J, Wakhloo D, Klein-Schmidt C, Ronnenberg A et al. *Uncoupling the widespread occurrence of anti-NMDAR1 autoantibodies from neuropsychiatric disease in a novel autoimmune model.* Molecular Psychiatry. 2018; *In press*
4. Mitjans M, Begemann M, Ju A, Dere E, Wüstefeld L, Hofer S, Hassouna I, Balkenhol J, **Oliveira B**, Van der Auwera S et al. *Sexual dimorphism of AMBRA1 related autistic features in human and mouse.* Translational Psychiatry. 2017; 710:e1247
5. Loureiro S, Almeida J, Café C, Conceição I, Mougá S, Beleza A, **Oliveira B**, de Sá J, Carreira I, Saraiva J et al. *Copy number variations in chromosome 16p13.11-The neurodevelopmental clinical spectrum.* Current Paediatric Research. 2017; 21 1: 116-129
6. Conceição IC, Rama MM, **Oliveira B**, Café C, Almeida J, Mougá S, Duque F, Oliveira G, Vicente AM. *Definition of a putative pathological region in PARK2 associated with autism spectrum disorder through in silico analysis of its functional structure.* Psychiatry Genetics. 2017; 272:54-61
7. Martins S, Maia N, Loureiro J, **Oliveira B**, Marques I, Santos R, Jorge P. *Contraction of fully-expanded FMR1 alleles to the normal range: predisposing haplotype or rare events?* Journal of Human Genetics. 2016; 622:269-275
8. Castillo-Gómez E*, **Oliveira B***, Tapken D*, Bertrand S, Klein-Schmidt C, Pan H, Zafeiriou P, Steiner J, Jurek B, Trippe R et al. *All naturally occurring autoantibodies against the NMDA receptor subunit NR1 have pathogenic potential irrespective of epitope and immunoglobulin class.* Molecular Psychiatry. 2017; 2212:1776-1784.
9. Ehrenreich H, Castillo-Gomez E, **Oliveira B**, Ott C, Steiner J, Weissenborn K. *Circulating NMDAR1 autoantibodies of different immunoglobulin classes modulates evolution of lesion size in acute ischemic stroke.* Neurology Psychiatry and Brain Research. 2016; 221.
10. Ott C, Martens H, Hassouna I, **Oliveira B**, Erck C, Zafeiriou M-P, Peteri U-K, Hesse D, Gerhart S, Altas B et al. *Widespread expression of erythropoietin receptor in brain and its induction by injury.* Molecular Medicine. 2015; 21:803-815.
11. Hadley D, Wu Z-I, Kao C, Kini A, Mohamed-Hadley A, Thomas K, Vazquez L, Qiu H, Mentch F, Pellegrino R, Kim C, Connolly J, **AGP Consortium** et al. *The impact of the*

APPENDIX

metabotropic glutamate receptor and other gene family interaction networks on autism.

Nature Communications. 2014; 5:4074.

12. Pinto D, Delaby E, Merico D, Barbosa M, Merikangas A, Klei L, Thiruvahindrapuram B, Xu X, Ziman R, Wang Z, ... **Oliveira B** et al. *Convergence of genes and Cellular Pathways dysregulated in Autism Spectrum Disorders.* American Journal Human Genetics. 2014; 5:677-94.
13. Correia CT, Conceição IC, **Oliveira B**, Coelho J, Sousa I, Sequeira AF, Almeida J, Café C, Duque F, Mougá S et al. *Recurrent duplications of the Annexin A1 gene ANXA1 in autism spectrum disorders.* Molecular Autism. 2014; 10;51:28.
14. Jorge P*, **Oliveira B***, Marques I, Santos R. *Development and validation of a multiplex-PCR assay for X-linked intellectual disability.* BMC Medical Genetics. 2013; 14:80.
15. Leblond CS, Heinrich J, Delorme R, Proepper C, Betancur C, Huguet G, Konyukh M, Chaste P, Ey E, Rastam M, ... **Oliveira B** et al. *Genetic and functional analyses of SHANK2 mutations provide evidence for a multiple hit model of autism spectrum disorders.* PLoS Genetics. 2012; 82: e1002521.

*Authors with equal contribution